



The
University
Of
Sheffield.

**The role of Sonic Hedgehog
signalling in
satellite cell-mediated myogenesis**

Sara Betania Cruz Migoni

The University of Sheffield
Department of Biomedical Science

This thesis is submitted on September, 2015 in partial fulfilment of the requirements for the degree of Doctor of Philosophy

ABSTRACT

Adult skeletal muscle regeneration depends on the existence of tissue-specific stem cells known as satellite cells. Satellite cells are found in a quiescent state in homeostatic conditions but become activated, re-enter the cell cycle, proliferate and differentiate or self-renew in response to muscle injury, exercise or disease. These events are tightly regulated by intrinsic and extrinsic cues, including well-characterised embryonic signalling cascades. The Sonic Hedgehog (Shh) signalling pathway has multiple roles in tissue patterning, cell fate determination, cell survival and proliferation in the embryo. Previous studies have shown that during embryonic myogenesis, Shh signalling controls the specification, migration and proliferation of muscle progenitor cells, as well as muscle patterning by the regulation of genes encoding basement membrane proteins. As the myogenic program carried out by satellite cells recapitulates, to a certain extent, embryonic myogenesis, I hypothesised that Shh signalling controls satellite cell activity in a manner reminiscent to its effect on muscle progenitor cells in the embryo. In this study, through a combination of *ex vivo* and *in vivo* approaches, I showed that, although quiescent satellite cells are refractory to Shh signals, activated satellite cells respond to Shh signalling. Shh response persists during the expansion phase and declines as satellite cells enter differentiation. Through the use of pharmacological agonists and antagonists of Shh signalling, as well as of an inducible conditional knockout mouse line of the Smoothed receptor in satellite cells, I demonstrated that Shh signalling contributes to satellite cell proliferation *ex vivo* and *in vivo* and to muscle regeneration following injury. Analysis of cell cycle dynamics showed that Shh signalling promotes the entry of satellite cells into the cell cycle and their progression through G1/S phase. Thus, the present study demonstrates that Shh signalling is required for adult skeletal muscle regeneration and provides novel insights into the role of Shh signalling in the control of satellite cell progression through the cell cycle and through myogenesis.

ACKNOWLEDGEMENTS

I would like to thank my supervisor Dr. Anne-Gaelle Borycki for giving me the opportunity to undertake this research project in her lab. It is really difficult to find words to express my gratitude for all her time, patience, guidance and support throughout my PhD.

I would also like to thank my advisors, Professor Marysia Placzek and Dr. Henry Roehl for their valuable advice and criticism. Thanks are also due to all current and past members of the Borycki lab for their constant discussions and enthusiasm while working in the lab. Special thanks to Dr. Shanti Rayagiri for her time and tuition, to Daniele Ranaldi for his help and humour and to Kamallia Mohd for her experimental support to finish this project. I also extend my gratitude to all members of the Placzek, Furley and Rivolta lab for their advice and help with reagents and equipment.

I would also like to acknowledge the experimental help I received for this project: Dr. Anne-Gaelle Borycki performed all cardiotoxin injections on the mice and Kamallia Mohd did all the estimations of recombination frequency presented in chapter 7.

I would like to thank Dr. James Briscoe for giving me the opportunity to work with his mice and to the members of his lab for their help during my visits to London. Special thanks go to Dr. Shahragim Tajbakhsh and Professor Ulrike Mayer for providing us with transgenic and knock-in mice.

Many thanks also go to all the members of Biological Services for dealing with the mice and providing them as and when required. Special thanks to William Sean Hague, Anne Marie Kimberly and Barry Bird for their help.

I would also like to express my gratitude to the National Council on Science and Technology (CONACyT) for the financial and academic support to carry out my postgraduate studies.

I would especially like to thank my dear friends Dr. Natasja Barki, Dr. Justyna Serba and Monika Tomecka for their moral support in tough times and for all the good moments we spent together. Special thanks also to all my Mexican friends and Son de America dancers for making me feel like home.

Last but not least, I would like to express my deepest gratitude to all my family for understanding and supporting me through all this adventure. Gracias mama y papa por

todo su apoyo, amor, comprensión y por estar siempre conmigo, aun en la distancia. Esta tesis es tanto suya como mía. Gracias a mis hermanos Abi y Bet por su cariño, por apoyarme y procurarme siempre. A mi pequeña Jolie por su amor incondicional. Y por último, gracias Sam por tu amor, apoyo, compañía y por todos los momentos que hemos pasado juntos, que han sido sin duda lo mejor de este PhD.

CONTENTS

1	Introduction	21
1.1	Adult skeletal muscle	21
1.1.1	Skeletal muscles have distinct levels of structural organisation . . .	21
1.1.2	Muscle fibre type and function	22
1.1.3	Different cell types coexist within skeletal muscles	23
1.2	Adult skeletal muscle repair	25
1.2.1	Evidence of regeneration in adult skeletal muscles	25
1.2.2	Cellular mechanisms of skeletal muscle repair	26
1.2.3	Satellite cells are responsible for muscle regeneration	27
1.2.3.1	Requirement for Pax3 and Pax7 in embryonic progenitors and satellite cells	29
1.2.3.2	Satellite cells are formed during embryogenesis	30
1.2.3.3	Satellite cells recapitulate embryonic myogenesis	31
1.2.3.4	Satellite cell heterogeneity	32
1.2.4	Non-myogenic cells also contribute to muscle repair	34
1.3	Satellite cell function	37
1.3.1	The quiescent state of satellite cells	37
1.3.1.1	The satellite cell quiescence signature	37
1.3.1.2	Regulation of satellite cell quiescence	39
1.3.2	Satellite cell activation	40
1.3.2.1	Molecular signature of activated satellite cells	40
1.3.2.2	Signals that control satellite cell activation	41
1.3.2.3	Markers of satellite cell proliferation	42
1.3.2.4	Signals that regulate satellite cell proliferation rate	43
1.3.2.5	Specific control of satellite cell progression through the cell cycle	44
1.3.3	Symmetric and asymmetric cell divisions	45
1.3.4	Satellite cell self-renewal: how the return to quiescence is regulated?	47
1.3.5	Satellite cell differentiation	48

1.3.5.1	Molecular signature of satellite cell differentiation	48
1.3.5.2	Signals that control satellite cell differentiation	49
1.4	The Hedgehog (Hh) signalling pathway	50
1.4.1	The Hh signalling ligands and their functions	50
1.4.2	The biosynthesis and secretion of Hedgehog proteins	52
1.4.3	Different receptors mediate Hh response	52
1.4.4	The mechanism of Hh signalling transduction	55
1.4.5	Hh proteins can act as morphogens and mitogens in different contexts	56
1.5	Shh signalling orchestrates embryonic myogenesis	58
1.5.1	Shh induces epaxial and hypaxial muscle cell fate specification . . .	58
1.5.2	Shh controls myotomal basal membrane assembly	59
1.5.3	Shh signalling regulates myofibre specificity in zebrafish	60
1.6	The Shh signalling pathway in adult skeletal muscles	62
1.6.1	Shh signalling activity is recapitulated during adult myogenesis . .	62
1.6.2	Pleiotropic effects of Shh signalling on adult muscle progenitors . .	62
1.6.3	Shh as a therapeutic for muscle repair	63
1.7	Conclusions	63
1.8	Hypothesis	64
1.9	Aims of the thesis	64
2	Material and Methods	67
2.1	Mouse models used	67
2.1.1	C57BL/6 mice	67
2.1.2	GBS-GFP mice	67
2.1.3	Pax7 ^{CreERT2} -Smo ^{flax/flax} mice	67
2.1.3.1	Induction of Cre-mediated recombination	68
2.1.4	Pax7GFP mice	68
2.1.5	Fucci2 mice	68
2.1.6	Genotyping	68
2.2	Single myofibre culture system	68
2.2.1	<i>Extensor digitorum longus</i> (EDL) and <i>Tibialis anterior</i> (TA) muscle harvesting	68
2.2.2	Isolation of single EDL muscle fibres	69
2.2.3	Culture of single EDL muscle fibres	69
2.2.3.1	Use of Shh signalling pathway agonist and antagonists . .	70
2.2.3.2	EdU assay	70
2.3	Immunofluorescence of single muscle fibres	70
2.4	Model of muscle injury <i>in vivo</i>	72

2.4.1	Cardiotoxin injections	72
2.5	Muscle transverse sections	72
2.5.1	Freezing protocol	72
2.5.2	Haematoxylin and eosin (H&E) staining	72
2.5.3	Immunofluorescence of muscle sections	72
2.5.4	Imaging	73
2.6	Cell cycle analysis by flow cytometry	73
2.6.1	Single cell isolation from cultured myofibres	73
2.6.2	Propidium iodide and RNase A treatment	73
2.6.3	Flow cytometry analysis	74
2.7	Cell sorting	74
2.7.1	Single cell preparation from bulk of muscle	74
2.7.2	Fluorescence activated cell sorting (FACS) analysis	75
2.8	Molecular biology techniques	75
2.8.1	Total RNA isolation from muscle fibres, whole embryo and cells grown in monolayer	75
2.8.2	Complementary DNA (cDNA) synthesis	75
2.8.3	Reverse transcription polymerase chain reaction (RT-PCR)	76
2.8.4	Quantitative real-time PCR (qPCR)	76
2.8.5	Primer design	77
2.9	Statistical analysis	77

3 *Ex vivo* and *in vivo* murine models to study satellite cell-mediated myogenesis **81**

3.1	Introduction	81
3.1.1	<i>In vitro</i> systems to study satellite cells	81
3.1.2	Study of satellite cells <i>ex vivo</i> : the myofibre culture system	82
3.1.3	Models to explore satellite cell function <i>in vivo</i>	84
3.1.4	Aim	85
3.2	Results	85
3.2.1	Satellite cell-mediated myogenesis can be studied <i>ex vivo</i> using the myofibre culture system	85
3.2.2	Adult myogenesis can be studied <i>in vivo</i> by inducing muscle injury with cardiotoxin	87
3.2.2.1	Satellite cells become activated and expand upon muscle injury <i>in vivo</i>	88
3.2.2.2	Satellite cells proliferate in response to muscle injury <i>in vivo</i>	92

3.2.2.3	Satellite cells differentiate <i>in vivo</i> to contribute to muscle regeneration	92
3.3	Discussion	94
3.3.1	The myofibre culture system recapitulates the events that happen during satellite-cell mediated myogenesis <i>ex vivo</i>	94
3.3.2	An acute model of muscle injury to study satellite cell myogenesis <i>in vivo</i>	96
4	Characterisation of the expression of Shh signalling pathway components in satellite cells	99
4.1	Introduction	99
4.1.1	Hypothesis and aim	100
4.2	Results	100
4.2.1	Components of the Shh signalling pathway are up-regulated during myofibre culture	100
4.2.2	Quiescent satellite cells are not responsive to Shh signalling but become responsive during their activation and expansion	101
4.2.3	Satellite cell progression through myogenesis and Shh response <i>ex vivo</i>	104
4.2.4	Shh response in satellite cells coincides with their entry into the cell cycle	105
4.2.5	Characterisation of Ptch1 distribution muscle regeneration <i>in vivo</i> .	107
4.3	Discussion	109
4.3.1	Quiescent satellite cells do not respond to Shh signalling.	109
4.3.2	Activated satellite cells become responsive to Shh signals.	112
4.3.3	Source of the Shh ligand during adult myogenesis <i>ex vivo</i> and <i>in vivo</i>	114
4.3.4	Non-muscle cells may be influenced by Shh signalling during adult skeletal muscle regeneration.	115
5	Effect of Shh signalling pathway activation and blockade on satellite cell progression through myogenesis <i>ex vivo</i>.	117
5.1	Introduction	117
5.1.1	Hypothesis and aim	118
5.2	Results	118
5.2.1	Effect of the stimulation of the Shh signalling pathway in satellite cells by the Smo agonist SAG	118

5.2.2	Chemical blockade of the Shh signalling pathway reduces the number of satellite cells in cultured myofibres	121
5.2.3	Blocking Shh signalling causes a delay in satellite cell-mediated myogenesis <i>ex vivo</i>	123
5.2.4	Inhibition of Shh signalling does not cause precocious differentiation of satellite cells	129
5.3	Discussion	130
5.3.1	Chemical manipulation of the Shh signalling pathway leads to a change in satellite cell numbers.	130
5.3.2	Shh signalling and apoptosis of satellite cells	131
5.3.3	Shh signalling and proliferation of satellite cells	132
5.3.4	Satellite cell progression through the myogenic program is affected by the Shh signalling pathway.	132
6	Shh signalling controls satellite cell progression through the cell cycle.	135
6.1	Introduction	135
6.1.1	Hypothesis and aim	136
6.2	Results	136
6.2.1	Effect of Shh signalling blockade on the expression of proliferation markers during satellite cell-mediated myogenesis <i>ex vivo</i>	136
6.2.2	Inhibition of Shh signalling delays satellite cell entry and progression through the cell cycle <i>ex vivo</i>	140
6.3	Discussion	144
6.3.1	The satellite cell proliferation profile <i>ex vivo</i> : insights from different experimental approaches.	144
6.3.2	Shh signalling affects the cell cycle dynamics of satellite cells at two different time points during myogenesis <i>ex vivo</i>	148
7	Skeletal muscle regeneration is impaired in the absence of Shh signalling	151
7.1	Introduction	151
7.1.1	Hypothesis and aim	152
7.2	Results	152
7.2.1	Generation of the Pax7 ^{CreERT2} -Smo ^{flax/flax} mutant mice.	152
7.2.2	Effect of satellite cell-specific deletion of Smo on muscle architecture following CTX injury.	153
7.2.3	Satellite cell-specific deletion of Smo increases fibrosis during muscle regeneration.	157

7.2.4	The absence of active Shh signalling in satellite cell delays muscle regeneration <i>in vivo</i>	157
7.3	Discussion	163
7.3.1	The absence of Shh signalling impairs muscle regeneration <i>in vivo</i>	163
7.3.2	Shh signalling is required for satellite cell progression through the myogenic program.	166
7.3.3	Dose-dependent effect of Shh signalling in satellite cell function	167
7.3.4	The role of Shh signalling in adult muscles differs from its role in embryonic myogenesis.	168
8	Final discussion	171
8.1	Thesis summary	171
8.2	Shh signalling activity is recapitulated during adult myogenesis	171
8.3	Control of cell cycle progression by Shh signalling	174
8.4	A requirement of Shh signalling in adult skeletal muscles	176
8.5	Shh signalling and implications in muscular diseases and therapies	177
8.6	Future directions	178
8.7	Final remarks	179
	Bibliography	214

LIST OF FIGURES

1.1	Structure of skeletal muscles	22
1.2	Different cell types are found in skeletal muscles	25
1.3	Cell dynamics during skeletal muscle repair	28
1.4	Parallels between embryonic and adult myogenesis.	33
1.5	The satellite cell cell cycle	38
1.6	Asymmetric and symmetric satellite cell division	47
1.7	Progression of the myogenic program in satellite cells	51
1.8	Biosynthesis and release of the Hh ligands	53
1.9	Transduction of the Hh signalling pathway	57
1.10	Different roles of Shh signalling in embryonic myogenesis.	60
1.11	Myofibre type specification depends on the concentration and timing of Shh exposure	61
3.1	Myogenic regulatory factor expression in single muscle fibres cultured <i>ex</i> <i>vivo</i>	86
3.2	Regeneration process following cardiotoxin-induced muscle injury.	89
3.3	Pax7 labels satellite cells during muscle regeneration.	90
3.4	Activated satellite cells expressed MyoD during muscle regeneration.	91
3.5	The satellite cell population expands during muscle regeneration.	93
3.6	Satellite cells activate Myogenin expression during muscle regeneration <i>in</i> <i>vivo</i>	95
3.7	The myofibre culture system recapitulates satellite cell-mediated myogenesis.	96
3.8	Cardiotoxin-mediated injury triggers muscle regeneration <i>in vivo</i>	97
4.1	Temporal expression of Shh and its downstream components in cultured myofibres	101
4.2	Ptch1 is expressed in activated satellite cells	102
4.3	Satellite cells become responsive to Shh signalling upon activation.	103

4.4	Ptch1 and Gli are indicators of Shh activity and are co-expressed in satellite cells	104
4.5	Shh signalling response during satellite cell-mediated myogenesis	106
4.6	Differentiating cells are the main target of Shh response at 72h	107
4.7	Gli response coincides with the entry of satellite into the cell cycle	108
4.8	Ptch1 expression is associated with satellite cells and non-muscle cells during muscle regeneration <i>in vivo</i>	110
4.9	Working model for Shh signalling activity in satellite cells	113
5.1	Proof of concept experiment to test the effect of the Smoothened agonist SAG on muscle cells.	119
5.2	Stimulation of Shh signalling with SAG does not affect the number of satellite cells <i>ex vivo</i>	120
5.3	Pilot experiment to test a concentration gradient of the Gli inhibitor GANT61 and the Smoothened agonist cyclopamine on <i>ex vivo</i> myofibre cultures. . .	121
5.4	Cyclopamine and GANT61 effectively block Shh response in satellite cells <i>ex vivo</i>	122
5.5	Blockade of Shh signalling with cyclopamine decreases the number of satellite cells <i>ex vivo</i>	124
5.6	Inhibition of Shh signalling with GANT61 affects satellite cell expansion <i>ex vivo</i>	125
5.7	Effect of Shh signalling inhibition on Pax7 and MyoD expression in satellite cells <i>ex vivo</i>	127
5.8	Shh signalling inhibition does not affect the number of Pax7+/Myf5- self-renewing satellite cells <i>ex vivo</i>	128
5.9	Shh signalling inhibition delays the onset of Myogenin expression <i>ex vivo</i> . .	129
5.10	Shh signalling inhibition does not cause premature differentiation of satellite cells.	130
6.1	Effect of Shh signalling inhibition on Ki67 expression <i>ex vivo</i>	138
6.2	Effect of Shh signalling inhibition on PH3 expression <i>ex vivo</i>	139
6.3	Effect of Shh signalling pathway stimulation and blockade on EdU incorporation <i>ex vivo</i>	141
6.4	Shh signalling inhibition affects satellite cell progression through the cell cycle.	142
6.5	Quantitative analysis of satellite cell cycle progression following Shh signalling inhibition <i>ex vivo</i>	143
6.6	Effect of Shh signalling inhibition on satellite cell cycle distribution <i>ex vivo</i> . .	145
6.7	Working model for satellite cell cell cycle control by Shh signalling	150

7.1	Tamoxifen (TM) and cardiotoxin (CTX) regimen and regeneration assay strategy.	152
7.2	Efficiencies of Cre-mediated recombination measured by YFP expression.	154
7.3	Regeneration following CTX-induced muscle injury in Smo ^{CKO} mice	155
7.4	Myofibre size declines in regenerating TA muscles of Smo ^{CKO} and Smo ^{Δ/+} mice.	156
7.5	Collagen type I deposition increases in Smo ^{CKO} and Smo ^{Δ/+} regenerating muscles.	158
7.6	Specific deletion of Smo in satellite cells does not affect the weight of regenerating muscles.	159
7.7	Loss of Smo affects the number of MyoD+ satellite cells in regenerating muscles.	161
7.8	Decrease of satellite cell differentiation in the absence of Shh signalling.	162
7.9	Regeneration at 21 days post-injury in Smo ^{CKO} and Smo ^{Δ/+} CTX-injured muscles.	163
7.10	Satellite cells remain proliferative at late stages of regeneration in the absence of Shh signalling.	164
7.11	Smo deletion impairs the expansion of activated satellite cells.	165
8.1	Shh signalling during adult muscle regeneration	172

LIST OF TABLES

2.1	Primary antibodies	71
2.2	Secondary antibodies	71
2.3	Standard PCR program	76
2.4	RT-PCR primers	78
2.5	qPCR primers	78
3.1	Satellite cell populations found during <i>ex vivo</i> culture as reported in the literature	83
3.2	Proportion of satellite cell populations found in this study during <i>ex vivo</i> culture	87
6.1	Distribution of satellite cells in the phases of the cell cycle using different experimental approaches	147

INTRODUCTION

1.1 Adult skeletal muscle

1.1.1 Skeletal muscles have distinct levels of structural organization

Skeletal muscle is highly contractile tissue representing around 40% of the total body mass. Skeletal muscles are not only important for support and locomotion but they are also critical for maintaining and regulating glucose homeostasis and carbohydrate metabolism (Richter et al., 1982).

Skeletal muscles are made up of bundles of multinucleated myofibres, which are the fundamental unit of the muscle. Each myofibre contains bundles of myofibrils, which are repetitions of filaments of actin (thin) and myosin (thick) that together form the sarcomere, the functional unit of the muscle fibre (Hanson and Huxley, 1953). Skeletal myofibres are surrounded by a 100 to 200nm thick layer of extracellular matrix (ECM) known as the basal lamina and a layer of connective tissue called the endomysium, which contains capillaries, nerves and lymphatics (Purslow and Trotter, 1994). These tightly-packed myofibres are assembled in bundles called fascicles, which are in turn surrounded by another layer of connective tissue called the perimysium (Davies and Nowak, 2006). Bundles of fascicles are covered by the epimysium, more connective tissue that surrounds the whole muscle and has continuity with the tendons (Fig.1.1) (Lieber, 2002).

The contractility of skeletal muscles relies on the action of the actin and myosin filaments of the sarcomere. Actin filaments are arranged in parallel and are joined by α -actinin at each end to form the Z-line. Myosin filaments are arranged in anti-parallel manner with the globular head bound to the actin filaments, which results in the sliding of actin towards the centre of the sarcomere during contraction (Huxley, 1957). This mech-

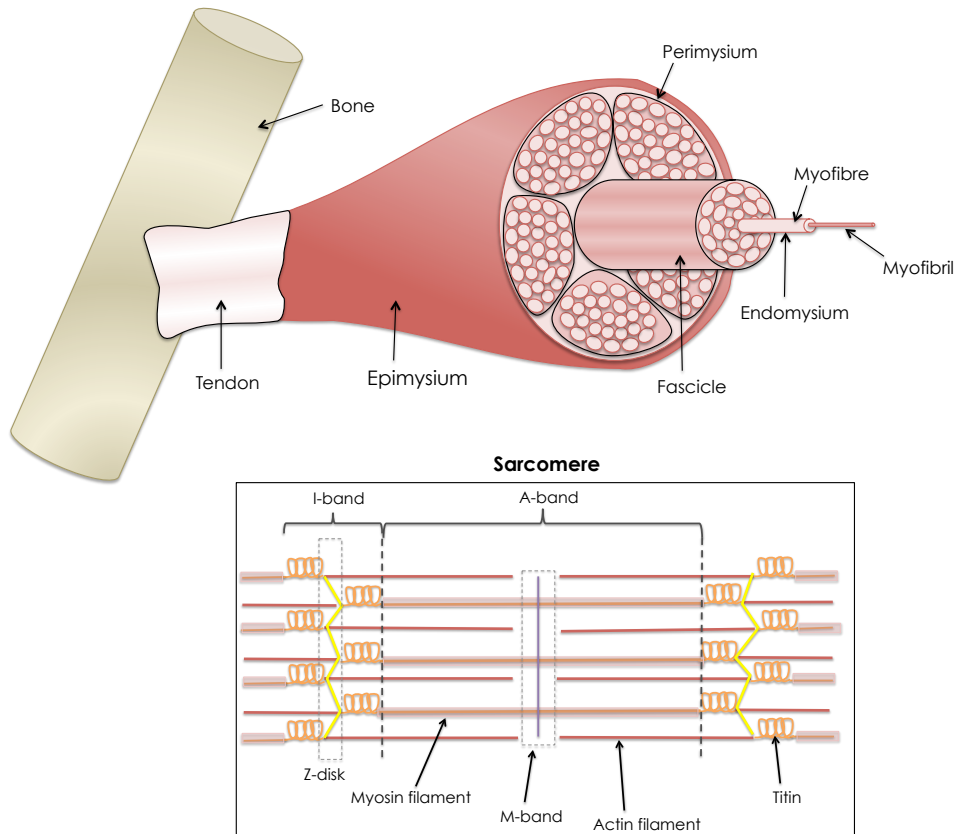


Figure 1.1: Structure of skeletal muscles. Skeletal muscles are intimately attached to the bones by tendons. The whole muscle is covered by the epimysium while bundles of myofibres are packed together by the perimysium. Finally, individual myofibres are surrounded by the endomysium. Each myofibre is composed of myofibrils, which contain sarcomeres. Each sarcomere is delimited by the Z-disks (or Z-lines), which are bound to actin filaments. Myosin filaments are arranged in anti-parallel manner and attached to the M band. Titin protein anchors the M to the Z line. The A-band corresponds to the alignment of myosin whereas the I-band extends in the area between two adjacent sarcomeres and only contains actin.

anism is mediated by calcium released from the sarcoplasmic reticulum, which binds to the troponin complex associated to the actin filaments. This binding unlocks tropomyosin from the actin binding site and allows the interaction of myosin with actin. This process continues as long as calcium is being released and finishes when the tropomyosin adopts its original position and covers the actin binding site (Szent-Györgyi, 2004).

1.1.2 Muscle fibre type and function

Skeletal muscle is a heterogeneous tissue made up of distinct myofibre types that determine the functional, molecular, metabolic and contractile activity of each muscle. First, myofibres can be classified as type I or slow-twitch fibres and type II or fast-twitch fibres (Schiaffino and Reggiani, 1994). Type I myofibres use aerobic metabolism and are resistant to fatigue. They are rich in mitochondria, have good blood supply and contain high levels of myoglobin and oxidative enzymes. These fibres are red in appearance due to the

high density of myoglobin. In contrast, type II myofibres rely on anaerobic metabolism and have faster contraction time but fatigue quickly. They contain little or no myoglobin and have fewer blood vessels and mitochondria, which gives them a pink/white colour (Eisenberg, 1983). Type II myofibres can be further categorised into type IIA and type IIB fibres. IIA fibres are fatigue-resistant with high succinate dehydrogenase (SDH) activity whereas IIB fibres are fatigue-resistant and have low SDH activity. An additional category of myofibres, the type IIX, describes fast-twitch fibres with a different composition of myosin heavy chain (MYHC) proteins and with a resistance to fatigue intermediate between IIA and IIB fibres (Schiaffino and Reggiani, 2011).

Different factors can determine the distribution of myofibre types in the whole organism. For instance, body size influences the functional demands of the musculature and it has been shown that small-sized mammals have more IIX and IIB fibres (high oxidation) than large-sized mammals, which have more type I and type IIA fibres (low oxidation) (Schiaffino and Reggiani, 2011). Myofibre distribution also varies between muscles and species. For example, type I fibres are abundant in the soleus muscle, whereas type II fibres are predominant in the extensor digitorum longus (EDL) muscle. Extraocular muscles (EOM) are of particular interest because they express a different type of MyHC isoform in fast-twitch fibres (MYH13) as well as embryonic and neonatal MyHCs (MYH3 and MYH8) (Sartore et al., 1987). Moreover, unlike mice and rats, human muscles only present type I, IIA and IIX myofibres (Ciciliot et al., 2013). Other determinants can also modify the myofibre profile, including hormones, aging, exercise and disease.

1.1.3 Different cell types coexist within skeletal muscles

The skeletal muscle system is made up of a complex network of distinct cell types that orchestrate the overall homeostatic activity of the tissue. First, bundles of muscle fibres are surrounded by layers of connective tissue and ECM that provide functional organisation and allow the attachment to tendons and bones. Underneath the most proximal layer of ECM, the basal lamina, quiescent muscle stem cells or satellite cells are found, which are responsible for muscle turnover and repair (Mauro, 1961). Additional cell types can be found, including fibroadipogenic progenitors (FAPs), endothelial cells, interstitial cells, vessel-associated cells (pericytes), fibroblasts and some immune cells (Bentzinger et al., 2013a). All these cells show little to no mitotic activity in normal homeostatic conditions but can enter proliferation in response to external stimuli, including injury and disease.

1. Endothelial cells

Muscles are supplied with nutrients and oxygen by a dense network of blood vessels and associated endothelial cells (Fig.1.2). Importantly, satellite cells are likely to

be found close to capillaries and endothelial cells (Christov et al., 2007). Following injury, endothelial cells secrete diverse growth factors needed for the formation of new capillaries (Ochoa et al., 2007). These factors also have mitogen and anti-apoptotic activities and can promote the proliferation of muscle stem cells (Christov et al., 2007).

2. Immune cells

Resting muscles contain few types of resident leukocytes such as mast cells and macrophages. Furthermore, healthy muscles are also supplied with a subpopulation of monocytes that patrol the tissue for rapid response in the event of injury (Auffray et al., 2007). Following muscle injury, resident monocytes quickly differentiate into M1 and M2 macrophages, which secrete pro-inflammatory and anti-inflammatory chemokines and cytokines, respectively (Arnold et al., 2007). Neutrophils also secrete pro-inflammatory molecules and remove muscle debris. Importantly, imbalance between neutrophils and M1 and M2 macrophages can impair the decrease of oxidative activity and clearance of muscle debris, strongly affecting muscle regeneration (Bentzinger et al., 2013a). More about the function of these cells during muscle regeneration is discussed in section 1.2.2.

3. Fibroadipogenic progenitors (FAPs) and fibroblasts

FAPs are non-myogenic mesenchymal stem cells that can give rise to fibroblasts, adipocytes and cartilage cells (Joe et al., 2010). These cells are found in the interstitial space of skeletal muscles in close contact with blood vessels (Fig.1.2). They express the platelet-derived growth factor receptor alpha (PDGFR α) and the Sca-1 marker (Joe et al., 2010, Uezumi et al., 2010). During muscle regeneration, FAPs promote fibrosis and fat deposition but can also induce proliferation of muscle stem cells (Joe et al., 2010).

In resting muscles, fibroblasts are located in the interstitial space between myofibres. These cells are the major source of ECM components and are essential for muscle regeneration (Murphy et al., 2011). They have a peculiar spindle-like morphology and are characterised by the expression of vimentin, desmin, α -actin-2 (ACTA2) and the fibroblast-specific protein 1 (FSP1) (Kalluri and Zeisberg, 2006, Strutz et al., 1995). The role of these cells during muscle regeneration is discussed in section 1.2.2.

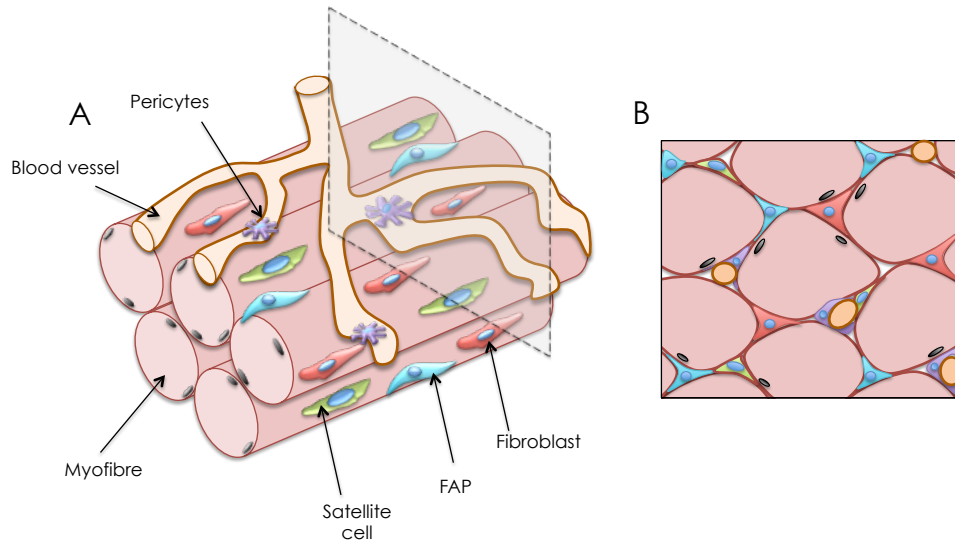


Figure 1.2: Different cell types are found in skeletal muscles. (A) Tridimensional and (B) cross-sectional representation of the cell identities found in the adult skeletal muscle system. Skeletal muscles are made up of multinucleated myofibres that intimately harbour satellite cells (green), which are located beneath the basal lamina. Blood vessels are intercalated between the fibres and are closely associated to vessel-associated cells (purple). Other cell types can also be found in the interstitial space, including mesenchymal progenitors (turquoise) and fibroblasts (red). Adapted from Pannérec et al. (2012).

1.2 Adult skeletal muscle repair

1.2.1 Evidence of regeneration in adult skeletal muscles

The idea of skeletal muscle regeneration dates back to the 19th century, with few studies describing the fusion of aligned corpuscles or round cells to form muscle fibres during embryogenesis (Scharner and Zammit, 2011). Further work by Wilhelm Waldeyer analysed muscle injuries in animals, including frogs, guinea pigs and rabbits, where he described the growth of muscle cells within the plasma membrane of degenerating myofibres (Scharner and Zammit, 2011). Another important piece of work was done by Rudolf Volkmann in 1893, who performed a wide range of muscle injuries on different animal species and concluded that muscles regenerate from nuclei of old myofibres and that this process could be continuous (new myofibres were formed from surviving fibres), discontinuous (new myofibres were formed from the fusion of single cells, similar to embryonic myogenesis) or a combination of both (Scharner and Zammit, 2011). This idea of "amitotic" regeneration from pre-existing myonuclei was further supported by a study describing the generation and multiplication of adult skeletal muscles *in vitro* by culturing small fragments of rat and human adult muscles (Pogogeff and Murray, 1946). Importantly, not only muscle repair in injured muscles was documented, but almost complete regeneration was observed in skeletal muscles of adult dystrophic rats supplemented with vitamin E (Pappenheimer, 1939). Further studies reported that upon injury, only mononucleated

cells such as myoblasts, leukocytes, fibroblasts and endothelial cells were labelled with tritiated thymidine, which incorporates into the DNA of proliferating cells. Interestingly, myoblasts were the most radioactive cells at early time points during regeneration and no radioactivity was observed in mature myofibres, disproving the idea of amitosis (Walker, 1962). The presence of myoblasts was also observed by electron microscopy in regenerating muscles of mice and rabbits (Allbrook, 1962). In 1961, the presence of mononucleated cells at the periphery of the adult skeletal myofibre was reported (Mauro, 1961). These so-called "satellite cells" were defined as dormant myoblasts that were morphologically indistinguishable from undifferentiated cells found at the site of injury during muscle regeneration (Muir et al., 1965). Interestingly, satellite cells were positively labelled for tritiated thymidine in regenerating skeletal muscles from adult mice, demonstrating the ability of these cells to synthesise DNA and divide mitotically (Reznik, 1969). Consistently, *ex vivo* culture of intact myofibres demonstrated that after 24 or 48 hours (h) in culture, mononucleated cells originating from myofibres had the ability to form colonies and fuse into myotubes (Bischoff, 1975). These findings led to the idea that satellite cells could be the precursors of the myoblasts found during skeletal muscle regeneration.

1.2.2 Cellular mechanisms of skeletal muscle repair

Adult skeletal muscle is a highly stable tissue that in homeostatic conditions shows little myonuclei turnover. Nevertheless, skeletal muscles have an incredible ability to grow and regenerate during normal development, as well as a result of intense exercise, mechanical load, injury or genetic diseases such as muscular dystrophies (Carlson, 1973). Importantly, adult muscles can be repaired within a period of 2 to 3 weeks after severe damage and also in response to repeated injury (Luz et al., 2002, Rosenblatt, 1992).

In general, adult skeletal muscle repair follows different phases, including degeneration, inflammation, regeneration and fibrosis. During muscle degeneration, mechanical/chemical trauma triggers the destruction of the integrity of the plasma membrane and basal lamina of the muscle fibre. As a consequence, myofibres undergo necrosis and protease mediated-degradation, increasing blood levels of muscle proteins like creatine kinases and myoglobin (Sorichter et al., 1998a). The necrotic area becomes infiltrated with immune cells and irrigated by small blood vessels. In particular, resident mast cells get activated immediately and start secreting histamine and tryptase as well as cytokines like tumour necrosis factor alpha (TNF- α) and interleukin 6 (IL-6) (Bentzinger et al., 2013a). These molecules are important since they can promote satellite cell activation and proliferation (Serrano et al., 2008) as well as neutrophil recruitment (Wang and Thorlacius, 2005). Neutrophils secrete several chemokines to attract monocytes, which eventually differentiate into macrophages (Arnold et al., 2007). Two distinct population of macrophages

are recruited during muscle regeneration. Pro-inflammatory or M1 macrophages are the first to appear, reaching a peak between days 2-3 and returning to basal numbers at days 7-9 post-injury (St Pierre and Tidball, 1994). These macrophages are characterised by the expression of CD11b, CD31, CD68 and iNOS and are mainly responsible for phagocytosis of any cell debris. They secrete the cytokines interleukin 1b (IL-1b), IL-6 and TNF- α , which promote the proliferation of satellite cells while inhibiting their differentiation (Saclier et al., 2013). On the other hand, anti-inflammatory or M2 macrophages appear later than M1 macrophages, peaking at days 3-5 and returning to basal numbers by days 8-10 after injury. They share the expression of some surface markers (CD11b, CD31 and CD68) with M1 macrophages but are also positive for CD206 and CD163 (McLennan, 1993). These M2 macrophages secrete interleukin 4 (IL-4) and insulin-like growth factor 1 (IGF-1), promoting satellite cell proliferation and differentiation (Fig.1.3) (Saclier et al., 2013).

Efficient muscle regeneration also requires the recruitment and proliferation of fibroblasts to synthesise ECM molecules including collagen, fibronectin, elastin, proteoglycans and laminins (Murphy et al., 2011). Importantly, fibroblasts also secrete metalloproteinases to control ECM deposition and remodel the muscle architecture (Lindner et al., 2012). Fibroblasts are mainly originated from mesenchymal stem cells or FAPs, which produce interleukin 6 to promote satellite cell differentiation (Fig.1.3) (Joe et al., 2010). Upon muscle injury, fibroblasts proliferate and reach a peak at 4-5 days post-injury and persist throughout the repair process (Bentzinger et al., 2013a). The deposition of ECM components by fibroblasts provide stability and support for the formation of new myofibres and the subsequent degradation of ECM excess by metalloproteinases facilitate satellite cell migration and differentiation (Chen and Li, 2009). Finally, endothelial cells also play an active role during muscle regeneration through the close interaction with myogenic precursors to promote both myogenesis and blood vessel formation. Endothelial cells peak at day 5 post-injury and secrete signalling proteins such as vascular endothelial growth factor (VEGF), which can stimulate myoblast proliferation (Christov et al., 2007). Thus, angiogenesis promotes the development of a new vasculature at the site of injury while stimulating satellite cell function, which contributes to efficient muscle repair.

1.2.3 Satellite cells are responsible for muscle regeneration

Satellite cells are adult muscle-specific stem cells that are defined by their anatomical position underneath the basal lamina (Mauro, 1961). Satellite cells have other particular morphological features, including a relative high nucleus-to-cytoplasm ratio with few organelles and an increased amount of nuclear heterochromatin compared to myonuclei (Schultz and McCormick, 1994). The frequency of satellite cells differs depending on age,

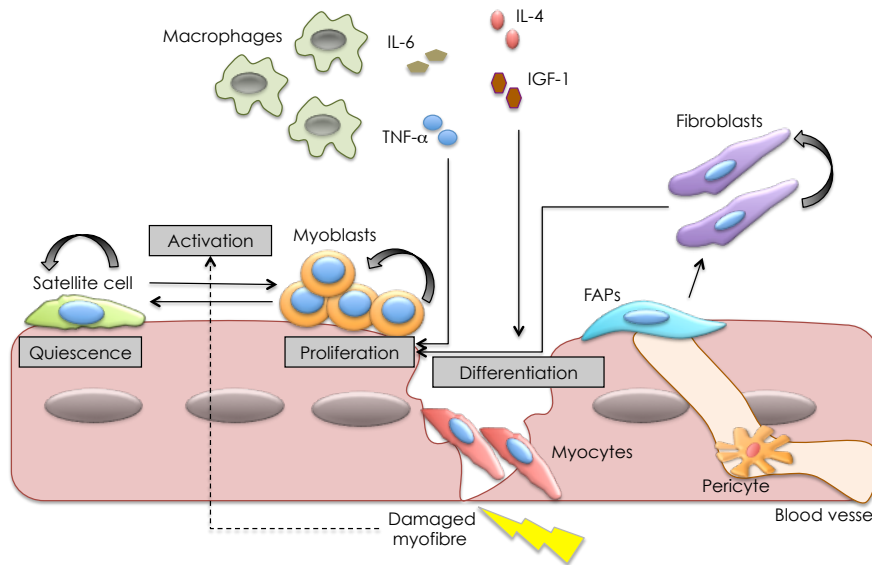


Figure 1.3: Cell dynamics during skeletal muscle repair. Following injury different signalling molecules (cytokines and growth factors) are released by damaged myofibres, infiltrating macrophages and fibroblasts to control satellite cell function, including their activation, proliferation and differentiation. Fibroadipogenic progenitors (FAP) give rise to fibroblasts that secrete both ECM components and metalloproteinases to promote remodelling of the muscle structure. Adapted from Wang and Rudnicki (2012).

myofibre type and species. Satellite cells constitute around 30% of the muscle nuclei in neonatal mice and decline to 4% in adult and 2% in old mice (Snow, 1977) and this is similar for human satellite cells (Schmalbruch and Hellhammer, 1976). This reduction in satellite cell number with age has been linked to changes in the satellite cell microenvironment or niche (Chakkalakal et al., 2012, Shefer et al., 2006). Satellite cell numbers also varies between different muscles; for example, the fast-twitch EDL muscle in mice contains less satellite cells (2.8%) than the slow-twitch soleus muscle (5.5%) (Zammit et al., 2002).

In normal healthy skeletal muscles, satellite cells are in quiescent state and only become activated in response to external factors released during injury or muscular disorders. Satellite cells then proliferate to become myoblasts and then undergo differentiation into myocytes and eventually fuse to form new fibres to repair the muscle (Charge and Rudnicki, 2004). As other stem cells, a fraction of satellite cells are able to self-renew and return to quiescence to repopulate the stem cell pool (Collins et al., 2005).

Early studies in muscle regeneration suggested that satellite cells were able to divide in response to injury (Reznik, 1969). Importantly, subsequent experiments showed that satellite cells incorporate into growing muscle fibres from young rats to later become myonuclei (Moss and Leblond, 1971). Other studies supported this observation through the use of isolated myofibres, showing the proliferation of satellite cells and their contribution to muscle fibres (Bischoff, 1975, Konigsberg et al., 1975). Indeed, transplantation of sin-

gle myofibres into irradiated muscles showed that donor satellite cells are able to produce myogenic progeny and self-renew *in vivo* (Collins et al., 2005). The ultimate proof that the regeneration of skeletal muscles *in vivo* is entirely dependent on satellite cells came from genetic studies. Using the Pax7^{DTR} mice, that express the diphtheria toxin fragment A (DTA) receptor (DTR) under control of the Pax7 promoter, it was shown that the depletion of Pax7-expressing satellite cells before muscle injury led to impaired muscle repair (Sambasivan et al., 2011). Similar approaches to eliminate satellite cells in adult skeletal muscles were applied, in which DTA expression was specifically induced in Pax7+ satellite cells prior to muscle injury, resulting in the failure of muscle regeneration. This was achieved using conditional recombination with Pax7^{iCreERT2/+}: R26R^{DTA/+} (83-91% ablation), Pax7^{iCE/+}: R26R^{DTA/+} (over 90% ablation) or Pax7^{CreERT2/+}: R26R^{GFP-DTA/+} (100% ablation) mice (Lepper et al., 2011, McCarthy et al., 2011, Murphy et al., 2011). Importantly, functional muscle regeneration in satellite cell-depleted injured muscles could be rescued by grafting Pax7-nGFP satellite cells, indicating that satellite cells are necessary and sufficient for muscle regeneration (Sambasivan et al., 2011).

1.2.3.1 Requirement for Pax3 and Pax7 in embryonic progenitors and satellite cells

Pax3 and Pax7 belong to a family of transcription factors characterised by the presence of a DNA-binding region known as the paired domain (Gruss and Walther, 1992). These genes are thought to be originated by duplication from a common ancestral gene and they share similarities at the protein level and in the expression pattern at some extent. *Pax3*-null mutant embryos display muscle abnormalities, including loss of both the epaxial and hypaxial dermomyotome (Tajbakhsh and Buckingham, 2000). In contrast, *Pax7*-null mutant embryos do not present defects in muscle development but fail to maintain their musculature postnatally (Mansouri et al., 1996). Therefore, Pax3 has a major role during embryonic myogenesis, whereas Pax7 is important for postnatal muscle development (Bryson-Richardson and Currie, 2008).

In the vertebrate embryo, Pax3 is expressed in the presomitic paraxial mesoderm (Goulding et al., 1994) and becomes restricted to the dorsal part of the somite following somite formation and is down-regulated when the myogenic regulatory factors (MRF) are activated (Williams and Ordahl, 1994). On the contrary, Pax7 is not expressed in the presomitic mesoderm or newly formed somites, but is progressively detected in the central part of the dermomyotome, following Pax3 expression (Borycki et al., 1999a, Jostes et al., 1990). In the hypaxial dermomyotome, Pax3 is required for the survival of progenitor cells and it directly induces Myogenic factor 5 (Myf5) expression in cells that migrate to the limb, which in turn activates myoblast determination protein (MyoD) (Bajard et al.,

2006, Borycki et al., 1999a, Tajbakhsh et al., 1997). On the other hand, in the epaxial dermomyotome, Pax3 can act independently of Myf5 to regulate MyoD (Tajbakhsh et al., 1997). In fact, Pax3, Myf5 and the muscle-specific regulatory factor 4 (MRF4) can promote myogenic differentiation through MyoD activation (Kassar-Duchossoy et al., 2004, Maroto et al., 1997, Tajbakhsh et al., 1997).

In adult skeletal muscles, Pax7 is specifically expressed by satellite cells and although a subset of satellite cells also express Pax3, this transcription factor is unable to compensate for the loss of Pax7 during postnatal myogenesis or adult muscle regeneration (Kuang et al., 2006, Relaix et al., 2006). *Pax7*-null mutant newborn die within two weeks after birth, display a decrease in muscle mass and are depleted of satellite cells, indicating the requirement for Pax7 for the specification of the satellite cell lineage (Seale et al., 2000). Consistently, over-expression of Pax7 in CD45⁺:Sca1⁺ cells isolated from injured *Pax7*-null muscles is sufficient to activate the myogenic program (Seale et al., 2004). Conditional inactivation of *Pax7* in Pax7⁺ satellite cells results also in impaired muscle regeneration after single or repeated injury, confirming the critical requirement for Pax7 during satellite cell-mediated myogenesis (von Maltzahn et al., 2013). Pax7 is expressed at high levels in quiescent satellite cells and becomes progressively down-regulated as satellite cells differentiate (McKinnell et al., 2008, Olguin and Olwin, 2004). siRNA-mediated knock-down of *Pax7* in satellite cells causes a reduction of Myf5 expression, and chromatin immunoprecipitation assays have showed that Pax7 recruits a histone methyltransferase (HMT) complex to directly activate *Myf5* transcription (McKinnell et al., 2008). Consistent with this, inactivation of Pax7 in Myf5⁺ satellite cells leads to a decline in satellite cell numbers in mice older than 8 weeks and to an impairment of muscle regeneration following injury, indicating a requirement of Pax7 for the maintenance of satellite cells (Günther et al., 2013).

1.2.3.2 Satellite cells are formed during embryogenesis

Skeletal muscles in vertebrates originate from the segmented somitic paraxial mesoderm, the unsegmented cranial paraxial mesoderm and the chorda mesoderm (Bryson-Richardson and Currie, 2008). Somites are epithelial patches of mesodermal cells flanking the neural tube and they give rise to various tissues, including skeletal muscles of the trunk and limbs. As development proceeds, the dorsal and ventral somite compartments differentiate into epithelial and mesenchymal structures known as dermomyotome and sclerotome, respectively. The sclerotome will give rise to cartilage and vertebrae, while the dermomyotome will generate skeletal muscle and dermal progenitors (Pownall et al., 2002). The first skeletal muscle progenitor cells (MPC) to form during embryonic development delaminate from the dorsal medial lip (DML) of the dermomyotome to incorporate

into a new structure, the myotome (Hollway and Currie, 2003). Cells entering the myotome grow bidirectionally to reach both the rostral and caudal edges of the somite. Subsequently, myogenic progenitors delaminate from the caudal, rostral and ventro lateral lip (VLL) domains and translocate to the myotome where they contribute to its expansion (Gros et al., 2004). In this way, progenitors derived from the DML will give rise to the epaxial myotome, while cells coming from the VLL will colonise the hypaxial myotome (Gros et al., 2004).

The origin of satellite cells has been a subject of debate for several years. Early quail-chick chimera strategies proposed that satellite cells were generated in the somites, but no progenitor cell population giving rise to these cells could be identified at the time (Armand et al., 1982). Other reports described that adult muscle progenitors in the chick originated during mid and late foetal development based on *in vitro* assays (Feldman and Stockdale, 1992). Lineage tracing experiments of GFP-electroporated dermomyotome cells showed that some GFP+ cells that migrated into the myotome were highly proliferative and expressed Pax7 and adopted a satellite cell position (Gros et al., 2005). Similarly, using Pax3^{GFP/+}:Pax7^{LacZ/+} reporter mice, β -gal+/GFP+ cells that do not express myogenic markers and are actively proliferating could be detected as early as at E.10.5 (Kassar-Duchossoy et al., 2005, Relaix et al., 2005). Around E.15.5, these Pax3+/Pax7+ progenitors localise along differentiated myofibres and between E.16.5 and 18.5 they become surrounded by a basal lamina (Kassar-Duchossoy et al., 2005, Relaix et al., 2005). Together, these data demonstrate that satellite cells of the trunk and the limb muscles are specified during embryogenesis from undifferentiated Pax3+/Pax7+ progenitors originating from the dermomyotome (Fig.1.4).

1.2.3.3 Satellite cells recapitulate embryonic myogenesis

Embryonic muscle progenitors and satellite cells share many similarities concerning the expression of the myogenic regulatory factors (MRFs) and the dynamics of the myogenic program during both embryonic and adult myogenesis.

In the developing embryo, the onset of Pax3 expression in the dorsal somites is followed by the activation of *Myf5* as early as at E.8 in the dorsal-medial somites and MyoD 2.5 days later (Cossu et al., 1996, Tajbakhsh et al., 1997). MRF4 expression starts at E.9.5 and gradually accumulates in the somites (Kassar-Duchossoy et al., 2004). Conversely, Myogenin transcripts are expressed at E.8.5 in the myotome before MyoD expression starts (Venuti et al., 1995). Both *Myf5*-null and *MyoD*-null mutant are viable. *Myf5*-null mice show a delay in myotome formation until the onset of MyoD expression and a reduction in the development of trunk musculature, but normal development of limb muscles (Kablar et al., 1997, Tajbakhsh et al., 1997). In *MyoD*-null mutant mice, Myf5

expression becomes up-regulated, probably compensating for the lack of MyoD (Rudnicki et al., 1992). Skeletal muscles can form in *Myf5::MyoD* double-mutant mice when MRF4 expression is not compromised but not in the absence of MRF4, indicating that Myf5, MyoD and MRF4 are essential for muscle progenitor formation (Kassar-Duchossoy et al., 2004). In contrast, Myogenin is a MRF that is important for myoblast differentiation, acting by regulating the transcription of genes involved in fibre formation and others that encode contractile muscle proteins. In *Myogenin*-null mutant mice, the muscular tissue consists of muscle progenitor cells but no differentiated myocytes are observed, confirming the role of Myogenin in initiating muscle differentiation (Venuti et al., 1995). As *Mrf4::MyoD* double mutants have a similar phenotype than *Myogenin*-null mice, it suggests that MyoD acts upstream of Myogenin to drive myoblast differentiation (Rawls et al., 1998).

In adult muscles, quiescent satellite cells express Pax7 rather than Pax3, although a small fraction of cells express also Pax3 (Relaix et al., 2006). Upon activation, satellite cells re-enter the cell cycle and initiate a myogenic program that recapitulates the events taking place during embryonic myogenesis (Fig.1.4) (Cooper et al., 1999). For instance, activated satellite up-regulate Myf5 and within the first 12 hours progressively up-regulate MyoD expression while continuing to express Pax7 (Cooper et al., 1999, Yablonka-Reuveni and Rivera, 1994, Zammit et al., 2004). Following the expansion phase, satellite cells down-regulate Pax7 and Myf5 and begin expressing Myogenin and MRF4 (Cornelison, 2008, Yablonka-Reuveni and Rivera, 1994, Yablonka-Reuveni et al., 1999a). Finally, differentiating myogenic cells fuse to each other to form new myofibres or fuse with damaged fibres to contribute to their regeneration. This sequence of events is reminiscent to the myogenic program that takes place in embryonic muscle progenitors (Fig.1.4).

1.2.3.4 Satellite cell heterogeneity

The satellite cell population is heterogeneous as evidenced by differences in the molecular/cellular signature of satellite cells. Studies using *Myf5-nlacZ* mice have shown that a proportion of quiescent satellite cells does not express *Myf5* or other satellite cell markers such as CD34 and M-cadherin (Beauchamp et al., 2000, Zammit et al., 2002). Accordingly, lineage tracing experiments using *Myf5-Cre/Rosa26-YFP* mice confirmed that around 10% of satellite cells never expressed *Myf5* and contribute efficiently to the stem cell pool upon transplantation (Kuang et al., 2007). Satellite cell heterogeneity also translates into differences in Pax7 expression. Although all satellite cells express *Pax7* mRNA, levels of the Pax7 protein in the satellite cell population are not homogeneous. Immunofluorescence analysis of single myofibres have shown that the satellite cell population is made up of one subset of cells that expresses Pax7 but no MRFs and another subset that

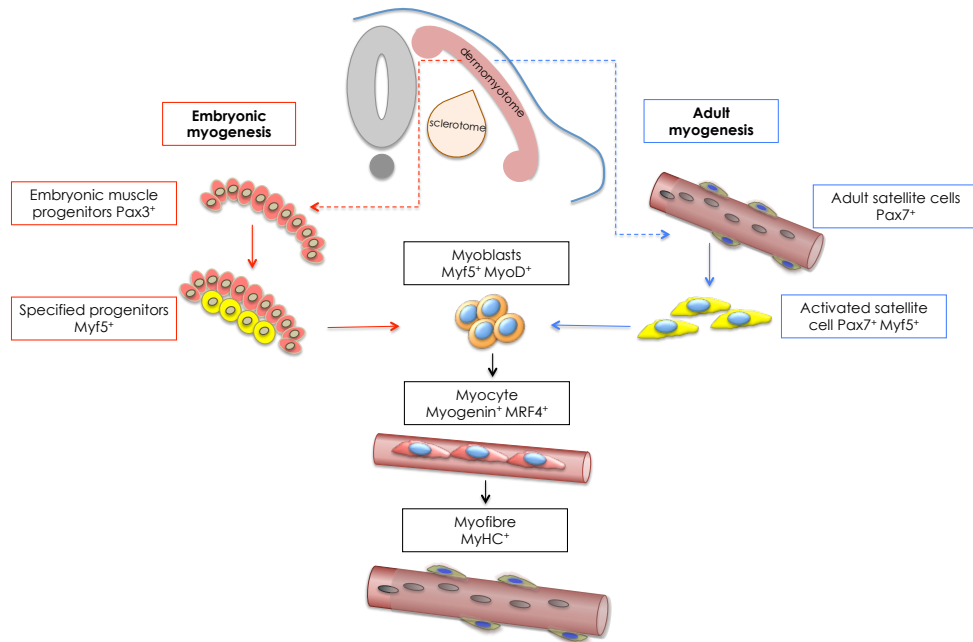


Figure 1.4: Parallels between embryonic and adult myogenesis. Muscle progenitor cells (Pax3+) and satellite cells (Pax7+) are formed during embryogenesis and they follow similar dynamics to generate fully differentiated myofibers. Both cell populations become specified and activate Myf5 and MyoD expressions. Their entry into differentiation is characterised by the expression of Myogenin and MRF4 expression, resulting in the formation of myotubes and functional myofibers.

is more prone to myogenic commitment and differentiation (Olguin and Olwin, 2004). Consistently, fluorescence-activated cell sorting (FACS) of satellite cells from post-natal Pax7-nGFP transgenic mice has revealed the existence of two distinct cell populations: Pax7-nGFP^{Hi}, which expresses high levels of Pax7 and contain more slow-dividing label-retaining cells (LRC), and Pax7-nGFP^{Lo}, which expresses low levels of Pax7. Upon muscle injury, Pax7-nGFP^{Hi} satellite cells are less prone to commitment than Pax7-nGFP^{Lo} and their first cell division is slower (Rocheteau et al., 2012). Importantly, Pax7-nGFP^{Hi} are the only satellite cell population able to give rise to Pax7-nGFP^{Lo} cells following several transplantations, indicating a strong self-renewal potential (Rocheteau et al., 2012). Similarly, experiments using the TetO-H2B-GFP mice, which carry a conditional transgene consisting of a fusion of the histone H2B to GFP and controlled by tetracycline (Tumbar et al., 2004), identified two satellite cell populations in adult mice on the basis of the cells ability to retain H2B-GFP: LRCs and non-LRCs. LRC satellite cells divide and differentiate less than non-LRCs and contribute to the maintenance of satellite cells that adopt a sublaminar position (self-renewal) (Chakkalakal et al., 2012). This is consistent with other studies showing that satellite cells fated to differentiate are fast-dividing cells, whereas self-renewing satellite cells are considered to be slow-dividing (Ono et al., 2012). Together, these studies support the idea that the satellite cell population is heterogeneous, with most of the cells being committed to the myogenic lineage and a subset representing

a stem cell population able to self-renew to sustain the regenerative potential of skeletal muscles.

1.2.4 Non-myogenic cells also contribute to muscle repair

Although Pax7+ satellite cells are required for skeletal muscle regeneration, other non-muscle cell types have the potential to contribute to the repair process. These cells include bone marrow-derived cells, pericytes and mesoangioblasts. Some of them can differentiate both *in vitro* and *in vivo* into multiple lineages depending on the extrinsic signals they are subjected to. Importantly, they have also shown potential to differentiate into the myogenic lineage.

1. Hematopoietic stem cells (HSCs)

HSCs are responsible for the continuous generation of blood and immune cells in the body. HSCs can be isolated from blood or the stroma of the bone marrow, and are characterised by their non-adherent behaviour *in vitro* (Domen et al., 2006). The injection of HSCs from MLC3f-LacZ mice (muscle specific promoter) into myotoxin-injured mouse muscles results in the incorporation of β -gal+ nuclei in regenerating myofibres (Ferrari et al., 1998), indicating that cells of HSC origin contribute to the regeneration program. A subpopulation of HSCs that express the cell surface marker CD45 has myogenic potential when grafted into injured muscles (McKinney-Freeman et al., 2002). Furthermore, HSCs expressing the CD133 marker also expressed myogenic markers, including Pax7, Myf5 and MyoD. Importantly, CD133+ cells isolated from humans contribute to myofibres when grafted into dystrophic mice (Torrente et al., 2004). This indicates that different populations of HSCs have a myogenic potential although their contribution to muscle regeneration *in vivo* is still low.

2. Mesenchymal stem cells (MSCs)

MSCs are found in the stroma of the bone marrow. MSCs adhere rapidly when cultured at low density, allowing separation from non-adherent hematopoietic cells (Bianco et al., 2001). MSCs can give rise to cells that express skeletal muscles markers and are able to fuse *in vitro* after treatment with basic fibroblast growth factor (bFGF), forskolin, platelet-derived growth factor (PDGF), Neuregulin and subsequent transfection with the Notch1 intracellular domain (NICD) gene. Importantly, following transplantation into dystrophic-nude mice, these cells incorporate into newly formed myofibres (Dezawa et al., 2005). Furthermore, MSCs can also be harnessed into the myogenic lineage by transfection of *Pax3*, which have a good engraftment efficiency but fail to improve the dystrophic phenotype in mice mainly

due to lack of contractility (Gang et al., 2009). This suggests that other factors than Pax3 may be required to improve the functionality of these cells *in vivo*.

3. Side population (SP) cells

SP cells were initially identified in the mouse bone marrow and were characterised by the exclusion of Hoechst 33342 dye, which gave them a particular pattern when analysed by fluorescence-activated cell sorting (FACS) (Goodell et al., 1996). A similar fraction of SP cells has been identified in the interstitium of skeletal muscles but these cells are different from bone marrow SP cells (Asakura et al., 2002). Similar to satellite cells, muscle SP cells have mainly an embryonic origin and are derived from Pax3+ cells in the hypaxial somite (Schienda et al., 2006). Muscle SP are multipotent, express the Sca-1 marker and do not express myogenic proteins like Myf5 (Asakura et al., 2002). Consistently, SP cells are still present in *Pax7*-null mice, indicating that SP and satellite cells are two distinct cell populations (Seale et al., 2000). Although when cultured *in vitro*, muscle SP cells (CD45+, Sca-1+) give rise to hematopoietic colonies, they can also adopt a myogenic fate if co-cultured with myoblasts (Asakura et al., 2002). Injection of muscle SP cells into injured muscles results in the incorporation of SP cells in regenerating fibres (Asakura et al., 2002). Moreover, SP cells injected intravenously into irradiated dystrophic mice can re-established the hematopoietic system and contribute to muscle regeneration (Gussoni et al., 1999).

4. Pericytes

Pericytes are vascular smooth muscle cells that surround the surface of blood vessels and capillaries. They originate from the embryonic sclerotome and in adult tissues express the alkaline phosphatase (ALP) protein and the endothelial marker CD31. Pericytes can usually differentiate into smooth muscles, osteoblasts and adipocytes but display also a low myogenic potential (Doherty et al., 1998). However, co-culture of pericytes with myogenic cells or muscle-differentiation medium increases the frequency of fusion into myofibres and the frequency of spontaneous differentiation into myotubes, respectively (Dellavalle et al., 2007). Unlike satellite cells, proliferating pericytes do not up-regulate Pax7 or the MRFs (Myf5 and MyoD), and the expression of these markers is only visible during terminal differentiation, indicating that distinct mechanisms of myogenesis occur in pericytes and satellite cells (Dellavalle et al., 2007). Nevertheless, the interarterial injection of isolated human pericytes into dystrophic mice resulted in the restoration of Dystrophin expression in regenerating myofibres (Dellavalle et al., 2007), demonstrating their myogenic potential *in vivo*.

5. Mesoangioblasts

Mesoangioblasts are foetal mesodermal progenitors that express endothelial and pericyte markers depending on the stage during which they are isolated (Cossu and Bianco, 2003). Mesoangioblasts isolated from the mouse dorsal aorta are able to form satellite cell-like colonies and express the myogenic markers MyoD, Myf5 and c-Met (De Angelis et al., 1999). Upon injection into injured muscles of immunodeficient mice, MLC3f-LacZ mesoangioblasts contribute to regenerating myofibres (De Angelis et al., 1999). One interesting feature of mesoangioblasts is their ability to cross the vessel wall in response to inflammation, allowing therapeutically relevant approaches such as their transplantation via arteries towards the interstitium of skeletal muscles. Using this approach, it has been shown that the injection of wild-type mesoangioblasts or mesoangioblasts isolated from α -*Sarcoglycan*-null mice and transfected with α -*Sarcoglycan*-encoding lentivirus ameliorates the dystrophic phenotype of mice lacking α -*Sarcoglycan* (Sampaolesi et al., 2003). Likewise, delivery of wild-type mesoangioblasts into dogs affected with golden retriever muscular dystrophy (GRMD) resulted in improvement of dystrophin expression and gain of muscle function (Sampaolesi et al., 2006). Therefore, mesoangioblasts are powerful candidates for the treatment of muscular disorders.

6. Fibroadipogenic progenitors (FAPs)

FAPs are important player of muscle regeneration, they proliferate rapidly in response to injury to generate adipocytes and fibroblasts and to secrete factors to promote myoblast proliferation, such as interleukin 6 (IL-6) (Heredia et al., 2013, Joe et al., 2010). FAPs show little to no myogenic differentiation even when co-cultured with muscle progenitors *in vitro* (Joe et al., 2010). Also, FAPs are thought to be responsible for ectopic fat formation and decreased muscle contractility during muscle regeneration (Uezumi et al., 2010). However, it has recently been shown that blockade of FAP adipogenic differentiation improves muscle regeneration of young dystrophic mice (Mozzetta et al., 2013). More specifically, the use of HDAC inhibitors can derepress FAPs myogenic potential by inducing MyoD and BAF60C expression, as well as specific miRNAs (miR-133 and miR-206), which can also promote myogenic differentiation (Saccone et al., 2014). Therefore, modification of FAPs behaviour and differentiation *in situ* is a promising strategy for the treatment of muscular dystrophies.

1.3 Satellite cell function

1.3.1 The quiescent state of satellite cells

Generally speaking, the eukaryotic cell cycle consists of four discrete phases: G1 (Gap 1), S (DNA synthesis), G2 (Gap 2) and M (Mitosis), which are active phases leading to the division of a cell (Nurse, 1994). An additional phase, named G0 (Gap 0), is an inactive, non-cycling state where cells do not divide at all (Fig.1.5). Cells in G0 state include terminally differentiated cells that have irreversibly exited the cell cycle and cells in quiescence, which is a reversible growth arrest where cells can re-enter the cell cycle upon stimulation (Cheung and Rando, 2013). Quiescence is an important characteristic of several stem cells, including hematopoietic, intestinal, epithelial and muscle stem cells. In healthy skeletal muscles, satellite cells are found in a quiescent state, which is essential to maintain the satellite cell pool and the homeostatic balance of the muscle.

Satellite cells transition into an intermediate state between G0 and G1, named GAlert state (Fig.1.5). Satellite cells at GAlert arise in response to injury-induced systemic signals and have an intermediate phenotype between G0 and G1 cells. For instance, GAlert satellite cells are larger, have a greater propensity to cycle and have a higher metabolic activity than G0 cells, making them comparable to G1 cells. However, when grafted into injured muscles, GAlert satellite cells exhibit similar engraftment and self-renewal efficiency to quiescent G0 satellite cells (Rodgers et al., 2014). The biological importance of this intermediate state translates into a greater and faster ability for satellite cells to carry out the first cell division compared to G0 cells.

1.3.1.1 The satellite cell quiescence signature

Quiescent satellite cells are characterised by high expression levels of the transcription factor Pax7, which is required for the specification of the satellite cell lineage (Fig.1.7) (Seale et al., 2000). Moreover, microarray analyses have shown that about 500 genes are exclusively up-regulated in quiescent satellite cells compared to activated and proliferating myoblasts. These genes include cell adhesion molecules, cell cycle regulators, cytoskeletal proteins, signalling molecules and extracellular components among others (Fukada et al., 2007).

Because quiescent satellite cells are in a G0 state, it is not surprising that some of the most relevant markers of quiescence are negative regulators of the cell cycle. This includes the G-protein signalling 2 and 5 (*Rgs2*, *Rgs5*), peripheral myelin protein 22 (*Pmp22*), cyclin-dependent kinase inhibitor 1A (*Cdkn1a/p21Cip1*), 1B (*Cdkn1b/p27Kip*) and 1C (*Cdkn1/p57Kip2/p57*), the retinoblastoma protein (*Rb1*) and the Sprouty homolog 1 *Spry1* (Dumont et al., 2015b, Fukada et al., 2007). These proteins inhibit cell cycle

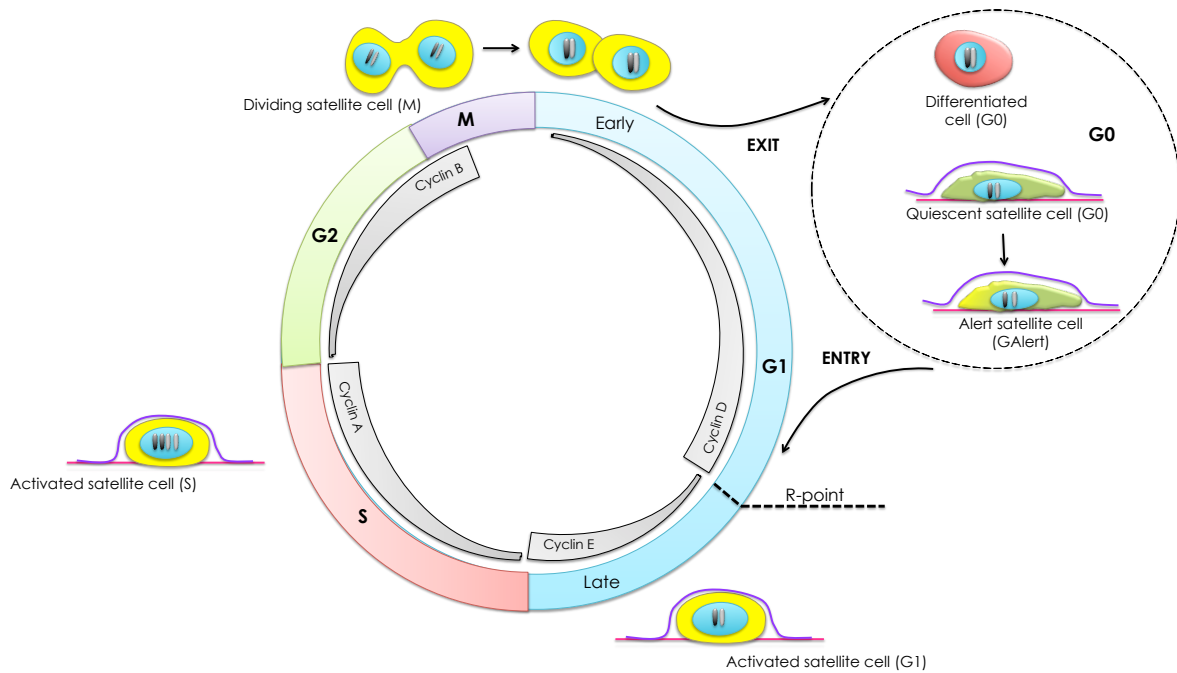


Figure 1.5: The satellite cell cycle. Quiescent satellite cells are in a reversible G0 state. Following muscle injury, satellite cells become activated and enter the mitogen-dependent early G1 phase, transitioning through the R-point and committing to the cell cycle. Hyperphosphorylation of retinoblastoma protein (Rb1) by Cdk4/Cyclin D is important for passage through the R point. Quiescent satellite cells can also transition into a GAlert state as a result of injury-induced systemic signals and enter the cell cycle from there. Activated satellite cells in G1 enter the S phase to replicate their DNA. The Cdk2-Cyclin E complex is an important regulator of the G1-S transition. Once the DNA is duplicated, activated satellite cells go the G2 phase. Cdk1/Cdk2-Cyclin A complexes regulate the completion of the S phase. Satellite cells then enter mitosis to generate two daughter cells. Transition from G2-M phase depends on the control of Cdk1-Cyclin B complex. The resulting cells continue into G1 phase, where they can undergo further cell divisions or if differentiating, exit the cell cycle into the G0 state.

entry or cell cycle progression, and are needed to prevent premature activation of satellite cells. Accordingly, muscles from *p27Kip*-null mice displayed a decrease in the number of quiescent LRCs and, as a consequence, an increase in the number of proliferating satellite cells (Chakkalakal et al., 2014). Likewise, the conditional deletion of the *Rb1* gene in satellite cells results in an accelerated cell cycle re-entry, leading to a drastic increase in the number of Pax7+ cells (Hosoyama et al., 2011).

Amongst the cell surface and cell adhesion molecules enriched in quiescent satellite cells are M-cadherin, the Notch co-receptor Syndecan-3, Caveolin-1, Sca-1, calcitonin receptor (CTR), Integrin α 7, the tyrosine kinase receptor c-Met, the sialomucin surface receptor CD34, VCAM-1 and NCAM-1 (Allen et al., 1995, Beauchamp et al., 2000, Fukada et al., 2007, Gnocchi et al., 2009, Irintchev et al., 1994). Some markers, like Caveolin-1 and M-cadherin are not only expressed during quiescence, but are maintained as satellite cells become activated (Gnocchi et al., 2009). Other markers are generally used in combination with other proteins because their expression is not exclusive of satellite cells. This is the case for the CD34 protein, which is also expressed by hematopoietic progenitor cells (Krause et al., 1994).

1.3.1.2 Regulation of satellite cell quiescence

1. The Notch signalling pathway

Quiescent satellite cells express high levels of components and targets of the Notch signalling pathway, including *Notch1*, *Notch2*, *Notch3*, *HeyL* and *Hesr3* (Fukada et al., 2007, Mourikis et al., 2012b), which are down-regulated when satellite cells become activated, suggesting a role for Notch signalling in the control of satellite cell quiescence (Fig.1.7) (Bjornson et al., 2012).

The Notch ligand delta-like 1 (Dll1) is expressed by myofibres and stimulates Notch activity by binding to Notch receptors, which are expressed by quiescent satellite cells (Conboy and Rando, 2002). Following ligand binding, the Notch receptor undergoes protease-mediated cleavage and releases the Notch intracellular domain (NICD), which translocate to the nucleus and interacts with recombining binding protein suppressor of hairless (Rbpj). Finally, the resulting NICD-RBPJ complex activates the transcription of Notch target genes, including *Hey* and *Hes* genes (Kopan, 2012). Notch signalling facilitates the transition of muscle progenitors into quiescence, as forced expression of the NICD in Myf5+ satellite cells at postnatal stages results in their precocious exit from the cell cycle and the return of quiescence (Mourikis et al., 2012a). Likewise, forced expression of NICD in Pax7+ satellite cells (Pax7-NICD^{OE}) promotes self-renewal and inhibits myoblast proliferation, as shown by Pax7 up-regulation and MyoD down-regulation (Wen et al., 2012). Conversely,

conditional deletion of *Rbpj* in adult satellite cells ($\text{Pax7}^{\text{CreERT2/+}}; \text{RBP-J}^{\text{flox/flox}}$) results in the loss of quiescence and spontaneous activation and differentiation of satellite cells, ultimately causing a depletion of the satellite cell pool (Bjornson et al., 2012, Mourikis et al., 2012b). *Hesr1/Hesr3* double mutant satellite cells display also an increased expression of proliferation and differentiation markers (Ki67 and MyoD) and fail to maintain quiescent satellite cells post-natally, indicating that the Notch signalling pathway is required for the generation of satellite cells and their maintenance in a quiescent state (Fukada et al., 2011).

2. Control of satellite cell quiescence by miRNAs

miRNAs are small RNA molecules that bind to specific coding mRNAs to inhibit mRNA translation or to promote mRNA degradation (Bartel, 2004). They are derived from longer hairpin-containing precursors named pri-miRNAs, which are processed in the nucleus by the RNase III Droscha. Pri-miRNAs are transferred to the cytoplasm where they undergo further processing by another RNase III enzyme, Dicer. Finally, the resulting miRNA molecules are coupled to the RNA-induced silencing complex (RISC) to regulate their targets (Han et al., 2009).

Conditional deletion of *Dicer* in satellite cells results in their spontaneous exit from quiescence and entry into the cell cycle. Consequently, muscle regeneration is severely impaired in the absence of a functional miRNA machinery (Cheung et al., 2012). Microarray analysis of quiescent versus activated satellite cells has shown that a group of miRNAs are highly expressed during quiescence and down-regulated upon satellite cell activation. Among these, miR-489 inhibits satellite cell activation and proliferation, and suppresses the *Dek* oncogene, which is strongly up-regulated during satellite cell activation and it is preferentially distributed in differentiating cells (Cheung et al., 2012). One of the mechanisms behind miRNA control of quiescence is illustrated by miR-31, which is another miRNA enriched in quiescent satellite cells and whose main target is the *Myf5* mRNA. miR-31 is associated to messenger ribonucleoprotein (mRNP) complexes, which control its localisation within the cell. When miR-31 is present, *Myf5* transcripts are sequestered into mRNP-miR-31 complexes and silenced during quiescence, and are released upon satellite cell activation, allowing their translation (Crist et al., 2012).

1.3.2 Satellite cell activation

1.3.2.1 Molecular signature of activated satellite cells

The activation of satellite cells involves their exit from quiescence and concomitant entry into the cell cycle, leading to a transition from G0 to G1 phase. G0 cells usually spend

more time to enter the S phase than G1 cells (Coller, 2007). This may result from the fact that some regulatory proteins required for the initiation of DNA replication complexes, such as the cyclin-dependent kinase 6 (Cdk6), are removed from the chromatin in quiescence cells but not in G1 cells (Madine et al., 2000). For instance, quiescent satellite cells express high levels of p27Kip, which inhibits Cdk6 and other kinases, preventing cell cycle progression from G0 to G1 and G1 to S (Toyoshima and Hunter, 1994).

Morphologically speaking, quiescent satellite cells have low cytoplasm-to-nucleus ratio and low transcriptional activity whereas activated satellite cells have a bigger size, a more expanded cytoplasm and increased transcriptional activity (Rodgers et al., 2014). This translates into the ability of most Pax7+ satellite cells to up-regulate the expression of MRFs, including Myf5 and MyoD as early as 3 hours following stimulation/injury, with particularly high levels of MyoD being expressed in cells in G1 phase (Cooper et al., 1999, Kitzmann et al., 1998, Rocheteau et al., 2012, Zammit et al., 2002). The expression of these factors is crucial for cell fate determination and for further mechanisms such as cell differentiation and self-renewal.

1.3.2.2 Signals that control satellite cell activation

Quiescent cells going into G1 phase can go back to the G0 state before they reach the restriction point (R-point) (Fig.1.5). The R-point occurs between the G1 and S phases (2 to 3 hours before the initiation of DNA synthesis), it depends on the presence of growth factors and once a cell reaches it, it becomes committed to the next phase of the cell cycle (Cheung and Rando, 2013, Pardee, 1974). Following muscle injury, mitogen factors released from damaged fibres and infiltrating cells induce quiescent satellite cells to enter the cell cycle. For instance, hepatocyte growth factor (HGF), insulin-like growth factor (IGF-1) and fibroblast growth factor (FGF2) can stimulate receptor tyrosine kinase (RTK)-mediated signalling pathways and induce satellite cell activation, probably by promoting their transition over the R-point (Fig.1.7) (Montarras et al., 2013).

One of the main signals that mediates the initial activation of satellite cells is nitric oxide (NO)-HGF signalling (Fig.1.7). Nitric oxide synthase (NOS) is normally associated to the dystrophin cytoskeleton of muscle fibres and mediates the synthesis of NO. The activity of NOS increases under the influence of shear forces generated by contraction/retraction of damaged myofibres, promoting the production of NO (Anderson, 2000). NO in turn activates matrix metalloproteinases (MMPs), which degrade proteoglycans in the ECM to release HGF (Tatsumi et al., 2002, Yamada et al., 2006). HGF then binds to the tyrosine kinase receptor c-Met, which is strongly expressed in satellite cells (Allen et al., 1995, Gonzatti-Haces et al., 1988). Thus, pharmacological inhibition of NOS or blockade of the HGF ligand using anti-HGF antibodies leads to decreased satellite cell

activation (Tatsumi et al., 2002, Yamada et al., 2006). Although the effectors acting downstream the NO-HGF cascade have yet to be defined, a recent report has found that HGF signalling lies upstream mTORC1 signalling, which controls the entry of quiescent G0 satellite cells into the GAlert state. Conditional deletion of the mTORC1 signalling inhibitor *TSC1* in satellite cells converts all quiescent satellite cells into GAlert. Conversely, conditional inactivation of the mTORC1 signalling component *Rptor* in satellite cells blocks their responsiveness to injury-induced systemic signals that leads to the transition into the GAlert state (Rodgers et al., 2014).

IGF-1 is another growth factor that can stimulate satellite cell activation. IGF-1 activates the phosphatidylinositol 3-kinase (PI3K)/AKT signalling cascade, which in turn phosphorylates the forkhead transcription factor FoxO1, causing its inactivation (Guo et al., 1999). This leads to the down-regulation of the kinase inhibitor p27Kip, which facilitates G1-S cell cycle progression (Chakravarthy et al., 2000, Machida et al., 2003). Interestingly, transcripts of the protein Igfbp6, which sequesters IGFs, are highly expressed in quiescent satellite cells, supporting the idea that IGF-1 signalling promotes satellite cell activation (Pallafacchina et al., 2010).

Another growth factor involved in satellite cell activation is FGF2, which activates MAPK signalling in satellite cells. FGF2 is associated with ECM components at the surface of muscle fibres, thus is released in response to injury (Clarke et al., 1993). Quiescent satellite cells express different FGF receptors, including FGFR1, FGFR4, Syndecan-3 and Syndecan-4 (Cornelison et al., 2001), indicating that they are responsive to FGF signalling. Exogenous administration of FGF2 in satellite cell cultures leads to an increase in ERK1/2 (Mapk3/1) signalling and in satellite cell numbers (Yablonka-Reuveni et al., 1999b). Moreover, chemical blockade of ERK1/2 pathway prevents the satellite cells transition from G1 to S phase (Jones et al., 2001). FGF2 can also stimulate the p38 α / β MAPK pathway and chemical blockade of p38 α / β MAPK decreases satellite cell proliferation due to their inability to enter the cell cycle. Interestingly, inhibition of this pathway drives satellite cells into a reversible quiescent-like state, confirming its requirement for cell cycle entry (Jones et al., 2005).

subsectionSatellite cell proliferation

1.3.2.3 Markers of satellite cell proliferation

Cell proliferation can be defined as the increase in cell number that results from cycles of cell division. Broadly speaking, activated satellite cells are proliferating cells because they have exited quiescence and have entered the cell cycle. Conversely, proliferating satellite cells are activated cells until they undergo terminal differentiation or self-renewal, returning to the G0 state. However, for the sake of simplicity, proliferating satellite cells

will be considered as those cells that have transitioned beyond the R-point and that have undergone a finite number of cell cycles.

Cycling satellite cells maintain the expression of the transcription factor Pax7 as well as Myf5 and MyoD (Fig.1.7). Furthermore, cycling satellite cells can be identified by the use of broad-spectrum proliferation markers like Ki67 or phase-specific markers like the proliferating cell nuclear antigen (PCNA), which labels cells in S phase, and the phospho-histone 3 protein (PH3), which labels cells undergoing mitosis (Madsen and Celis, 1985, Scholzen et al., 2000). Satellite cells in S phase can also be identified by the incorporation of the thymidine analogs 5-bromo-2-deoxyuridine (BrdU) or 5-ethynyl-2-deoxyuridine (EdU). More recently, the use of fluorescent ubiquitynation-based cell-cycle indicator (Fucci) system in cultured myofibres and the mVenus-p27K⁻ mice on whole muscle sections has deepened the understanding of the proliferative status of satellite cells (de Lima et al., 2014, Oki et al., 2014).

1.3.2.4 Signals that regulate satellite cell proliferation rate

As mentioned earlier, satellite cells that have exited quiescence (G0) have a prolonged G1 phase and enter the S-phase around 18h after injury *in vivo* or when plated after FACS isolation (Mourikis et al., 2012b, Rocheteau et al., 2012). Satellite cells complete their first division between 24 and 48h after stimulation *in vivo*, *in vitro* and *ex vivo*, with satellite cells expressing high levels of Pax7 (Pax7-nGFP^{Hi}) taking the longest to complete it (Rocheteau et al., 2012, Siegel et al., 2011). Subsequent satellite cell divisions occur in average every 8 to 10h (Rocheteau et al., 2012, Siegel et al., 2011).

Several signalling molecules are known to modify the rate of satellite cell proliferation, influencing the overall number of satellite cells (Fig.1.7). For instance, the canonical Wnt- β -catenin signalling pathway has been implicated in the control of satellite cell proliferation. Quiescent satellite cells express non-activated β -catenin, which becomes functional in activated satellite cells (between 24 and 48h in *ex vivo* cultured myofibres) (Otto et al., 2011). Indeed, following satellite cell activation, Wnt ligands are expressed, including Wnt1, Wnt3, Wnt4, Wnt5, Wnt6 and Wnt11, and the exogenous administration of Wnt1, Wnt3 or Wnt5 induces satellite cell proliferation, whereas Wnt4 and Wnt6 have the opposite effect (Otto et al., 2011). The mechanism responsible for this mitogenic effect appears to be linked to the translocation of active β -catenin into the nucleus and the subsequent activation of cell cycle regulators (Otto et al., 2011).

Another signalling molecule involved in satellite cell proliferation is Sonic Hedgehog (Shh). Treatment of primary myoblasts or C₂C₁₂ cells with recombinant Shh protein increases BrdU incorporation, and this effect can be reversed by cyclopamine, an inhibitor of the Shh pathway (Elia et al., 2007, Straface et al., 2009). However, the mechanism by

which Shh signalling modulate satellite cell proliferation is still poorly understood.

Bone morphogenetic proteins (BMP), which are members of the transforming growth factor-beta (TGF- β) family, have also been implicated in the control of the balance between proliferation and differentiation of satellite cells. BMP binds to BMP receptors at the cell surface, which leads to the phosphorylation of Smad proteins and the regulation of target genes (Feng and Derynck, 2005). Studies have shown that transcripts of BMP signalling components are enriched in quiescent satellite cells and that exogenous administration of the BMP signalling inhibitor Noggin to cultured myofibres results in precocious differentiation and a decrease in satellite cell numbers (Ono et al., 2011, Pallafacchina et al., 2010). The same effect is observed when BMP receptor 1, Smad5 or Smad4 are knocked down by siRNA, and is mediated by Inhibitor of differentiation (Id1), a downstream target of BMP signalling and a negative regulator of MyoD expression (Ono et al., 2011).

1.3.2.5 Specific control of satellite cell progression through the cell cycle

1. G1/S transition

Myostatin is a member of the TGF- β family and has an important regulatory role in skeletal muscles. *Myostatin*-null mice have an increased size and muscle mass due to muscle hyperplasia and hypertrophy (McPherron et al., 1997). Conversely, overexpression of Myostatin in skeletal muscles leads to loss of muscle mass and decreased myofibre size, indicating that Myostatin negatively controls muscle growth (Reisz-Porszasz et al., 2003). *Myostatin*-null mice have also a higher number of activated satellite cells and an increased number of cells in S phase compared to control satellite cells. Indeed, Myostatin inhibits the G1-S transition by up-regulating *p21* expression, which represses Cyclin E-cyclin dependent kinase 2 (*Cdk2*) complex activity (McCroskery et al., 2003). More recently, it has been shown that this mechanism is likely to be transduced via Smad3 protein (Ge et al., 2011).

2. S phase

One of the main regulators of the completion of the S phase is the Cyclin A2-Cdk2 complex, which accumulates during early S phase and drops in prometaphase (Girard et al., 1991, Morgan, 2007). The Cyclin A2-Cdk2 complex mediates the phosphorylation of the cell division control protein 6 (CDC6), which ensures that only one round of DNA replication occurs in every cycle (Bendris et al., 2011). Reports have shown that C₂C₁₂ muscle cells cultured in mitogen-rich medium can be synchronised in a reversible arrest in a quiescent-like state without differentiation (Sachidanandan et al., 2002). Under these conditions, mixed lineage leukemia 5

(MLL5), a tumour suppressor gene that encodes for a methyltransferase able to regulate gene expression, is induced (Sebastian et al., 2009). RNAi-mediated *Mll5* knock-down in C₂C₁₂ cells results in the up-regulation of both *Cyclin E* and *Cyclin A2*, which regulate the entry and exit from S-phase, respectively. Therefore, MLL5 represses Cyclin A2 to prevent transition into the S-phase and to maintain cells in a quiescent-like state (Sebastian et al., 2009). However, whether this mechanism is conserved in satellite cells *in vivo* has yet to be determined.

3. G2/M transition

Cyclin B1 is one of the main positive regulators of the G2/M transition in vertebrates. Cyclin B1 accumulates during G2 and peaks during metaphase. Cyclin B1 associates with cyclin dependent kinase 1 (Cdk1). However, the complex is maintained inactive by Wee1 kinase-mediated phosphorylation (Morgan, 2007), until its dephosphorylation mediated by Cdc25 phosphatase, which allows the cell to transit into M phase (Berry and Gould, 1996). A recent mass spectrometry-based protein analysis has also shown that the histone arginine methyltransferase Prmt5 affects the activity of satellite cells by repressing the expression of *p21*, which regulates Cyclin B1-Cdk1 negatively (Zhang et al., 2015). Consistently, conditional deletion of *Prmt5* in Pax7+ satellite cells results in impaired muscle regeneration and a drastic arrest of cell proliferation linked to the up-regulation of *p21* (Zhang et al., 2015).

1.3.3 Symmetric and asymmetric cell divisions

Activated satellite cells divide symmetrically to give rise to two identical daughter cells, or asymmetrically to generate two daughter cells that are different in size, protein profile or developmental potential (Knoblich, 2008). One of the key determinants of the type of cell division is the orientation of the division plan (and mitotic spindles) with respect to the basal lamina (basal surface) and the plasma membrane (apical surface) of the muscle fibre. Symmetric cell divisions occur mainly in a planar orientation (parallel to the fibre) and promote satellite cell expansion, whereas asymmetric cell divisions occur mainly in an apico-basal orientation (perpendicular to the fibre) and generate two daughter cells with distinct fates: the daughter cell close to the apical surface commits to the myogenic lineage and the daughter cell close to the basal lamina maintains the stem cell identity (Fig.1.6) (Wang and Rudnicki, 2012).

Lineage tracing analysis using the Myf5-Cre/Rosa26-YFP mice has shown that 10% of the total number of satellite cells never express *Myf5* (YFP-) during development. Importantly, these YFP- (Pax7+/Myf5-) cells can undergo both symmetrical cell division to generate more YFP- (Pax7+/Myf5-) daughter cells and asymmetrical cell division to

produce one YFP⁻ (Pax7⁺/Myf5⁻) and one YFP⁺ (Pax7⁺/Myf5⁺) cell (Kuang et al., 2007). Using this model, it has been observed that around 30-40% of YFP⁻ first cell divisions are symmetric, whereas the rest are asymmetric (Le Grand et al., 2009).

One characteristic of asymmetric cell division is the differential distribution of cellular components or cell fate determinants into only one of the two daughter cells. For instance, components of the Notch signalling pathway display a differential localisation in satellite cells: the Notch ligand Dll1 is expressed in Pax7⁺/Myf5⁺ cells and the Notch-3 receptor is highly expressed in Pax7⁺/Myf5⁻ cells (Kuang et al., 2007). Similarly, the Notch inhibitor Numb is asymmetrically expressed in satellite cells and cosegregate with BrdU-retaining cells, suggesting a role for this protein in the control of self-renewal (Conboy and Rando, 2002, Shinin et al., 2006). The partitioning-defective proteins (PAR) are also asymmetrically distributed in satellite cells. For instance, the PAR3-PKCl complex segregates into one daughter cell and activates p38 α / β MAPK signalling and MyoD expression, resulting in its commitment into the myogenic lineage. The other daughter cell does not activate the p38 α / β MAPK pathway and instead returns to quiescence (Troy et al., 2012). Another characteristic of asymmetric cell division is the differential segregation of old and new DNA strands, also known as non-random DNA segregation. As DNA is replicated semiconservatively, this results in chromatids containing new and old DNA strands and it has been proposed that the older DNA strand is maintained through successive asymmetric cell division in only one of the two daughter cells. Through this mechanism, stem cells ensure the protection of DNA against damage (Cairns, 2006). One way to study this phenomenon is through pulse-chase experiments to mark DNA so that slowly dividing cells (such as stem cells) would retain the label (LRC) and the progeny of myoblasts would dilute the label after random DNA segregation (non-LRC). Using this approach it has been observed that the majority of Pax7-nGFP^{Hi} satellite stem cells perform non-random DNA segregation whereas Pax7-nGFP^{Lo} perform random DNA segregation (Rocheteau et al., 2012). Importantly, old DNA strands tend to segregate with Pax7, whereas nascent DNA strands are more likely to segregate with Myogenin (Yennek et al., 2014).

In contrast, symmetric cell expansion of satellite cells are regulated by the Wnt planar cell polarity (PCP) pathway. Following muscle injury, Wnt7a is up-regulated at the time satellite cells replenish the stem cell pool (6 days post-injury), and bind to the Wnt receptor Frizzled 7 (Fzd7), which is expressed in both quiescent and activated satellite cells (Le Grand et al., 2009). Stimulation of YFP⁻ satellite cells from Myf5-Cre/Rosa26-YFP mice with Wnt7a results in a drastic increase in the proportion of symmetrical cell divisions (Pax7⁺/Myf5⁻) without affecting proliferation rate or differentiation (Le Grand et al., 2009). Wnt7a treatment promotes the symmetric distribution of the polarity effector Vangl2, and in the absence of the latter, Wnt7a can not stimulate symmetric cell

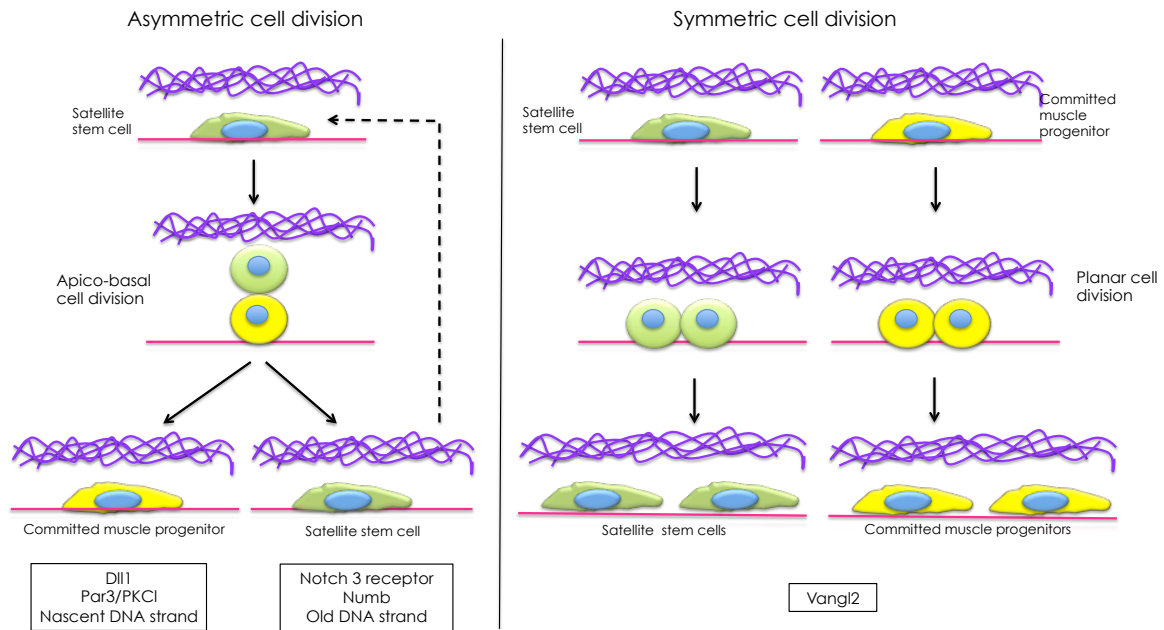


Figure 1.6: Asymmetric and symmetric satellite cell division. During asymmetric cell division, satellite stem cells (green) divide following an apico-basal orientation to give rise to one committed muscle progenitor (yellow) associated to the plasma membrane (pink line) and one satellite cell (green) located close to the basal lamina (purple mesh). On the other hand, during symmetric cell division, both satellite stem cells and committed muscle progenitors divide following a planar orientation to give rise to identical daughter cells. Adapted from Dumont et al. (2015a).

division (Le Grand et al., 2009). Consistently, Wnt7a over-expression in injured muscles results in enhanced muscle repair linked to a greater number of satellite cells, bigger fibre size and increased muscle mass (Le Grand et al., 2009).

1.3.4 Satellite cell self-renewal: how the return to quiescence is regulated?

Self-renewal is the process by which stem cells divide to generate a progeny that has the same developmental potential as the mother cell. This mechanism is essential to maintain the stem cell pool within a tissue after regeneration (Shenghui et al., 2009). The regulation of self-renewal is closely linked to the ratio of symmetric and asymmetric cell divisions, which were discussed in section 1.3.3. Indeed, asymmetric cell division generates 50% of daughter cells with a self-renewal fate, whereas symmetric cell division yields 100% of daughter cells that either self-renew or differentiate. Hence, depending on the tissue requirement and the overall environment, symmetric or asymmetric cell division will be privileged to ensure that homeostasis is preserved (Fig.1.6).

The process of self-renewal involves the exit of satellite cells from the cell cycle. This return to the quiescent state occurs when cells are in G1 phase and re-enter G0 before reaching the R-point, so they do not commit to the next round of the cell cycle. As

mentioned in section 1.3.1, the maintenance of quiescence largely depends on the expression of negative regulators of the cell cycle. For instance, p27Kip1 is required for self-renewal, as *p27*-null mice have a decreased ability to cope with repeated rounds of muscle regeneration (Chakkalakal et al., 2014). Another important regulator of satellite cell self-renewal is the negative regulator of RTK signalling, Sprouty (SPRY1). SPRY1 is highly expressed in quiescent satellite cells, is down-regulated during activation but it is re-expressed in cells returning to quiescence (Fukada et al., 2007). Conditional deletion of *Spry1* in satellite cells results in a 40% decrease in the number of Pax7+ satellite cells found at 50 days post-injury, when the satellite stem cell pool is thought to be completely replenished (Shea et al., 2010). Importantly, SPRY1 promotes self-renewal by inducing cell cycle exit via ERK signalling inhibition (Shea et al., 2010).

The satellite cell niche also plays an essential role in the maintenance of satellite cell stemness and in the control of self-renewal. Indeed, several ECM components can influence satellite cell behaviour (Bentzinger et al., 2013b, Urciuolo et al., 2013). For instance, the glycoprotein Fibronectin binds to the Syndecan-4/Fzd7 complex at the surface of satellite cells, resulting in the stimulation of Wnt7a signalling and the symmetric expansion of satellite cells (Bentzinger et al., 2013b). Also, Collagen VI (COL6A1), a major component of the ECM of skeletal muscles, has been implicated in the control of satellite cell self-renewal. *Col6a1*-null mice show a delay in muscle regeneration, accompanied by a decrease in satellite cell numbers. Furthermore, mutant mice display aberrant muscle repair following repeated muscle injury, indicating a failure to replenish the satellite cell pool after the initial round of regeneration. One mechanism by which Collagen VI may regulate the return to quiescence is an increase in muscle stiffness, which enhances the biomechanical properties of the satellite cell niche (Urciuolo et al., 2013). Consistently, satellite cells are able to self-renew *in vitro* when cultured in soft hydrogels that have similar elasticity and stiffness as myofibres (Gilbert et al., 2010). This indicates that the biophysical and mechanical characteristics of the satellite cell niche are essential cues to control satellite cell self-renewal.

1.3.5 Satellite cell differentiation

1.3.5.1 Molecular signature of satellite cell differentiation

Differentiating satellite cells are characterised by the expression of the transcription factor Myogenin, which is an important driver of differentiation (Fig.1.7). Following crush injury, *Myogenin* mRNA is detected as early as 6h post-injury, reaching the highest levels between 24 and 48h and progressively declining at 8 days post-injury (Grounds et al., 1992). *Myogenin*-deficient mice die perinatally and have loss of differentiated myofibres (Hasty et al., 1993). MRF4 is not expressed in quiescent satellite cells but is co-expressed with

MyoD and Myogenin in regenerating myofibres following muscle injury, indicating a role in terminal differentiation (Zhou and Bornemann, 2001). Both Myogenin and MRF4 induce the expression of other muscle specific differentiation markers, including creatine kinase (Ckm) and MyHC proteins (Molkentin and Olson, 1996).

Other proteins up-regulated during muscle regeneration and satellite cell differentiation are the Myocardin family of transcription factors MASTR and MRTF-A (Mokalled et al., 2012). Conditional *MASTR* removal in Pax7+ satellite cells results in an incapacity to regenerate skeletal muscles in response to injury and in low expression levels of Desmin, an intermediate filament protein essential for muscle structure (Mokalled et al., 2012). Interestingly, both MASTR and MRTF-A positively regulate MyoD expression, promoting satellite cell differentiation. Furthermore, the transcription factors MEF2A, C, and D, which belong to the family of the myocyte enhancer factor 2 (MEF2) are also required for satellite cell differentiation. These factors become up-regulated during muscle regeneration and their conditional deletion in Pax7+ satellite cells impairs the regeneration process in response to injury. More specifically, *MEF2*-deficient satellite cells do not differentiate in culture and they down-regulate muscle differentiation proteins like MRF4, Ckm, MyHC1 and MyHC4 (Liu et al., 2014).

Finally, the satellite cell markers Pax7 and Caveolin-1 become progressively down-regulated as satellite cells enter differentiation (Gnocchi et al., 2009). Indeed, Pax7 and Myogenin expression are mutually exclusive and Pax7 over-expression prevents Myogenin induction and alters muscle differentiation (Fig.1.7) (Olguin and Olwin, 2004, Zammit et al., 2006). Interestingly, Pax7 is repressed post-transcriptionally during satellite cell differentiation by microRNA-1 and microRNA-206, which regulate negatively proliferation of satellite cells while promoting their differentiation (Chen et al., 2010a).

1.3.5.2 Signals that control satellite cell differentiation

Similar to satellite cells returning to quiescence, differentiated myocytes need to exit the cell cycle (Fig.1.5). Myogenin dictates the commitment to differentiation and its expression in myoblasts is accompanied by the up-regulation of the cell cycle inhibitor p21, inducing irreversible cell cycle exit (Walsh and Perlman, 1997). The retinoblastoma protein (Rb1) is also of interest during differentiation, as is required for mitotic arrest, for maintaining the post-mitotic state and for protecting myotubes against apoptosis (Burkhart and Sage, 2008). Suppression of *Rb1* expression in primary mouse myotubes leads to cell cycle re-entry and up-regulation of the tumour suppressor p19ARF. Interestingly, inhibition of *p19ARF* alone does not have any obvious effect on differentiation but inactivation of *Rb1* and *p19ARF* together results in extensive loss of myoblast differentiation, indicating the requirement of both proteins for cell cycle arrest (Pajcini et al., 2010). More

recently, it has been reported that one of the catalytic subunits of the SWI/SNF chromatin remodelling complex, Brahma (Brm), directly binds to *Cyclin D1* (a R-point regulator) to repress its expression, leading the exit of myoblasts from the cell cycle (Albini et al., 2015).

Signals that control satellite cell differentiation include Wnt, Shh and BMP. Canonical Wnt signalling promotes satellite progression through the myogenic program. Indeed, treatment of primary myoblasts or single myofibres with Wnt3A results in an increase in the number of differentiated Desmin+ cells and the opposite effect is observed upon Wnt inhibition both *in vitro* and *in vivo* (Brack et al., 2008). Another signalling pathway that has been implicated in the control of muscle differentiation is Shh. Treatment of C₂C₁₂ cells or primary chick adult myoblasts with recombinant Shh protein results in an increase of muscle differentiation marked by the expression of MyHC. In this context, Shh mediates its signal through Akt phosphorylation, leading to the stimulation of MAPK/ERK and phosphoinositide 3-kinase (PI3K) pathways (Elia et al., 2007). Finally, consistent with the role of the BMP signalling in muscle proliferation, it has been shown that blocking BMP signalling results in increased cell differentiation and myotube formation in primary satellite cells. During muscle regeneration *in vivo*, the effect of BMP signalling inhibition on satellite cell differentiation seems to be mediated by *Chordin*, whose expression follows the onset of Myogenin expression (Friedrichs et al., 2011).

1.4 The Hedgehog (Hh) signalling pathway

1.4.1 The Hh signalling ligands and their functions

The Hedgehog (Hh) proteins are widely conserved in both invertebrates and vertebrates. The *hh* gene was initially discovered in a screen aimed at identifying genes involved in embryonic segment polarity in the fruit fly *Drosophila melanogaster* (Nüsslein-Volhard and Wieschaus, 1980). Whilst one single *hh* gene has been identified in *D. melanogaster*, in birds and mammals three *hh* homologues have been described: Sonic Hedgehog (*Shh*), Indian Hedgehog (*Ihh*) and Desert Hedgehog (*Dhh*) (Tabata et al., 1992). In contrast, in zebrafish five homologues have been identified: sonic (*shha* and *shhb*), indian (*ihha* and *ihhb*) and desert (*dhh*) (Cruz-Migoni and Borycki, 2014, Currie and Ingham, 1996, Krauss et al., 1993).

The importance of Hh genes during mammalian development has come from studies of the *Shh* gene, which is the most widely expressed member of the family. The Shh protein is involved in the control of proliferation, fate determination, patterning and survival of different tissues, including muscles, brain, neural tube, eyes, testes and gut (Chiang et al., 1996, Cruz-Migoni and Borycki, 2014, Wolff et al., 2003) In the early vertebrate

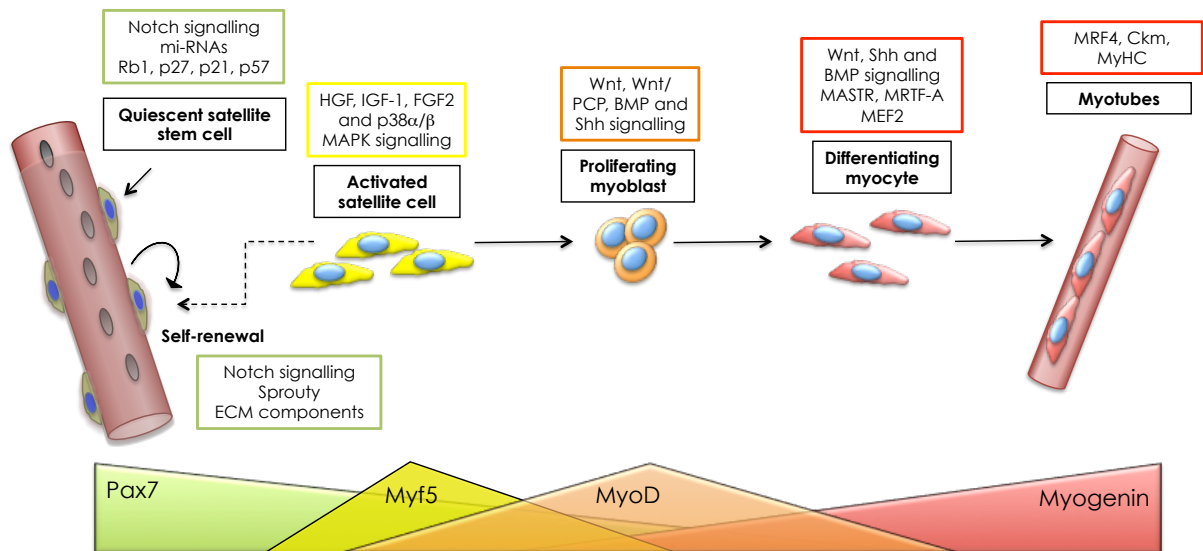


Figure 1.7: Progression of the myogenic program in satellite cells. In resting conditions, regulators like Notch signalling and mi-RNAs maintain satellite cells (Pax7+) in a reversible quiescent state. Satellite cells become activated by the influence of HGF, IGF-1 and FGF signalling pathways and up-regulate Myf5 and then MyoD expression. Satellite cells can then undergo several rounds of cell division under the control of extrinsic signals like Wnt, BMP and Shh cascades. Cycling myoblasts exit the cell cycle and become differentiating myocytes that express Myogenin and MRF4. Myocytes can then fuse to each other to form multinucleated myotubes that express Myogenin, MRF4 and MyHC. Satellite cells also self-renew to repopulate the stem cell pool and this mechanism is regulated by increased activity of Notch signalling and Sprouty.

embryo, Shh is mainly produced by the notochord, the floor plate of the neural tube and the polarising region or zone of polarising activity (ZPA) of the limb bud (Riddle et al., 1993). In these tissues Shh acts as a morphogen that establishes a gradient to dictate cell fate in a dose-dependent manner (Ericson et al., 1996). Shh is also produced during late embryonic and post-natal stages by other tissues, including Purkinje neurones in the cerebellum and progenitor cells in the retina, where it mainly acts as a mitogen (Masai et al., 2005, Wechsler-Reya and Scott, 1999). Loss of *Shh* expression in mice is embryonically lethal and results in the absence of ventral cell types in the neural tube as well as truncated fore and hindlimbs (Chiang et al., 2001, 1996), a phenotype also observed in mice carrying a germline mutation in *Smoothed* (*Smo*) (Zhang et al., 2001).

Shh and *Ihh* mRNA are both expressed in the early gut, where they have a redundant role in the control of foregut development. In contrast, *Ihh* transcripts are specifically detected in chondrocytes of early cartilage and embryonic bones (Bitgood and McMahon, 1995). Consequently, *Ihh*-null mutant mice have skeletal defects, including shortening of the bones and partial formation of the joints, resulting in perinatal death (St-Jacques et al., 1999). The *Dhh* gene has a more restricted expression domain in the Sertoli cells of the male gonad and in Schwann cells of peripheral nerves (Bitgood and McMahon, 1995) and is important in the control of spermatogenesis (Bitgood et al., 1996). Although

Dhh-null female mice have a normal development and are fertile, *Dhh*-null male mice are infertile, have small gonads and develop as phenotypic females (Bitgood et al., 1996).

1.4.2 The biosynthesis and secretion of Hedgehog proteins

Prior to their secretion, the Hh proteins undergo several post-translational modifications to generate active ligands. First, a 45kDa Hh protein precursor is generated in the endoplasmic reticulum (ER) by signal sequence cleavage, triggering its entry into the secretory pathway. This precursor is autocatalytically cleaved by its own C-terminal domain and produces a 19 kDa N-terminal fragment (N-Hh), which is responsible for all signalling activities of the protein (Bumcrot et al., 1995, Lee et al., 1994). The N-Hh product is subsequently modified by the addition of an ester-linked cholesterol at its C-terminus and a palmitic acid group at its N-terminus (Porter et al., 1996). The latter modification is thought to enhance Hh protein secretion and is carried out by *skinny hedgehog*, (*ski*) in *Drosophila* and Hh acyltransferase (HHAT) in mammals (Ingham and McMahon, 2001, Pepinsky et al., 1998). The secretion of the lipidated N-Hh to the extracellular space requires the function of the twelve-pass transmembrane protein Dispatched (Disp) and the glycoprotein Scube2 (Fig.1.8). Both proteins bind to different fragments of the cholesterol moiety of Hh and promote its secretion (Burke et al., 1999). Upon release, Hh stabilisation at the cell surface and subsequent diffusion require the participation of heparin sulphate proteoglycans (HSPGs), which are synthesized by the *tout-velu* (*ttv*) gene product in *Drosophila* and *EXT-1* in humans (Bellaiche et al., 1998). Also of interest are glypicans, which are glycosylphosphatidylinositol (GPI)-linked HSPGs associated to lipid rafts that facilitate the recruitment of Hh into clusters (Fig.1.8). In particular *division abnormally delayed* (*dally*) and *dally-like protein* (*dlp*) promote cluster formation of N-Hh into lipoproteins for long-range diffusion and also interact with *shifted* (*shf*), the fly homolog of the vertebrate Wnt inhibitory factor-1 (WIF-1), to couple N-Hh with HSPGs and regulate its distribution (Fig.1.8) (Eugster et al., 2007).

1.4.3 Different receptors mediate Hh response

Most of the knowledge on the reception of the Hh signal comes from studies in *D. melanogaster*, although the mechanism is well conserved in vertebrates. In the fruit fly, Hh response initiates with the binding of the Hh ligand to the receptors Ihog and Boi (Cdo and Boc in vertebrates) located at the plasma membrane of responding cells (Allen et al., 2011). These proteins bind to Hh via fibronectin domains and potentiate Hh association with Patched (Ptc), the main receptor of Hh proteins (Allen et al., 2011). In vertebrates, two additional proteins, the growth arrest-specific gene 1 (Gas1) and the

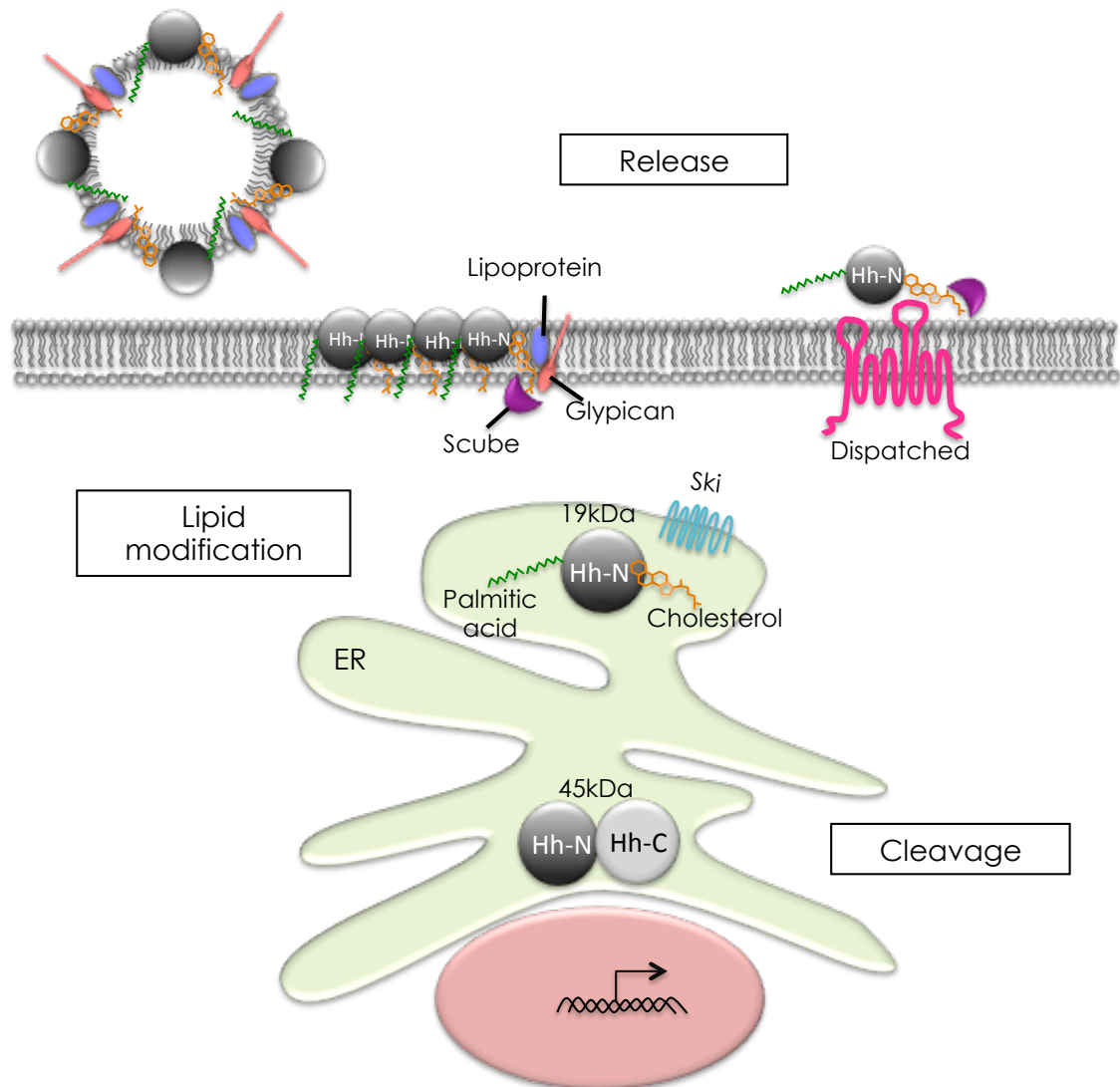


Figure 1.8: Biosynthesis and release of the Hh ligands. Hh proteins are synthesised as 45kDa precursors that are subjected to autoproteolytic cleavage to form a 19kDa product, which undergoes lipid modifications in the endoplasmic reticulum (ER). Such modifications include the addition of cholesterol to the C-terminus and the attachment of palmitic acid in the N-terminus, which is mediated by the Ski/HHAT acyltransferase. Lipidated Hh proteins are released via Dispatched and Scube, which bind to the cholesterol modification of the ligand. Additional mechanisms of Hh proteins release also include the interaction with glypicans and lipoproteins to form soluble particles that are secreted to the extracellular space. Adapted from Cruz-Migoni and Borycki (2014)[†].

[†]All images taken/adapted from this source were made by the author (Sara Cruz-Migoni) and modified for this thesis.

Hedgehog interacting protein (Hhip1) have the ability to interact with the Hh ligand to enhance or inhibit the signal, respectively (Martinelli and Fan, 2007).

Ptc is a twelve-transmembrane pass protein containing a sterol-sensing domain (SSD), which has similarities with members of the Resistance-Nodulation-Cell Division (RND) superfamily (Nakano et al., 1989, Tseng et al., 1999). The SSD domain is thought to mediate Ptc intracellular trafficking and to be involved in the regulation of the seven-transmembrane G protein-coupled receptor protein Smoothened (Smo) (Strutt et al., 2001). A single *ptc* gene has been described in *D. melanogaster*, whereas two *ptc* genes are found in vertebrates (*Ptch1* and *Ptch2*) (Carpenter et al., 1998). Whilst loss of *Ptch2* expression in mice only results in a mild phenotype, *Ptch1*-null mice die before birth and display aberrant activation of Hh targets (Goodrich et al., 1997, Ingham et al., 1991, Nieuwenhuis et al., 2006). In *Drosophila*, Ptc localises in intracellular vesicles and at the plasma membrane (Capdevila et al., 1994). In vertebrates, the dynamics of Ptch1 and Smo trafficking largely depends on their location at the primary cilium, a microtubule-associated non-motile structure that extend from the plasma membrane of most cells (Huangfu et al., 2003).

Ptc is a transcriptional target of the Hh signalling and it is generally expressed at high levels close to the source of the ligand (Nakano et al., 1989). Interestingly, studies in the wing imaginal discs of the fly larvae and the mouse spinal cord have shown that Hh-mediated *ptc* up-regulation results in a feedback mechanism, where Ptc sequesters Hh and limits its range of signalling (Chen and Struhl, 1996, Jeong and McMahon, 2005). Furthermore, mutations in Ptc phenocopy Hh over-expression and importantly, heterozygous loss-of-function mutations in the *PTCH1* human gene account for some cancers and this is linked to Hh signalling over-activation (Ingham et al., 1991). In the absence of Hh ligand, Ptc/Ptch1 is enriched at the plasma membrane (or primary cilia membrane) and maintains the pathway in an "off" state by preventing the translocation of vesicle-associated Smo into the plasma membrane (or primary cilia membrane), repressing Smo activity (Alcedo et al., 1996, Huangfu and Anderson, 2005). A single *Smo* gene has been found in both *D. melanogaster* and vertebrates and its removal in mice is embryonically lethal and results in a Hh loss-of-function phenotype (Alcedo et al., 1996, Zhang et al., 2001). The mechanisms by which Ptc/Ptch1 inhibits Smo might involve the function of the SSD of Ptc, since mutations affecting this motif abolish Ptc-induced Smo repression (Taipale et al., 2002). Because no direct interaction between Ptc/Ptch1 and Smo has been reported, it has been suggested that Ptc/Ptch1 might control the transport of another ligand, possibly a sterol-like molecule that can regulate Smo function. Consistently, Ptc is able to sequester lipophorin (Lpp) lipids and promote their accumulation at the membrane of endosomes, preventing Smo trafficking to the plasma membrane and inducing its degradation (Khaliullina et al., 2009). Binding of the Hh ligand to Ihog/Cdo, Boi/Boc

and Ptc/Ptch1 receptors triggers the internalisation of Ptc/Ptch1 in endocytic vesicles, which relieves the constitutive repression over Smo and triggers Smo accumulation at the cell surface or at the primary cilia tip via intraflagellar transport proteins (Fig.1.9) (Huangfu and Anderson, 2005).

1.4.4 The mechanism of Hh signalling transduction

Downstream of Smo, Hh signalling transduction continues with the processing of the zinc-finger transcription factor *cubitus interruptus*, (*ci*) in a microtubule-bound complex in *Drosophila* and of the three Ci homologs, the Gli proteins (Gli1, Gli2 and Gli3) in the primary cilia in vertebrates (Alexandre et al., 1996). In the fly, *ci* mutant embryos lose the transcription of Hh-responsive genes and the opposite effect is observed when Ci is over or misexpressed (Alexandre et al., 1996, Forbes et al., 1992). Similar to Ci, Gli2 and Gli3 can act as both transcriptional activators or repressors whereas Gli1 mainly acts as an activator to potentiate Gli2 activity (Aza-Blanc et al., 2000). Post-translational modifications of Ci/Gli are responsible for the activator or repressor activities; for instance full-length Ci (155kDa) functions as an activator upon Hh stimulation or it is cleaved into a repressor (75kDa) in the absence of Hh signalling (Aza-Blanc et al., 1997).

In the "off" state, the kinesin-like protein Costal-2 (Cos2) (Kif7 in vertebrates) recruits Hedgehog signalling complex (HSC) components, including Protein kinase A (PKA), Glycogen synthase kinase-3 β (Gsk3 β), Casein kinase Ia (CKIa) and the Fused (Fu) kinase (Chen et al., 1999, Jia et al., 2002, Robbins et al., 1997). These proteins cooperatively sequester Ci (or Gli2/Gli3) in a microtubule-bound (or primary cilium's basal body-bound) complex and mediate the sequential phosphorylation of full-length Ci/Gli2/Gli3. Ci is then targeted for ubiquitination by Slimb, leading to its degradation by the proteasome (Jiang and Struhl, 1998). Upon Hh signalling activation, Smo is phosphorylated successively by HSC kinases, including PKA, CKIa, CK2 and the G-protein coupled receptor kinase 2 (Gprk2) (Chen et al., 2010b). This stabilises Smo and leads to its accumulation at the cell surface (or at tip of the primary cilia), where it associates with the HSC via Cos2/Kif7 and undergoes Fu-mediated phosphorylation (Jia et al., 2003). This in turn induces Fu-dependent phosphorylation of Suppressor of Fused (SuFu), which results in the release of full-length Ci/Gli from the HSC and its translocation into the nucleus to activate Hh target genes (Fig.1.9) (Aza-Blanc and Kornberg, 1999).

Defects in primary cilia biogenesis or activity phenocopy the loss of Hh activity or result in defective transduction of the Hh signal (Murdoch and Copp, 2010). Consistently, it has been shown that Gli regulation in vertebrates requires the primary cilia (Huangfu et al., 2003). Indeed, the processing of the Gli proteins creates a balance between activators and repressors, which is important for the optimal function of the pathway in

different contexts. Genetic analysis in cultured cells have shown that both Gli2 and Gli3 have a C-terminal activator domain and a N-terminal repressor domain, whereas Gli1 only has the activation domain (Sasaki et al., 1999). *Gli1* is a transcriptional target of the Hh signalling and this is mediated by the Gli2 activator, which is able to bind to the *Gli1* promoter and in some cases also to its own promoter (Hu et al., 2006, Lee et al., 1997). Therefore, Gli1 is not the initial transducer of the Hh signal, but instead potentiates Gli2-mediated activation (Bai et al., 2002). Accordingly, *Gli1^{zfd}* mutant mice (lacking the zinc finger domain) are viable and only show a phenotype when the *Gli2* allele is also mutated (Park et al., 2000). Although known as bipotential transcription factors, Gli2 predominantly acts as an activator and Gli3 as a repressor (i Altaba, 1998, Litingtung and Chiang, 2000). *Gli2^{zfd}* mutant mice display a phenotype similar to *Shh* mutants, with numerous neural and skeletal defects (Mo et al., 1997). *Gli3* mutant mice also have neural defects and display polydactyly (Hui and Joyner, 1993). *Gli2/Gli3* double mutants have a more severe phenotype than either single mutant, indicating that these transcription factors have some non-overlapping functions (Motoyama et al., 1998).

1.4.5 Hh proteins can act as morphogens and mitogens in different contexts

The members of the Hh protein family have largely been known to function as morphogens. These proteins act at a distance (short or long) from their source of synthesis and diffuse to establish a gradient of activity across a tissue. This results in cells being exposed to different concentrations of the proteins, a mechanism that can dictate their fate. In vertebrates, examples of the long range morphogen activity of the Hh signalling have been observed in the patterning of the spinal cord and the limb bud. In the spinal cord, Shh secreted from the notochord and the neural tube establishes a gradient along the dorso-ventral (D-V) axis, with high concentrations of Shh in the most ventral part and low concentrations at the centre (Ribes and Briscoe, 2009). Therefore, progenitors are exposed to different levels of Shh and, as a consequence, to different activities of the Gli transcription factors. In the limb bud, Shh produced in the ZPA (posterior) creates a gradient along the antero-posterior (A-P) axis (Riddle et al., 1993, Yang et al., 1997). This gradient symmetrically mirrors a Gli3R gradient, which contributes to the specification of digit identity. Therefore, the most posterior digits are exposed to the highest levels of Shh (and to Gli2 and Gli3 positive activity) whereas the most anterior digits are exposed to lower levels of Shh (and to Gli3 repressor activity) (Bowers et al., 2012).

On the other hand, Hh proteins can also act as mitogens and control cell proliferation by affecting cell cycle dynamics. In vertebrates, some of the most representative tissues where Shh functions as a mitogen are the post-natal cerebellum and retina. For instance,

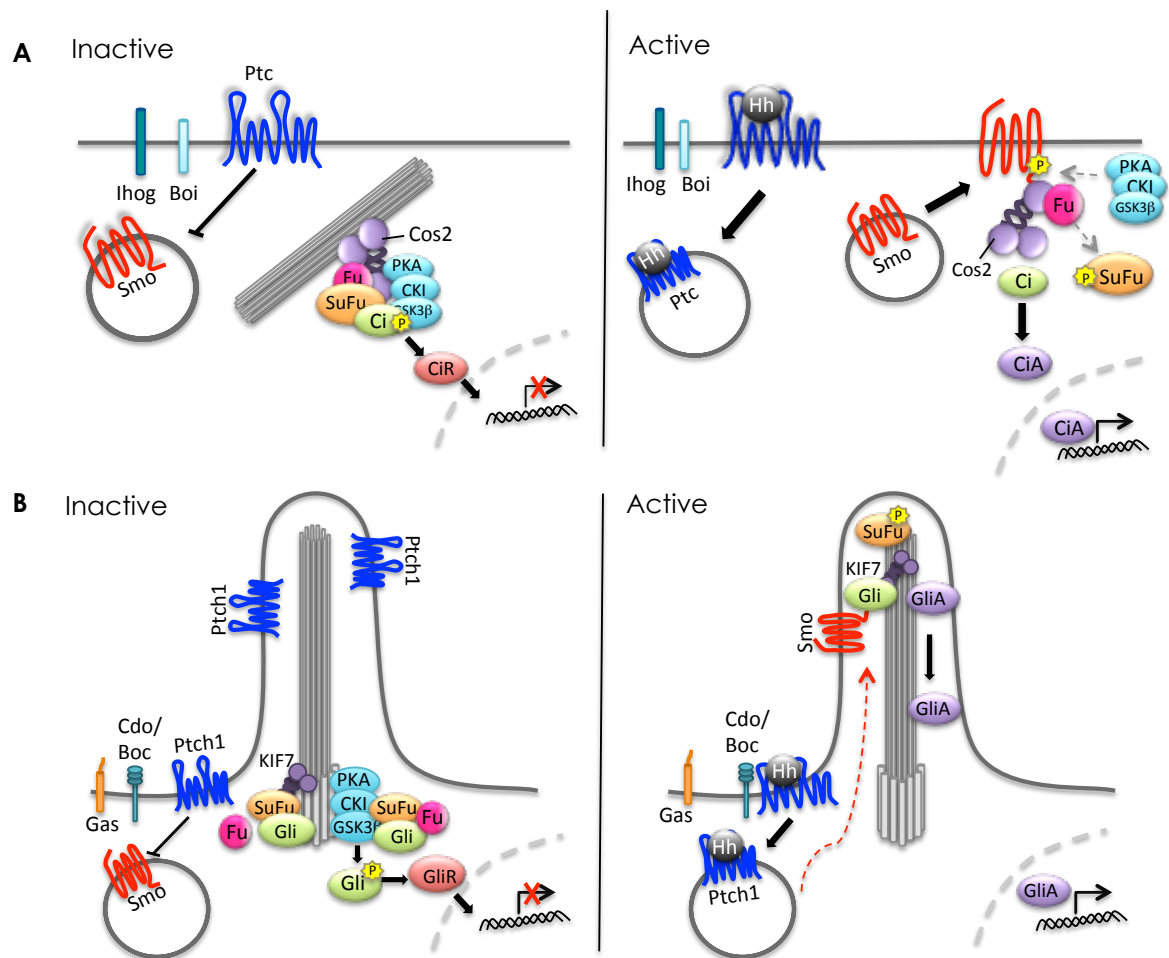


Figure 1.9: Transduction of the Hh signalling pathway. A. In *D. melanogaster*, the receptors Ihog and Boi cooperatively promote the binding of the Hh protein to Ptc. In the absence of ligand (inactive), Ptc constitutively represses the translocation of vesicle-associated Smo and promotes its degradation. As a consequence, the HSC complex (PKa, CKIa, GSK3 β , Fu and Ci) becomes associated to microtubules, where the HSC kinases sequentially phosphorylate Ci to be processed into a repressor form (CiR). Binding of the Hh ligand (active) relieves Ptc-mediated Smo repression, allowing its translocation to the plasma membrane and its subsequent phosphorylation by PKA, CKIa and Gprk2. This leads to the phosphorylation of Cos2 and SuFu by Fu, which results in the dissociation of the HSC and the release of the activator form of Ci (CiA). B. In vertebrates, the receptors Cdo, Boc and Gas1 promote the binding of the Hh ligand to Ptch1. In the absence of Hh (inactive), Ptch1 accumulates in and at the base of the primary cilia and prevents the translocation of Smo. Consequently, Kif7 accumulates at the base of the cilia and promotes the recruitment of HSC kinases, resulting in the phosphorylation of Gli2 and Gli3 and their cleavage into repressors (GliR). Binding of the Hh ligand (active) to Ptch1 promotes its release from the primary cilia, allowing Smo translocation into the organelle. Smo and SuFu phosphorylation by HSC kinases induces the dissociation of full-length Gli activators (GliA) from the HSC complex to travel to the nucleus and positively regulate Hh target genes. Taken from Cruz-Migoni and Borycki (2014).

in the cerebellum, SHH is secreted by Purkinje neurons and control the proliferation of cerebellar granular neural precursors by inducing the expression of type D Cyclins, which control the R-point transition (Kenney et al., 2004). Similarly, Shh secreted by a still undefined source induces the proliferation of retinal progenitor cells by controlling *Cyclin D1* expression during early retinal development (Locker et al., 2006, Wall et al., 2009). However, during late retinal development, Shh also controls the expression of *Cyclin B1* and the *cell division cycle 25 homolog C (Cdc25c)*, which are positive regulators of the G2-M phase transition (Locker et al., 2006).

It is important to bear in mind that during development, progenitor cells can proliferate and commit to a particular lineage synchronously and therefore the morphogen and mitogen activities of Hh proteins can be coupled. This is the case of the limb bud, where Shh acts as a morphogen to establish digit identity but also as a mitogen to control tissue growth by the regulation of *Cyclin D1* (Towers et al., 2008).

1.5 Shh signalling orchestrates embryonic myogenesis

1.5.1 Shh induces epaxial and hypaxial muscle cell fate specification

The epaxial and hypaxial domains of the myotome are defined based on the innervation of the different muscles derived from these regions: epaxial muscles include the deep muscles of the back whereas hypaxial muscles are the muscles of the body wall and limbs (Cheng et al., 2004, Christ and Brand-Saberi, 2002). The transcription factor Pax3 labels all trunk muscle progenitor cells (Goulding et al., 1994). Myogenic differentiation of both hypaxial and epaxial precursor cells is a highly dynamic regulated process where MRFs orchestrate the determination and terminal differentiation of myoblast into functional myofibres (Berkes and Tapscott, 2005, Pownall et al., 2002).

Different signalling pathways control the induction of MRFs expression and embryonic skeletal muscle development. These signalling molecules are produced by tissues surrounding the paraxial mesoderm. For instance, epaxial precursor cells specification and determination depends on signals from the neural tube and the notochord, while hypaxial myogenesis requires signals coming from the surface ectoderm and the lateral plate mesoderm (Bryson-Richardson and Currie, 2008, Buckingham, 2001). Among the signals known to direct myogenesis is Shh signalling, which along with BMP and Wnt, orchestrates the precise spatio-temporal expression of MRFs leading to muscle formation.

During vertebrate embryogenesis, the Shh ligand is produced by cells in the notochord

and the floor plate of the neural tube and this signal is an essential driver of epaxial myogenesis. For instance, studies in the chick embryo showed that Shh and Wnt proteins were capable of inducing myogenesis *in vitro*, as culture of presegmental plate mesoderm explants with both Shh and Wnt family members was sufficient to induce the expression of muscle-specific markers such as MyoD and MYHC (Münsterberg et al., 1995). Additionally, bead implantation assays showed that recombinant Shh was sufficient to activate MyoD expression in the dorsal somite, mimicking the function of the notochord (Borycki et al., 1998). Moreover, knocking down of *Shh* using antisense oligonucleotides showed a significant inhibition of *myoD* and *myf5* activation in the anterior somites of the quail embryo (Borycki et al., 1998). Further studies in the mouse embryo have shown that SHH is required for Myf5 activation in epaxial muscle progenitor cells (Fig.1.10) (Borycki et al., 1999b). More specifically, SHH controls directly the transcription of Myf5 in these cells through the binding of GLI2/GLI3 to the epaxial enhancer of Myf5 (Gustafsson et al., 2002, McDermott et al., 2005).

Shh transcripts are also detected in the posterior mesenchyme of emerging limb buds, in the so-called zone of polarising activity (ZPA) (Riddle et al., 1993). *Shh*-null mutant mice display reduced limb muscle formation (Kruger et al., 2001). Accordingly, gain-of-function experiments have shown that addition of Shh-coated beads or grafting of Shh-expressing cells in the chick limb bud (HH-20-24) causes the expansion of Pax3 and MyoD expression, and this effect is accompanied by muscle hypertrophy (Duprez et al., 1998, Johnson and Tabin, 1997). The effects of Shh on myogenic progenitor cells (MPCs) remains controversial and has been reported to promote proliferation (Duprez et al., 1998), survival (Kruger et al., 2001) or repress terminal differentiation (Bren-Mattison and Olwin, 2002). However, the specific deletion of *Smo* in Pax3+ cells using Pax3^{Cre};Smo^{flox/flox} mice showed a delay in the initiation of *Myf5* and *MyoD* expressions and a drastic decrease in the number of Pax3+ and Myf5+ cells in ventral limbs without affecting cell proliferation or survival (Anderson et al., 2012, Hu et al., 2012). Further analyses showed that, similar to epaxial MPCs, SHH signalling directly controls *Myf5* expression in ventral limb MPCs through the interaction of the Gli proteins with the *Myf5* enhancer (Anderson et al., 2012) and controls the distal migration of limb MPCs to the muscle of the paw (Hu et al., 2012).

1.5.2 Shh controls myotomal basal membrane assembly

During embryonic development, MPCs are in close contact with ECM components to support their proliferation, migration and differentiation. The myotomal basement membrane is a specialised ECM made up of laminins (mainly Laminin-111 and Laminin-5111), type IV collagen, nidogen and proteoglycans and it is the first basement membrane found in

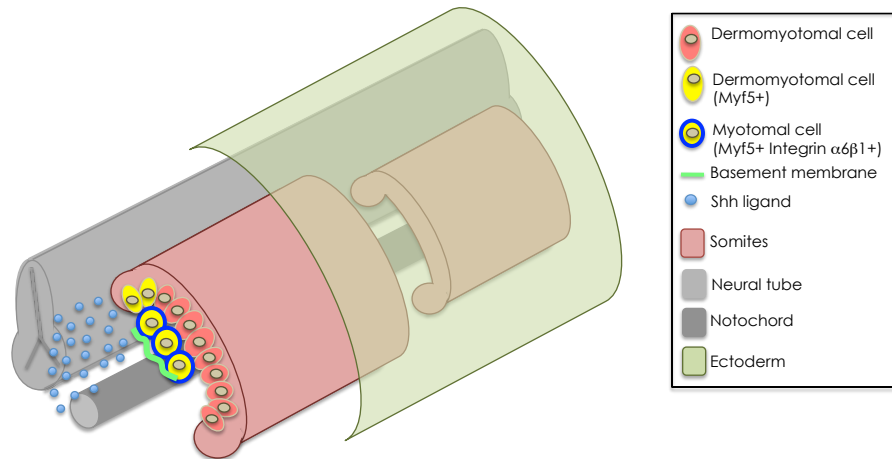


Figure 1.10: Different roles of Shh signalling in embryonic myogenesis. The first skeletal MPCs to form during embryogenesis delaminate from the dorsal part the dermomyotome (red cells) to incorporate into the myotome (yellow cells). The Shh ligand (blue dots) secreted from the neural tube and the notochord is required for *Myf5* activation in the dermomyotome. *Myf5*+ cells up-regulate the expression of the Laminin receptor Integrin $\alpha6\beta1$ (dark blue), which allows the incorporation of Laminin-111 and Laminin-511 and the assembly of the basement membrane. Adapted from Anderson et al. (2009).

embryogenesis (Tosney et al., 1994). As *Myf5*-expressing progenitor cells translocate into the myotome, they up-regulate the expression of the Laminin receptors Integrin $\alpha6\beta1$ and Dystroglycan, leading to the onset of myotomal basal membrane assembly, separating the myotome from the sclerotome (Anderson et al., 2007, Bajanca et al., 2006). Importantly, blockade of the Laminin-Integrin interaction alters the structure of the basal membrane, leading to aberrant differentiation of MPCs (Bajanca et al., 2006). Shh signalling pathway plays a role in the assembly of the myotomal membrane by controlling *Lama1* expression, which encodes one of the subunits of the basement membrane protein Laminin-111, essential for the assembly of the myotomal membrane (Anderson et al., 2009). Therefore, the Shh signalling pathway is not only required for cell fate specification during embryonic myogenesis, but it also important for the deposition of ECM components in the muscle-associated basement membrane myotome, which in turn regulates MPC behaviour (Fig.1.10).

1.5.3 Shh signalling regulates myofibre specificity in zebrafish

Muscle fibre specification is a major event during myogenesis occurring in foetal and postnatal development in vertebrates. In general, the identity of myofibres is dictated by the expression pattern of different MyHC isoforms and by innervation and is biologically relevant as the content in slow and fast fibres in a muscle determines its contractile and metabolic properties (see section 1.1.2).

In the zebrafish embryo, fibre specificity is determined during embryogenesis. Slow

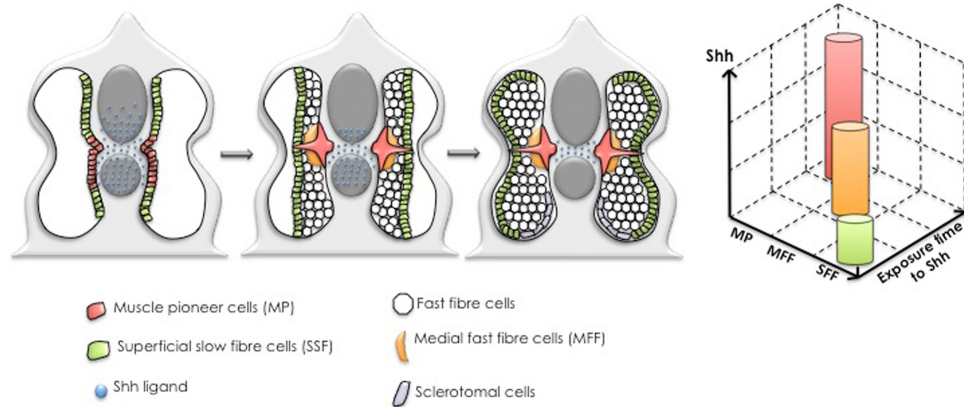


Figure 1.11: Myofibre type specification depends on the concentration and timing of Shh exposure. Muscle precursor cells (MP) and superficial slow fibre cells (SSF) arise from adaxial cells adjacent to the notochord. Unlike MP, SSF need to migrate to the surface of the somite to differentiate. During migration, medial fast fibre (MFF) and fast muscle cells are also specified. Shh ligand is secreted by the notochord is required for MP specification by high levels of Shh compared to MFFs and SSFs. MPs require longer exposure times to Shh signalling than MFFs and SSFs, whereas fast fibre formation does not depend on Shh signalling. Adapted from Cruz-Migoni and Borycki (2014).

muscle fibres are derived from adaxial cells, mesodermal cells situated at either sides of the notochord that give rise to two different cell populations: muscle pioneer (MP) cells that generate from the myoseptum and superficial slow fibres (SSFs), which are generated from medial cells that migrate to form a layer of slow fibres at the surface of the myotome (Wolff et al., 2003). Finally, the medial fast fibres (MFFs) expressing fast MyHC isoforms, are the last to form and develop from somitic, non-adaxial cells (Roy et al., 2001, Wolff et al., 2003). The Hh ligand secreted from the fish notochord controls the formation of slow muscle. Treatment of zebrafish embryos with increasing concentrations of the Smo inhibitor cyclopamine led to the progressive loss of MPs, MFFs and SSFs; therefore, MPs require the greatest concentrations of Shh ligand for their specification compared to MFFs and SSFs. Importantly, Hh-mediated myofibre specification occurred in a time-dependent manner, where MP and MFFs require longer exposure to Shh ligand than SSTs (Wolff et al., 2003). This demonstrates that the specification of the muscle lineage by Hh signalling depends on both the concentration and the time of exposure to the signal (Fig.1.11) (Wolff et al., 2003). How does Hh signalling mediate slow myofibre lineage specificity? Hh signalling activates Prdm1/Blimp1 in adaxial cells, which negatively regulates Sox6 expression and results in the repression of fast myofibre specification (Baxendale et al., 2004, Wang et al., 2011).

1.6 The Shh signalling pathway in adult skeletal muscles

1.6.1 Shh signalling activity is recapitulated during adult myogenesis

Because of its essential and multiple functions in embryonic muscle development, the role of the Shh signalling pathway in adult myogenesis, and more specifically in satellite cells has been explored in vertebrate systems. Some studies have examined the effect of Shh and the Smo inhibitor, cyclopamine, on cultures of the mouse myogenic C₂C₁₂ cell line (Elia et al., 2007, Koleva et al., 2005, Li et al., 2004, Madhala-Levy et al., 2012, Straface et al., 2009) or on primary cultures of adult myoblasts from chick, mice and frogs (Elia et al., 2007, Koleva et al., 2005, Yamane et al., 2011). Additionally, one study has explored the role of Shh in satellite cells *in vivo* by using a transgenic mice strain that express the reporter *LacZ* under the control of the *Ptch1* promoter (Straface et al., 2009).

Most reports have shown that both quiescent satellite cells and normal skeletal muscles do not express Shh or any of its signalling components (Elia et al., 2007, Koleva et al., 2005, Straface et al., 2009). However, up-regulation of *Shh*, *Ptch1* and *Gli1* mRNA as well as the Gli3 protein has been observed in regenerating skeletal muscles following injury such as crush, cardiotoxin (CTX) injection and ischemia (Piccioni et al., 2014b, Pola et al., 2003, Renault et al., 2013a, Straface et al., 2009). Moreover, C₂C₁₂ cells and primary myoblasts up-regulate the Shh target genes *Ptch1* and *Gli1* following ligand-triggered stimulation or induced differentiation (Elia et al., 2007, Fu et al., 2014, Koleva et al., 2005, Li et al., 2004). This suggests that although no formal demonstration has been reported yet, satellite cells may become responsive to Shh signals during muscle regeneration. In the embryo, Shh functions as a paracrine factor and there is no evidence of autocrine mechanism. In the adult muscle, the source of Shh remains elusive, although it has been suggested that both *Ptch1* and Shh proteins are expressed by interstitial mesenchymal fibroblasts (Pola et al., 2003) or by Pax7-expressing satellite cells (Elia et al., 2007), suggesting an autocrine mode of action.

1.6.2 Pleiotropic effects of Shh signalling on adult muscle progenitors

The role of Shh in adult muscles is also controversial. Studies using C₂C₁₂ cells or primary myoblasts support the idea that Shh promotes proliferation, as shown by increase in thymidine and BrdU incorporation upon Shh administration (Elia et al., 2007, Koleva

et al., 2005, Straface et al., 2009). Other studies have reported that Shh induces terminal differentiation, as the expression of myogenic proteins such as Myf5, MyoD and MYHC increases in response to Shh (Elia et al., 2007, Koleva et al., 2005, Li et al., 2004, Straface et al., 2009, Yamane et al., 2011) an effect that can be blocked by the addition of cyclopamine (Straface et al., 2009). However, one report claims that Shh maintains C₂C₁₂ myoblasts in an undifferentiated state (Koleva et al., 2005). Additional roles of Shh have been reported, including the promotion of angiogenesis (Pola et al., 2003, Straface et al., 2009), inhibition of apoptosis (Koleva et al., 2005) and activation of the MAPK/ERK and PI3K/AKT pathways (Elia et al., 2007, Madhala-Levy et al., 2012). Thus, although Shh signalling appears to act on adult muscle progenitor cells, its role and the mechanisms involved have not been clearly determined yet. One major caveat in the studies carried out previously is the absence of focus on satellite cells, leading to inappropriate interpretations.

1.6.3 Shh as a therapeutic for muscle repair

Few studies have explored the effect of Shh signalling *in vivo* in models of muscle regeneration. However, the systemic injection of cyclopamine in CTX-injured mice results in a decrease in the levels of VEGF and stromal-derived factor (SDF)-1alpha, which promotes angiogenesis and impairs muscle regeneration (Straface et al., 2009). In another study, a targeted knockout model of Gli3 (HSACre^{ERT2}; Gli3^{flox/flox}) reported that Gli3 deletion in post-mitotic skeletal muscles (using human α -skeletal actin promoter, which is active in the myofibre but not in satellite cells) delays ischemia-induced myogenesis and impairs angiogenesis (Renault et al., 2013b). Finally, another study using Smo haploinsufficient mice has demonstrated that loss of a single copy of the Smo receptor alters muscle repair (Renault et al., 2013a). On the other hand, two reports have demonstrated that intramuscular injection of a plasmid encoding human SHH (phShh) (Kusano et al., 2005) in injured and dystrophic muscles results in a reduction of fibrosis, increased number of activated satellite cells, increased myofibre size and angiogenesis, and an overall improvement of the muscle repair (Piccioni et al., 2014a,b). These studies suggest a role for the Shh signalling pathway in adult muscle regeneration. However, the effects observed following Shh therapy are diverse and systemic and the mechanism underlying them remains unknown.

1.7 Conclusions

Satellite cells are muscle specific stem cells responsible for muscle growth and regeneration. They are found in a quiescent state in homeostatic conditions but become activated,

re-enter the cell cycle, proliferate and exit the cell cycle to differentiate or self-renew in response to muscle injury. These events are tightly regulated by intrinsic and extrinsic mechanisms to ensure that sufficient differentiating progeny is generated and that the satellite stem cell pool is replenished. One of the extrinsic signals that has been implicated in the control of satellite cell behaviour is the Shh signalling pathway. This pathway is one of the key modulators of tissue patterning, cell fate determination, cell survival and proliferation in both the embryo and the adult. Shh signalling controls skeletal myogenesis in the embryo by activating muscle-specific transcription factors and genes encoding basement membrane proteins (Anderson et al., 2009, 2012, Borycki et al., 1999b) In the adult, the Shh pathway components are up-regulated in skeletal muscles after injury, and treatment of muscle cell lines or primary myoblasts with Shh has multiple effects, from enhanced cell proliferation, increased differentiation and improved cell survival (Elia et al., 2007, Koleva et al., 2005, Straface et al., 2009). Systemic injections of cyclopamine in muscle-injured mice reduces the efficiency of muscle regeneration (Straface et al., 2009). Conversely, injection of a plasmid encoding human Shh in injured and dystrophic mouse muscles can alleviate the dystrophic phenotype to some extent and improve the regeneration process (Piccioni et al., 2014a,b). While these findings suggest a role for Shh signalling in adult myogenesis, fundamental questions about the role of the Shh pathway on satellite cells remain unanswered, and the molecular mechanisms of Shh-mediated effects have not been described yet.

1.8 Hypothesis

I hypothesised that the target of Shh-mediated effects in adult muscles were satellite cells and that Shh signalling controls satellite cell activity function in mammalian adult muscles.

1.9 Aims of the thesis

To test the hypotheses of this project, the aims were:

1. To investigate the expression of Shh signalling components during satellite cell activation *ex vivo* and during muscle regeneration *in vivo*.
2. To determine the effect of Shh signalling blockade and stimulation on satellite cells.
3. To conditionally inactivate Smo expression in Pax7-expressing satellite cells to assess the requirements of Shh signalling during muscle regeneration *in vivo*.

The requirement of the Shh signalling pathway in the specification of mouse embryonic muscle progenitors and the growing evidence for its role in adult muscles makes Shh a potential candidate for muscle regeneration. Unravelling the role of Shh signalling in satellite cells and adult myogenesis will improve our understanding of this process and may yield to novel therapeutic strategies for the treatment of muscle injuries and disorders.

MATERIAL AND METHODS

2.1 Mouse models used

2.1.1 C57BL/6 mice

6 to 8 week-old adult mice were maintained in accordance with the UK Home Office regulation and the UK Animal Act of 1986 (ASPA) under a UK Home Office licence. All mouse lines were kept on a C57BL/6 background, referred also as wild-type (WT) mice. Animal care and husbandry were carried out at Biological Services at The University of Sheffield.

2.1.2 GBS-GFP mice

The Gli response Tg:GBS-GFP mouse line was generated as described (Balaskas et al., 2012). Briefly, eight fragments of a FoxA2 enhancer, which contains a Gli binding site, were cloned upstream the *hsp68* promoter to drive the expression of *eGFP*. Mice were kindly provided by James Briscoe at the National Institute of Medical Research (NIMR), London.

2.1.3 Pax7^{CreERT2}-Smo^{flox/flox} mice

Smo^{flox/flox};Pax7^{CreERT2/+} mice, referred here as Smo^{CKO}, were generated by crossing Smo^{flox/+}; Pax7^{CreERT2/+} mice (Lepper et al., 2009) with Smo^{flox/flox} mice (Long et al., 2001). Control animals used were Smo^{flox/+} and Pax7^{CreERT2/+} mice.

2.1.3.1 Induction of Cre-mediated recombination

Tamoxifen (TM, Sigma-Aldrich) (10mg/ml diluted in corn oil; Sigma-Aldrich) was administered in mice by intraperitoneal (IP) injections at a dose of 3mg/40g of body weight daily for 4 days before injury. Subsequently, mice were fed with Tamoxifen chow (approximately 40 mg/kg/day; Harlan Laboratories) until sacrifice.

2.1.4 Pax7GFP mice

The Tg:Pax7-GFP mouse line was generated as described (Sambasivan et al., 2009). These mice carry a BAC transgene containing approximately 200 kbp of mouse genomic DNA that includes the locus encoding *Pax7*, which drives the expression of a nuclear localised EGFP (nGFP). This construct recapitulates the endogenous expression of Pax7 in both embryo and adult mice (Sambasivan et al., 2009).

2.1.5 Fucci2 mice

The fluorescent ubiquitination-based cell cycle indicator (Fucci2) mice have been described elsewhere (Abe et al., 2013). These mice carry a single transgene, in which the *Rosa26* promoter drives the expression of *mCherry-hCdt1* and *mVenus-hGem*. *mCherry-hCdt1* consists of the fluorescent reporter mCherry fused to the ubiquitylation domain of the Cdt1 protein, which accumulates in the cell nucleus during G0/G1. *mVenus-hGem* consists of the fluorescent protein mVenus fused to the ubiquitylation domain of the Geminin protein, which accumulates in the cell nucleus during S, G2 and M phases.

2.1.6 Genotyping

Mice were ear-clipped to provide tissue samples for genotyping. The clips were digested in 10mM NaOH and boiled at 95°C for 30 minutes. Samples were neutralised with 1M Tris (pH 8.0). Genomic DNA was precipitated with ammonium acetate and ethanol before gene amplification (see section 2.8.3).

2.2 Single myofibre culture system

2.2.1 *Extensor digitorum longus* (EDL) and *Tibialis anterior* (TA) muscle harvesting

EDL and TA muscles were dissected out from 6 to 8 week-old mouse hindlimbs as follows. First, mice were culled by cervical dislocation and one of the hindlimbs was cleared out

of hair using a scalpel and 70% ethanol. When the skin was visible, toothed forceps were used to tear the skin and peel it off to expose the muscles. Mice were then pinned down on a polystyrene foam board with needles and observed under a stereo microscope. Next, the superficial connective tissue covering the TA muscle was carefully removed using forceps. Then, the excess of skin from the paw was removed to exposed one TA and four EDL distal tendons. All tendons were cut carefully using springbow dissecting scissors and they were looped out from the paw at the level of the ankle. Next, the EDL proximal tendon was visualised on the external side of the knee and cut off with scissors. The TA muscle was pulled away from the limb by grabbing it from the distal tendon and cutting it off at its proximal end, as close to the bone as possible. The EDL muscle, which is located beneath the TA muscle, was gently removed by holding it from its distal tendon. Dissected TA muscles were fixed for 1 hour (h) at 4°C in 2% paraformaldehyde (PFA, Sigma-Aldrich) with 0.25% Triton 100-X (Sigma-Aldrich) in PBS. Dissected EDL muscles were placed in collagenase solution for muscle fibre isolation.

2.2.2 Isolation of single EDL muscle fibres

EDL muscles were digested with Collagenase Type I (2 mg/ml in Dulbecco's Modified Eagle's medium (DMEM) supplemented with Glutamax; Sigma-Aldrich) at 37°C for 80 minutes. Meanwhile, three 60mm Petri dishes (numbered 1 to 3) were coated with 5% sterile bovine serum albumin (BSA; Sigma-Aldrich) in PBS and prepared with 5ml of isolation medium (DMEM+Glutamax; Life Technologies and 1% Penicillin-Streptomycin-Fungizone (PSF); Sigma-Aldrich) and kept at 37°C. Single muscle fibres were obtained from muscles under the dissection microscope using two heat-polished Pasteur pipettes pre-coated with BSA as follows: a digested EDL muscle was transferred with a large bore Pasteur pipette to Petri dish number 1 and gently pipetting was applied to flush the muscle with the medium and release fibres. Individual myofibres were then transferred to dish number 2 and then to dish number 3 using the small bore Pasteur pipette to wash off non-muscle cells. This procedure was repeated several times to get about 180 fibres from one EDL muscle. Individual muscle fibres were immediately fixed in 4% PFA in PBS or cultured for further analysis.

2.2.3 Culture of single EDL muscle fibres

60mm petri dished were coated with 5% sterile BSA in PBS and prepared with 5ml of complete medium (DMEM+Glutamax,10% horse serum; GIBCO/Invitrogen, 0.5% chick embryo extract; Seralab, and 1% PSF) and kept at 37°C until use. 25 to 30 individual muscle fibres were transferred into a dish with complete medium and incubated at 37°C and 5% CO₂. Fibres were collected at the indicated time.

2.2.3.1 Use of Shh signalling pathway agonist and antagonists

Myofibre and primary cultures were incubated with either 100nM of Smoothened Agonist (SAG, Millipore) in dimethyl sulfoxide (DMSO, Sigma-Aldrich), 4 μ M of Gli Antagonist (GANT61, Tocris Bioscience) in DMSO or 5 μ M of Cyclopamine in ethanol (Calbiochem) for the indicated time points. Optimal concentrations were determined by treating floating myofibres and C₂C₁₂ myoblasts with different concentrations and by assessing *Gli1* expression levels by RT-PCR.

2.2.3.2 EdU assay

Satellite cells in S-phase of the cell cycle were detected using the Click-iT EdU assay (Invitrogen) following the manufacturer instructions. Briefly, myofibre cultures were incubated with 10 μ M EdU for 1h at 37°C prior to their harvest and subsequently fixed in 3.7% formaldehyde for 10 minutes. Fibres were washed three times with 3% BSA in PBS and permeabilized with 0.5% Triton 100-X in PBS for 15 minutes and then washed again twice with 3% BSA in PBS. Fibres were incubated with EdU reaction mix for 30 minutes at room temperature (RT) in the dark. Next, fibres were washed with 3% BSA in PBS and blocked with 1% goat serum in PBS for 30 minutes at RT. Immunofluorescence staining was then performed as described below.

2.3 Immunofluorescence of single muscle fibres

Individual muscle fibres were collected in a crystal clear eppendorf tube and fixed in 4% PFA in PBS for 8 minutes and washed three times with PBS. Fixed myofibres were permeabilized with 0.5% Triton 100-X in PBS for 8 minutes, washed three times with PBS and blocked for 30 minutes at RT in 20% horse serum in PBS. Fibres were then incubated with primary antibodies diluted in PBS overnight at 4°C with agitation. Next day, fibres were washed 3 times with 0.025% Tween 20 (Sigma-Aldrich) in PBS (PBST) and incubated with secondary antibodies diluted in PBS for 1h at RT with agitation. Single fibres were washed 3 times with PBST and mounted on microscope slides in Vectashield with DAPI (Vector Laboratories) for imaging. Primary and secondary antibodies used in this study are shown in tables 2.1 and 2.2.

Table 2.1: Primary antibodies

Name	Host	Reference	Supplier	Dilution
Pax7	Mouse monoclonal	Pax7 supernatant	DSHB	1:20
Myf5	Rabbit polyclonal	sc-302	Santa Cruz	1:1000
MyoD	Rabbit polyclonal	sc-304	Santa Cruz	1:2000
Caveolin-1	Rabbit polyclonal	sc-894	Santa Cruz	1:400
Myogenin	Mouse monoclonal	F5D	DSHB	1:50
Myogenin	Rabbit polyclonal	sc-576	Santa Cruz	1:50
GFP	Chicken	ab13970	Abcam	1:600
Ki67	Rabbit polyclonal	Ki67	Leica	1:300
PH3	Rabbit polyclonal	MC463	Millipore	1:300
Laminin alpha2	Rat monoclonal	mAb(4H8-2)	Enzo	1:300
Patched1	Rabbit polyclonal	sc-9016	Santa Cruz	1:50
Laminin	Rabbit polyclonal	L9393	Sigma-Aldrich	1:1000
Collagen	Rabbit polyclonal	AB765	Millipore	1:350

Table 2.2: Secondary antibodies

Name	Host	Reference	Supplier	Dilution
Alexa 594 anti-mouse	Goat	A11005	Life Technologies	1:500
Alexa 594 anti-rabbit	Goat	A11037	Life Technologies	1:500
Alexa 488 anti-rabbit	Goat	A11034	Life Technologies	1:500
Alexa 488 anti-chicken	Goat	A11039	Life Technologies	1:500
Alexa 488 anti-rat	Donkey	A21208	Life Technologies	1:500
Alexa 633 anti-rabbit	Goat	A21070	Life Technologies	1:500
Alexa 633 anti-mouse	Goat	A21046	Life Technologies	1:500

2.4 Model of muscle injury *in vivo*

2.4.1 Cardiotoxin injections

Mice were maintained anaesthetised with Isoflurane (IsoFlo, Abbott) and 50µl of Cardiotoxin (CTX) (10µM in PBS) from *Naja mossambica* were injected in the TA muscle with insulin syringes to induce localised injury. The injections were carried out by Dr. Anne-Gaelle Borycki. Injured and control muscles were harvested at the indicated time points after damage.

2.5 Muscle transverse sections

2.5.1 Freezing protocol

TA muscles were harvested as mentioned in section 2.2.1 and then immediately fixed in 2% PFA with 0.25% Triton 100-X in PBS for 1h at 4°C. Muscles were washed several times with ice-cold PBS and then placed in 20% sucrose (VWR Chemicals) in PBS overnight at 4°C with agitation. Next day, muscles were embedded in O.C.T compound and rapidly frozen in cold isopentane (both from VWR Chemicals). Frozen muscles were kept at -80°C for long-term storage.

Frozen muscles were mounted on a dry ice-chilled metal chuck with O.C.T compound and 8 to 10µm transverse sections were generated on a Bright cryostat. Sections were collected on superfrost slides (Thermo Scientific) and were air-dried for 2h at RT for immediate immunolabelling or stored at -20°C until further use.

2.5.2 Haematoxylin and eosin (H&E) staining

Frozen muscle sections were air-dried for 30 minutes at RT and then rehydrated with 1X PBS for 1h in a coplin jar. Sections were then incubated for 5 minutes in 1% eosin in methanol (both from Fisher Scientific), rinsed with tap water, stained for 5 minutes in haematoxylin (Richard-Allan Scientific) and rinsed again with tap water. Sections were then dehydrated through an ethanol gradient (70 to 100% in water). Slides were finally incubated for 10 minutes in Xylene (Fisher Scientific) and mounted with DPX mountant (Sigma-Aldrich) for analysis.

2.5.3 Immunofluorescence of muscle sections

Frozen transverse sections were air-dried for 30 minutes before processing. Next, slides were hydrated for 5 minutes with PBS and then blocked for 1h in 5% BSA, 1% foetal

bovine serum (FBS), 1% heat-inactivated goat serum and 0.5% Triton 100-X in PBS in a humidified chamber. Sections were then incubated overnight at 4°C with primary antibodies diluted in PHT (PBS with 1% heat-inactivated goat serum and 0.5% Triton 100-X). After incubation, sections were washed 3 times with PHT and incubated for 1h at RT with secondary antibodies diluted in PHT. Finally, sections were washed 3 times with PHT and then mounted in Vectashield with DAPI for imaging. For some primary antibodies like Pax7, an unmasking or antigen retrieval step was applied before staining. To do so, air-dried sections were immersed in a coplin jar with 50ml of pre-warmed 1X citrate buffer pH 6 in PBS. The slides were microwaved at high power until boiling (around 1 minute) and then at low power for 10 minutes. The coplin jar was kept in the microwave for additional 10 minutes and then the slides were removed from the jar and cooled down at RT for 5 minutes. Finally, the slides were rinsed once with PBS and blocked as mentioned above.

2.5.4 Imaging

H&E sections were observed with a Leica DMR upright microscope. Samples used for immunofluorescence were observed under Olympus BX51 microscope with X-cite 120 illumination system (EXFO, Quebec, Canada). Immunofluorescence images were taken with a Zeiss Apotome with ZEN pro imaging system. Images were assembled using Photoshop CS5 version 12.0.4. Cross-sectional area (CSA), fluorescence intensity and cell counting were analysed with the ImageJ software.

2.6 Cell cycle analysis by flow cytometry

2.6.1 Single cell isolation from cultured myofibres

Myofibres in culture were collected in a 15ml conical tube and spun down at 100g for 3 minutes to obtain a pellet. The supernatant was discarded and fibres were incubated for 1h at 37°C in a water bath in digestion buffer (DB), which contains a mixture of collagenase A (100µg/µl, Roche) and Dispase II (2.4U/ml, Roche) in PBS. The mixture was vortexed every 10 minutes during the incubation period to help digestion. Digested fibres were then dissociated by mechanical action with a 19-gauge syringe for 5 minutes and filtered through a 70µm strainer (Falcon) to obtain a single cell suspension.

2.6.2 Propidium iodide and RNase A treatment

Isolated satellite cells in solution were spun down at 1000g for 10 minutes to obtain a pellet. The supernatant was discarded and the cell pellet was washed once with PBS

and transferred to a 1.5ml eppendorf tube. The solution was spun down again at 1000g for 5 minutes and the supernatant was discarded. Cells were carefully fixed with 1ml of 70% ethanol; to do so, the tube was placed on a vortex and ice-cold ethanol was added drop-wise. At this point, cells could be stored at -20°C until analysis.

For further processing, the cell solution was spun down at 1000g for 5 minutes at 4°C to discard the supernatant. Cells were then incubated for 30 minutes at 37°C with propidium iodide (PI, 10µg/ml) and RNase A in PBS. Finally, cells were taken to the flow cytometry facility for analysis.

2.6.3 Flow cytometry analysis

Labelled cells were analysed according to their DNA content with an Attune Autosampler (Life Technologies) and using the Attune Cytometric Software (Applied Biosystems).

2.7 Cell sorting

2.7.1 Single cell preparation from bulk of muscle

6 to 8 week-old Pax7-GFP mice were culled by cervical dislocation and hair from one of the hindlimbs was shaved with a scalpel and 70% ethanol. The skin was pinched and torn off with toothed forceps to expose the muscles. Large leg skeletal muscles (TA, gastrocnemius, quadriceps and biceps femoris) were removed under the stereo microscope using scissors for ophthalmology and forceps. The muscles were transferred to ice-cold PBS in a 10 cm Petri dish to remove connective tissue, tendons, blood vessels and fat. Muscles were placed into another dish with fresh ice-cold PBS for washing. Clean muscles were then transferred into another dish and minced into a smooth pulp using scissors for ophthalmology. The pulp was placed into a 50ml Falcon tube containing 7ml of collagenase type 2 (0.2% Worthington collagenase type II (CLS2) and 10% FBS in DMEM) and incubated for 1h at 37°C in a water bath. The solution was vortexed every 10 minutes during the incubation period to help digestion. After incubation, digested muscles were triturated with a 19-gauge syringe and the mixture was incubated for another 15 minutes at 37°C. The solution was then filtered through a 70µm strainer to obtain a single cell suspension. The solution was spun down at 1000g for 10 minutes and the supernatant was discarded. The cell pellet was then resuspended in chilled medium (10%FBS and 1%PSF in DMEM) and kept on ice until analysis.

2.7.2 Fluorescence activated cell sorting (FACS) analysis

Single cell solutions were brought to the Medical School flow cytometry core facility at the Royal Hallamshire Hospital, Sheffield. Cell suspensions were transferred into flow cytometry test tubes with cell strainer cap (Falcon, Corning) and analysed by the technical staff in a BD FACSAria cell sorter. To perform the analysis, control cells from C57BL/6 mice were also prepared as mentioned above to gate the fluorescence signal.

2.8 Molecular biology techniques

2.8.1 Total RNA isolation from muscle fibres, whole embryo and cells grown in monolayer

RNA extraction was carried out with sterile and RNase free reagents. Muscle fibres were collected in a 2ml eppendorf tube and allowed to sit at the bottom of the tube to aspirate culture medium. Fibres were washed once with PBS and then 200 μ l of Trizol reagent (Invitrogen) was added to the tube. Fibres were carefully homogenised with a pellet pestle motor (Kontes) and the mixture was left for 5 minutes at RT to help dissociation of nucleoproteins. 40 μ l of chloroform was added and the solution was mixed vigorously for 15 seconds and incubate for 3 minutes at RT. The solution was spun down at maximum speed for 15 minutes at 4°C. After centrifugation, the aqueous phase was carefully transferred to a new, clean tube and two volumes of ethanol were added to the sample, along with 1/20 volume of LiCl and 1 μ l of glycogen. Samples were incubated overnight at -20°C. After incubation, samples were centrifuged at maximum speed for 10 minutes at 4°C. The supernatant was discarded and the pellet was washed in 75% ethanol and centrifuged again at 7500g for 5 minutes at 4°C. The supernatant was discarded and the pellet was air-dried and dissolved in pre-warmed RNase-free water (diethylpyrocarbonate (DEPC) water).

To extract RNA from whole embryos or cells grown in monolayer, 1ml of Trizol reagent was directly added to the tissue or culture dish and the lysate was passed several times through the pipette. The mixture was transferred to a 1.5 ml eppendorf tube and was further homogenised using a vortex or a pestle motor. After 5 minutes of incubation at RT, 0.2ml of chloroform was added per 1ml of Trizol used. From this point, all the steps were the same as described above.

2.8.2 Complementary DNA (cDNA) synthesis

cDNA synthesis was carried out as described in the Invitrogen Superscript First Strand Synthesis handbook. Briefly, 1 to 5 μ g of mRNA was primed with 50 μ M oligo(dT) and

Table 2.3: Standard PCR program

Step	Temperature °C	Time	Cycles
Initial denaturation	94	5 minutes	1
Denaturation	94	30 seconds	30
Annealing	Primer T _m	30 seconds	30
Extension	72	30 seconds	30
Final extension	72	10 minutes	1
Hold	4	undefined	1

10mM dNTP mix into a final volume of 20 μ l of DEPC water. The samples were incubated at 65°C for 5 minutes and then chilled on ice for 1 minute. Next, 10 μ l of synthesis mix (10X RT buffer, 25mM MgCl₂, 0.1M DTT, RNaseOUT (40U/ μ l) and Superscript III reverse-transcriptase (200U/ μ l)) was added to the samples and incubated 50 minutes at 50°C. After incubation, the reactions were terminated at 85°C for 5 minutes and then chilled on ice. Finally, 1 μ l of RNase H was added to each sample and incubated for 20 minutes at 37°C. At this point the samples could be used immediately for PCR or stored at -20°C.

2.8.3 Reverse transcription polymerase chain reaction (RT-PCR)

Semi-quantitative RT-PCR was used to detect transcripts of different Shh signalling pathway components in cultured muscle fibres. cDNA was used as a template and primers listed in table 2.4 were used to amplify the region of interest. Primer stock concentration was 100 μ M but 20 μ M aliquotes were made to prevent contamination of the main the stock. PCR reactions were prepared by adding 10 μ l of 2x RedTaq ReadyMix (Sigma), 800nM of each primer and 500ng of cDNA adjusted to a final volume of 20 μ l of autoclaved milliQ water. PCR reactions were performed in a Eppendorf mastercycler gradient PCR machine (Eppendorf). Temperature and time conditions were optimised by adjusting the melting temperature (T_m) in a gradient program. A standard PCR program was as shown in table 2.3.

Finally, RT-PCR amplification products were run in 1% agarose/TAE gel containing ethidium bromide (4 μ l/100ml of agarose). 1kb DNA ladder (Fermentas) was also loaded to indicate band sizes.

2.8.4 Quantitative real-time PCR (qPCR)

qPCR was used to estimate relative expression levels of specific genes. These expression levels can also be considered as the amount of PCR product (amplicon) that is synthesised

as the reaction occurs. This amount of amplicon is directly related to the fluorescence emitted by a reporter dye, in this case SYBR Green, which binds to double-stranded DNA. The cycle threshold (Ct) value is taken as a reference of fluorescence accumulation, and it is defined as the number of cycles required for the fluorescence to cross a threshold or background level. The greater the initial concentration of the target gene in the sample, the fewer the number of cycles required to amplify the product.

Before starting with the analysis, qPCR primer concentrations were optimised by dilution series of forward and reverse primers in different combinations (from 1000 to 62.5nM), using embryo cDNA (150ng) or milliQ water as template. Primers and templates were mixed with 2x SYBR Green JumpStart Taq ReadyMix (Sigma) to a final concentration of 1.25 units of Taq DNA polymerase in a 20 μ l reaction adjusted with milliQ water. Samples were read with a iCycler instrument (Biorad) and using the iCycler software. Optimal primer concentrations were determined using the melt curve to identify a single peak that corresponds to the target amplicon.

Routine qPCR analysis was performed by preparing 20 μ l reaction mix as for primer optimisation (2x SYBR Green JumpStart Taq ReadyMix, forward and reverse primers at optimal concentrations, template DNA (150ng) adjusted with milliQ water). Samples were run as triplicates in a non-skirted 96-well plate (Cell Projects), sealed with a Microseal film (Biorad) and analysed in an iCycler. Transcription levels were calculated using the $\Delta\Delta$ Ct method. For qPCR analysis of cultured myofibres, Ct values were normalised by subtracting the Ct value of the housekeeping gene *Gapdh* from the Ct value of each target gene. Next, the relative mRNA levels of cultured myofibres at 24, 48 and 72h compared to freshly isolated myofibres at 0h were calculated.

2.8.5 Primer design

Primers were obtained either from the literature or designed using Primer Premier 5. Primer-BLAST tool was used to verify the specificity of the primers and to prevent partial binding to other sequences. Primer sequences for RT-PCR and qPCR are listed in tables 2.4 and 2.5 respectively. For qPCR analysis, forward RT-PCR primers for *GAPDH*, *Ptch1* and *Gli1* were used.

2.9 Statistical analysis

The number of positive cells per individual myofibre per experimental condition per mouse were counted and averaged. The average number of positive cells on muscle cryosections was based on four to six cross-sectional fields (x20 or 0.154 mm²) of regenerating muscle per mouse. Mean values per experiment were then averaged across all subjects in each

Table 2.4: RT-PCR primers

Gene	Primer	Sequence	T _m °C	Reference
<i>Shh</i>	Forward	CTGCGAGTGACCGAGGGCTG	65	This work
<i>Shh</i>	Reverse	GCGGTCCAGGAAGGTGAGG	62.4	This work
<i>Ptch1</i>	Forward	CAACACCTGGACTCAGCACTCC	61.6	This work
<i>Ptch1</i>	Reverse	GTGGCAGGGCAATCTGGGTC	62.5	This work
<i>Gli1</i>	Forward	GAGAGCAGACTGACTGTGCC	60.2	This work
<i>Gli1</i>	Reverse	CCTGCGGCTGACTGTGTAAG	60.8	This work
<i>Gli3</i>	Forward	GAAATGTCCCACGAGAACAGATGTC	59.8	This work
<i>Gli3</i>	Reverse	GAGGAGGGTGGTAGTGAGGC	62.2	This work
<i>Smo</i>	Forward	TGCCACCAGAAGAACAAGCCA	59.8	(Zhao et al., 2006)
<i>Smo</i>	Reverse	GCCTCCATTAGGTTAGTGCGG	61.8	(Zhao et al., 2006)
<i>Hip</i>	Forward	CAAAGCCCAGTGACCAAGCAATG	62.6	This work
<i>Hip</i>	Reverse	CACGCTGGCTCACACTTGGC	64.3	This work
<i>GAPDH</i>	Forward	ACTCCACTCACGGCAAATTC	57.3	(Morita et al., 2005)
<i>GAPDH</i>	Reverse	ACTGTGGTCATGAGCCCTTC	59.4	(Morita et al., 2005)
<i>Acta1</i>	Forward	GGCACCCAGGGCCAGAGTCA	66.5	(Londhe and Davie, 2011)
<i>Acta1</i>	Reverse	TCATCCCCGGCAAAGCCAGC	65.6	(Londhe and Davie, 2011)

Table 2.5: qPCR primers

Gene	Primer	Sequence	T _m °C	Reference
<i>GAPDH</i>	Reverse	GACTCCACGACATACTCAGCACC	59.4	This work
<i>Ptch1</i>	Reverse	GCAAGGGTAAAGGTATTCTATTATCTG	57.7	This work
<i>Gli1</i>	Reverse	CATCTCCACGCCGCTGTCCG	65.8	This work
<i>Gli2</i>	Forward	AGAACCTGAAGACACACCTGCG	62.7	(Rowbotham et al., 2007)
<i>Gli2</i>	Reverse	GAGGCATTGGAGAAGGCTTTG	59.5	(Rowbotham et al., 2007)

group. Values were expressed as either mean \pm standard error of the mean (SEM) or boxes (interquartile ranges, RQ) and whiskers (minimum and maximum values). Where percentage data were used, these were transformed before statistical analysis. A minimum of three individual mice were analysed for each experiment, unless stated otherwise in the figure legend.

To determine significance between two groups, comparisons were made using unpaired two-tailed Student's t-test. Analyses of multiple groups (qPCR data and GBS-GFP inhibition) were performed with one-way ANOVA and Tukey's multiple comparison post-hoc test. All data were analysed using Prism version 6.00 for Mac (GraphPad Software). $p < 0.05$ was considered statistically significant.

Ex vivo AND *in vivo* MURINE MODELS TO STUDY SATELLITE CELL-MEDIATED MYOGENESIS

3.1 Introduction

Since their initial anatomical characterisation through electron microscopy by Mauro in 1961, satellite cells have been largely studied using *in vitro* approaches to explore their behaviour and myogenic potential. Subsequently, *in vivo* strategies to determine the contribution of satellite cells during muscle regeneration have been established. More recently, *ex vivo* culture strategies have also been implemented, which offer great advantages over *in vitro* systems but without substituting for *in vivo* models.

3.1.1 *In vitro* systems to study satellite cells

There are two main *in vitro* approaches to study satellite cells and their progeny: immortalised muscle cell lines derived from satellite cells and primary myogenic cell cultures. The C₂ cell line, which was generated from adult injured thigh muscles of C3H mice (Yaffe and Saxel, 1977) and one of its subclones, the C₂C₁₂, is one of the most widely used myogenic cell lines due to its ability to differentiate easily (Blau et al., 1985). Furthermore, the use of these lines has provided extensive knowledge on biochemical and molecular characteristics and requirement of muscle cells in culture (Semmesarian et al., 1999) (Conboy and Rando, 2002) (Katagiri et al., 1997).

The second *in vitro* strategy to study satellite cells is the direct isolation of primary myoblasts from whole muscles. This approach has been extensively used to study satellite cell progeny as they proliferate, differentiate and fuse but also to overcome some

issues with established cell lines, such as senescence, poor transplantation potential and alteration of their phenotype and responsiveness to stimuli linked to constant passaging (Rando and Blau, 1994). Moreover, primary myoblasts can be isolated from practically any animal model, which is useful to study age-specific processes or when using genetically engineered mice. It is important to mention, however, that *in vitro* cultures of satellite cells might not mimic entirely the biological behaviour that satellite cells have *in vivo*, mainly because satellite cells are taken out from their native environment, including the muscle fibre, the basal lamina and other non-myogenic cells.

3.1.2 Study of satellite cells *ex vivo*: the myofibre culture system

The isolation and culture of single myofibres from adult rat *flexor digitorum brevis* (FDB) muscles was first established by Bekoff and Betz (Bekoff and Betz, 1977) and then optimised and further characterised by Bischoff (Bischoff, 1986). Later, isolation of mouse *extensor digitorum longus* (EDL), tibialis anterior (TA) and soleus muscle fibres was also implemented (Rosenblatt et al., 1995). Slightly different protocols of this *ex vivo* system are available (Collins and Zammit, 2009, Pasut et al., 2013, Shefer and Yablonka-Reuveni, 2005), but all of them rely on the culture of individual muscle fibres in floating conditions to study satellite cells in their native position, i.e. packed between the sarcolemma and the basal lamina of the muscle fibre. Although this is a simplified system that removes external cues coming from non-myogenic cell types, such as blood and connective tissue cells (Zammit et al., 2004), when single muscle fibres are cultured in serum-rich medium for 72h, satellite cells quickly activate, proliferate and eventually differentiate, mimicking the events that happen during myogenesis *in vivo* (Beauchamp et al., 2000). Moreover, single satellite cells can be visualised using specific satellite cell and myogenic markers and different cell populations can be identified within the 72h-period, as shown in table 3.1).

The *ex vivo* culture system has provided a better understanding of the biology of satellite cells, as well as meaningful information on the intrinsic and extrinsic cues required in different stages of adult myogenesis. Importantly, this approach was not only key to confirm the "stemness" and ability of satellite cells to give rise to other muscle cells (Bischoff, 1975) but also to study satellite cell behaviour with live imaging techniques (Siegel et al., 2009). Finally, molecular and biochemical approaches are also possible using this system (Pasut et al., 2013). Nevertheless, single myofibres cannot survive in floating conditions for long periods of time (up to 96 or 120 hours), so later events like satellite cell fusion into myotubes cannot be studied using this system.

Table 3.1: Satellite cell populations found during *ex vivo* culture as reported in the literature

Population	Description
Pax7+/Myf5-	Population made by either quiescent satellite cells or satellite cells that have not activated myogenic factors yet (Collins et al., 2007, Gnocchi et al., 2009)
Pax7-/Myf5+	Satellite cell population that has switched off Pax7 expression and is expected to also express MyoD (Zammit et al., 2002)
Pax7+/Myf5+	Population of satellite cells that have become activated (Zammit et al., 2004)
Pax7+/MyoD-	Self-renewing satellite cell population (Halevy et al., 2004, Ono et al., 2011, Zammit et al., 2004)
Pax7-/MyoD+	Satellite cell population that has entered the differentiation phase and would be expected to express Myogenin (Ono et al., 2011, Zammit et al., 2004)
Pax7+/MyoD+	Satellite cell population undergoing expansion (Zammit et al., 2004)
Caveolin-1+/Myogenin-	Population made by either quiescent satellite cells or satellite cells that express MyoD but have not switched on Myogenin expression yet. These cells are expected to also express Pax7 (Gnocchi et al., 2009, Zammit et al., 2004)
Caveolin-1-/Myogenin+	Satellite cells that have reached terminal differentiation and do not express Pax7 (Gnocchi et al., 2009)
Caveolin-1+/Myogenin+	Differentiating satellite cells. These cells are expected to also express MyoD but not Pax7 (Gnocchi et al., 2009, Zammit et al., 2004)

3.1.3 Models to explore satellite cell function *in vivo*

Contribution of satellite cells to repair muscles *in vivo* can be explored with injury models, where two main phases can be identified: a degenerative and a regenerative phase (Charge and Rudnicki, 2004). The degeneration phase begins with cell necrosis caused by the breakage of muscle fibres, which is accompanied by an increase in fibre permeability and in cytosolic protein levels such as creatine kinases (Sorichter et al., 1998b). Calcium homeostasis is also disrupted, triggering calpain-mediated proteolysis (Alderton and Steinhardt, 2000). During the degeneration phase, damaged fibres release chemotactic factors that activate and recruit mononucleated cells, including inflammatory and muscle cells (Tidball, 1995). Within few hours after damage, the first inflammatory cells that migrate to the injury site are neutrophils followed by macrophages, which can also affect satellite cell behaviour (Merly et al., 1999).

Muscle degeneration is followed by a regeneration phase, which is characterised by satellite cell activation, expansion, differentiation and fusion to repair damaged fibres (Snow, 1978). This leads to the appearance of small, newly formed myofibres with centrally located myonuclei that express embryonic forms of the Myosin Heavy Chain (MYHC) protein (Whalen et al., 1990). Once satellite cells have repaired the damage, new muscle fibres increase their size and some myonuclei might migrate to the periphery. At this point, the muscle architecture is completely restored.

Different models of muscle injury have been established. These include models of chronic muscle injury such as the *mdx* mouse, a genetic homologous equivalent of Duchenne muscular dystrophy (DMD) and characterised by the absence of the protein Dystrophin (Carnwath and Shotton, 1987). Acute models of muscle injury are also widely used and contrary to chronic injury models, these are characterised by a single round of degeneration with transient collagen accumulation and inflammatory response and restoration of muscle architecture by 3 to 4 weeks after damage. These models include the injection of myotoxins like bupivacaine, cardiotoxin (CTX) or neotexin, which results in around 80-90% damage of muscle membranes and necrosis without affecting satellite cell survival, or the injection of BaCl₂, which causes myofibre death by membrane depolarisation, exocytosis and Ca²⁺ efflux blockage (Boldrin et al., 2012, Relaix and Zammit, 2012). Other methods to induce acute injury are muscle crushing, freezing, denervation and ischemia (Charge and Rudnicki, 2004). Both chronic and acute injury models present degeneration and regeneration phases but their progression and duration may vary depending on the extent of the injury, the muscle injured and the age and pathological status of the animal used.

3.1.4 Aim

The aim of this chapter is to reproduce different established models to study satellite cell function, one *in vitro*, one *ex-vivo* and one *in vivo*, which form the methodological basis of this project.

3.2 Results

3.2.1 Satellite cell-mediated myogenesis can be studied *ex vivo* using the myofibre culture system

The *ex vivo* myofibre culture system has been widely used since the discovery of the protocol to isolate single myofibres from whole muscles (Bischoff, 1975). To reproduce this system in the lab, single muscle fibres from 6 to 8 week-old wild-type C57/BL6 mouse EDL muscles were either immediately fixed to preserve satellite cell quiescence (time 0h) or cultured *ex vivo* for 24, 48 and 72 hours. Quiescent satellite cells were identified at time 0h by the expression of the transcription factor Pax7 (Seale et al., 2000) (Fig.3.1 A-C). A mean of four Pax7+ satellite cells were counted on each freshly isolated myofibre at 0h (Fig.3.1 M), consistent with previous reports (Beauchamp et al., 2000). After 24h in culture, Pax7+ satellite cells exited quiescence and became activated, as shown by the expression of the myogenic transcription factor Myf5 (Fig.3.1 D-F). At this time point, around 84.6% of the cells co-expressed both Pax7 and Myf5, indicating that the majority of satellite cells become activated upon culture (Fig.3.1 M and table 3.1). Furthermore, following activation, satellite cells underwent morphological changes, as they appeared more round compared to quiescent satellite cells. A mean of six Pax7+/Myf5+ satellite cells could be observed per fibre and this number was similar to time 0h (Fig.3.1 M).

In the *ex vivo* culture system, satellite cells undergo their first cell division between 24 and 48h (Siegel et al., 2011, Zammit et al., 2004). Consistently, I observed a 3-fold increase in the number of satellite cells between 24 and 48h (Fig.3.1 M) and satellite cells were characterised by the co-expression of Pax7 and the myogenic transcription factor MyoD, which follows Myf5 expression (Zammit et al., 2002) (Fig.3.1 G-I). By 48h, 86.7% of Pax7+ cells co-expressed MyoD, whereas 7.3% just expressed Pax7 and 6% expressed only MyoD (Fig.3.1 M and table 3.2). The fraction of Pax7+/MyoD- cells might correspond to self-renewing satellite cells needed to maintain the stem cell pool or to Pax7+ satellite cells that have not up-regulated MyoD expression yet (Zammit et al., 2004).

At 72h, as Pax7 is down-regulated in differentiating cells (Ono et al., 2011, Zammit et al., 2004), I labelled satellite cells with the marker Caveolin-1, which labels most of the satellite cell progeny at 72h and is down-regulated only in a small fraction of fully

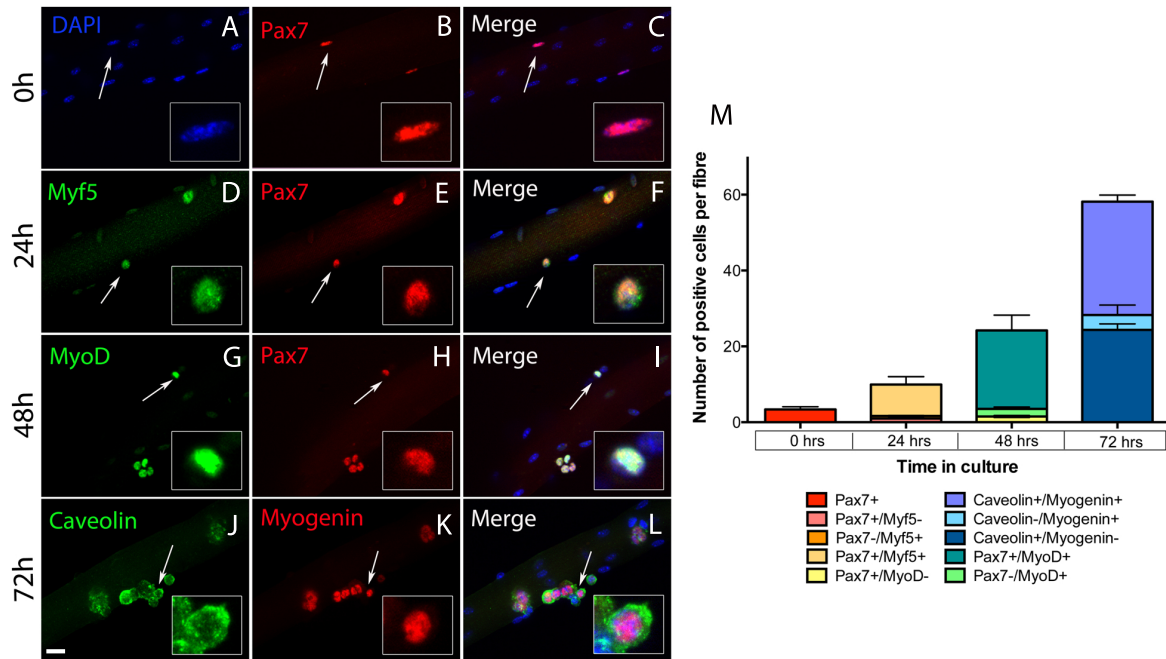


Figure 3.1: Myogenic regulatory factors expression on satellite cells from single muscle fibres cultured *ex vivo*. Individual mouse skeletal muscle fibres were cultured in floating conditions for 0, 24, 48 and 72h. Myofibres were immunostained to detect Pax7 in red (B, D and G), Myf5 in green (E), MyoD in green (H), Caveolin-1 in green (J) and Myogenin in red (K). Nuclei were counterstained with DAPI in blue, as shown in A. Merged images for each time point are shown in C, F, I and L. Magnified views for every channel are shown (regions indicated by an arrow). Scale bar represents 20 μ m. Quiescent satellite cells at 0h expressed Pax7. Upon 24h in culture, satellite cells became activated and up-regulated Myf5 and by 48h, MyoD. Beyond 48h, satellite cells expanded and most cells entered differentiation so that, by 72h, Myogenin+ satellite cells could be detected. At this point, satellite cells can also down-regulate myogenic factors and return to quiescence (Halevy et al., 2004, Ono et al., 2011, Zammit et al., 2004). The onset of amplification of the satellite cell population occurred between 24 and 48h and a maximum expansion could be observed by 72h (M). Representative data from at least three individual mice are shown, with 15 individual fibres per mouse counted for each time point. Values are mean and error bars indicate standard error of the mean (SEM).

Table 3.2: Proportion of satellite cell populations found in this study during *ex vivo* culture

Population	Percentage \pm SEM
Pax7+/Myf5-	8.2 \pm 5.9
Pax7-/Myf5+	7.2 \pm 5.4
Pax7+/Myf5+	84.6 \pm 10.6
Pax7+/MyoD-	7.3 \pm 6.7
Pax7-/MyoD+	6.0 \pm 5.3
Pax7+/MyoD+	86.7 \pm 8.2
Caveolin-1+/Myogenin-	39.8 \pm 9.1
Caveolin-1-/Myogenin+	8.6 \pm 4.9
Caveolin-1+/Myogenin+	51.6 \pm 9.8

differentiated cells (Gnocchi et al., 2009). As shown in Fig.3.1 J-L, most satellite cells were labelled with Caveolin-1 at 72h and expanded greatly, increasing their numbers by around four-fold (Fig.3.1 M). By 72h, 51.6% of cells expressed both Caveolin-1 and Myogenin, which represent differentiating satellite cells, while 8.6% only expressed Myogenin and are terminally differentiated cells. The 39.8% remaining cells that were Caveolin-1+/Myogenin-, may either not have switched Myogenin expression on yet or have already down-regulated MyoD and returned to quiescence (Tables 3.1 and 3.2) (Gnocchi et al., 2009, Zammit et al., 2004).

Together, using the *ex vivo* culture system, I managed to show the transition of satellite cells from the activation phase (Myf5+) to the expansion phase (MyoD+) and to the differentiation phase (Myogenin+), which goes in line with previous reports within the literature (Gnocchi et al., 2009, Zammit et al., 2004).

3.2.2 Adult myogenesis can be studied *in vivo* by inducing muscle injury with cardiotoxin

6 to 8 week-old C57/BL6 TA muscles were injected with cardiotoxin as described in section 2.4.1. The left TA muscle was injured and the right muscle was kept as uninjured control. Injured and control TA muscles were harvested at 2, 4, 7 and 14 days following induced injury and were processed as described in section 2.5. Muscle transverse sections were then analysed by hematoxylin and eosin staining (H&E). Normal uninjured TA muscles had a highly homogeneous appearance, with muscle fibres of similar size and myonuclei located at the periphery of fibres (Fig.3.2 A-C). In contrast, 2 days after CTX-induced injury, the whole architecture of the muscle changed: myofibres lost their defined

shape due to necrosis and infiltration of mononucleated cells to the site of injury was observed, which are likely to be inflammatory cells, fibroblasts and satellite cells (Fig.3.2 D-F). At 4 days following injury, the infiltration of cells was still visible and some newly formed myofibres were readily detected, as shown by the appearance of centrally located myonuclei (Fig.3.2 G-I). Newly regenerated myofibres were more abundant at 7 days post-injury (Fig.3.2 J-L). Finally, the architecture of the muscle was visibly restored at 14 days after CTX-induced injury, showing larger fibres with centrally located nuclei (Fig.3.2 M-O) (Charge and Rudnicki, 2004). Beyond 14 days, inflammation reduces greatly so by day 21, little or no inflammatory cells can be observed (Mann et al., 2011). Finally by day 28 post-injury, the muscle displays a normal morphology with myofibres of almost the same diameter as non-injured ones, although centrally located nuclei are still visible (Charge and Rudnicki, 2004, Rosenblatt, 1992). Thus, localised CTX muscle injury allows us to follow the progression of muscle regeneration over time, with discrete events that span over a 28 day-period.

3.2.2.1 Satellite cells become activated and expand upon muscle injury *in vivo*

In order to identify satellite cells during adult muscle regeneration *in vivo*, immunofluorescence analysis of Pax7 and Laminin was performed in uninjured and CTX-injured TA muscles at 2, 4, 7 and 14 days post-injury. Non-injured muscles presented quiescent Pax7+ satellite cells located under the basal lamina of muscle fibres, here labelled with Laminin (Fig.3.3 A-D). Satellite cell activation occurs within a few hours after injury (Cooper et al., 1999) and at 2 days following CTX-induced damage, satellite cells likely to be activated were detected at the site of injury (Fig.3.3 E-H). By day 4 the satellite cell population expanded as more Pax7+ cells were visible, which coincided with the appearance of newly formed myofibres with centrally located nuclei (Fig.3.3 I-L). Beyond day 7, the muscle architecture was progressively restored and Pax7+ satellite cells were less abundant and were re-positioned beneath the basal lamina of regenerating myofibres (Fig.3.3 M-P), so that by day 14, CTX-injured muscles looked similar to uninjured control muscles apart from the presence of centrally located myonuclei (Fig.3.3 Q-T).

To detect activated satellite cells, immunofluorescence analysis of MyoD and Laminin alpha 2 was performed in uninjured and CTX-injured TA muscles at 2, 4, 7 and 14 days post-injury. Unlike non-injured muscles, CTX-injured muscles at 2, 4 and 7 days expressed MyoD+ satellite cells (Fig.3.4). MyoD+ satellite cells were more abundant at 4 days post-injury (Fig.3.4 I-L) and declined at 7 days post-injury (Fig.3.4 M-P) to become nearly undetectable by 14 days (Fig.3.4 Q-T), indicating a gradual completion of the myogenic program once the muscle architecture was restored.

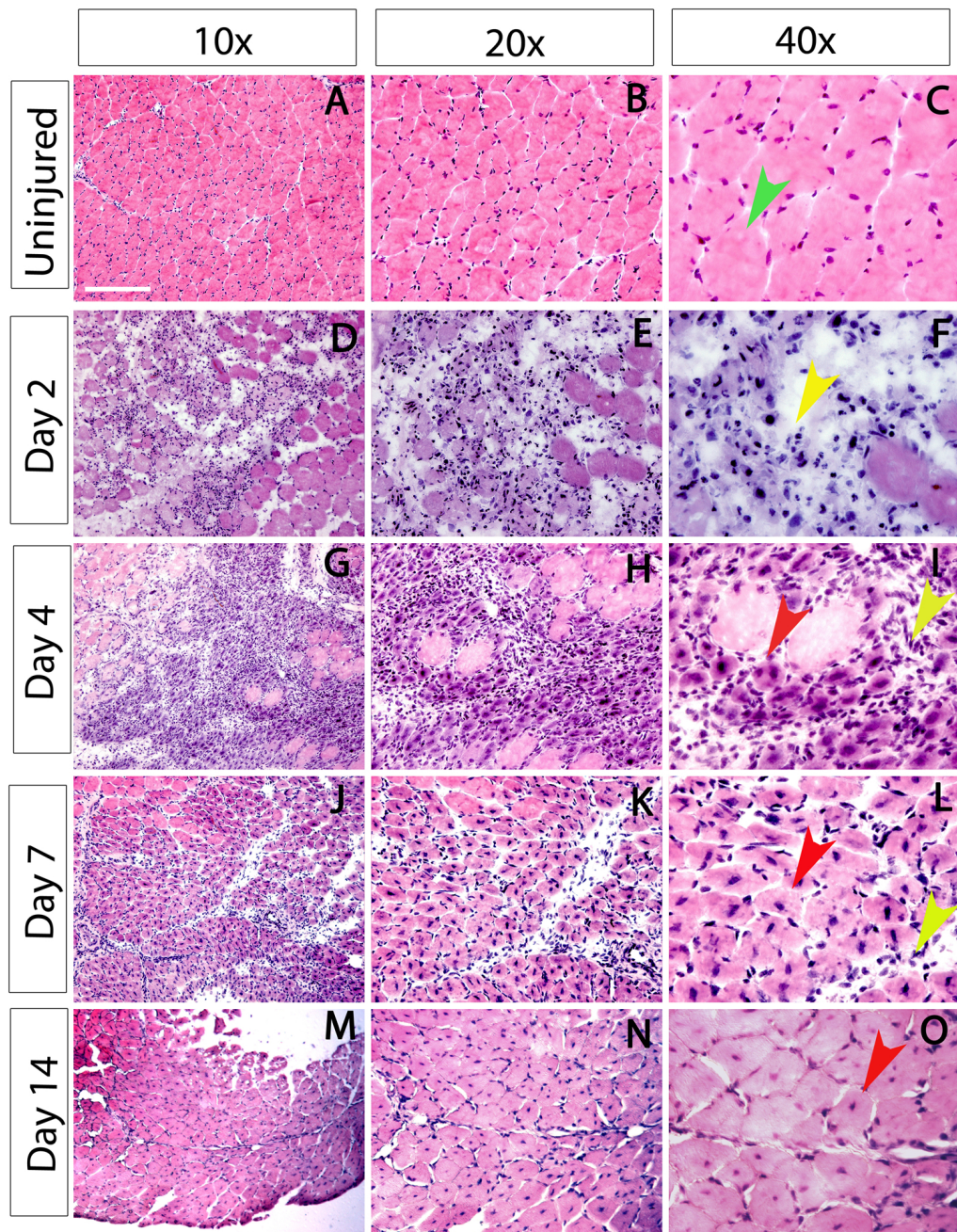


Figure 3.2: Regeneration process following cardiotoxin induced muscle injury. Uninjured and cardiotoxin-injured (2, 4, 7 and 14 days post-injury) TA muscles from C57/BL6 mice were analysed by H&E staining to assess changes in muscle architecture. Non-injured TA muscle fibres had an homogeneous size and appearance (A-C). In contrast, injured muscles were characterised by changes in myofibre shape due to necrosis and cell infiltration of different types of mononuclear cells at 2 (D-F) and 4 days (G-I) post-injury. Newly regenerating myofibres were visible from day 4 but more evident by day 7 post-injury (J-L). Muscle architecture was restored by 14 days post-injury (M-O), with the presence of fully regenerated myofibres. Non-injured areas, infiltrated cells and fibres with centrally located nuclei are shown with green, yellow and red arrows, respectively. Representative images from three individual mice for each time point are shown. Scale bar represents 200 μ m.

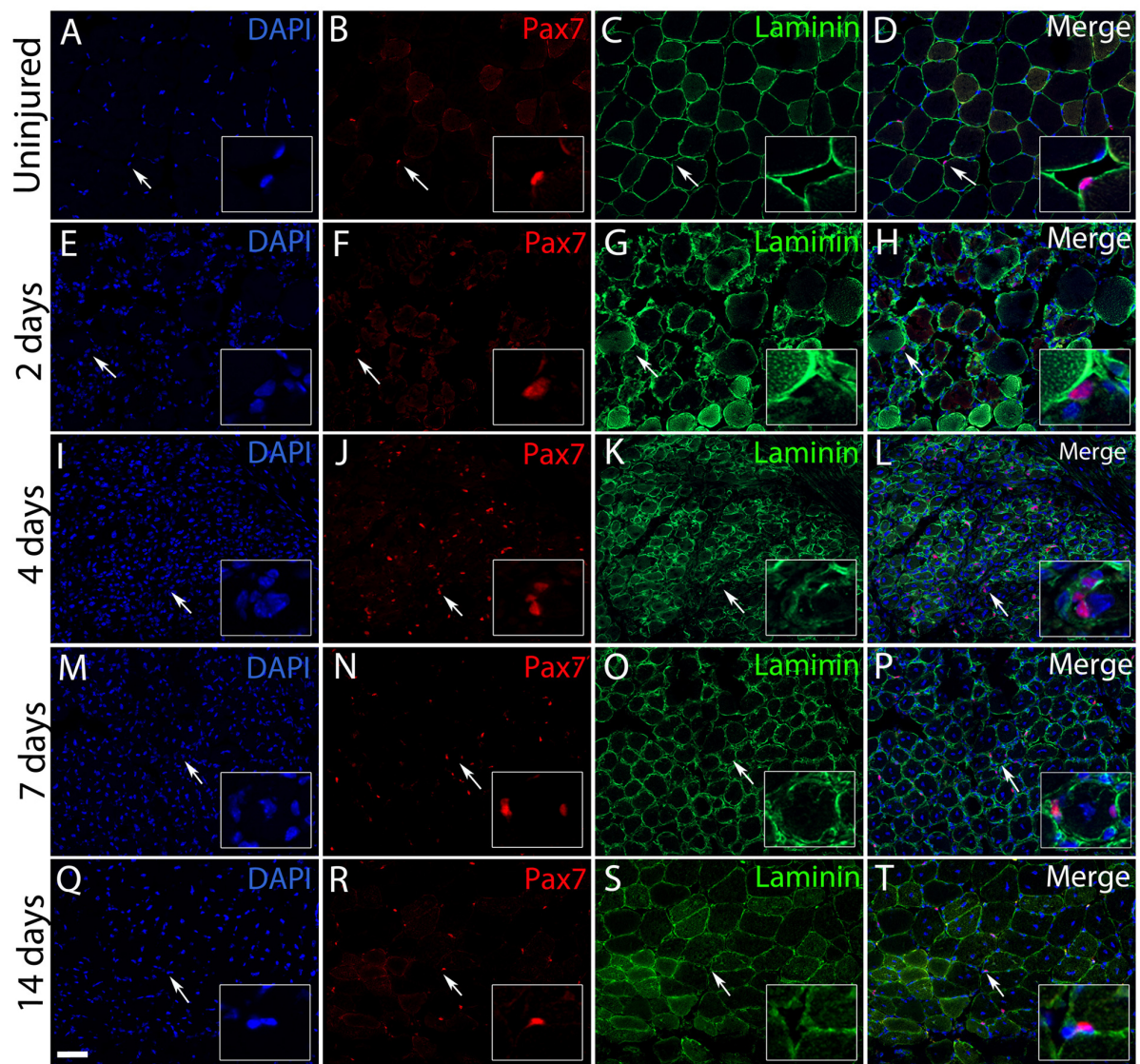


Figure 3.3: Pax7 labels satellite cells during muscle regeneration. Uninjured and CTX-injured (2, 4, 7 and 14 days post-injury) TA muscles from C57/BL6 mice were analysed by immunofluorescence using antibodies against Pax7 (red) and Laminin (green). Cell nuclei were counterstained using DAPI (blue). Merge images from three channels are shown for non-injured and 2, 4, 7 and 14 injured muscles in D, H, L, P and T, respectively. Magnified views for every channel are shown (regions indicated by an arrow). Non-injured TA muscles had quiescent Pax7+ cells positioned beneath the basal lamina (A-D). 2 days after CTX-induced injury, Pax7+ satellite cells migrated to the site of injury (E-H). By 4 days post-injury (I-L) the satellite cell population expanded and persisted until day 7 (M-P). Finally, at 14 days post-injury, the restoration of the muscle architecture was accompanied by a decline in the number of Pax7+ satellite cells and the reintegration of self-renewing cells under the basal lamina (Q-T). Representative images from three individual mice for each time point are shown. Scale bar represents 50 μ m.

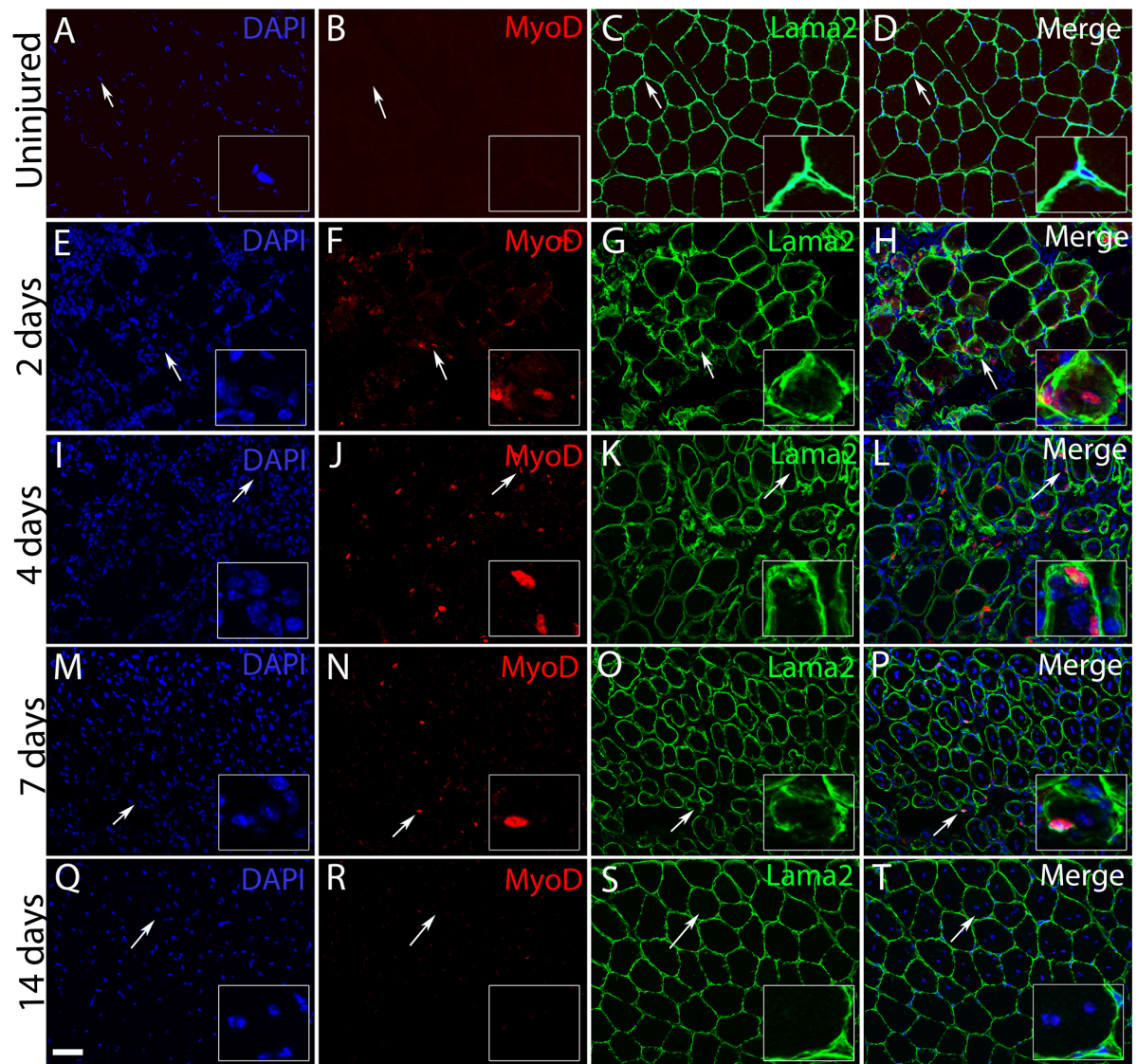


Figure 3.4: Activated satellite cells expressed MyoD during muscle regeneration. Uninjured and CTX-injured (2, 4, 7 and 14 days post-injury) TA muscles from C57/BL6 mice were analysed by immunofluorescence using antibodies against MyoD (red) and Laminin alpha 2 (green). Cell nuclei were counterstained using DAPI (blue). Merge images from three channels are shown for non-injured and 2, 4, 7 and 14 injured muscles in D, H, L, P and T, respectively. Magnified views for every channel are shown (regions indicated by an arrow). Uninjured TA muscles had quiescent satellite cells that did not express MyoD (A-C). Upon CTX-induced muscle injury, satellite cells became activated and expressed MyoD at 2 (E-H), 4 (I-L) and 7 days (M-P) but this expression declined by 14 days post-injury (Q-T). Representative images from three individual mice for each time point are shown. Scale bar represents 50 μ m.

3.2.2.2 Satellite cells proliferate in response to muscle injury *in vivo*

To assess the proliferative status of satellite cells during muscle regeneration, a pilot experiment was carried out using muscles from Tg:Pax7-EGFP mice, which express EGFP under the control of the regulatory elements of Pax7 and label all satellite cells (Sambasivan et al., 2009). These muscles were sectioned and analysed by immunofluorescence using antibodies against GFP and the proliferation marker Ki67 at 1, 2, 4, 7 and 14 days post-injury. Uninjured TA muscles had quiescent GFP+ satellite cells (average of 39 cells/mm²) and did not express Ki67 (Fig.3.5 A-D and Y). In contrast, an important increase in the number of Ki67+ cells was observed at 1 day post-injury, where an average of 62 cells/mm² were GFP-/Ki67+, 7 cells/mm² were GFP+ only and 39 cells/mm² were GFP+/Ki67+ (which represents 85.4% of the Pax7+ population), indicating that the majority of satellite cells have become activated and entered the cell cycle. In addition, other cell types proliferate in response to injury (Fig.3.5 E-H and Y). The expression of proliferating Pax7+ satellite cells increased by 3.6-fold at day 2 post-injury (143 cells/mm²) (Fig.3.5 I-L and Y), as was the number of non-myogenic cells (GFP-/Ki67+, 203 cells/mm²).

Between 2 and 4 days post-injury, the Pax7+ satellite cell population expanded further although the overall number of Ki67+ cells decreased. By 4 days post-injury, an average of 557 cells/mm² were GFP+/Ki67-, 232 cells/mm² were only positive for Ki67 and 51 cells/mm² were both GFP+ and Ki67+ cells (just 8.5% of all Pax7+ cells) (Fig.3.5 M-P and Y). At day 7 post-injury, there was a drastic reduction in the overall number of both GFP+ and Ki67+ cells (Fig.3.5 Q-T and Y), with an average of 12 cells/mm² co-expressing GFP and Ki67. Finally, by 14 days post-injury, a mean of 132 cells/mm² only expressed GFP, 12 cells/mm² only expressed Ki67 and no GFP/Ki67 co-expression could be detected (Fig.3.5 U-X and Y). This suggests that satellite cells undergo an important expansion between 2 and 4 days post-injury to reach a maximum number by 4 days. Satellite cell numbers decline beyond 4 days post-injury, which coincides with the progressive down-regulation of Ki67 expression.

3.2.2.3 Satellite cells differentiate *in vivo* to contribute to muscle regeneration

The progressive decline of proliferating Pax7 expressing-satellite cells from 4 days post-injury suggests that myoblasts have initiated differentiation. To identify differentiating progenitor cells, another pilot experiment was performed using Tg:Pax7-EGFP mice. Here, Tg:Pax7-EGFP were analysed by immunofluorescence using antibodies against GFP and the myogenic transcription factor Myogenin at 1, 2, 4, 7 and 14 days post-injury. In uninjured TA muscles, quiescent GFP+ satellite cells did not express Myogenin (Fig.3.6

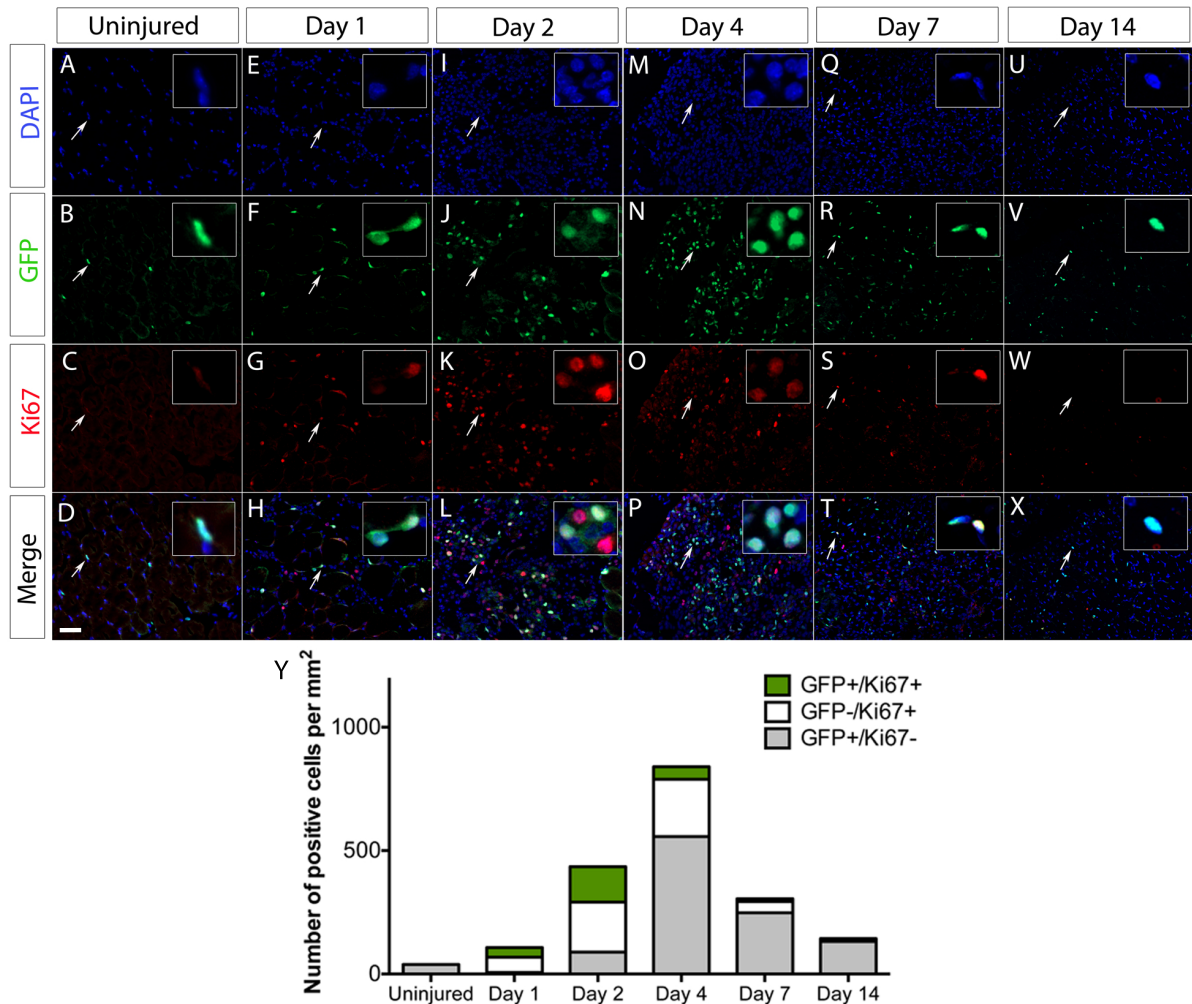


Figure 3.5: The satellite cell population expands during muscle regeneration. Uninjured and cardiotoxin-injured (1, 2, 4, 7 and 14 days post-injury) TA muscles from Tg:Pax7-EGFP mice were analysed by immunofluorescence using antibodies against Ki67 (red) and GFP (green). Cell nuclei were counterstained using DAPI (blue). Merge images from three channels are shown for non-injured and 1, 2, 4, 7 and 14 injured muscles in D, H, L, P, T and H respectively. Magnified views for every channel are shown (regions indicated by an arrow). Scale bar represents 50 μ m. Uninjured TA muscles had quiescent GFP+ satellite cells that did not show any Ki67 expression (A-D). Following CTX-induced muscle injury, satellite cells became activated and expressed Ki67 at 1(E-H), 2 (I-L) and 4 (M-P) days post-injury. By day 7 (Q-T), the number of Ki67+ satellite cells declined so that by 14 days, no Ki67 expression was observed (U-X). (Y) shows the quantification of the number of Ki67 and GFP expression in Tg:Pax7-EGFP uninjured and CTX-injured TA muscles. Mean values are shown. Each mean is based on four to six random 0.154 mm² regenerating areas from one mouse per each time point.

A-D and Y). At 1 day post-injury GFP+ satellite cells were activated but had not induced Myogenin expression yet (Fig.3.6 E-H and Y). In contrast, from 2 days post-injury, some Myogenin+ cells could be detected (26 cells/mm²) (Fig.3.6 I-L and Y) and this number increased further at 4 days post-injury, with 103 cells/mm² being Myogenin+ (Fig.3.6 M-P and Y). By day 7, just 23 cells/mm² were Myogenin+ (Fig.3.6 Q-T and Y) and by 14 days post-injury the number of Myogenin+ cells was a little bit higher than at 7 days (48 cells/mm²) (Fig.3.6 U-X and Y). Together, these data suggest that satellite cell differentiation starts as early as 2 days post-injury, peaks at 4 days post-injury and progressively decreases from 7 days. This reduction coincides with the increase of fibres with centrally located nuclei.

3.3 Discussion

3.3.1 The myofibre culture system recapitulates the events that happen during satellite-cell mediated myogenesis *ex vivo*

The myofibre culture system is a simple yet useful approach to study satellite-cell mediated myogenesis *ex vivo* (Fig.3.7). This system preserves satellite cells in their native environment while removing input from non-myogenic cells. Although this system does not substitute for the *in vivo* system, it offers great advantages over *in vitro* models. In particular, feedback mechanisms between satellite cells and the niche are preserved in the *ex vivo* culture system. For instance, quiescent satellite cells express nitric oxide synthase (NOS) and shear forces that occurs during myofibre isolation stimulate nitric oxide (NO) synthesis (Anderson, 2000). This results in the release of hepatocyte growth factor (HGF) from the extracellular matrix and the binding to its receptor c-Met, expressed by satellite cells (Tatsumi et al., 2002, Yamada et al., 2006). Interestingly, NO is also involved in the regulation of satellite cell migration along the muscle fibre following a blebbing movement (Otto et al., 2011).

Here, I used the transcription factor Pax7 to identify quiescent and activated satellite cells in freshly isolated myofibres. However, other satellite cell markers have been described, including the proteins C-Met, Caveolin-1, M-Cadherin, Integrin $\alpha 7$ and CD34 among others (Yin et al., 2013). A mean of four Pax7+ satellite cells was detected in freshly isolated myofibres from EDL muscles, which is in agreement with previous reports (Ono et al., 2010, Shefer et al., 2006). Furthermore, the proportion of satellite cells progressing into the different stages of the myogenic program reported here, including activation at 24h, proliferation at 48h and differentiation at 72h, was also consistent with the literature (Gnocchi et al., 2009, Zammit et al., 2002).

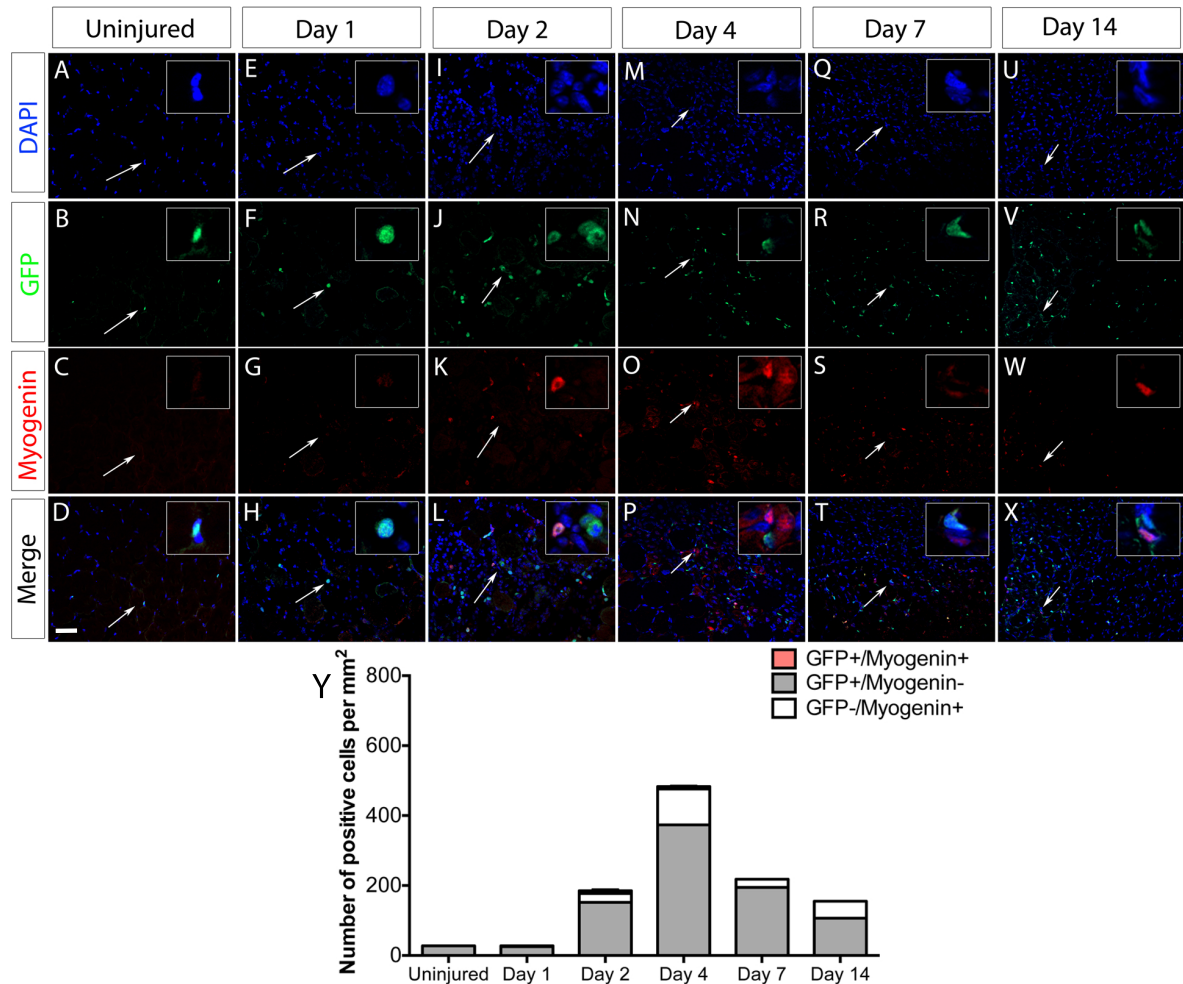


Figure 3.6: Satellite cells activate Myogenin expression during muscle regeneration *in vivo* Uninjured and cardiotoxin-injured (1, 2, 4, 7 and 14 days post-injury) TA muscles from Tg:Pax7-EGFP mice were analysed by immunofluorescence using antibodies against GFP (green) and Myogenin (red). Cell nuclei were counterstained using DAPI (blue). Merge images from three channels are shown for non-injured and 1, 2, 4, 7 and 14 injured muscles in D, H, L, P, T and H respectively. Magnified views for every channel are shown (regions indicated by an arrow). Scale bar represents 50 μ m. Quiescent GFP+ satellite cells in uninjured muscles cells did not express Myogenin, a marker of muscle differentiation (A-D). At 1 day following muscle injury, satellite cells became activated but did not express Myogenin (E-H). However, Myogenin expression was detected at 2 (I-L), 4 (M-P), 7 (Q-T) and 14 days (U-X) post-injury. (Y) shows the quantification of Myogenin and GFP expression in Tg:Pax7-EGFP uninjured and injured TA muscles. Mean values are shown. Each mean is based on four to six random 0.154 mm² regenerating areas from one mouse per each time point.

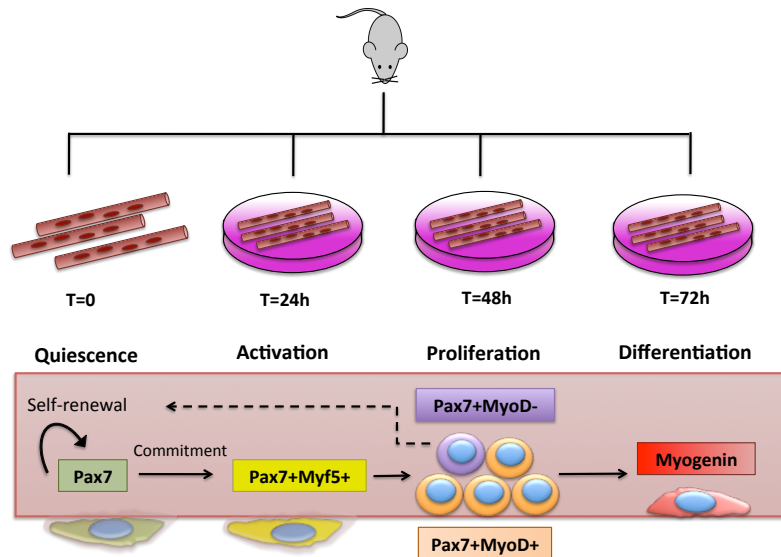


Figure 3.7: The myofibre culture system recapitulates satellite cell-mediated myogenesis. In this culture system, satellite cells maintain their association with the fibre and the basal lamina (niche) and are able to undergo myogenesis *ex vivo*. Importantly, harvesting fibres at different time points allows for the analysis of different cellular events, such as satellite cell in quiescent state labelled with Pax7 (T=0), Pax7+/Myf5+ activated satellite cells (T=24h), Pax7+/MyoD+ proliferative cells (T=48h) and Myogenin+ differentiating satellite cells (T=72h).

3.3.2 An acute model of muscle injury to study satellite cell myogenesis *in vivo*

In this chapter I reproduced a previously described cardiotoxin-mediated acute model of muscle injury to study satellite cell-mediated muscle regeneration. Satellite cell-mediated muscle regeneration *in vivo* was visualised by immunolabelling of Pax7 and by immunolabelling Tg:Pax7-EGFP mice using an anti-GFP antibody. Both methods allowed me to follow satellite cells as they progress through activation at 1-2 days post-injury, proliferation between 2-4 days post-injury and differentiation from 4 days post-injury onwards (Fig.3.8) (Cooper et al., 1999, Yan et al., 2003). However, experiments done with Tg:Pax7-EGFP mice should be taken exclusively for reference purposes, as just one Tg:Pax7-EGFP mouse per time point was available for analysis.

My quantification of the number of satellite cells at the site of injury showed that the number of GFP+ cells in injured muscles in the Tg:Pax7-EGFP mice peaked at 4 days post-injury, with 91.2 cells/0.154 mm² and then declined to 39 cells/0.154 mm² by 7 days post-injury. These figures are consistent with previous studies reporting 90.33 cells/0.154 mm² by 5 day post-injury (Lepper et al., 2011) and around 38 cells/0.154 mm² by 7 days post-injury (Wen et al., 2012). In contrast, although I observed that Myogenin+ cells peaked at day 4 post-injury, the numbers I recorded were lower than those reported previously (Lepper et al., 2011). This discrepancy may be due to differences in the sensitivity

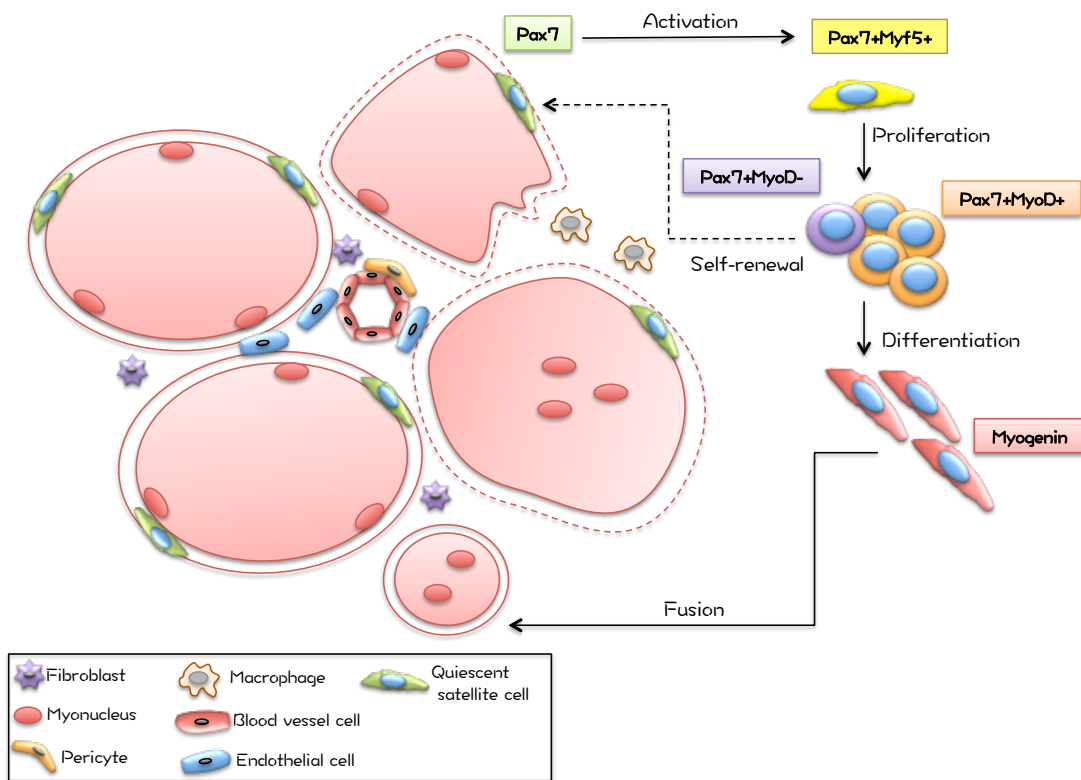


Figure 3.8: Cardiotoxin-mediated injury triggers muscle regeneration *in vivo*. Satellite cells are located at the periphery of muscle fibres and become rapidly activated upon CTX injection, which results in 80-90% muscle degeneration (dotted lines) without affecting satellite cell survival. Once activated, some satellite cells proliferate and differentiate to fuse to damaged myofibres and other return to quiescence. Different non-myogenic cells, such as inflammatory cells, endothelial cells and fibroblasts are important components of the satellite cell niche and also contribute to muscle repair. Adapted from (Schaaf, 2012)

of the Myogenin antibody used (F5D mouse monoclonal versus sc-576 rabbit polyclonal) or to the insufficient number of Tg:Pax7-EGFP mice used for these experiments. Nevertheless, I observed that satellite cells are rapidly activated in response to injury and that their proliferation and differentiation peak between 2 and 4 days post-injury (Fig.3.5). Following this phase, the formation of new fibres with centrally located nuclei takes place, a phenomenon that continues at 14 days post-injury (Charge and Rudnicki, 2004, Pastoret and Sebillé, 1995). In line with this, cross-sectional area (CSA) analysis indicate that fibre size in 14 day-injured muscles is comparable to uninjured muscles (Le Grand et al., 2012), indicating the progressive restoration of the muscle architecture. Although not analysed in this chapter, fibroblast-mediated collagen deposition and quantification of inflammatory cells like macrophages are two additional strategies to assess the extent of muscle repair *in vivo*, since persistent inflammation and fibrosis reflect perturbations in the regeneration process (Mann et al., 2011).

CHARACTERISATION OF THE EXPRESSION OF SHH SIGNALLING PATHWAY COMPONENTS IN SATELLITE CELLS

4.1 Introduction

Adult stem cells reside in a niche or microenvironment where they interact with neighbouring supporting cells and extracellular matrix (ECM) components (Lane et al., 2014). The niche provides physical and biochemical cues for the adequate function of stem cells. Satellite cells have a specialised niche made up of the muscle fibre, non-myogenic cells and the basal lamina (Fig.3.8). This microenvironment provides extrinsic signals that maintain an adequate balance between self-renewing and committed muscle progenitors.

Several signalling pathways involved in embryonic muscle development, including Wnt, Notch and FGF have roles in satellite cell expansion, self-renewal, quiescence and activation, respectively (Chakkalakal et al., 2012, Le Grand et al., 2009, Mourikis et al., 2012b). In contrast, the role of Shh signalling, another signalling pathway with essential role during embryonic myogenesis, has not been explored in satellite cells. Although Shh signalling pathway is inactive in normal adult skeletal muscles, up-regulation of *Ptch1*, *Gli1* and *Smo* mRNAs as well as Gli3 protein has been observed in regenerating skeletal muscles following injury (Piccioni et al., 2014b, Pola et al., 2003, Renault et al., 2013a, Straface et al., 2009). Moreover, C₂C₁₂ mouse myoblasts and primary myoblasts up-regulate the Shh target genes *Ptch1* and *Gli1* following culture in the presence of Shh (Elia et al., 2007, Fu et al., 2014, Koleva et al., 2005, Li et al., 2004), suggesting that satellite cells may become responsive to Shh signals during muscle regeneration.

In this chapter, I examined the expression of Shh signalling components in cultured

muscle fibres and in satellite cells. Specifically, Shh response was monitored in quiescent and activated satellite cells using a Gli reporter mice and Ptch1 immunostaining.

4.1.1 Hypothesis and aim

My first hypothesis is that satellite cells are able to respond to Shh signalling. Therefore, the aim of this chapter is to characterise the expression of the Shh signalling components in satellite cells and to assess Shh response during satellite cell-mediated myogenesis using *ex vivo* and *in vivo* approaches.

4.2 Results

4.2.1 Components of the Shh signalling pathway are up-regulated during myofibre culture

To investigate the temporal expression of Shh and Shh signalling components, mRNA expression levels were evaluated by semi-quantitative RT-PCR and real-time PCR (qPCR) analysis. cDNA was prepared from mRNA extracted from 0, 24, 48 and 72h-cultured myofibres as described in section 2.8.2. RT-PCR analysis was carried out using primers for *Shh*, *Ptch1*, *Gli1*, *Gli3*, *Smo* and *Hip* and primers for glyceraldehyde-3 phosphatedehydrogenase (*Gapdh*) and alpha-actin (*Acta1*) were used as internal controls. cDNAs from E.11.5 mouse embryos and H₂O were used as positive and negative controls, respectively. *Shh* expression could not be detected at any time point using this technique, which suggests that neither muscle fibres nor satellite cells are the source of Shh (Fig.4.1 A, first panel). Likewise, most of Shh signalling components were not expressed in freshly isolated myofibres. However, the expression of the Shh receptor *Ptch1* and the G protein-coupled receptor *Smo* was up-regulated at 48h and progressively down-regulated at 72h (Fig.4.1 A, second and fifth panels). Additionally, the transcription factor *Gli1* and the Shh inhibitor *Hip*, which along with *Ptch1* are transcriptional targets of Shh signalling, were detected as early as 24h after culture. Finally, I observed that the expression of *Gli1*, *Hip* and *Gli3* peaked at 72h (Fig.4.1, third, fourth and sixth panels).

To confirm these RT-PCR data, I performed qPCR analyses to quantify *Ptch1*, *Gli1* and *Gli2* expression in myofibres cultured for 0, 24, 48 and 72h. qPCR primers for *Shh*, *Smo*, *Hip* and *Gli3* were also designed, but could not be optimised due to the prevalent formation of primer dimers and were not included in the study. For the rest of the primers used, the analysis showed that *Ptch1* and *Gli2* expression was significantly up-regulated in cultured myofibres at 48h and then down-regulated at 72h (Fig.4.1 B). In contrast, although *Gli1* expression also increased at 48h, no significant difference was

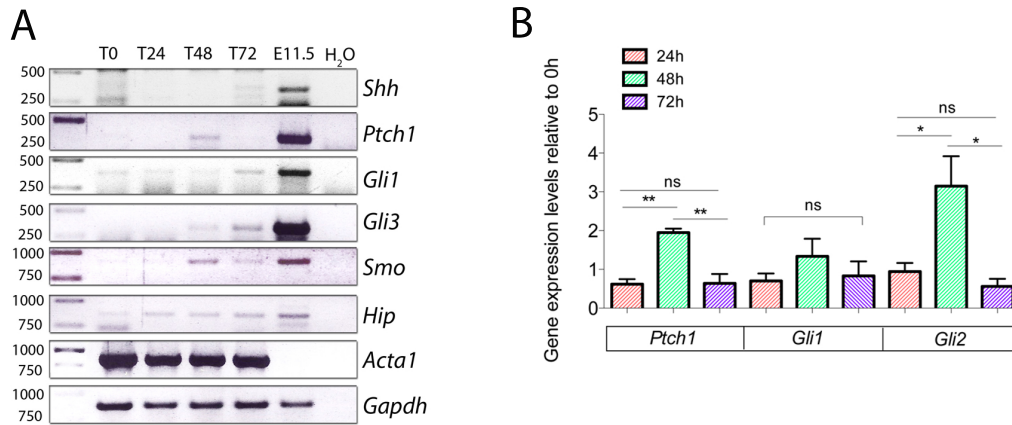


Figure 4.1: Temporal expression of Shh and its downstream components in cultured myofibres. (A) mRNA expression levels evaluated by semi-quantitative RT-PCR analysis using *Gapdh* and *Acta1* as internal controls. *Shh* expression was not detected at any time point with this method. *Ptch1* and *Smo* were up-regulated at 48h, while *Gli1*, *Gli3* and *Hip* expressions peaked at 72h. Representative images of myofibre cDNA coming from three individual mice are shown. (B) qPCR analysis of *Ptch1*, *Gli1* and *Gli2* expression levels normalised to 0h. For *Ptch1*, $p=0.0022$ (between 24h and 48h and between 48h and 72h); for *Gli1*, $p=0.4667$ and for *Gli2* $p=0.0173$ (between 24h and 48h and between 48h and 72h). Values are mean and error bars show SEM. Each mean is based on log₂-fold expression change in myofibre cDNA from three individual mice. Statistical analysis was performed using one-way ANOVA.

observed compare to other time points (Fig.4.1 B), suggesting that *Gli1* expression levels remained fairly constant over the culture time. Thus, components of the Shh signalling are up-regulated following *ex vivo* culture, peak at 48h before being down-regulated at 72h, when the main repressors of the pathway (*Gli3* and *Hip*) increase their expression. This suggests that satellite cells have a dynamic Shh response.

4.2.2 Quiescent satellite cells are not responsive to Shh signalling but become responsive during their activation and expansion

To further address Shh response in satellite cells, I assayed the expression of *Ptch1*, the receptor of Shh as it is a transcriptional target of Shh signalling (Nakano et al., 1989). In order to validate the reactivity of the anti-*Ptch1* antibody used in this study, immunofluorescence analysis was performed on E.10.5 mouse embryo cross sections, where *Ptch1* is expressed in the floor plate of the neural tube. Additionally, myofibres were immunostained with secondary antibody alone to control for non-specific binding (data not shown). In freshly isolated muscle fibres, *Ptch1* expression was not detected in quiescent Pax7+ satellite cells (Fig.4.2 A-D). However, after 24h in culture, *Ptch1* expression was detected in 42% of Pax7-expressing satellite cells (Fig.4.2 E-H and Q) and this number increased to 92% as cells began proliferating at 48h (Fig.4.2 J-L and Q). Interestingly, by 72h, the

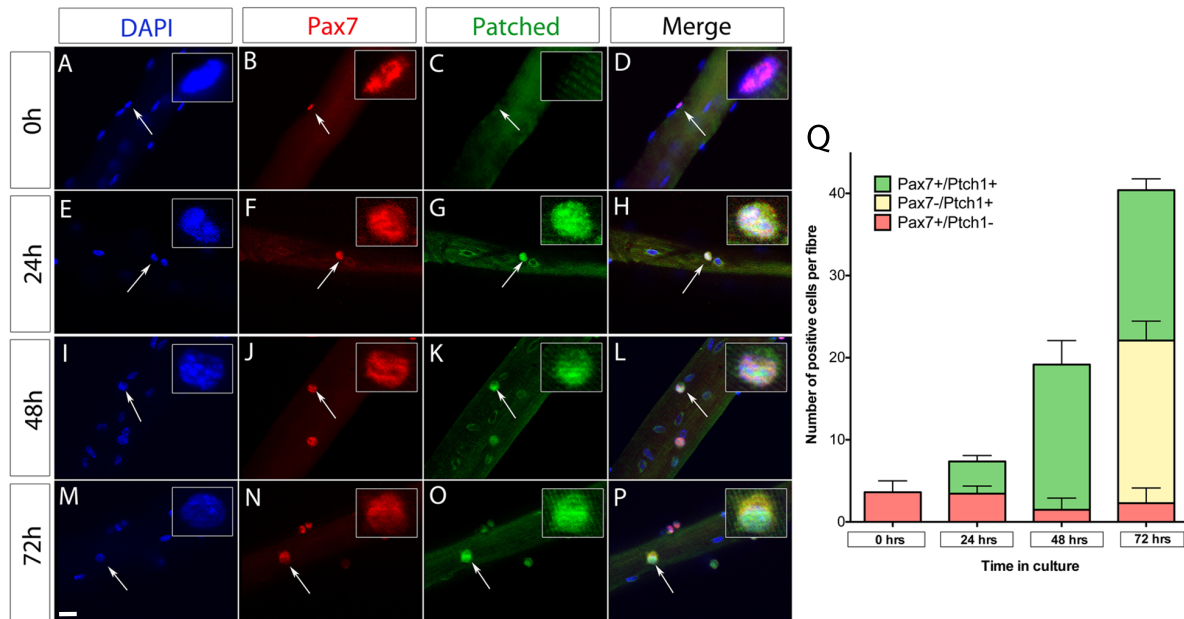


Figure 4.2: Ptch1 is expressed in activated satellite cells. EDL muscle fibres were cultured for 0, 24, 48 and 72h. Myofibres were immunostained to detect Pax7 in red (B, F, J and N) and Ptch1 in green (C,G, K and O). Nuclei were counterstained with DAPI in blue(A, E, I and M). Merged images for each time point are shown in D, H, L and P. Magnified views for every channel are shown (regions indicated by an arrow). Scale bar represents 20 μ m. Quiescent Pax7 satellite cells at 0h did not express Ptch1. Following activation at 24h in culture, Pax7+ satellite cells up-regulated Ptch1 and by 48h most of Pax7+ satellite cells co-expressed Ptch1. By 72h, Ptch1 was expressed in both Pax7+ and Pax7- satellite cells. (Q) Quantification of Pax7 and Ptch1 expression in 0, 24, 48 and 72h myofibre cultures. Representative data from three individual mice are shown, with 10 to 20 individual fibres per mouse counted for each time point. Values are mean and error bars indicate standard error of the mean (SEM).

number of Pax7+/Ptch1+ cells decreased to 46.3% of the total cell population, with a concomitant increase in the number of Pax7-/Ptch1+ cells (49%), which may correspond to differentiating satellite cells (MyoD+/Myogenin+) (Fig.4.2 M-P and Q). These data are in agreement with my RT-PCR/qPCR results and indicate that quiescent satellite cells are not responsive to Shh signalling but initiate Shh response upon satellite cell activation.

To confirm these observations, Gli response was directly assessed in cultured myofibres from Tg(GBS-GFP) mice, in which eight concatemerized binding sites for the Gli transcription factor drive GFP expression (Balaskas et al., 2012). To validate the reactivity of the anti-GFP antibody used in this study, immunofluorescence analysis was performed on larvae fish cross sections, where a GFP construct was expressed in motoneurons. Additionally, GFP immunofluorescence analysis was performed on hippocampal cross sections from 8-week-old Tg(GBS-GFP) mice, which show Shh response in the dentate gyrus (data not shown) (Ahn and Joyner, 2005). In agreement with my observations using a Ptch1 antibody, GFP expression was not detected in quiescent Pax7+ satellite cells (Fig.4.3 A-D and Q). However, Gli response was observed as satellite cells became activated at 24h, in

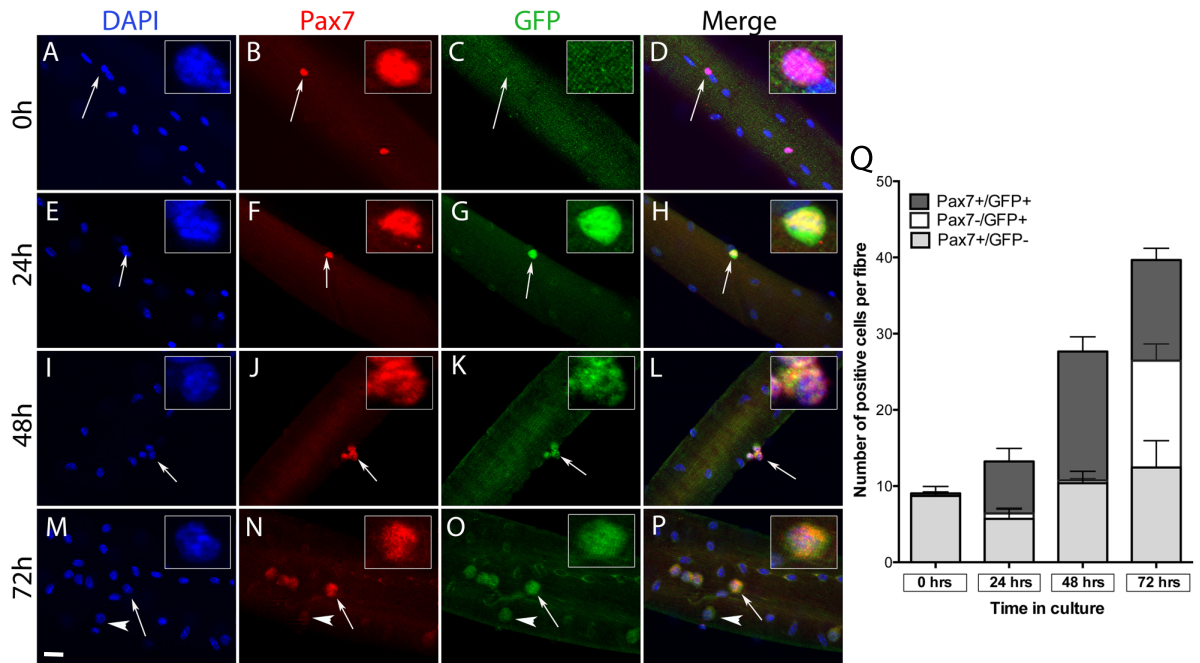


Figure 4.3: Satellite cells become responsive to Shh signalling upon activation. EDL muscle fibres from Tg(GBS-GFP) mice were cultured for 0, 24, 48 and 72h. Myofibres were immunostained to detect Pax7 in red (B, F, J and N) and GFP in green (C,G, K and O). Nuclei were counterstained with DAPI in blue (A, E, I and M). Merged images for each time point are shown in D, H, L and P. Magnified views for every channel are shown (regions indicated by an arrow). Scale bar represents 20 μ m. Quiescent Pax7 satellite cells at 0h did not show any Gli response. Following activation at 24h in culture, Pax7+ satellite cells started up-regulating GFP and this number increased as cells proliferated at 48h. By 72h, Gli response was detected in both Pax7+ (arrow) and Pax7- (arrowhead) satellite cells. (Q) Quantification of Pax7 and GFP expression in 0, 24, 48 and 72h myofibre cultures from Tg(GBS-GFP) mice. Representative data from three individual mice are shown, with 7 to 15 individual fibres per mouse counted for each time point. Values are mean and error bars indicate standard error of the mean (SEM).

51.5% of Pax7+ (Fig.4.3 E-H and Q). At 48h, 61% of Pax7+ satellite cells were positive for GFP (Fig.4.3 I-L and Q), and by 72h, GFP expression was associated with both Pax7+ and Pax7- cells, confirming that Shh response occurs in differentiating (Pax7-) as well as proliferating (Pax7+) satellite cells (Fig.4.3 M-P and Q). These results confirm that Shh response occurs in satellite cells that exit quiescence and become activated. Furthermore, Gli response persists during satellite cell proliferation and differentiation *ex vivo*.

As the number of Ptch1+ satellite cells was noticeably higher than the number of GFP+ satellite cells in 48h (92% vs 61%) and 72h (95% vs 68%) *ex vivo* cultures, I decided to investigate whether Ptch1 and Gli response occurred in the same cells. Confirming that quiescent Pax7-satellite cells did not respond to Shh signals, neither Gli response nor Ptch1 expression was detected at 0h (Fig.4.4 A-E). However, from 24h onwards, Ptch1 and GFP were co-expressed in Pax7+ satellite cells (Fig.4.4 F-J, K-O and P-T). Interestingly, Pax7+ cells expressing Ptch1 but very low GFP were also observed (Fig.4.4 K-O arrowhead), suggesting that Ptch1 and GFP are expressed by the same type of

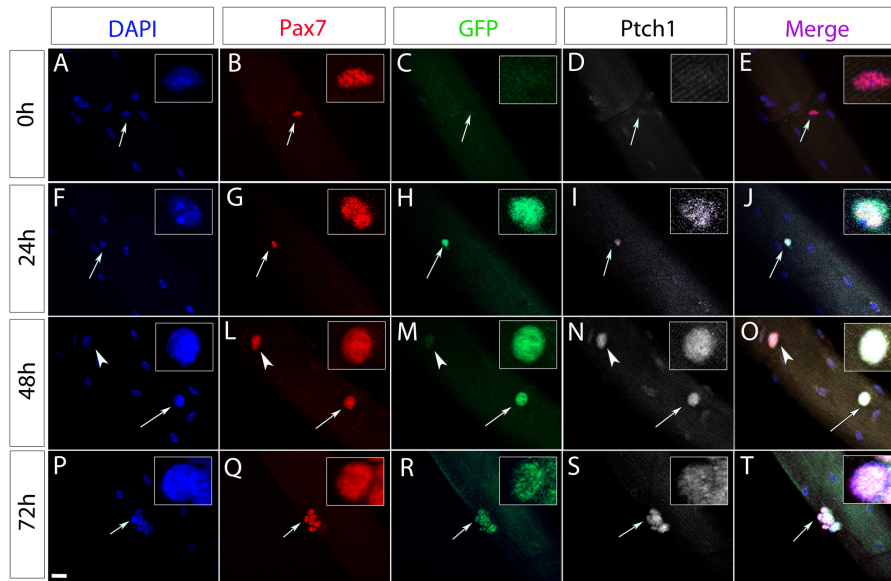


Figure 4.4: Ptch1 and Gli are indicators of Shh activity and are co-expressed in activated satellite cells. EDL muscle fibres from Tg(GBS-GFP) mice were cultured for 0, 24, 48 and 72h. Myofibres were immunostained to detect Pax7 (B, G, L and Q), GFP (C, H, M and R) and Ptch1 (D, I, N and S). Nuclei were counterstained with DAPI (A, F, K and P). Merged images for each time point are shown in E, J, O and T. Magnified views for every channel are shown (regions indicated by an arrow). Neither GFP nor Ptch1 were detected in quiescent Pax7+ satellite cells in freshly isolated myofibres at 0h. However, from 24h, Pax7+ satellite cells co-expressed GFP and Ptch1. Furthermore, Pax7+ cells expressing Ptch1 and low levels of GFP were also observed (arrowhead). Representative data from three individual mice are shown. Scale bar represents 20 μ m.

satellite cells but Tg(GBS-GFP) detects high levels of Shh response while Ptch1 detects high and low levels.

4.2.3 Satellite cell progression through myogenesis and Shh response *ex vivo*.

Shh response throughout the satellite cell myogenic program suggests that Shh signalling occurs in proliferating and differentiating progenitor cells. To investigate this I immunolabelled 24, 48 and 72h-cultured myofibres from Tg(GBS-GFP) mice for Pax7/Myf5/GFP, Pax7/MyoD/GFP and Caveolin-1/Myogenin/GFP to distinguish cells undergoing activation, proliferation or differentiation, respectively. In agreement with my previous results, Gli response was associated with half of activated satellite cells (47.5% of Pax7+/Myf5+ cells) at 24h, suggesting that Shh response is downstream of activation (Fig.4.5 A-E and P). In contrast, Pax7+/Myf5- did not contain Gli-driven GFP, confirming that the Shh signalling pathway is not active in quiescent satellite cells.

As shown in section 4.2.2, the total number of satellite cells responding to Shh signalling increased over time *ex vivo*. At 48h, for instance, Pax7/MyoD double-positive cells remained the major population showing Shh response (around 60% of total cells counted)

(Fig.4.5 F-J and Q). Interestingly, a proportion of proliferating Pax7+/MyoD+ cells (30%) were GFP-, suggesting that not all the cells undergoing active proliferation respond to Shh signalling. At 72h around 40% of total cells counted were Caveolin-1+/Myogenin+ differentiating satellite cells. From this population, 62.5% of cells also expressed GFP, confirming that Shh response persists during the differentiation phase (Fig.4.5 K-O and R). However, the remaining fraction of Caveolin-1+/Myogenin+ satellite cells (37.5%) did not express GFP, indicating that some satellite cells undergoing differentiation may progressively become desensitised to Shh signalling and down-regulate Gli response, a process known as "adaptation" (Balaskas et al., 2012). This is consistent with the fact that no terminally differentiated satellite cells (Caveolin-1-/Myogenin+) expressed GFP.

Next, 46.6% of total cells counted at 72h were Caveolin-1+/Myogenin-. Within this population, 26% were also GFP+ and expected to express MyoD, indicating that proliferating satellite cells respond to Shh signalling (Fig.4.5 K-O and R). In contrast, 74% of Caveolin-1+/Myogenin- cells were GFP-, which means that these cells may have never expressed GFP or that have switched off GFP expression by the time of analysis. This population is likely to be composed mainly by self-renewing/quiescent satellite cells, supporting the idea that Shh signalling is not active in satellite cells undergoing self-renewal.

Strikingly, a small proportion of the total cells counted at 72h were GFP+ only (12.8%). This was a very rare event, since most of the cells at 72h are either positively labelled for Caveolin-1, Myogenin or both (see section 3.2.1). Given that Myogenin labelling is generally very neat and precise in *ex vivo* myofibre cultures, it is possible that these GFP+ cells expressed low levels of Caveolin-1 protein, which was not clearly detected during counting. In fact, MyoD/Myogenin immunofluorescence analysis of Tg(GBS-GFP) myofibres at 72h shows that only 3.6% of total cells counted were MyoD-/Myogenin-/GFP+ (Fig.4.6), confirming the previous statement. This analysis shows that the Shh signalling pathway is not active in both quiescent and self-renewing satellite cells (Pax7+/Myf5-/MyoD- and Caveolin-1+/MyoD-/Myogenin-) and that Shh response predominantly occurs in activated satellite cells undergoing proliferation and early differentiation (Pax7+/Myf5+/MyoD+ and Caveolin-1+/MyoD+/Myogenin+).

4.2.4 Shh response in satellite cells coincides with their entry into the cell cycle

The transition from quiescence to activation involves the entry of satellite cells into the cell cycle. To investigate the cell cycle status of satellite cells that respond to Shh signalling, I immunolabelled cultured myofibres from Tg(GBS-GFP) mice for Pax7, GFP and the proliferation marker Ki67. As previously shown, Pax7-positive satellite cells

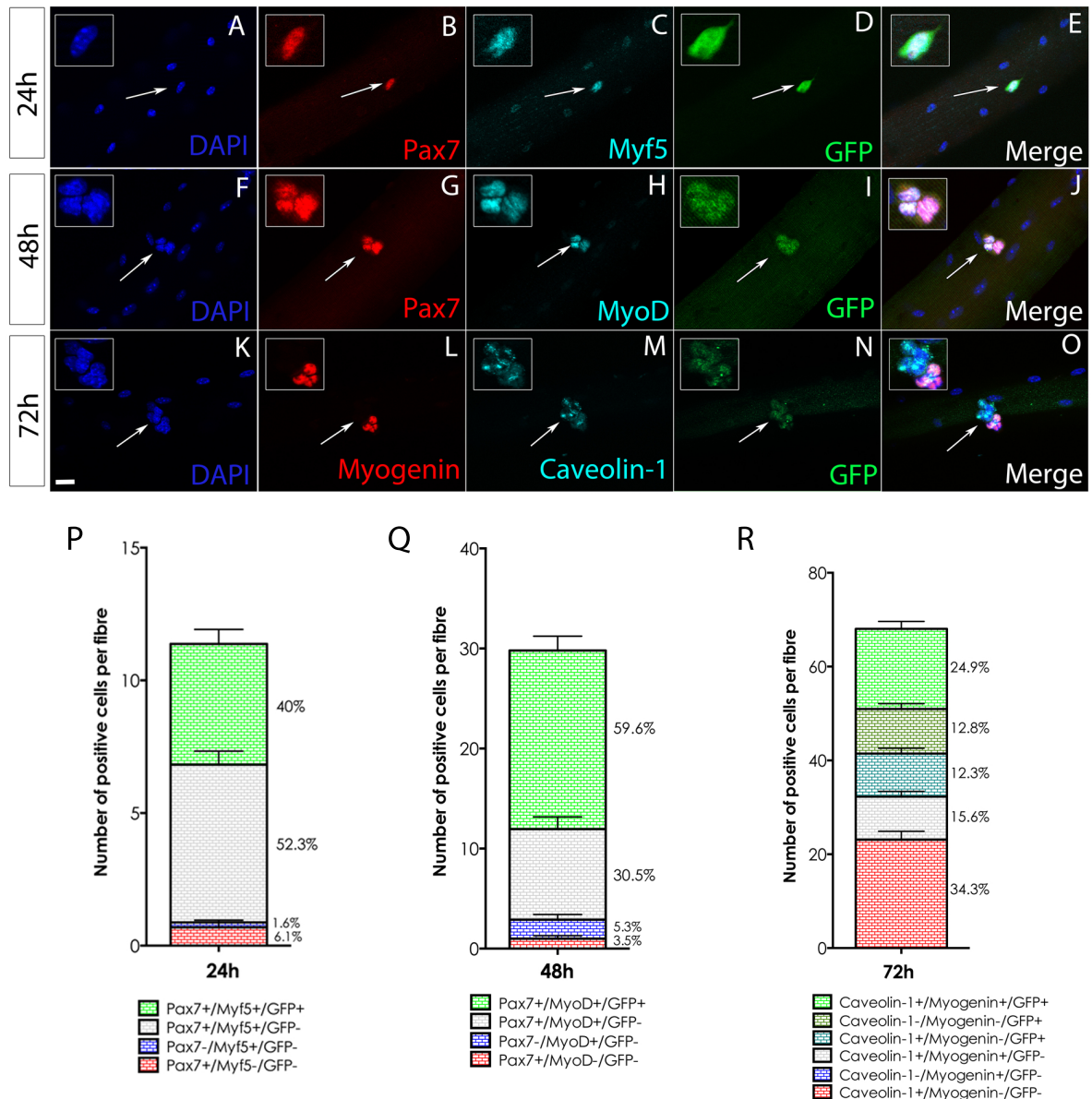


Figure 4.5: Shh signalling response during satellite cell-mediated myogenesis. EDL muscle fibres from Tg(GBS-GFP) mice were cultured for 24, 48 and 72h. Myofibres were immunostained to detect Pax7 (B and G), Myf5 (C), MyoD (H), Myogenin (L), Caveolin-1 (M) and GFP (D, I and N). Nuclei were counterstained with DAPI (A, F and K). Merged images for each time point are shown in E, J and O. Magnified views for every channel are shown (regions indicated by an arrow). Scale bar represents 20µm. At 24h, a fraction of Pax7+/Myf5+ satellite cells also expressed GFP (A-E). Likewise, at 48h the majority of Pax7+/MyoD+ cells were also GFP+ (F-J). At 72h, a proportion of differentiating (Caveolin-1+/Myogenin+) and proliferating (Caveolin-1+/Myogenin-) satellite cells preserved GFP expression (K-O). P, Q and R respectively show the quantification of Pax7/Myf5/GFP, Pax7/MyoD/GFP and Caveolin/Myogenin/GFP in 24, 48 and 72h myofibre cultures from Tg(GBS-GFP) mice. Representative data from three individual mice are shown, with 12 to 15 individual fibres per mouse counted for each time point. Values are mean and error bars indicate standard error of the mean (SEM).

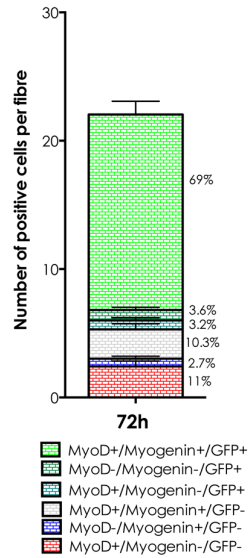


Figure 4.6: Differentiating cells are the main target of Shh response at 72h. EDL muscle fibres from Tg(GBS-GFP) mice were cultured for 72h and immunostained to detect MyoD, Myogenin and GFP. This graph shows the percentage of the different cell populations that respond or not to Shh signalling (GFP+/GFP-). Representative data from three individual mice are shown, with 14 to 15 individual fibres per mouse counted for each time point. Values are mean and error bars indicate SEM.

at 0h did not show any Gli response. At this time point, Pax7+ satellite cells did not express Ki67, which is associated with G1, S, G2 and M phases, consistent with these cells being quiescent (Fig.4.7 A-E). As satellite cells became activated at 24h, they expressed both Ki67 and GFP and continued to do it at 48 and 72h (Fig.4.7 F-J, K-O and P-T), suggesting a correlation with their entry into the cell cycle. Interestingly, some satellite cells that did not respond to Shh signalling or stopped responding to it by the time of analysis remained Ki67+, suggesting that cell cycle exit is not necessarily linked to the cessation of Shh response. This is consistent with my previous finding that some satellite cells undergoing active proliferation/differentiation did not respond to Shh signalling (see section 4.2.3). Taken together, these results indicate that satellite cell responsiveness to Shh signalling coincides with their exit from quiescence and their entry into the cell cycle.

4.2.5 Characterisation of Ptch1 distribution muscle regeneration *in vivo*

To examine whether Shh signalling occurred in satellite cells *in vivo*, I performed a pilot experiment using muscles from Tg:Pax7-EGFP mice¹. To do so, TA muscles were harvested at different time points after CTX-mediated injury and GFP and Ptch1 expression was analysed by immunofluorescence.

¹For this experiment, only one Tg:Pax7-EGFP mouse per time point was analysed because no more mice were available due to breeding issues.

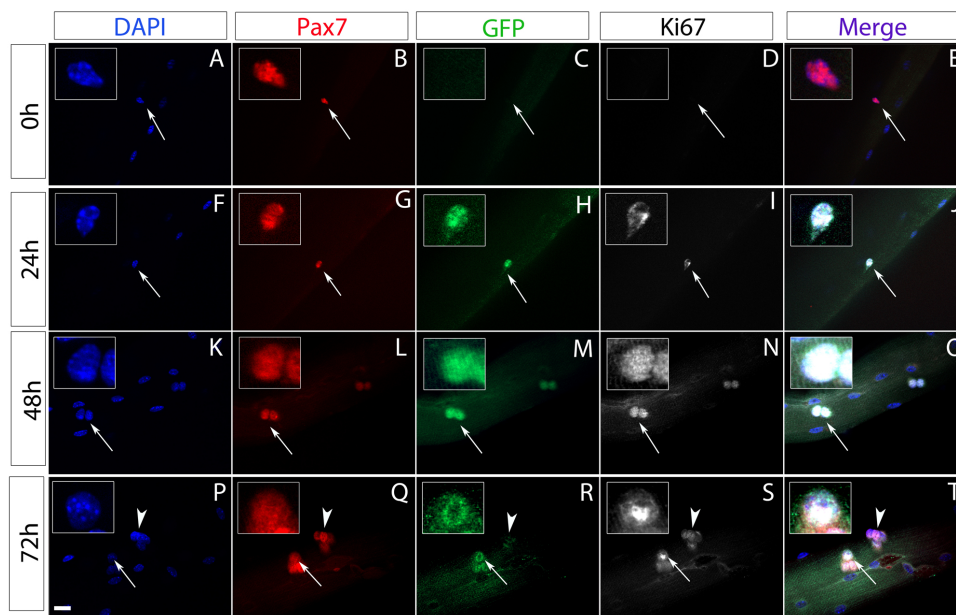


Figure 4.7: Gli response coincides with the entry of satellite into the cell cycle. EDL muscle fibres from Tg(GBS-GFP) mice were cultured for 0, 24, 48 and 72h. Myofibres were immunostained to detect Pax7 (B, G, L and Q), GFP (C, H, M and R) and Ki67 (D, I, N and S). Nuclei were counterstained with DAPI (A, F, K and P). Merged images for each time point are shown in E, J, O and T. Magnified views for every channel are shown (regions indicated by an arrow). Quiescent satellite cells at 0h did not express GFP or Ki67. At 24h, Pax7+ satellite cells co-expressed GFP and Ki67 and these expressions persisted at 48h. At 72h, some Pax7+ cells still co-expressed GFP and Ki67 (arrow) whereas some other Pax7-expressing satellite cells just expressed Ki67 (arrowhead). Representative data from three individual mice are shown. Scale bar represents 20 μ m.

Ptch1 expression was observed in activated satellite cells at 1, 2 and 4 day post-injury muscles (Fig.4.8 2a-2e, 3a-3e and 4a-4e, respectively). There was no Ptch1 expression in GFP+ satellite cells in non-injured and in 7 and 14 day post-injury muscles (Fig.4.8 1a-1e, 5a-5e and 6a-6e). Quantitative analysis showed that the number of GFP+/Ptch1+ cells increased from 1 day (48 cells/mm²) to 2 day post-injury (90.6 cells/mm²) by almost two-fold and then progressively declined between 2 and 4 days post-injury (30 cells/mm²) until no GFP+/Ptch1+ cells were detected at day 7 and 14 post-injury (Fig.4.8 F). In previous results (see section 3.2.2.2), I have shown that during muscle regeneration *in vivo* Pax7+ satellite cells actively proliferate between day 1 and 4, peaking at 2 days and declining by 7 days post-injury. Furthermore, differentiating satellite cells (Myogenin+) can be detected from day 2 post-injury and persist after 14 days, reaching a maximum by 4 days post-injury (see section 3.2.2.3). Together, these data suggest that readily activated satellite cells respond to Shh signalling and that the peak of responsiveness overlaps with the expansion phase of satellite cells (2 days post-injury). Moreover, Ptch1 expression importantly declines beyond 4 days post-injury, which correlates with the reduction in the number of satellite cell undergoing proliferation and an increase of those reaching terminal differentiation. Therefore, consistent with the data I generated with the *ex vivo* culture system, I found that most of the satellite cells undergoing proliferation and early differentiation may respond to Shh signalling *in vivo*.

Interestingly, I also observed a number of Pax7- cells that were positive for Ptch1 (Fig.4.8). These cells were detected at day 1 (55 cells/mm²), day 2 (172 cells/mm²), day 4 (185 cells/mm²), day 7 post-injury (82 cells/mm²) and absent at day 14 post-injury (Fig.4.8 F). A previous study has reported that in ischemic nls-Ptc1-lacZ muscles, Vimentin-expressing fibroblasts are positive for β -galactosidase (Pola et al., 2003), suggesting that the GFP-/Ptch1+ cells observed are fibroblasts. Further analyses would be required to confirm this possibility.

4.3 Discussion

4.3.1 Quiescent satellite cells do not respond to Shh signalling.

In embryonic myogenesis, Shh signalling controls the specification of muscle progenitors, the expression of basement membrane components in the somites and the development of ventral autopod muscles in the limb (Anderson et al., 2009, 2012, Borycki et al., 1999b). In contrast, the role for Shh signalling pathway in postnatal myogenesis is still poorly understood. The origin and identity of Shh-responding cells in muscles had not been fully characterised. In this chapter, I have shown unequivocally that satellite cells respond to Shh signalling in a dynamic manner. For instance, there is no Shh response in satellite

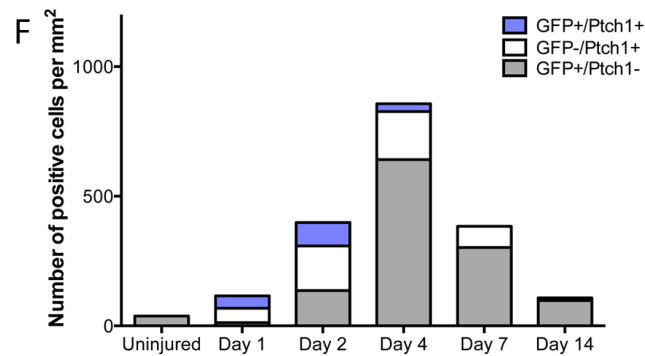
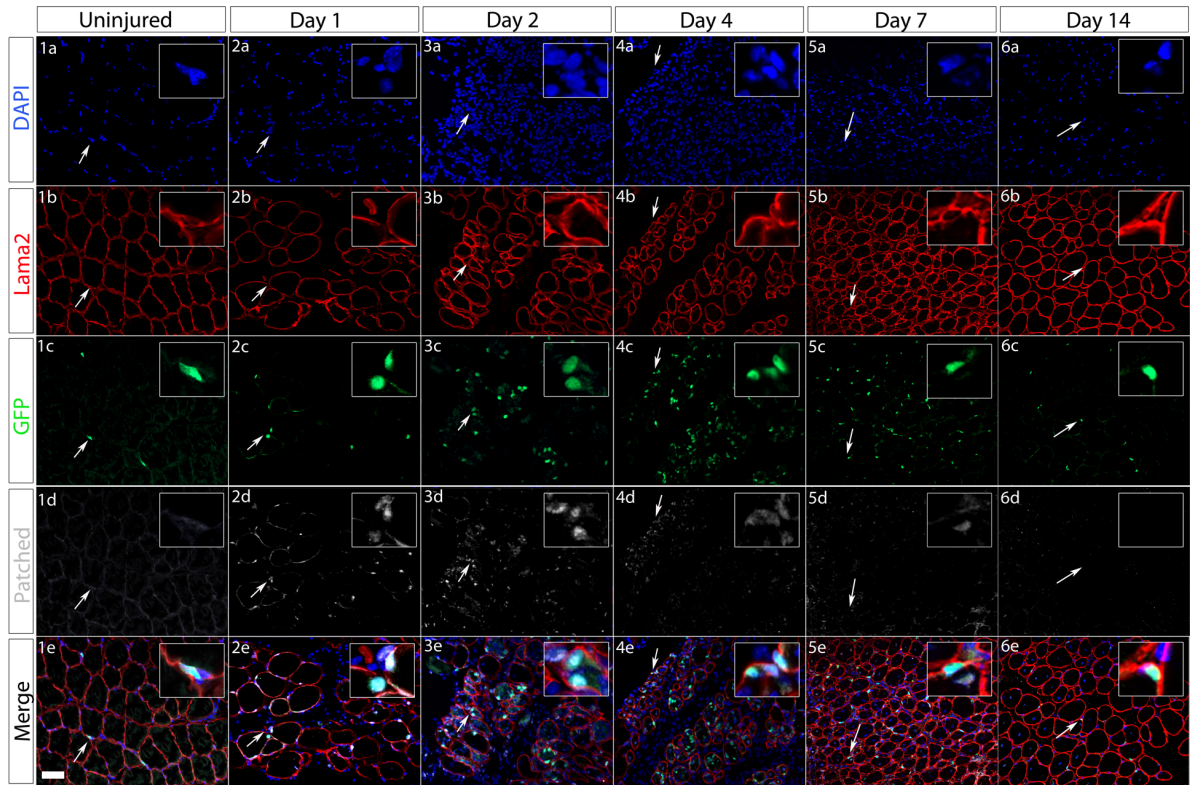


Figure 4.8: Ptch1 expression is associated with satellite cells and non-muscle cells during muscle regeneration *in vivo*. Uninjured and cardiotoxin-injured (1, 2, 4, 7 and 14 days post-injury) TA muscles from Tg:Pax7-EGFP mice were analysed by immunofluorescence using antibodies against Laminin alpha-2 (Lama2, red), GFP (green) and Ptch1 (white). Cell nuclei were counterstained using DAPI (blue). Merge images from four channels are shown for non-injured and 1, 2, 4, 7 and 14 injured muscles in 1e, 2e, 3e, 4e, 5e and 6e, respectively. Magnified views for every channel are shown (regions indicated by an arrow). Scale bar represents 50µm. Quiescent GFP+ satellite cells in uninjured muscles did not express Ptch1 (1a-1e). However, Ptch1 expression was observed at 1, 2 and 4 days following CTX muscle injury in both GFP+ satellite cells and in non-myogenic cells (2a-2e, 3a-3e, 4a-4e). Ptch1 expression in GFP+ cells declined at day 7 post-injury but it was maintained in non-muscle cells (5a-5e). No Ptch1 expression was observed at 14 days post-injury (6a-6e). (F) shows the quantification of Ptch1 and GFP expression in Tg:Pax7-EGFP uninjured and CTX-injured TA muscles. Mean values are shown. Each mean is based on four to six random 0.154 mm² regenerating areas from one mouse per each time point.

cells of freshly isolated myofibres or of non-injured skeletal muscles, which are mostly quiescent. This is the first clear evidence showing the absence of Shh activity in quiescent satellite cells, as previous studies used myoblast cell lines or primary cell cultures, which lack quiescent cells (Elia et al., 2007, Koleva et al., 2005).

So, how do quiescent satellite cells become responsive to Shh signalling? Several mechanisms for the control of Shh responsiveness have been previously reported during embryogenesis. In the developing somite, the initiation of Shh responsiveness depends on the activation of *Gli2* and the repression of *Gli3* by surface ectoderm and neural tube-derived canonical Wnt signalling (Borycki et al., 2000). Canonical Wnt signalling promotes satellite cell progression through the myogenic program, especially during differentiation (Brack et al., 2008). Although loss of β -catenin in satellite cells ($\text{Pax7}^{\text{CreERT2/+}};\beta\text{-catenin}^{\text{flox/flox}}$) does not affect muscle regeneration, constitutive activation of β -catenin in satellite cells prolongs the regenerative response upon muscle injury (Murphy et al., 2014). Conditional removal of the tumour suppressor adenomatous polyposis coli (APC), a component of the β -catenin destabilisation complex in Pax7+ satellite cells results in cell death and failure to enter the cell cycle and is associated with increased levels of β -catenin (Parisi et al., 2015). Thus, although inactivation of Wnt signalling appears to be required for satellite cell progression through the cell cycle, it is unclear whether Wnt signalling acts upstream Shh to regulate the expression of *Gli* genes in satellite cells. To address this, Shh response in satellite cells could be assessed in the absence of Wnt signalling by using specific Wnt signalling inhibitors on myofibres cultures from Tg(GBS-GFP) mice or in β -catenin conditional knockout mice. An alternative mechanism may be that used in the neural tube, where Notch signalling is required for maintaining neural progenitor cells (NPCs) in an undifferentiated state and for the maintenance of Shh responsiveness (Huang et al., 2012). Notch signalling mediates also the trafficking and accumulation of Smo in the primary cilia, sensitising NPCs to Shh signals (Kong et al., 2015, Stasiulewicz et al., 2015). Given that Notch signalling is required to maintain satellite cells in a quiescent state and that its activity decreases as satellite cells become activated (Bjornson et al., 2012, Mourikis et al., 2012b), it seems unlikely that Notch signalling induces Shh response in satellite cells as Shh response is observed in activated satellite cells, when Notch signalling activity decreases. Consistent with the activity of Notch in quiescent satellite cells, recent work from our lab uncovered that quiescent satellite cells have primary cilia, which are rapidly resorbed when satellite cells become activated (Jaafar Marican et al., unpublished data). Therefore, my observations converge towards a possible mechanism of Shh signalling independent of primary cilia. The primary cilium is critical for processing Gli proteins into repressors and it is also important for the accumulation of Shh signalling components such as Gli2 and Smo (Huangfu et al., 2003). However, some studies have shown that Smo accumulation in the primary cilia is not a prerequisite for Shh signalling

activation (Chong et al., 2015, Fan et al., 2014). For instance, the Smo/SAG complex or SmoM2 protein, which carries activating oncogenic mutations, can signal without ciliary accumulation (Fan et al., 2014). Moreover, disruption of Shh signalling activity can be achieved even when Smo is enriched in the cilia (Chong et al., 2015, Rohatgi et al., 2009, Yang et al., 2015), indicating that Smo accumulation in the primary cilium and Shh activation via Gli proteins can be uncoupled (Chen et al., 2009). It remains to be seen, however, whether any Shh signalling component is enriched in the primary cilia of quiescent satellite cells.

4.3.2 Activated satellite cells become responsive to Shh signals.

I have shown that activated Pax7+ satellite cells become responsive to Shh signalling both *ex vivo* and *in vivo*. Furthermore, Shh response in satellite cells coincides with their entry into the cell cycle and persists during their expansion. Indeed, activated/proliferating satellite cells are highly responsive to Shh, but Shh response is down-regulated over time, especially in self-renewing satellite cells and terminally differentiated cells. This heterogeneous response to Shh signalling may arise from an asynchronous initiation of the cell cycle (Siegel et al., 2011) and from the known heterogeneity of satellite cells (Kuang et al., 2007). Shh response, as measured through Ptch1 accumulation was more widespread than Shh response measured using the Gli reporter transgenic mice Tg(GBS-GFP). This may reflect some intrinsic differences between the control of Ptch1 up-regulation and Gli activity, in particular in the stability of the Gli proteins (activated versus repressor forms). However, I favour the possibility that low levels of Gli activity are not detected by the Tg(GBS-GFP) reporter mouse line, and this may account for the difference in the number of Ptch1+ versus GFP+ cells (Balaskas et al., 2012, Kahane et al., 2013). Therefore, my working model for the dynamics of Shh response is described in Fig.4.9. First, quiescent satellite cells do not respond to Shh signalling. Upon activation or muscle injury, satellite cells become responsive to Shh signals and up-regulate Ptch1 expression/Gli response. As satellite cells enter the proliferation phase, Shh response peaks and persists during early satellite cell differentiation to become progressively down-regulated as cells complete differentiation or self-renew. This down-regulation may be linked to the up-regulation of Gli3 and Hip, which are both repressors of Shh signalling, during the differentiation phase. Another factor that may contribute to the termination of Shh signalling is the negative feedback exerted by Ptch1 expression (Chen and Struhl, 1996).

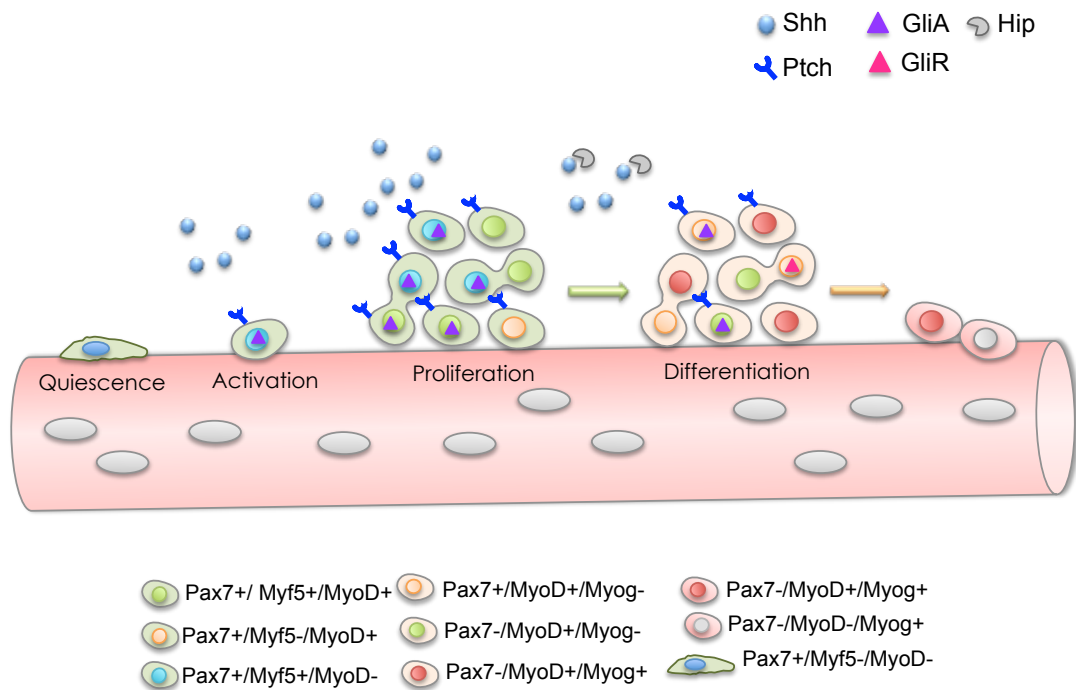


Figure 4.9: Working model of Shh signalling activity in satellite cells. During the initial stages of adult myogenesis, activated satellite cells become responsive to Shh signalling and up-regulate Ptch1 expression. During the expansion phase, Shh acts on proliferating satellite cells. Later, differentiating satellite cells may express specific Shh signalling repressors (Hip and Gli3) and may become less responsive to Shh signalling, resulting in lower levels of Ptch1. This lesser response to Shh signalling may facilitate satellite cell differentiation and/or the return to quiescence.

4.3.3 Source of the Shh ligand during adult myogenesis *ex vivo* and *in vivo*.

The response of satellite cells to Shh signalling suggests the presence of ligands during the activation phase of muscle regeneration. *Shh* mRNAs have been observed in the interstitium of skeletal myofibres and in whole skeletal muscle preparations following mechanical crush, CTX injury and ischemia (Pola et al., 2003, Renault et al., 2013a, Straface et al., 2009). The expression of the Shh ligand has also been reported in Pax7+ cells and in Ptch1+ interstitial cells, suggesting an autocrine signalling mechanism (Elia et al., 2007, Pola et al., 2003). However, my own PCR data showed that no *Shh* mRNA could be detected at any time point in *ex vivo* cultured myofibres, arguing against Shh being produced by myofibres or satellite cells. Where does Shh come from? In the *ex vivo* system, it is highly likely that Shh is present in the chick embryo extract added to the culture medium. *In vivo*, as Pola et al. reported, it is possible that Shh is synthesised and released by interstitial cells within skeletal muscles (Pola et al., 2003). However, it is also possible that secreted Shh proteins are maintained inactive in the muscle tissue and recruited following muscle injury. A precedent for this was reported in the cerebellum, where Shh interacts with different ECM components, including Vitronectin and Laminin-1 (Blaess et al., 2004, Pons et al., 2001), indicating that Shh can be sequestered in the ECM. Shh binding partners may also limit the availability of the protein by sequestering it away from its target cells. This is the case of the Boi-Hh interaction, where Boi sequesters the Hh ligand in apical cells to regulate its levels in the follicle stem cell niche of the *Drosophila* ovary (Hartman et al., 2010). Likewise, the binding of Shh to Ptch1, Ptch2 and Hip1 restricts its activity in patterning the ventral neural tube (Holtz et al., 2013, Jeong and McMahon, 2005). Finally, it is also possible that Shh is delivered systemically in the event of muscle injury. For instance, Shh is produced by stromal cells of the bone marrow and lymph nodes, and this secreted protein could be delivered via lymphatic vessels connected to skeletal muscles (Dierks et al., 2007, Korthuis, 2011). Shh is also synthesised by smooth muscle cells and can be found in the blood plasma, opening the possibility that this protein can be delivered to skeletal muscles through blood vessels (El-Zaatari et al., 2012, Yao et al., 2014). Finally, Shh protein could be delivered to skeletal muscles through peripheral nerves, as in the case of rodent incisors and adult mouse skin (Brownell et al., 2011, Zhao et al., 2014). Nevertheless, the ultimate experiment to determine which cell population is the source of the Shh protein will be the analysis of different cell types from CTX-injured muscles isolated by FACS, including satellite cells, fibroblasts, interstitial, blood and immune cells before, after and at the time of satellite cell activation *in vivo*.

4.3.4 Non-muscle cells may be influenced by Shh signalling during adult skeletal muscle regeneration.

In vivo, I observed that non-myogenic cell types respond to Shh signalling. This is consistent with a previous publication reporting that β -galactosidase expression was observed in Vimentin+ fibroblasts upon ischemia in nls-Ptc1-lacZ muscles (Pola et al., 2003). The high number of non-muscle cells that express Ptch1 in my *in vivo* analysis is consistent also with the abundant number of Tcf4+ fibroblasts found in skeletal muscles following BaCl₂ injury (Murphy et al., 2011). This suggests that Shh response may occur in fibroblasts in addition to satellite cells. This is interesting given that depletion of fibroblasts in skeletal muscles affects muscle regeneration by inducing premature differentiation and depletion of satellite cells (Murphy et al., 2011).

Endothelial cells and macrophages are other non-myogenic cells that have been reported to respond to Shh signalling (Fabian et al., 2012, Ghorpade et al., 2013, Yao et al., 2014). Indeed, the induction of Shh signalling activity in endothelial cells is in line with the role of this pathway in promoting angiogenesis following skeletal muscle ischemia (Pola et al., 2003, Straface et al., 2009). However, the expression of Shh signalling components has not been reported yet in these cell types during muscle regeneration *in vivo*. Investigation of the role of the Shh signalling in these cells would highlight a role for Shh signalling in the coordinated response between satellite cells and non-myogenic cells during muscle regeneration.

EFFECT OF SHH SIGNALLING PATHWAY ACTIVATION AND BLOCKADE ON SATELLITE CELL PROGRESSION THROUGH MYOGENESIS *ex vivo*.

5.1 Introduction

I have previously shown that activated satellite cells respond to Shh signalling *ex vivo* and *in vivo*. During adult myogenesis, Shh signalling response corresponds with the entry of satellite cells into the cell cycle and it persists during their expansion. Notably, Shh signalling response becomes gradually down-regulated as satellite cells enter differentiation or return to quiescence. Thus, Shh signalling activity in satellite cells is transient and accompanies activation, expansion and early differentiation of adult myogenesis.

Shh signalling has multiple roles in patterning, cell proliferation and differentiation during early development. Previous studies from the lab have shown that Shh signalling controls skeletal myogenesis in the embryo by activating the muscle-specific transcription factor *Myf5* and genes encoding basement membrane proteins (Anderson et al., 2009, 2012, Borycki et al., 1999b). In contrast, in skeletal muscle regeneration, Shh has been proposed to function as a proliferation and differentiation factor that can improve muscle repair (Piccioni et al., 2014a). However, *in vitro* analyses of muscle cell lines and primary myoblasts have yielded contradictory results, some demonstrating that Shh signalling promotes proliferation (Koleva et al., 2005, Straface et al., 2009) differentiation (Elia et al., 2007, Straface et al., 2009) and cell survival (Koleva et al., 2005) and others showing that it inhibits muscle differentiation (Koleva et al., 2005). To date, it is unclear how Shh

signalling affects satellite cell behaviour, and in particular, how this signalling pathway may regulate the myogenic program.

In this chapter, I investigated the effect of Shh signalling in satellite cells from myofibres cultured *ex vivo*. I performed gain and loss-of-function experiments using Shh signalling agonists and antagonist to dissect the stages of adult myogenesis requiring Shh signals.

5.1.1 Hypothesis and aim

As activated satellite cells respond to Shh signals, I hypothesised that stimulation or blockade of Shh signalling will impair satellite cell behaviour. Therefore, the aim of this chapter was to manipulate pharmacologically the Shh signalling pathway in cultured myofibres and investigate the effects on satellite cell-mediated myogenesis *ex vivo*.

5.2 Results

5.2.1 Effect of the stimulation of the Shh signalling pathway in satellite cells by the Smo agonist SAG

The induction of Shh responsiveness during satellite cell activation suggests a role for Shh signalling in adult myogenesis. To investigate the function of Shh signalling in muscle stem cells, I used experimental approaches to stimulate Shh signalling in the *ex vivo* myofibre culture system and examined the effect on satellite cell behaviour. An initial concentration of 100nM was chosen based on the dose-response curve of SAG in the Shh-LIGHT2 cell line, which is a NIH3T3 clone that incorporates a Gli-luciferase reporter (Chen et al., 2002b). However, a pilot experiment (proof of concept) was also performed to determine whether this SAG concentration had an effect on satellite cells, in which EDL myofibres isolated from C57BL/6 mice were cultured in the presence or in the absence of a SAG gradient (from 20nM to 500nM) for 72h. 100nM was shown to be the SAG concentration that yielded the highest mean value of Caveolin-1+ and Myogenin+ cells at 72h (Fig.5.1 A). Interestingly, higher concentrations of SAG did not show any effect on satellite cells, which was consistent with the finding that concentrations closer and higher than 1 μ M dramatically decrease SAG-mediated effect (Chen et al., 2002b). To further assess whether this concentration was able to modulate Shh response, C₂C₁₂ cells were cultured for 48h in the presence of DMSO (control) or 100nM of SAG and cDNA was prepared from these cultures. *Gli1* mRNA expression levels were evaluated by semi-quantitative RT-PCR. cDNAs from E.11.5 mouse embryos and H₂O were used as positive and negative controls, respectively. I observed an increased of 59 \pm 11.3% in the expression

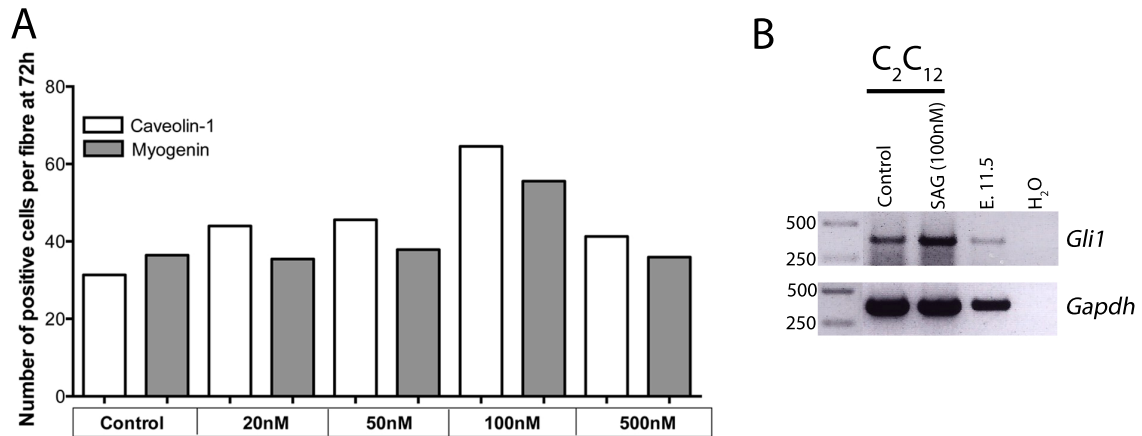


Figure 5.1: Proof of concept experiment to test the effect of the Smoothened agonist SAG on muscle cells. (A) EDL muscle fibres from C57BL/6 mice were cultured for 72h in the presence of DMSO (control) or a gradient of SAG (from 20nM to 500nM). Myofibres were immunostained to detect Caveolin-1 and Myogenin. Treatment with 100nM of SAG yielded the highest number of Caveolin-1+ and Myogenin+ cells per fibre at 72h. Mean values are shown. Each mean is based on 15 myofibres from one mouse. (B) mRNA expression levels in C₂C₁₂ cells after SAG (100nM) treatment for 48h were evaluated by semi-quantitative RT-PCR analysis using *Gapdh* as internal control. Changes in gene expression were calculated by normalising *Gli1* to *Gapdh* band intensity using the ImageJ software. *Gli1* expression was visibly up-regulated in the presence of SAG compared to the control. Representative images of C₂C₁₂ cDNA coming from two independent sets of cell cultures are shown.

of *Gli1* in the presence of SAG compared to the control (DMSO) (Fig.5.1 B). Therefore, this concentration was used for further experiments.

Single EDL muscle fibres from C57BL/6 mice were cultured in the presence of the Smoothened agonist SAG (100nM) or DMSO (control) and the distribution of Pax7/Myf5, Pax7/ MyoD and Caveolin-1/Myogenin was determined by immunofluorescence analysis at 24, 48 and 72h, respectively. Treatment of isolated myofibres with 100nM of SAG for 24h did not have any obvious effect on satellite cell behaviour, since Pax7+ cells were activated normally as shown by the co-expression of Myf5 and Pax7 compared to control (Fig.5.2 A-D and A'-D'). Moreover, the number of satellite cells did not change at 24h upon Shh signalling stimulation (Fig.5.2 M). Likewise, treatment with SAG did not have any effect on the number of Pax7+ nor MyoD+ satellite cells at 48h (Fig.5.2 E-H, E'-H' and M). Finally, no significant effect was observed in the number of Caveolin-1+ and Myogenin+ cells at 72h after SAG treatment, although a tendency towards larger clusters of differentiating satellite cells attached to the fibres under SAG conditions compared to the control was observed (Fig.5.2 I-L and I'-L' and M). These results suggest that stimulation of the Shh signalling pathway using SAG is not sufficient to help expand the population of satellite cells *ex vivo*. Moreover, SAG effect is highly variable from experiment to experiment and may not affect all satellite cells in the same way.

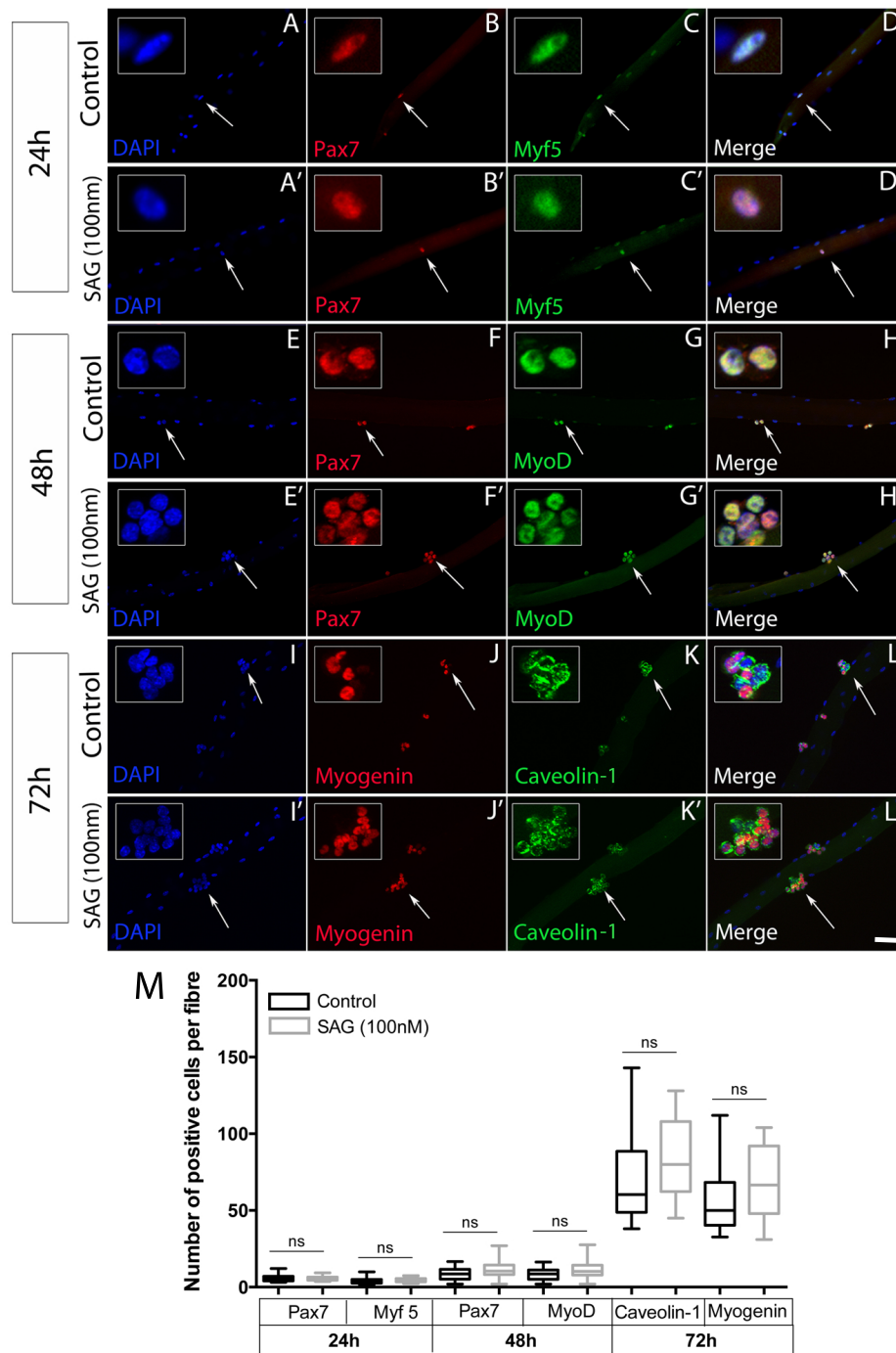


Figure 5.2: Stimulation of Shh signalling with SAG does not affect the number of satellite cells *ex vivo*. EDL muscle fibres from C57BL/6 mice were cultured for 24, 48 and 72h in the presence of DMSO (control) or SAG (100nM). Myofibres were immunostained to detect Pax7 in red (B, B', F and F'), Myf5 (C and C'), MyoD in green (G and G'), Myogenin in red (J and J') and Caveolin-1 in green (K and K'). Nuclei were counterstained with DAPI in blue (A, A', E, E', I and I'). Merged images for each time point are shown in D, D', H, H', L and L'. Magnified views for every channel are shown (regions indicated by an arrow). SAG treatment did not affect the behaviour of satellite cells at 24h. At 48h and 72h following stimulation of the Shh signalling pathway with SAG, larger cluster of satellite cells could be observed. Scale bar represents 50 μ m. (M) shows the quantitative analysis of the number of satellite cells at 24h (Pax7 and Myf5), 48h (Pax7 and MyoD) and 72h (Caveolin-1 and Myogenin) per fibre in the presence of DMSO (black boxes) or 100nM of SAG (gray boxes). No significant difference in the number of satellite cells under SAG treatment was observed. Representative data from three individual mice are shown, with 10 to 20 individual fibres per mouse for each time point. Boxes represent interquartile ranges (RQ) and whiskers show minimum and maximum values. Statistical analysis was performed using Student's t-test.

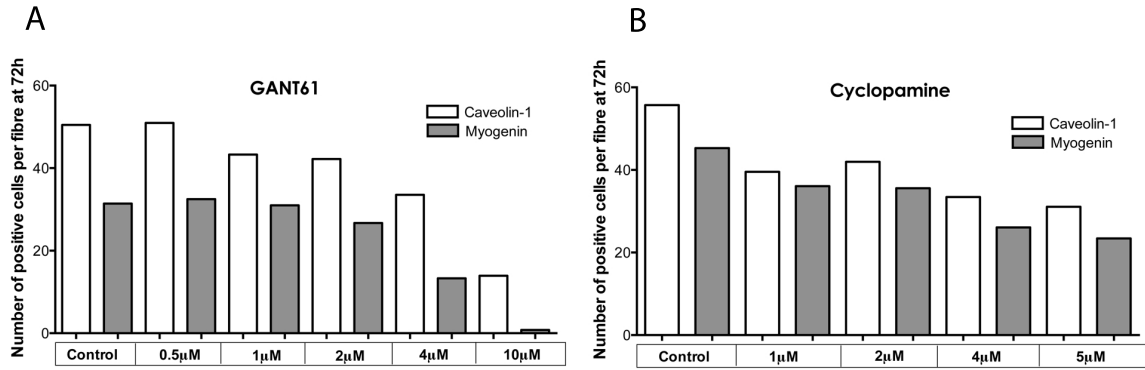


Figure 5.3: Pilot experiment to test a concentration gradient of the Gli inhibitor GANT61 and the Smoothened agonist Cyclopamine on *ex vivo* myofibre cultures. EDL muscle fibres from C57BL/6 mice were cultured for 72h in the presence of DMSO (control) or a gradient of GANT61 (A) (from 0.5µM to 10µM) and Cyclopamine (B) (from 1µM to 5µM) and myofibres were immunostained to detect Caveolin-1 and Myogenin. (A) Treatment with 4 and 10µM of GANT appeared to decrease the number of both Caveolin-1+ and Myogenin+ cells per fibre at 72h. (B) Treatment with 4 and 5µM of Cyclopamine showed a tendency towards fewer Caveolin-1+ and Myogenin+ cells per fibre at 72h. Mean values are shown. Each mean is based on 20 to 30 myofibres from one mouse.

5.2.2 Chemical blockade of the Shh signalling pathway reduces the number of satellite cells in cultured myofibres

As Shh signalling pathway stimulation showed a tendency towards an increase in satellite cell numbers, I asked whether Shh signalling was necessary for satellite cell activity. To block Shh signalling in adult muscle stem cells, I inhibited the Shh pathway activity using two pharmacological inhibitors: cyclopamine, which directly binds to the receptor Smoothened and impedes its function (Taipale et al., 2000) and GANT61, which represses Gli-mediated transcription by acting downstream of Smoothened (Lauth et al., 2007). An initial concentration of 10µM of GANT61 was chosen based on the dose-response curve of GANT61 in the NIH 3T3 cell line, where IC₅₀ was of around 5µM (Lauth et al., 2007). However, this concentration used by Lauth and colleagues had a cytotoxic effect on the myofibres. The compound was then re-tested in a pilot experiment in our system by applying a concentration gradient on 72h-cultured myofibres and the ideal working concentration found was 4µM (Fig.5.3 A). On the other hand, the concentration of 5µM of cyclopamine was chosen based on a gradient pilot experiment on 72h-cultured myofibres (Fig.5.3 B). This cyclopamine concentration was also shown to be optimal to inhibit a Gli-luciferase reporter in the NIH3T3 cell line (Taipale et al., 2000).

An initial proof-of-concept experiment was performed in which individual EDL muscle fibres from Tg(GBS-GFP) mice were cultured in the presence of either DMSO (control), 4µM of GANT61 or 5µM of cyclopamine and the distribution of GFP-expressing cells was determined by immunofluorescence analysis at 24, 48 and 72h (Fig.5.4 A-E, A'-

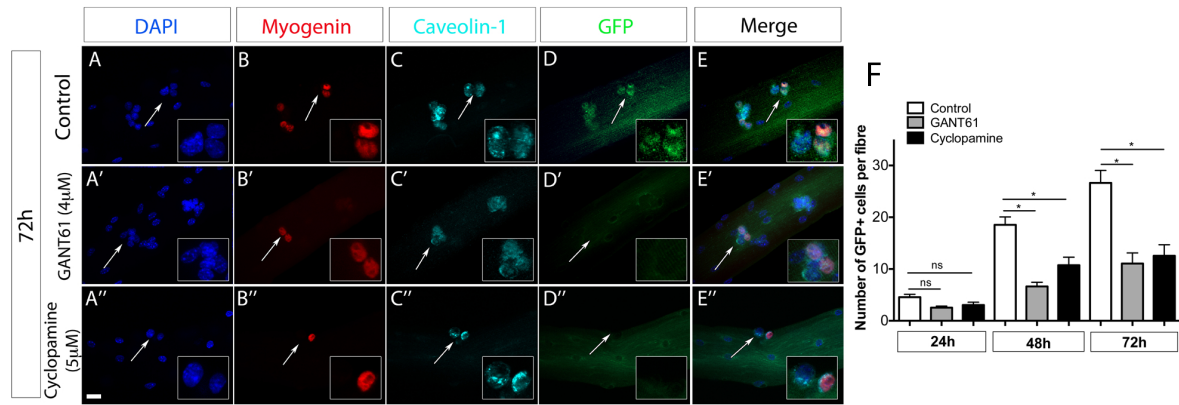


Figure 5.4: Cycloamine and GANT61 effectively block Shh response in satellite cells *ex vivo*. EDL muscle fibres from Tg(GBS-GFP) mice were cultured for 72h in the presence of DMSO (control), Cycloamine (5µM) or GANT61 (4µM). Myofibres were immunostained to detect Myogenin (red, B, B' and B''), Caveolin (cyan, C, C' and C'') and GFP (green, D, D' and D''). Nuclei were counterstained with DAPI (blue, A, A' and A''). Merged images for each time point are shown in E, E' and E''. Magnified views for every channel are shown (regions indicated by an arrow). Scale bar represents 20µm. (F) shows the quantitative analysis of the number of GFP+ satellite cells at 24h, 48h and 72h per fibre in the presence of DMSO (white), 4 µM of GANT61 (gray) or 5µM of cycloamine (black). There was no difference in the number of GFP+ cells at 24h treated with either GANT61 nor cycloamine. In contrast, at 48h and 72h there was a significant difference in the number of GFP-expressing cells with both treatments compared to control conditions (p=0.0143 and p=0.0081, respectively). Values are mean and SEM. Each mean is based on 10 to 15 myofibres from two mice per time point. Statistical analysis was performed using one-way ANOVA.

E' and A''-E''). Immunofluorescence analysis at 24h showed that the number of Shh responsive satellite cells (GFP+) was not significantly different after culturing myofibres in the presence of either GANT61 nor cycloamine compared to the control (Fig. 5.4 F). However, by 48h, a reduction of 64% and 42% of GFP+ satellite cells was observed upon GANT61 and cycloamine treatment, respectively (Fig.5.4 F). Finally, more than 50% reduction of GFP expression was observed at 72h with both inhibitors (Fig.5.4 A-E, A'-E' and A''-E''), indicating that cycloamine and GANT61 can effectively block Shh signalling response in satellite cells *ex vivo*.

Next, muscle fibres from C57BL/6 mice were cultured in the presence of cycloamine (5µM) or DMSO (control) and the distribution of Pax7/Myf5, Pax7/ MyoD and Caveolin-1/Myogenin was determined by immunofluorescence analysis at 24, 48 and 72h, respectively. Blockade of the Shh signalling pathway with cycloamine in isolated myofibres for 24h did not affect the activation of satellite cells, since the number and proportions of Pax7+ and Myf5+ cells remained similar to control conditions (Fig.5.5 A-D, A'-D' and M). Likewise, treatment with cycloamine did not change the number of Pax7+ and MyoD+ satellite cells at 48h compared to the control (Fig.5.5 E-H, E'-H' and M). Interestingly, myofibres treated with cycloamine for 72h showed a significant decrease in the number of both Caveolin-1+ (44%) and Myogenin+ (47%) cells (Fig.5.5 M), with

smaller clusters of differentiating satellite cells attached to the fibres compared to the control (Fig.5.5 I-L and I'-L'). These results suggest that inhibition of Shh signalling using cyclopamine leads to a decrease in satellite cell numbers, including cells undergoing differentiation *ex vivo*.

A similar experiment blocking the Shh pathway activity with GANT61 (5 μ M) or DMSO (control) was carried out. Treatment of isolated C57BL/6 myofibres with GANT61 had no effect on satellite cells at 24h (Fig.5.6 A-D, A'-D' and M), confirming previous observations with cyclopamine and indicating that Shh signalling is not required for satellite cell activation. Importantly, GANT61 treatment resulted in a decrease in the number of proliferating and differentiating satellite cells at both 48h and 72h compared to control. For instance at 48h upon GANT61 treatment, a reduction of 42% in the number of Pax7+ and MyoD+ cells was observed compared to control conditions (Fig.5.6 E-H, E'-H' and M). Furthermore, blockade of Gli activity with GANT61 at 72h caused a reduction in the number of Caveolin-1+ and Myogenin+ cells by 40% and 60%, respectively (Fig.5.6 I-L, I'-L' and M). Taken together, these data corroborate that blocking Shh signalling results in a decrease in satellite cell expansion with a concomitant reduction in satellite cell differentiation.

5.2.3 Blocking Shh signalling causes a delay in satellite cell-mediated myogenesis *ex vivo*

Treatment of isolated myofibres with Shh signalling inhibitors causes an overall reduction in the number of satellite cells at 72h, particularly in differentiating cells (Myogenin+) compared to control conditions. Given that by 48h in *ex vivo* culture satellite cells have completed their first cell divisions and beyond that point they greatly expand, I decided to look at an intermediate time point between 48 and 72h in order to identify in more details the satellite cell population affected by Shh signalling blockade. To do so, I treated single myofibres with GANT61, harvest them at 60 and 72h after culture and performed a Pax7/MyoD immunofluorescence analysis. 48h-cultured fibres in the presence of DMSO or GANT61 were also included and taken as starting point for the analysis.

As previously shown, at 48h in control conditions, 93% of total cells counted were proliferative progenitor cells (Pax7+/MyoD+), whereas 10% were self-renewing cells (Pax7+/MyoD-) and 7% were progenitors entering differentiation (Pax7-/MyoD+) (Fig.5.7 I). Upon GANT61 treatment, there was a 2-fold reduction in the number of Pax7+/MyoD+ cells (Fig.5.7 I). However, Shh signalling inhibition just caused a subtle change in the proportion of the distinct satellite cell populations: around 94% of satellite cells were now Pax7+/MyoD+, 3.7% were just Pax7+ and 2.3% expressed MyoD only (Fig.5.7 I). These results suggest that inhibition of Shh signalling leads to an increase in the proportion of

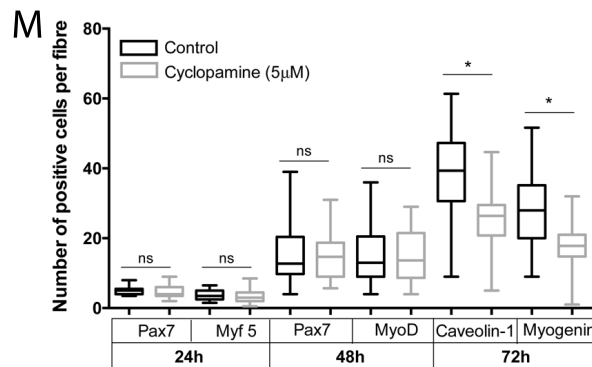
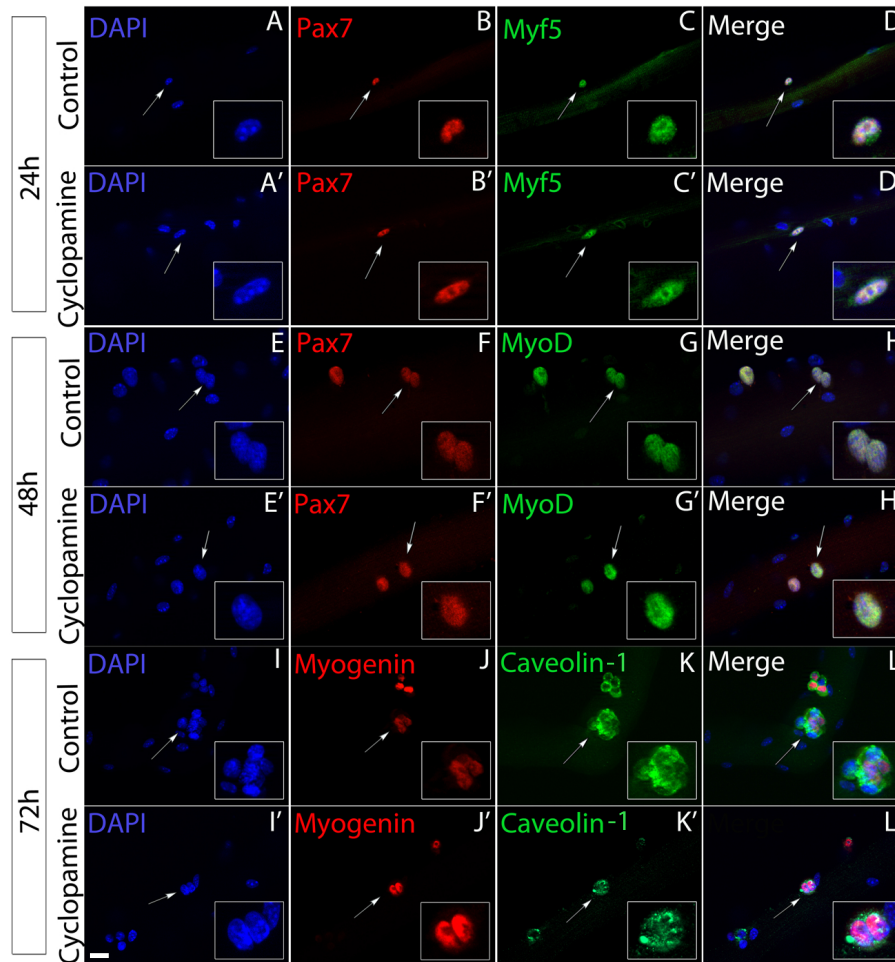


Figure 5.5: Blockade of Shh signalling with cyclopamine decreases the number of satellite cells *ex vivo*. EDL muscle fibres from C57BL/6 mice were cultured for 24, 48 and 72h in the presence of DMSO (control) or Cyclopamine (5µM). Myofibres were immunostained to detect Pax7 (red, B, B', F and F'), Myf5 (green, C and C'), MyoD (green, G and G'), Myogenin (red, J and J') and Caveolin-1 (green, K and K'). Nuclei were counterstained with DAPI (blue, A, A', E, E', I and I'). Merged images for each time point are shown in D, D', H, H', L and L'. Scale bar represents 20µm. (M) shows the quantitative analysis of the number of satellite cells at 24h (Pax7 and Myf5), 48h (Pax7 and MyoD) and 72h (Caveolin-1 and Myogenin) per fibre in the presence of DMSO (black boxes) or 5µM of cyclopamine (gray boxes). There was a significant difference in the number of Caveolin+ (p=0.0305) and Myogenin+ (p=0.0299) cells at 72h upon Smoothened inhibition with cyclopamine compared to the control. Representative data from three individual mice are shown, with 10 to 30 individual fibres per mouse for each time point. Boxes represent interquartile ranges (RQ) and whiskers show minimum and maximum values. Statistical analysis was performed using Student's t-test.

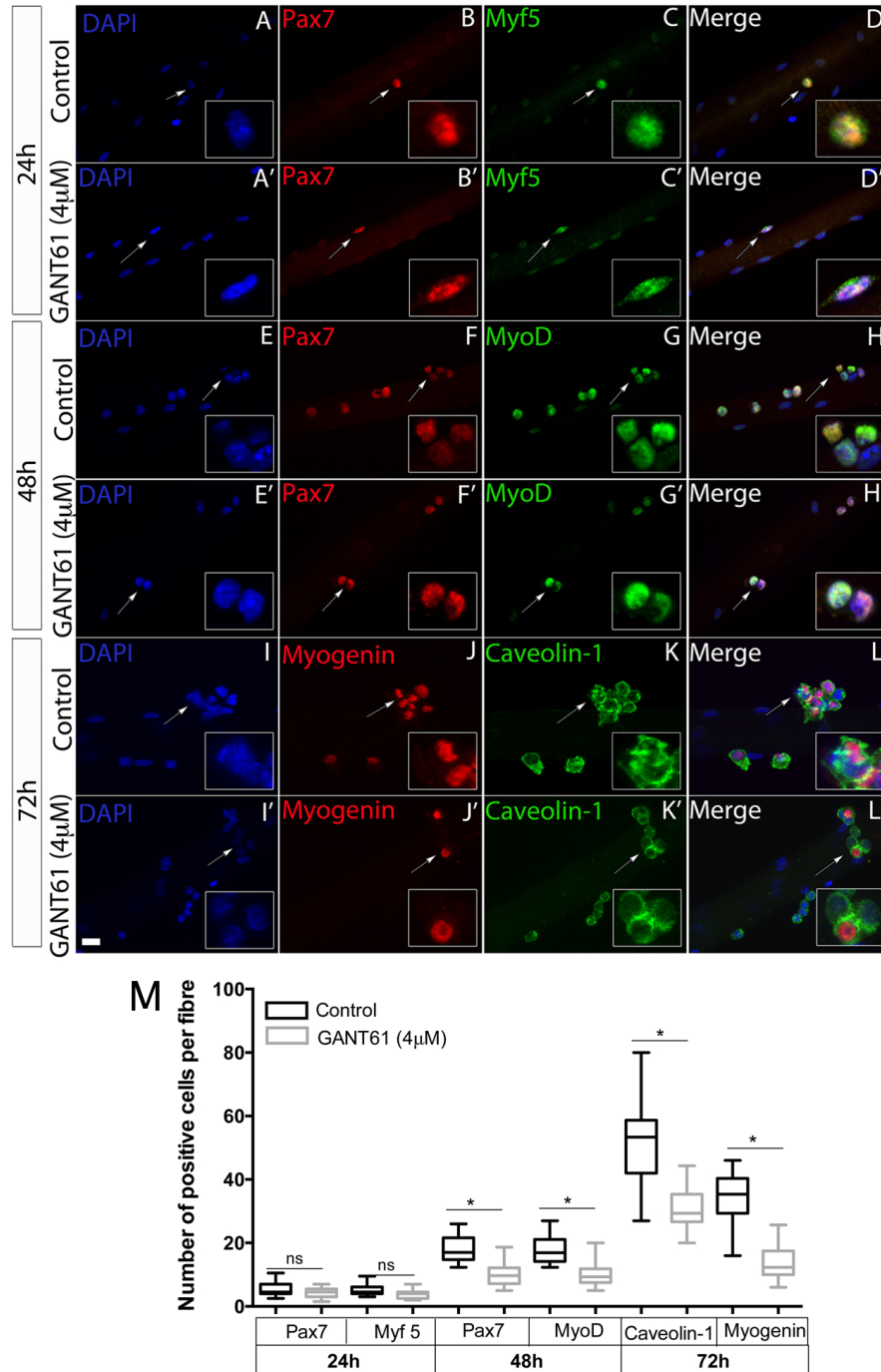


Figure 5.6: Inhibition of Shh signalling with GANT61 affects satellite cell expansion *ex vivo*. EDL muscle fibres from C57BL/6 mice were cultured for 24, 48 and 72h in the presence of DMSO (control) or GANT61 (4 μ M). Myofibres were immunostained to detect Pax7 (red, B, B', F and F'), Myf5 (green, C and C'), MyoD (green, G and G'), Myogenin (red, J and J') and Caveolin-1 (green, K and K'). Nuclei were counterstained with DAPI (blue, A, A', E, E', I and I'). Merged images for each time point are shown in D, D', H, H', L and L'. Magnified views for every channel are shown (regions indicated by an arrow). Scale bar represents 20 μ m. M) shows the quantitative analysis of the number of satellite cells at 24h (Pax7 and Myf5), 48h (Pax7 and MyoD) and 72h (Caveolin-1 and Myogenin) per fibre in the presence of DMSO (black boxes) or 4 μ M of GANT61 (gray boxes). There was a significant difference in the number of Pax7+ ($p=0.0412$) and MyoD+ ($p=0.0483$) cells at 48h upon GANT61 treatment. Moreover, there was a significant decrease in the number of Caveolin+ ($p=0.0342$) and Myogenin+ ($p=0.0136$) cells at 72h upon Gli inhibition compared to the control. Representative data from three individual mice are shown, with 13 to 25 individual fibres per mouse for each time point. Boxes represent interquartile ranges (RQ) and whiskers show minimum and maximum values. Statistical analysis was performed using Student's t-test.

proliferative progenitor cells (Pax7+/ MyoD+).

Between 48 and 60h, proliferating progenitor cells begin differentiating leading to a 2.5-fold reduction in the proportion of Pax7+/MyoD+ (22.2%) cells and a 3 and a 7-fold increase in the number of Pax7+/MyoD- (26.4%) and Pax7-/MyoD+ (51.4%) cells, respectively at 60h in control conditions (Fig.5.7 A-D, I and J). This trend exacerbates at 72h in control conditions, where 6% of satellite cells were Pax7+/MyoD+, 32% were Pax7+/MyoD- and 62% expressed MyoD only (Fig.5.7 E-H, I and J). This shows that over time the population of proliferative progenitors (Pax7+/MyoD+) decreases with a concomitant increase in the number of differentiating satellite cells (Pax7-/MyoD+), which progressively up-regulate Myogenin expression and reach terminal differentiation.

Following inhibition of Shh signalling with GANT61, a 30% and 26% reduction in the overall number of satellite cells was observed at 60 and 72h, respectively (Fig.5.7 I and J). Concomitantly, proliferating progenitor cells (Pax7+/MyoD+, 58.9% compared to 22.2%) were maintained and differentiating cells (Pax7-/MyoD+, 28.8% compared to 51.4%) and self-renewing cells (Pax7+/MyoD-, 12.3% compared to 26.4%) were fewer at 60h upon GANT61 treatment (Fig.5.7 A'-D', I and J). By 72h, 32% of satellite cells were still proliferating (Pax7+/MyoD+) in GANT61 treated cultures whereas 22% were Pax7+/MyoD- and 46% were Pax7-/MyoD+ (Fig.5.7 E'-H', I and J). This indicates that a higher proportion of cells remained proliferative (Pax7+/MyoD+) at both 60 and 72h in the presence of GANT61 compared to control conditions. Interestingly, the distribution of satellite cell populations in GANT61-treated cultures at 72h resembles that of non-treated cultures at 60h (Fig.5.7 I, compare bars 3 and 6), suggesting that blocking Shh signalling causes a 12-hour delay in the progression of satellite cells through the myogenic program.

As shown in Fig.5.7 I and J, at 60h upon GANT61 treatment there was a reduction in the proportion of Pax7+/MyoD- cells. This cell population comprises cells that have not switched on MyoD yet and cells that have returned to quiescence. To determine which cell population was predominantly affected at this point, I performed an immunofluorescence analysis of Pax7/Myf5 in 60h-cultured myofibres under GANT61 treatment. In control conditions, 6.7% of satellite cells were quiescent satellite cells (Pax7+/Myf5-), 40.6% were proliferative and differentiating progenitors (Pax7-/Myf5+) and 52.7% were committed cells (Pax7+/Myf5+), indicating that just a small proportion of satellite cells are fated to self-renew. Following GANT61 treatment, I observed an overall reduction of 75% in the number of Pax7-/Myf5+ cells (Fig.5.8 E). Furthermore, there was a change in the distribution of satellite cells, with 7.7% of satellite cells expressing Pax7 alone, 14% expressing only Myf5 and 78.3% expressing both proteins. This indicates that inhibition of the Shh signalling pathway at 60h causes a decrease in the number and proportion of differentiating satellite cells (Pax7-/Myf5+) without affecting the proportion of cells

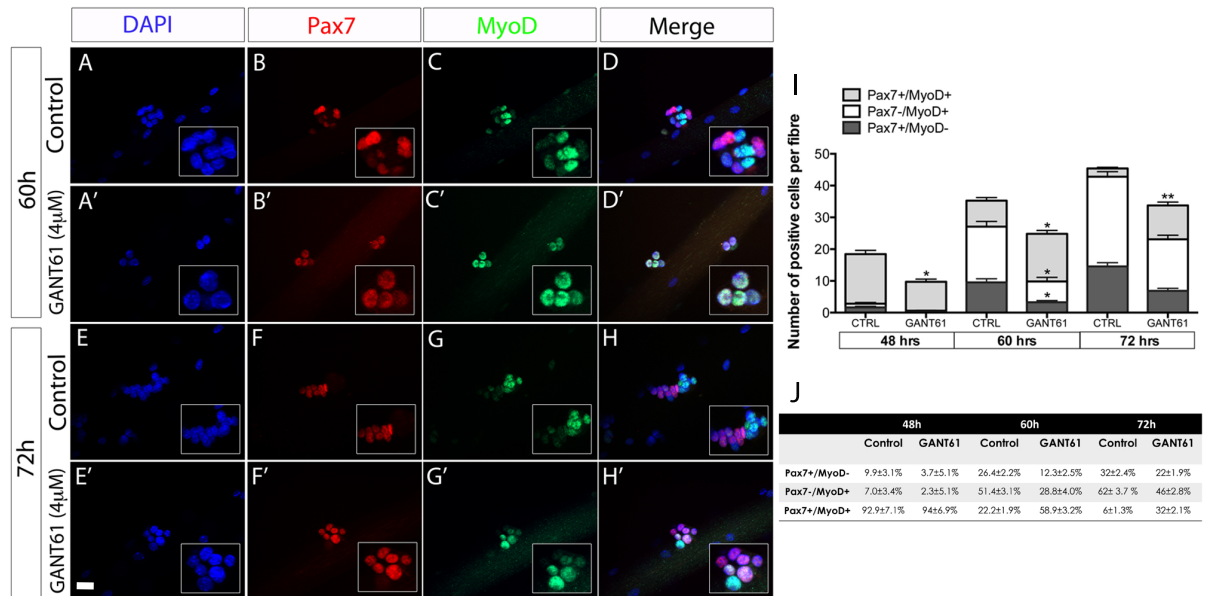


Figure 5.7: Effect of Shh signalling inhibition on Pax7 and MyoD expression in satellite cells *ex vivo* EDL muscle fibres from C57BL/6 mice were cultured for 48, 60 and 72h in the presence of DMSO (control) or GANT61 (4μM). 60 and 72h-cultured myofibres were immunostained to detect Pax7 (red, B, B', F and F') and MyoD (green, C,C', G and G'). Nuclei were counterstained with DAPI (blue, A, A', E and E'). Merged images for each time point are shown in D, D', H and H'. Magnified views for every channel are shown. Inhibition of Shh signalling causes an increase in the proportion of Pax7+/MyoD+ cells with a concomitant reduction of the Pax7+/MyoD- and Pax7-/MyoD+ cell populations, suggesting that Shh inhibition delays the myogenic programme. Scale bar represents 20μm. (I) shows the quantitative analysis of the number of Pax7+ and MyoD+ satellite cells at 48, 60h and 72h per fibre in the presence of DMSO or 4μM of GANT61. There was a significant difference in the number of Pax7+/MyoD+ cells at 48h upon Gli inhibition with GANT61 compared to the control (p=0.0310). At 60h under GANT61 treatment, the number of Pax7+/MyoD- cells increased, with a concomitant decrease in the number of Pax7+/MyoD- and Pax7-/MyoD+ cells (p=0.0260 for Pax7+/MyoD-, p=0.0194 for Pax7-/MyoD+ and p=0.0212 for Pax7+/MyoD+). By 72h, there was an increase in the number of Pax7+/MyoD+ cells upon GANT61 treatment compared to the control (p=0.0077). Representative data from three individual mice are shown, with 13 to 25 individual fibres per mouse for each time point. Values are mean and SEM. Statistical analysis was performed using Student's t-test. (J) shows the mean percentage ±SEM of Pax7 and MyoD populations at 48, 60h and 72h per fibre in control or under GANT61 treatment.

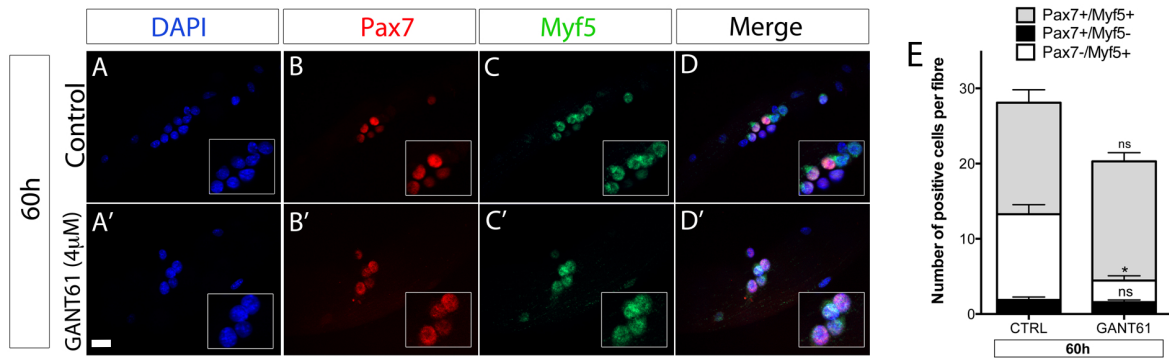


Figure 5.8: Shh signalling inhibition does not affect the number of Pax7+/Myf5- self-renewing satellite cells *ex vivo*. EDL muscle fibres from C57BL/6 mice were cultured for 60h in the presence of DMSO (control) or GANT61 (4µM). Myofibres were immunostained to detect Pax7 (red, B and B') and Myf5 (green, C and C'). Nuclei were counterstained with DAPI (blue, A and A'). Merged images for control and treatment are shown in D and D'. Magnified views for every channel are shown. Inhibition of Shh signalling causes an increase in the proportion of Pax7+/Myf5+ satellite cells at the expense of more differentiated muscle progenitor cells (Pax7-/Myf5+). Scale bar represents 20µm. Quantitative analysis of the number of Pax7+ and Myf5+ satellite cells at 60h per fibre in the presence of DMSO or 4µM of GANT61 is shown in E. There was a significant difference in the number of Pax7-/Myf5+ ($p=0.0339$) cells at 60h upon Gli inhibition with GANT61 compared to the control. Representative data from three individual mice are shown, with 13 to 15 individual fibres per mouse for each time point. Values are mean and SEM. Statistical analysis was performed using Student's t-test.

returning to quiescence (Pax7+/Myf5-). This is consistent with the possibility that loss of Shh signalling causes a delay in myogenesis.

Next, to determine the identity of differentiating cells affected by GANT61, I performed a MyoD/Myogenin immunofluorescence analysis on 72h-cultured myofibres. In control conditions, 10% of satellite cells were initiating differentiation (MyoD+/Myogenin-), 14% were reaching terminal differentiation (MyoD-/Myogenin+) and 76% were differentiated myoblasts (MyoD+/Myogenin+) (Fig.5.9 A-D and E). Following Gli inhibition with GANT61, there was an increase of 60% in the number of MyoD+/Myogenin- cells, along with a 38% reduction in the number of MyoD+/Myogenin+ cells, respectively. This also had an impact on the distribution of cell populations, as 33% of cells were now initiating differentiation (MyoD+/Myogenin-), 2% only reached terminal differentiation (MyoD-/Myogenin+) and 65% were differentiated myoblasts (MyoD+/Myogenin+) (Fig.5.9 A'-D' and E). This demonstrates that Shh signalling inhibition increases the proportion of myoblasts that initiate differentiation at the expense of fully differentiated myoblasts at 72h. This reinforces the idea that Shh signalling inhibition leads to a delay in the myogenic process.

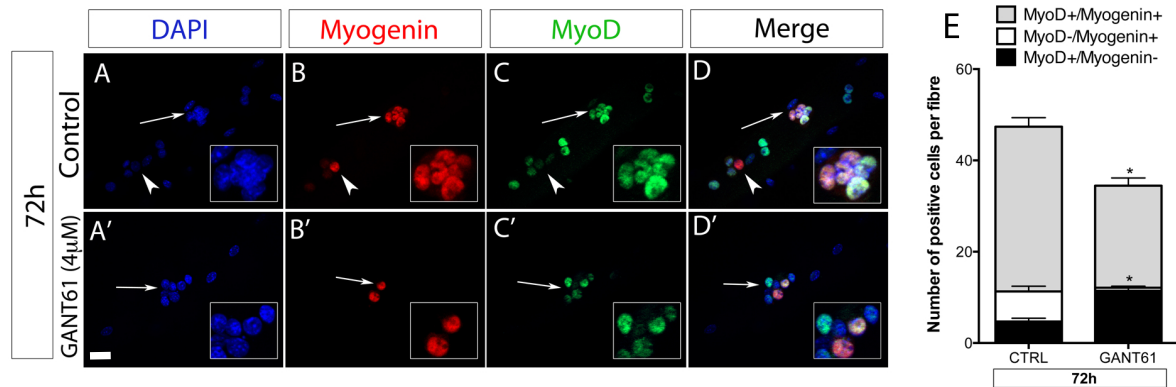


Figure 5.9: Shh signalling inhibition delays the onset of Myogenin expression *ex vivo*. EDL muscle fibres from C57BL/6 mice were cultured for 72h in the presence of DMSO (control) or GANT61 (4μM). Myofibres were immunostained to detect Myogenin (red, B and B') and MyoD (green, C and C'). Nuclei were counterstained with DAPI (blue, A and A'). Merged images for control and treatment are shown in D and D'. Magnified views for every channel are shown (regions indicated by an arrow). Scale bar represents 20μm. (E) shows that inhibition of Shh signalling causes an increase in the number and proportion of MyoD+/Myogenin- satellite cells (p=0.046) and a decrease in the number and proportion of MyoD+/Myogenin+ satellite cells (p=0.045) compared to the control. Representative data from three individual mice are shown, with 14 to 15 individual fibres per mouse for each time point. Values are mean and SEM. Statistical analysis was performed using Student's t-test.

5.2.4 Inhibition of Shh signalling does not cause precocious differentiation of satellite cells

Inhibition of Shh signalling leads to an overall decrease in proliferating and differentiating satellite cells. This effect can be due to different mechanisms, including premature differentiation of muscle progenitor cells. To assess this possibility, I cultured EDL myofibres from C57BL/6 mice in the presence of 4μM of GANT61 or DMSO (control) for 48h to analyse the expression of the myogenic regulatory factor Myogenin, which labels differentiated satellite cells. Therefore, the distribution of Caveolin-1/Myogenin and MyoD/Myogenin was determined by immunofluorescence analysis at 48h.

At 48h in control conditions some satellite cells undergoing early differentiation could be observed, as shown by the early expression of Myogenin (Fig.5.10 A-D, E-H, I and J). Indeed, 17% and 24% of total satellite cells counted were positive for Caveolin-1/Myogenin and MyoD/Myogenin, respectively. Following Shh signalling inhibition with GANT61, the number of Myogenin+ cells dramatically decreased, representing then just 4% of the total cells counted (Fig.5.10 A'-D', E'-H', I and J), indicating that inhibition of Shh signalling does not cause premature differentiation of satellite cells and instead delays it. Furthermore, in line with previous data, following GANT61 treatment the number of proliferative cells, including Caveolin-1+/Myogenin- cells was reduced by 2-fold. Taken together, these results confirm that the Shh signalling pathway positively affects satellite

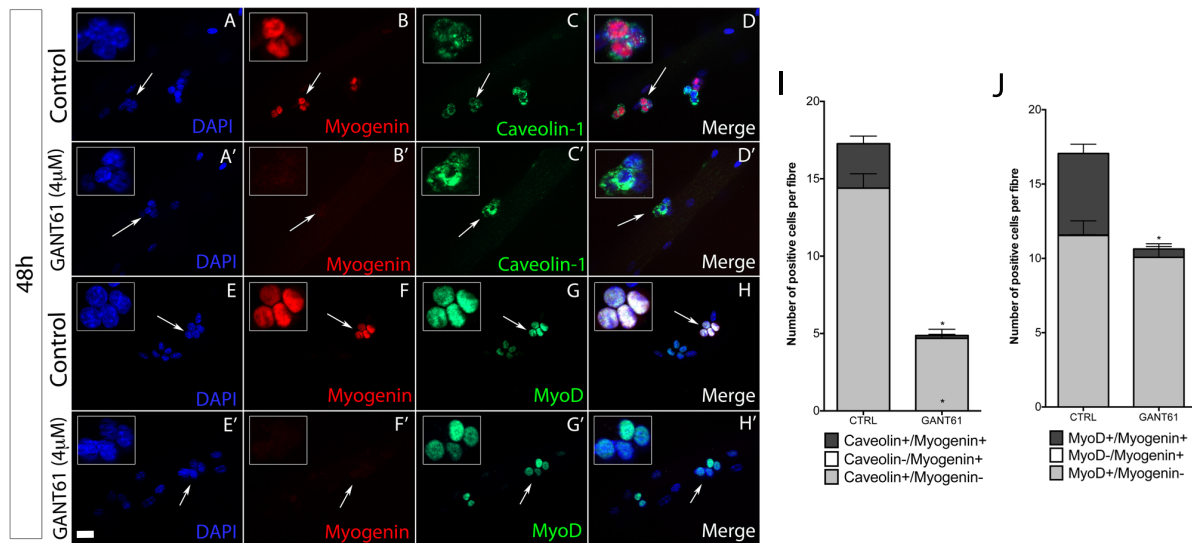


Figure 5.10: Shh signalling inhibition does not cause premature differentiation of satellite cells. EDL muscle fibres from C57BL/6 mice were cultured for 48h in the presence of DMSO (control) or GANT61 (4μM). Myofibres were immunostained to detect Myogenin (red, B and B') and Caveolin-1 (green, C and C') or Myogenin (red, F and F') and MyoD (green, G and G'). Nuclei were counterstained with DAPI (blue, A, A', E and E'). Merged images for control and treatment are shown in D, D', H and H'. Magnified views for every channel are shown (regions indicated by an arrow). Scale bar represents 20μm. (I) and (J) show the quantitative analyses of the number of Caveolin/Myogenin and Myogenin/MyoD positive satellite cells at 48h per fibre in the presence of DMSO or 4μM of GANT61. Inhibition of Shh signalling causes a decrease in the number of both Caveolin+/Myogenin- (p=0.0095) and Caveolin+/Myogenin+ (p=0.05) satellite cells compared to the control. Furthermore, GANT61 treatment also had a negative effect in the number of MyoD+/Myogenin+ (p< 0.0348) cells compared to the control. Representative data from three individual mice are shown, with 16 to 20 individual fibres per mouse for each time point. Values are mean and SEM. Statistical analysis was performed using Student's t-test.

cell progression through the myogenic program.

5.3 Discussion

5.3.1 Chemical manipulation of the Shh signalling pathway leads to a change in satellite cell numbers.

During vertebrate embryonic development, Shh signalling controls the specification, growth and patterning of epaxial, hypaxial and limb muscle progenitor cells (Anderson et al., 2012, Borycki et al., 1999b, Gustafsson et al., 2002, Hu et al., 2012, Kruger et al., 2001, McDermott et al., 2005). In the adult muscle, the role of Shh signalling remains ambiguous, as some *in vitro* analyses have shown that Shh can promote muscle differentiation (Elia et al., 2007, Li et al., 2004, Straface et al., 2009), whereas others claimed that it prevents it (Koleva et al., 2005). These reports relied on the use of myogenic cell lines

or primary cultures, which have the inconvenience of taking satellite cells out of their native environment. Furthermore, these studies did not examine in details the sequence of myogenic events that lead to satellite cell differentiation, and how these events may be affected by Shh signalling stimulation or inhibition.

Here, I have performed gain and loss-of-function experiments using pharmacological drugs that activate and inhibit Shh signalling in the *ex vivo* myofibre culture system and showed that loss-of-function approaches lead to a decrease of satellite cell numbers. Specifically, I showed that following treatment with the Shh signalling inhibitors cyclopamine and GANT61, which caused a reduction in GFP expression in Tg(GBS-GFP) satellite cells, there was a decrease in the number of Pax7+/MyoD+ and Caveolin-1+/Myogenin+ proliferating progenitor cells at 48 and 72h, respectively. The greater effect of GANT61 compared to cyclopamine (notably at 48h) could be due to the different nature of these inhibitors. Cyclopamine is a steroidal alkaloid found in the plant *Veratrum californicum* that inhibits Shh signalling by direct binding to the Smo heptahelical bundle (Chen et al., 2002a). In contrast, GANT61 is a hexahydropyrimidine derivative that binds to the Gli1 protein and prevents its binding to the DNA (Agyeman et al., 2014, Lauth et al., 2007). As GANT61 acts at the level of Gli proteins, which can be modulated in a Smo-independent manner (Nolan-Stevaux et al., 2009, Stecca et al., 2007, Varjosalo et al., 2008), this may explain its stronger activity. In addition, similar to SAG, cyclopamine can promote Smo accumulation in the primary cilia, which may result in attenuated ability to inhibit the pathway (Wang et al., 2009).

5.3.2 Shh signalling and apoptosis of satellite cells

Several mechanisms may explain the effect of Shh signalling on the expansion and differentiation of satellite cells. First, it is possible that Shh signalling increases satellite cell numbers by preventing apoptosis as described by others (Koleva et al., 2005). Indeed, Shh signalling can directly regulate the expression of the anti-apoptotic factor Bcl2, promoting survival of neural progenitor cells in the developing chick embryo (Cayuso et al., 2006). Shh signalling has also been described as survival factor during tumour progression through interaction with the pro-apoptotic protein CDON or the cytoprotective protein polo-like kinase (Delloye-Bourgeois et al., 2013, 2014, Fingas et al., 2013). Other mechanism by which Shh signalling mediates apoptosis includes the induction of cell death by the Ptc/Caspase-9 complex in the chick spinal cord (Fombonne et al., 2012, Mille et al., 2009, Thibert et al., 2003). However, despite several attempts at assaying cell death in the *ex vivo* culture system, including TUNEL assay and Caspase-3 staining, these experiments were not optimised and did not yield any convincing results. Therefore, a role of Shh signalling in satellite cell survival cannot be ruled out and further analyses are

needed to explore this possibility.

5.3.3 Shh signalling and proliferation of satellite cells

An alternative mechanism to explain the effect of Shh signalling in satellite cell expansion is an increase in the proliferation of activated satellite cells as previously reported (Elia et al., 2007, Koleva et al., 2005, Straface et al., 2009). Indeed, Shh is a well-known mitogen of different embryonic cell types, including progenitor cells of the cerebellum and the retina (Corrales et al., 2006, Locker et al., 2006). It also controls the proliferation of adult stem cells in the hair follicle, the cervical loop of the teeth and the brain (Hsu et al., 2014, Petrova et al., 2013, Seidel et al., 2010). Because a role of Shh signalling in satellite cell proliferation is highly plausible, a whole chapter exploring this possibility will be discussed later.

5.3.4 Satellite cell progression through the myogenic program is affected by the Shh signalling pathway.

An interesting finding was that Shh signalling inhibition via GANT61 results in a delay in satellite progression through the myogenic program *ex vivo*, leading to presence of cells in a more primitive state at any given time and a concomitant decrease in the proportion of more committed or differentiating muscle progenitor cells. As a result, the proportion of satellite cells reaching terminal differentiation was reduced in GANT61-treated cultures.

What is mechanism implicated in this delay? During adult myogenesis, satellite cells progress through the myogenic program by the sequential expression of the MRFs. Myf5 is the first MRF to be expressed in embryonic muscle progenitor cells and its mRNA is already transcribed in around 90% of quiescent satellite cells, reflecting their commitment to the myogenic lineage (Kuang et al., 2007). Once activated, satellite cells up-regulate Myf5 and then MyoD and begin their expansion before activating Myogenin, which initiates the differentiation program. One possibility is that in the absence of Shh signalling, satellite cell activation is delayed. However, stimulation or inhibition of Shh signalling had no effect on satellite cell activation, as the number and proportion of Pax7+ cell expressing Myf5 at 24h was not altered. Alternatively, satellite cells may be delayed because their entry into the cell cycle is also delayed. Quiescent satellite cells express negative regulators of the cell cycle including cyclin-dependent kinase inhibitors (p27 and p57) and the retinoblastoma protein (Rb1) among others (Chakkalakal et al., 2014, Hosoyama et al., 2011). Following muscle injury, damaged myofibres release signalling molecules that stimulate cell cycle entry, including the insulin-like growth factor (IGF-I), which inactivates FoxO1 through phosphorylation to down-regulate p27 expression (Machida et al.,

2003). Therefore, it is possible that Shh signalling promotes cell cycle entry or progression through the cell cycle by acting on one or several of these cell cycle regulators. Indeed, in the cerebellum, the retina and the limb, cell cycle regulators like D-type cyclins, N-myc, p27 and p57 have been identified as Shh signalling targets (Shkumatava and Neumann, 2005, Towers et al., 2008, Wall et al., 2009). Likewise, different MAPK pathways are functional in activated satellite cells and are required to initiate the cell cycle or to control transitions between cell cycle phases (Jones et al., 2005). This is relevant in the context of this project, as some reports have suggested a link between Shh and the modulation of MAPK/ERK and PI3K/Akt pathways in muscle progenitors (Elia et al., 2007).

And how is cell division coupled with myogenic differentiation? Satellite cells perform both symmetric and asymmetric cell divisions. During the latter, cell fate determinants are segregated asymmetrically to generate one stem cell and one committed cell that differentiates. For instance, after asymmetric cell division, the arginine methyltransferase *Carm1* is segregated into the committed daughter cell, resulting in Pax7-mediated control of *Myf5* expression (Kawabe et al., 2012). Therefore, if the rate of satellite cell division is altered in the absence of Shh signalling, the balance between symmetric versus asymmetric cell division may be affected and may result in changes in the proportion of committed differentiating cells. However, additional experiments are needed to explore this possibility.

SHH SIGNALLING CONTROLS SATELLITE CELL PROGRESSION THROUGH THE CELL CYCLE.

6.1 Introduction

I have previously shown that Shh signalling controls the expansion of satellite cells and their progression through the myogenic program likely via control of the cell cycle (chapter 5). Specifically, loss-of-function experiments using pharmacological Shh antagonists led to a decrease of satellite cell numbers. Furthermore, Shh signalling inhibition results in a delay in satellite cell-mediated myogenesis *ex vivo*. However, how this pathway regulates the cell cycle dynamics or how this is linked to cell fate determination is still unknown.

Following skeletal muscle injury, satellite cells proliferate extensively between the second and fourth days of regeneration (see chapter 3). Quiescent satellite cells, which are in a reversible G0 state, become activated as early as 6 hours upon injury *in vivo* (Grounds et al., 1992) and carry out their first S phase between 14 and 18h post-injury, indicating the existence of a prolonged G1 phase that follows the exit from quiescence (Rocheteau et al., 2012). Satellite cells complete their first cell division between 24 and 48h post-injury and subsequent cell divisions occur every 8 to 10h until the onset of myogenic differentiation (Rocheteau et al., 2012). This results in the expansion of both committed and self-renewing satellite cells needed to contribute to myogenesis and to the stem cell pool, respectively.

In this chapter I used the *ex vivo* myofibre culture system to explore changes in satellite cell proliferation following Shh signalling inhibition. More specifically, experimental strategies to assess differences in cell cycle dynamics were applied, which allow to propose

a role of the Shh signalling pathway in the control of satellite cell cell cycle progression.

6.1.1 Hypothesis and aim

I hypothesise that Shh signalling controls satellite cell proliferation. Therefore, the aim of this chapter is to assess the proliferative status of satellite cells in the absence of Shh signalling.

6.2 Results

6.2.1 Effect of Shh signalling blockade on the expression of proliferation markers during satellite cell-mediated myogenesis *ex vivo*.

I have previously showed that treatment of cultured muscle fibres with the Shh signalling inhibitors cyclopamine or GANT61 results in an overall decrease in the number of satellite cells. This change in cell numbers could be due to a decrease in cell proliferation. To test this, I measured the proliferation rate of satellite cells using different proliferation markers in the absence of Shh signalling.

First, single EDL muscle fibres from C57BL/6 mice were cultured in the presence of the Gli inhibitor GANT61 (4 μ M) or DMSO (control), and the distribution of Pax7 and the proliferation marker Ki67 was determined by immunofluorescence analysis at 24, 48 and 72h. Ki67 is an antigen present in the nuclei of cells during all active phases of the cell cycle (G1, S, G2 and M) but absent in resting cells (G0) (Scholzen et al., 2000), as shown by the absence of Ki67 expression in quiescent satellite cells (see figures 3.5 and 4.7). Ki67 is detected in about 32% of Pax7+ cells at 24h in control conditions. Following GANT61 treatment at 24h, no changes in satellite cell numbers were observed, although there was a tendency towards a decreased proportion of Pax7+ cells expressing Ki67 (16%) (Fig.6.1 A-D, A'-D' and M). At 48h in control conditions, 92% of satellite cells counted expressed both Pax7 and Ki67, which shows that most of the cells are undergoing active proliferation. As previously shown, upon GANT61 treatment the number of satellite cells decreased drastically by 2-fold, but about 85% of the remaining cells were Pax7+/Ki67+, indicating that these cells did not lose their proliferative potential (Fig.6.1 E-H, E'-H' and M). At 72h in control conditions, Ki67 expression was detected in Pax7+ (45.6%) and Pax7- (39%) cells, which shows that at this time point differentiating satellite cells (Pax7-/Ki67+) were still cycling. The remaining cells (15.4%) were Pax7+/Ki67- cells, which are the cells deemed to self-renew. In agreement with my previous data, following Shh signalling inhibition the differentiating progeny (Pax7-/Ki67+) was no longer detected

and most of the remaining cells were either proliferating (Pax7+/Ki67+, 77.3%) or self-renewing (Pax7+/Ki67-, 17.6%) cells (Fig.6.1 I-L, I'-L' and M). Thus, satellite cells entry into the cell cycle is delayed at 24h and a larger proportion of cells remain in the cell cycle at 72h in the absence of Shh signalling. This suggests that inhibition of Shh signalling impairs satellite cell progression through the cell cycle and as a consequence, the number of cells entering differentiation.

To investigate whether a specific phase of the cell cycle was affected in the absence of Shh signalling, I performed immunostaining analysis using the proliferation marker phospho-histone 3 (PH3), which labels cells undergoing mitosis (Hans and Dimitrov, 2001). To do so, single EDL muscle fibres from C57BL/6 mice were cultured in the presence of GANT61 (4 μ M) or DMSO (control) and the distribution of Pax7 and PH3 was determined by immunofluorescence analysis at 24, 48 and 72h. At 24h in control conditions, a small proportion of Pax7+ cells were PH3+ (5%). This proportion was reduced to 1% following Shh signalling inhibition with GANT61, which is in line with the Ki67 analysis and shows that fewer satellite cells undergo mitosis in the absence of Shh signalling (Fig.6.2 A-D, A'-D' and M). At 48h, while the total number of satellite cells was reduced in the presence of GANT61, the proportion of Pax7+/PH3+ cells was not changed in GANT61-treated compared to control myofibres (28% versus 29%). This indicates that the same proportion of cells were in mitosis in the absence of Shh signalling and in control fibres (Fig.6.2 E-H, E'-H' and M). However at 72h, cells in mitosis (PH3+) represented about 6% of the total cells (4% were Pax7+/PH3+ and 1% were Pax7-/PH3+) in control conditions and 15% following GANT61 administration (Fig.6.2 I-L, I'-L' and M). This indicates that by 72h, a higher proportion of cells remaining in M phase are observed in the absence of Shh signalling.

To assess the S phase of the cell cycle, I measured cells undergoing DNA synthesis by incubating cultured muscle fibres with 5-ethynyl-2-deoxyuridine (EdU). EdU is a thymidine analogue that incorporates into DNA during replication and can be detected with fluorescent azides through a Cu-mediated reaction (Salic and Mitchison, 2008). Thus, myofibres were cultured in the presence of SAG (100nM), cyclopamine (1 μ M), GANT61 (4 μ M) or DMSO (control), incubated with EdU for 1 hour before harvesting and the proportion of Caveolin-1+ satellite cells that have incorporated EdU was determined by immunofluorescence analysis at 24, 48 and 72h.

At 24h, around 32% of Caveolin-1+ satellite cells were also positive for EdU in control conditions. Following Shh signalling stimulation with SAG, the percentage of EdU+ cells showed a slight increase but it was not significant. In contrast, upon Shh signalling inhibition with either cyclopamine or GANT61, 19.3% and 4.3% of satellite cells were EdU+, respectively (Fig.6.3 1A-1D and E). This indicates that Shh signalling promotes satellite cell proliferation at 24h. As shown before, by 48h most of the satellite cells are

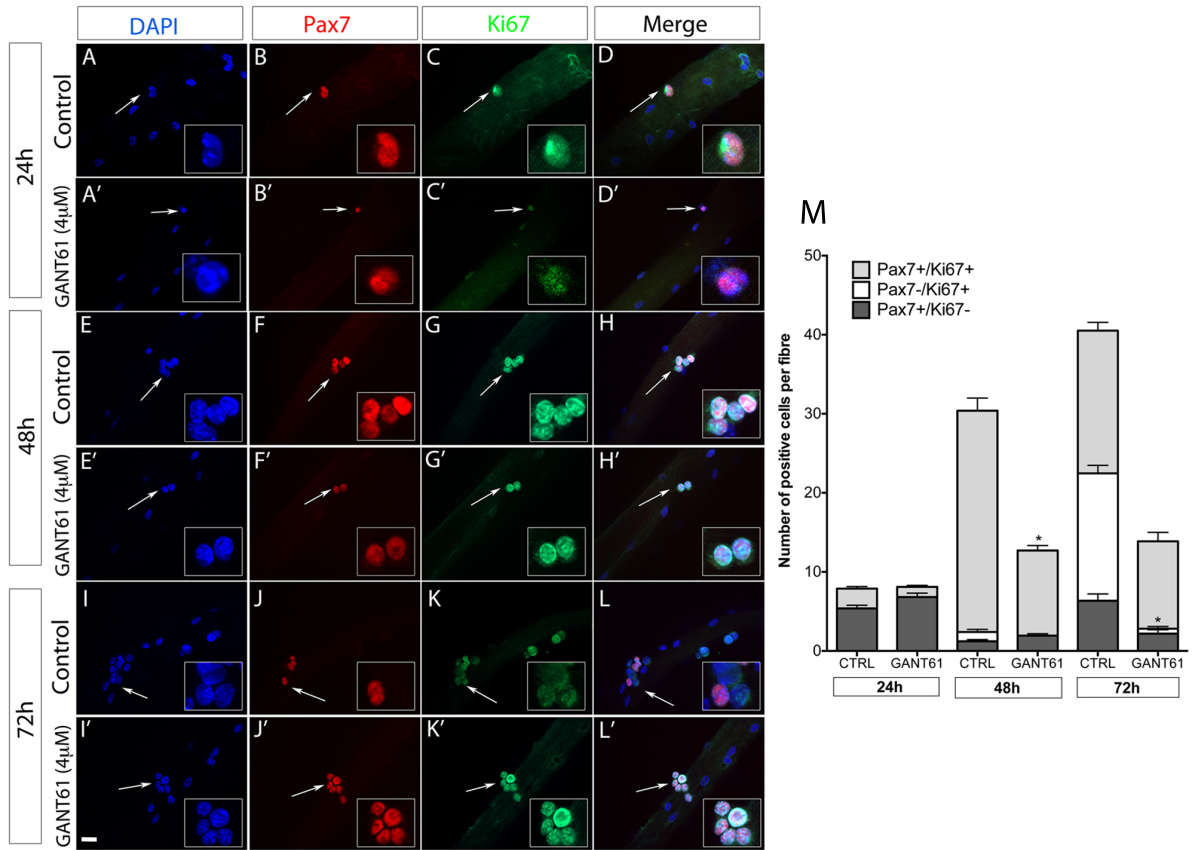


Figure 6.1: Effect of Shh signalling inhibition on Ki67 expression *ex vivo*. EDL muscle fibres from C57BL/6 mice were cultured for 24, 48 and 72h in the presence of DMSO (control) or GANT61 (4µM). Myofibres were immunostained to detect Pax7 (red, B, B', F, F', J and J') and Ki67 (green, C, C', G, G', K and K'). Nuclei were counterstained with DAPI (blue, A, A', E, E', I and I'). Merged images for each time point are shown in D, D', H, H', L and L'. Magnified views for every channel are shown (regions indicated by an arrow). Scale bar represents 20µm. (M) shows the quantitative analysis of the number of Pax7+ and Ki67+ satellite cells at 24h, 48h and 72h per fibre in the presence of DMSO or 4µM of GANT61. There was a significant difference in the number of Pax7+/Ki67+ cells upon GANT61 treatment at 48h compared to the control (p=0.0043). Moreover, there was a significant decrease in the number of Pax7-/Ki67+ cells at 72h following Gli inhibition compared to the control (p=0.0049). Representative data from three individual mice are shown, with 10 to 30 individual fibres per mouse for each time point. Values are mean and SEM. Statistical analysis was performed using Student's t-test.

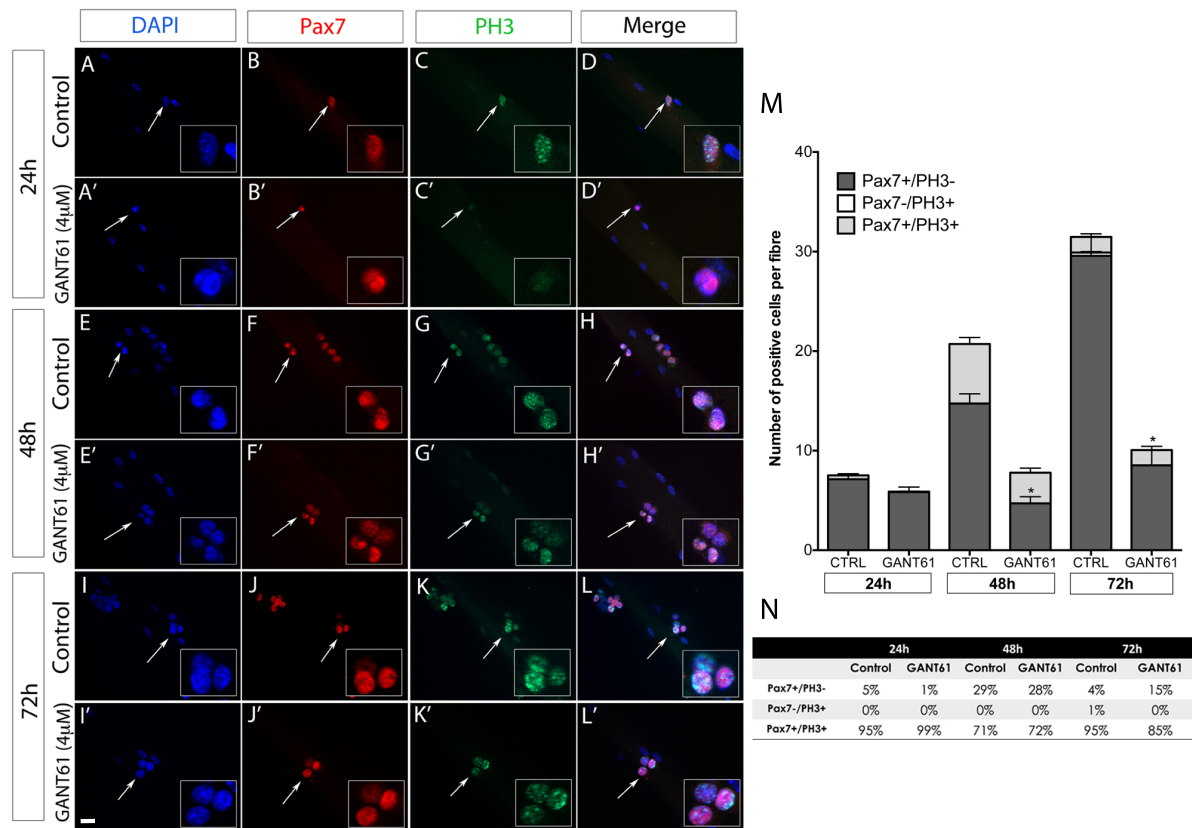


Figure 6.2: Effect of Shh signalling inhibition on PH3 expression *ex vivo*. EDL muscle fibres from C57BL/6 mice were cultured for 24, 48 and 72h in the presence of DMSO (control) or GANT61 (4µM). Myofibres were immunostained to detect Pax7 (red, B, B', F, F', J and J') and PH3 (green, C, C', G, G', K and K'). Nuclei were counterstained with DAPI (blue, A, A', E, E', I and I'). Merged images for each time point are shown in D, D', H, H', L and L'. Magnified views for every channel are shown (regions indicated by an arrow). Scale bar represents 20µm. (M) shows the quantitative analysis of the number of Pax7+ and PH3+ satellite cells at 24h, 48h and 72h per fibre in the presence of DMSO or 4µM of GANT61. There was a significant difference in the number of Pax7+/PH3- cells at both 48 (p=0.0155) and 72h (p=0.0146) upon GANT61 treatment compared to the control. (N) shows the average percentage of Pax7 and PH3 populations at 24, 48h and 72h per fibre in control or under GANT61 treatment. Representative data from three individual mice are shown, with 10 to 15 individual fibres per mouse for each time point. Values are mean and SEM. Statistical analysis was performed using Student's t-test.

actively cycling. Here, EdU incorporation revealed that 61.4% of Caveolin-1+ were in S phase in control conditions and no difference was observed in the percentage of EdU+ cells after Shh signalling stimulation or inhibition (Fig.6.3 2A-2D and E), suggesting that after an initial delay in entering the cell cycle, satellite cells are able to divide independently of Shh signalling. However, as Shh signalling inhibition with cyclopamine or GANT61 caused an increase in EdU incorporation from 13.8% of Caveolin-1+ cells/fibre to 18.2% and 33.2% (Fig.6.3 3A-3D and E), it suggests that Shh signalling is required for satellite cell progression through the S phase of the cell cycle and in its absence, satellite cells remain cycling for a longer period in S phase or fail to pass the checkpoint at the G/S transition.

6.2.2 Inhibition of Shh signalling delays satellite cell entry and progression through the cell cycle *ex vivo*.

To gain further insight into the role of Shh signalling in satellite cell proliferation, I performed Shh signalling inhibition experiments on cultured myofibres from the *R26p-Fucci2* mice. *R26p-Fucci2* mice carry a single transgene, in which the *Rosa26* promoter drives the expression of *mCherry-hCdt1* and *mVenus-hGem*. mCherry-hCdt1 is a fusion between the fluorescent reporter mCherry and the ubiquitinylation domain of the Cdt1 protein, which accumulates in the cell nucleus during G0, G1, and early S phases. mVenus-hGem is a fusion of the fluorescent protein mVenus to the ubiquitinylation domain of the Geminin protein, which accumulates in the cell nucleus during S, G2 and M phases (Fig.6.4 A) (Abe et al., 2013).

Single EDL muscle fibres from *R26p-Fucci2* mice were cultured in the presence of GANT61 (4 μ M) or DMSO (control) and the distribution of green and red satellite cells was determined by immunofluorescence analysis at 0, 24, 48 and 72h. First, I observed that myonuclei, which are post-mitotic, strongly expressed mCherry-hCdt1. Similarly, 97.4% of all Pax7+ cells counted in freshly isolated myofibres at 0h showed comparable levels of mCherry-hCdt1 than myonuclei, confirming that these cells were in a quiescent state (Fig.6.4 B and Fig.6.5). At 24h, 56% of satellite cells were in G1/S phase (low levels of mVenus-hGem while still expressing mCherry-hCdt1). In addition, around 24% of cells were in S phase (stronger levels of mVenus-hGem and low mCherry-hCdt1 expression), 11% were in G2/M phase (mVenus-hGem expression only) and 9% remained in the G0/G1 phase (Fig.6.4 C and Fig.6.5). Following GANT61 treatment, 45% of cells were in G1/S, 9% were in S and less than 2% were in G2/M phase. The remaining 44% of cells were in G0/G1 (Fig.6.4 C' and Fig.6.5). This indicates that fewer satellite cells entered into G1/S the absence of Shh signalling, and confirming my EdU data, fewer cells were in S phase.

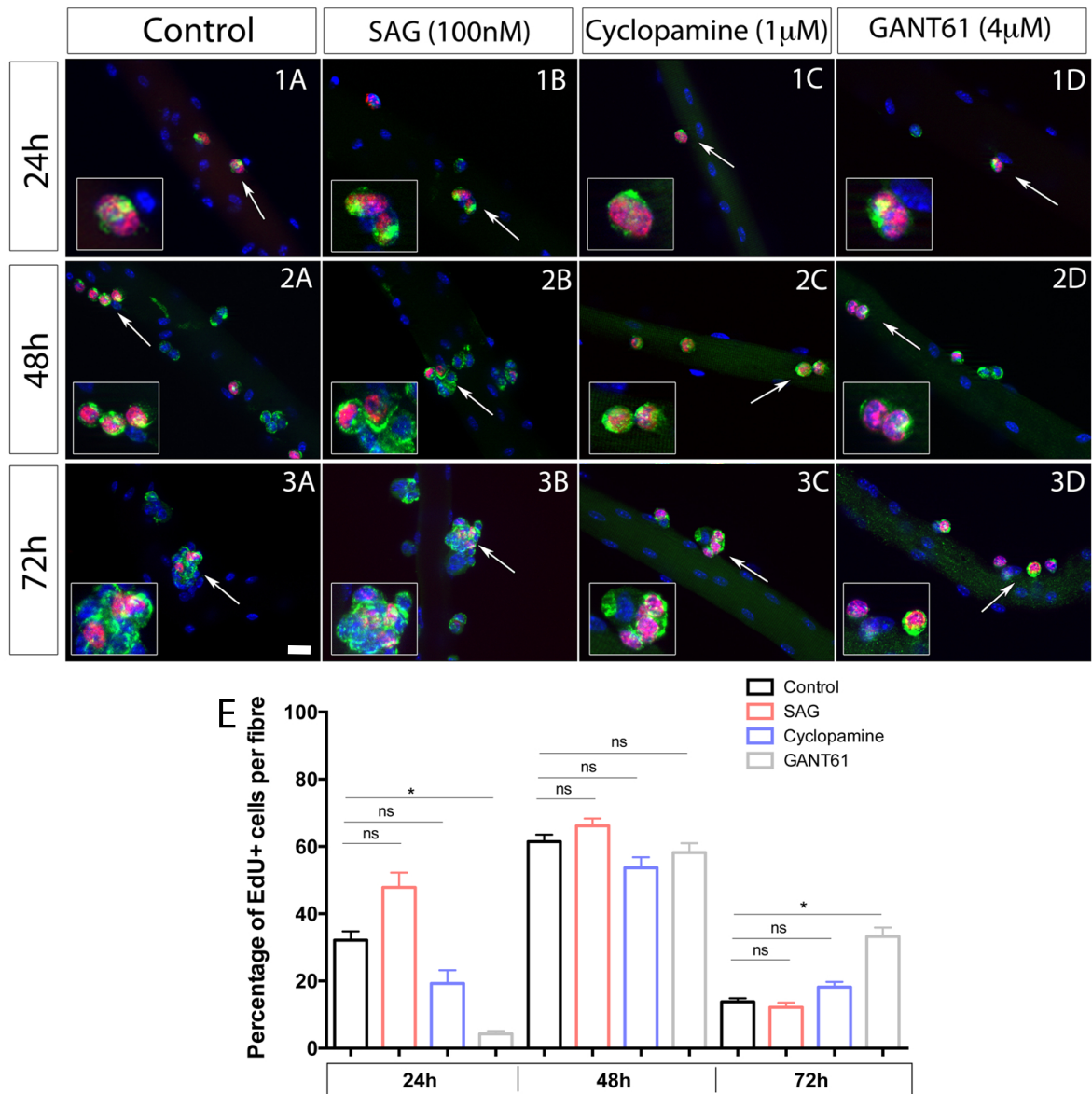


Figure 6.3: Effect of Shh signalling pathway stimulation and blockade on EdU incorporation *ex vivo*. EDL muscle fibres from C57BL/6 mice were cultured for 24, 48 and 72h in the presence of DMSO (control), SAG (100nM), cyclopamine (1µM) or GANT61 (4µM). Myofibres were incubated with 10µM of EdU for 1 hour before harvesting and EdU was detected using the Click-iT kit. Merged images for each time point and treatment are shown, where satellite cells are labelled with Caveolin-1 (green) and cells in S-phase have incorporated EdU (red). Nuclei were counterstained with DAPI (blue). Magnified views for every channel are shown (regions indicated by an arrow). Scale bar represents 20µm. (E) shows the percentage of Caveolin-1+ that incorporated EdU at 24h, 48h and 72h per fibre in the presence of DMSO, SAG (100nM), cyclopamine (1µM) or GANT61 (4µM). There was a significant difference in the proportion of Caveolin-1+ cells expressing EdU at 24h upon GANT61 treatment ($p=0.0019$) compared to the control. No change in the percentage of EdU+ cells was observed at 48h with any treatment compared to the control. Finally, there was a significant difference in the proportion of Caveolin-1+ cells expressing EdU at 72h upon GANT61 treatment ($p=0.0001$) compared to control conditions. Representative data from three individual mice are shown, with 12 to 33 individual fibres per mouse for each time point. Values are mean and SEM. Statistical analysis was performed using Student's t-test.

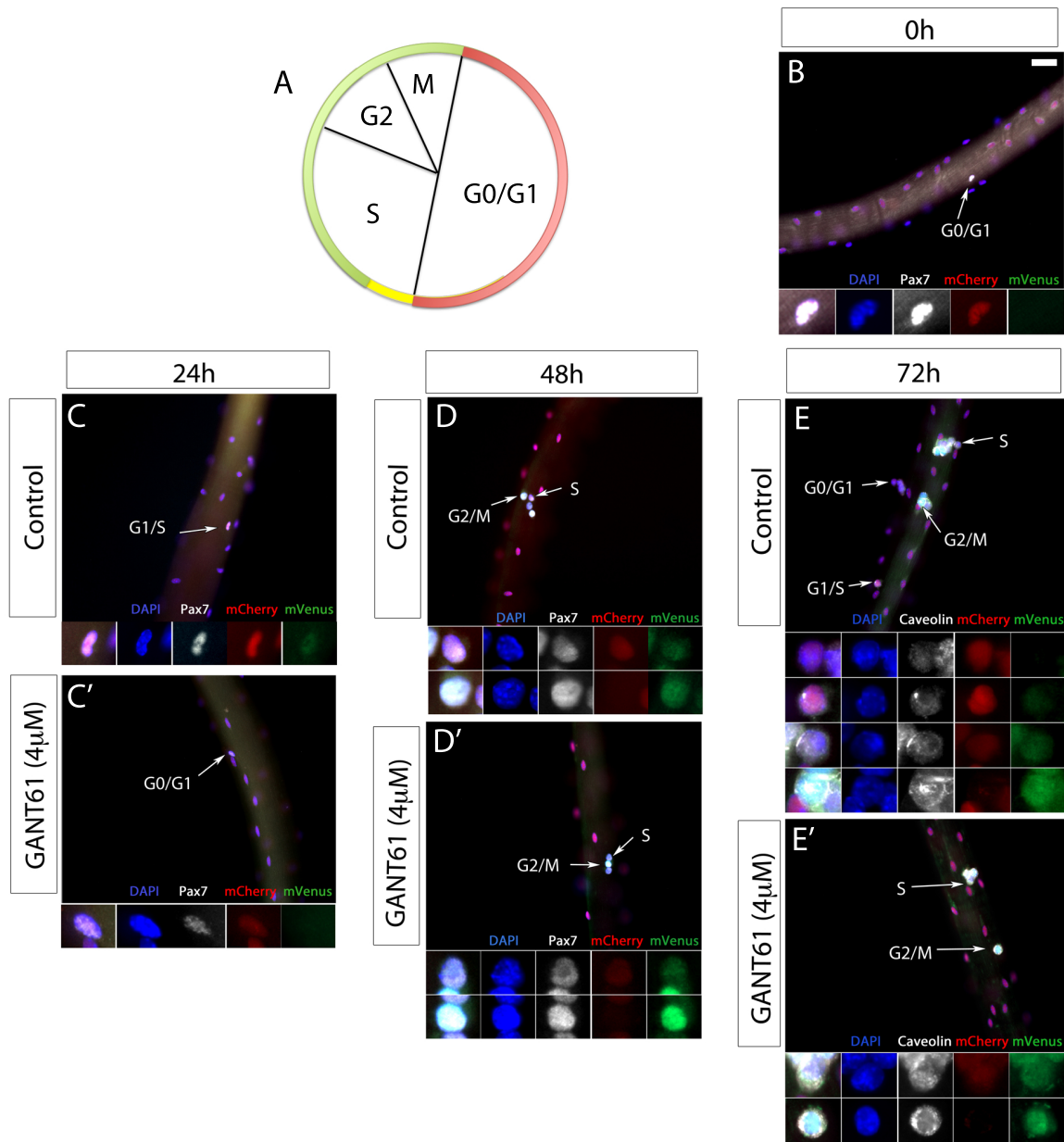


Figure 6.4: Shh signalling inhibition affects satellite cell progression through the cell cycle. EDL muscle fibres from *R26p-Fucci2* mice were cultured for 24, 48 and 72h in the presence of DMSO (control) or GANT61 (4 μ M). Freshly isolated myofibres at 0h were also analysed. A shows a diagram of the expression of the Fucci2 transgene. mCherry-hCdt1 labels G0, G1 and early S phase nuclei in red, whereas mVenus-hGem labels S, G2 and M phase nuclei in green. Yellow indicates overlapping expression of red and green signals. Myofibres were immunostained to detect Pax7 or Caveolin-1 and mVenus-hGem (GFP). mCherry-hCdt1 signal was detected without antibody amplification. Nuclei were counterstained with DAPI. Merged images for each time point are shown in B, C, C', D, D', E and E'. Magnified views for every channel are displayed in small panels, corresponding to regions indicated by an arrow. Scale bar represents 20 μ m.

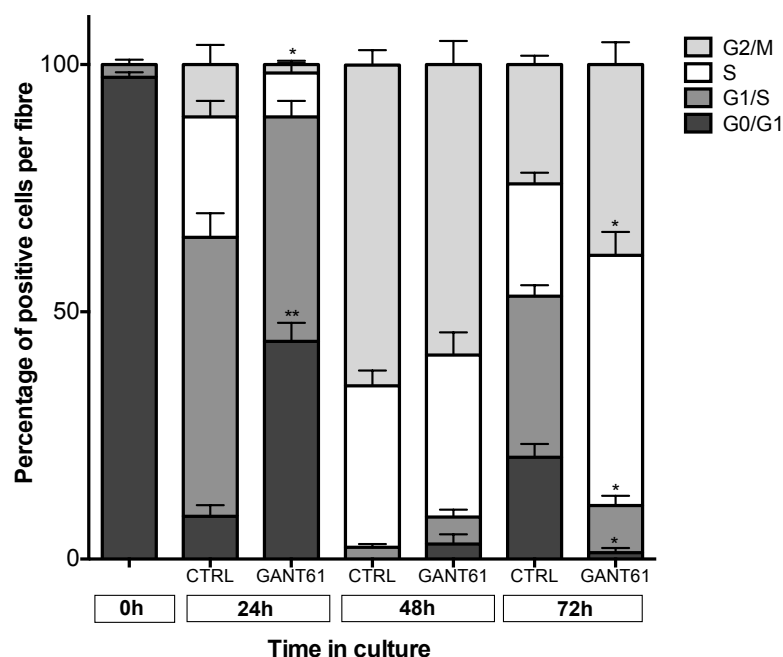


Figure 6.5: Quantitative analysis of satellite cell cycle progression following Shh signalling inhibition *ex vivo*. EDL muscle fibres from *R26p-Fucci2* mice were cultured for 0, 24, 48 and 72h in the presence of DMSO (control) or GANT61 (4 μ M). Myofibres were immunostained to detect Pax7/Caveolin-1, mVenus-hGem and mCherry-hCdt1 and the percentage of cells in G0/G1, G1/S, S and G2/M was quantified. There was a significant difference in the proportion of cells in G0/G1 ($p=0.0066$) and S ($p=0.0236$) at 24h upon GANT61 treatment. In contrast, no significant difference was found at 48h after Shh signalling inhibition. Finally, at 72h there was a significant difference in the proportion of G0/G1 ($p=0.0150$), G1/S ($p=0.0129$) and S ($p=0.0275$) phases following GANT61 administration. Representative data from three individual mice are shown, with 10 to 12 individual fibres per mouse for each time point. Values are mean and SEM. Statistical analysis was performed using Student's t-test.

At 48h, 65% of satellite cells were in the G2/M phase, 33% in S and 2% in G1/S in control conditions. In agreement with my Ki67 and EdU data, I observed that following Shh signalling inhibition, the proliferative status of satellite cells barely changed, as 59% of cells were in G2/M phase, 33% in S, 5% in G1/S and 3% in G0/G1 (Fig.6.4 D and D' and Fig.6.5). This indicates that following the initial delay in initiating the cell cycle, satellite cells succeed in entering the cell cycle. Finally, at 72h, 24% of the cells were in G2/M phase, 23% in S, 33% in G1/S and 21% in G0/G1, suggesting that half of the satellite cell population is still cycling whereas the other half has stopped dividing or is close to exit the cell cycle to differentiate in control conditions (Fig.6.4 E and Fig.6.5). In contrast, upon GANT61 treatment, 39% of satellite cells were in G2/M phase, 50% in S, 10% in G1/S and just 1% were in G0/G1 (Fig.6.4 E' and Fig.6.5). This indicates that once entered into the cell cycle, satellite cells progress through the cell cycle more slowly in the absence of Shh signalling than in control conditions. Specifically, satellite cells remained in the S phase for longer, and failed to progress to G1 or G0 phase.

To confirm that satellite cells remain in the cell cycle upon inhibition of Shh signalling,

single satellite cells were isolated from cultured myofibres and labelled with propidium iodide (PI) to measure their DNA content. To obtain a cell cycle profile, the initial cell population was gated according to the forward-scattered light (FSC) and the side-scattered light (SSC), which give information on the size and granularity of the cells. These features have to be determined experimentally for a particular cell type and in this case, the C₂C₁₂ muscle cell line was used to do so. Next, doublets were excluded from the analysis by plotting the area of the fluorescence light pulse (BL3-A) against the width (BL3-W). Doublets usually have greater pulse width than single cells and therefore were excluded from the analysis. The premise with PI staining is that it binds DNA proportionally to the amount of DNA present in a given cell. Thus, cells in S phase have more DNA than cells in G1 so they take up proportionally more dye and fluoresce more brightly. Likewise, cells in G2/M phase are approximately twice as bright as cells in G1. Therefore, the cell cycle profile is represented graphically in a histogram as the amount of fluorescence emitted (X axis, BL3-H) and the number of cells that would emit that fluorescence (Y axis, count).

PI-labelled satellite cells were analysed to determine the proportion of cells at different stages of the cell cycle and compare this profile to satellite cells that have been treated with GANT61. I found that around 57% of satellite cells isolated from 48h-cultured myofibres were in G0/G1, whereas 18% and 25% of cells were in S and G2/M, respectively. Following GANT61 treatment, 55% of satellite cells were in G0/G1, 23% in S and 22% in G2/M (Fig.6.6 A, A' and C). By 72h, analysis of satellite cells from myofibres cultured in control conditions indicated that 78% of cells were in G0/G1, 8% in S and 14% in G2/M. Following Shh signalling inhibition 72% of cells were in G0/G1, 11.5% in S and 16.5% in G2/M (Fig.6.6 B, B' and C). This indicates that Shh signalling inhibition causes an accumulation of satellite cells in the S and G2/M phases at the expense of G0/G1.

6.3 Discussion

6.3.1 The satellite cell proliferation profile *ex vivo*: insights from different experimental approaches.

At the time of activation, satellite cells enter the cell cycle to expand and supply progeny to repair muscle damage. In this chapter, using different markers and experimental approaches I examined the normal proliferative behaviour of satellite cells during adult myogenesis *ex vivo*.

Ki67 is a broad-spectrum marker of cell proliferation as it is detected in all active phases of the cell cycle (G1, S, G2 and M) but not in resting cells. Thus, quiescent satellite cells did not show any Ki67 expression at 0h. However, when examined using

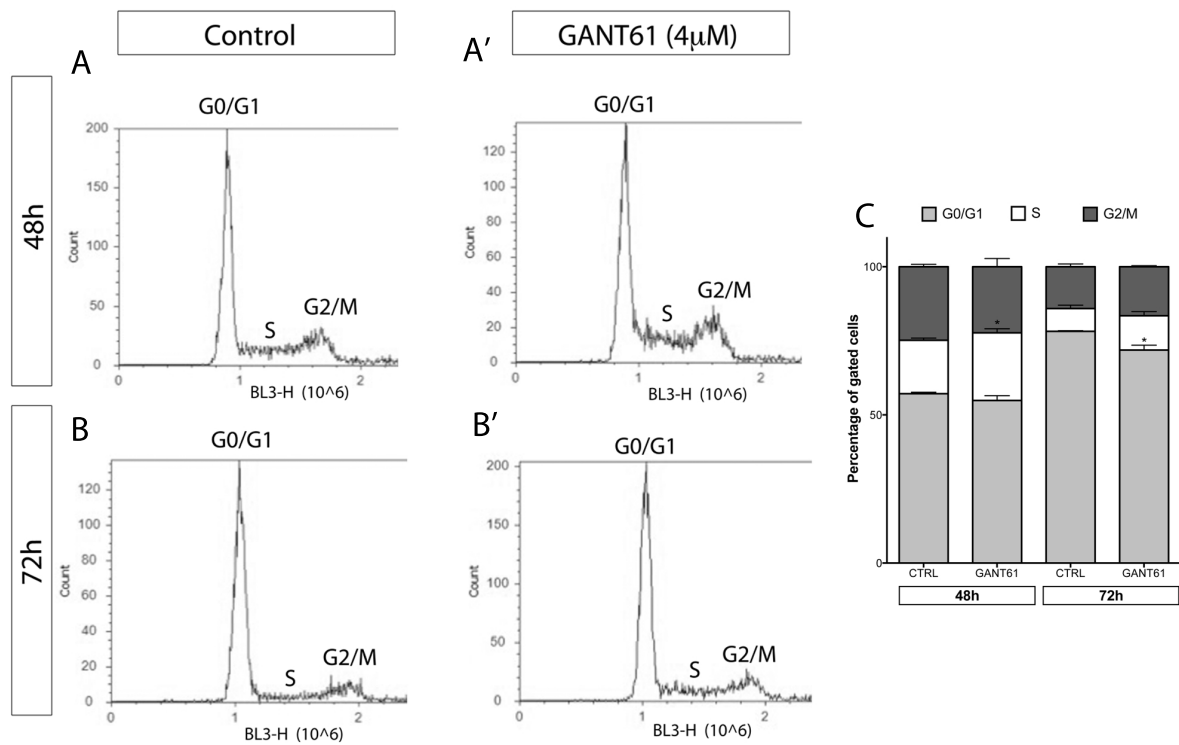


Figure 6.6: Effect of Shh signalling inhibition on satellite cell cycle distribution *ex vivo*. Single EDL myofibres from C57BL/6 mice were cultured in the presence of either DMSO (control) or GANT61 (4 μ M). Satellite cells were subsequently isolated by enzymatic and mechanical dissociation to obtain single cells. Isolated satellite cells were labelled with PI and were analysed according to their DNA content. A, A', B and B' show the cell cycle profile of 48 and 72h-cultured satellite cells treated with DMSO or GANT61. The G0/G1 interval would include both differentiating satellite cells and cells that are actually in the G1 phase. C. The graph shows the percentages of satellite cells in different phases of the cell cycle at 48 and 72h in control condition and GANT61 treatment. There was a difference in the proportion of cells in S phase at 48h following GANT61 treatment compared to the control ($p=0.037$). Additionally, less cells in G0/G1 phase were observed upon Gli inhibition compared to the control ($p=0.0190$). Representative data from three independent experiments are shown. Values are mean and SEM. Statistical analysis was performed using Student's t-test.

the *R26p-Fucci2* mice, quiescent satellite cells were strongly labelled with mCherry-Cdt1, which marks both G0 and G1 phases. This finding contradicts a previous study that reported the absence of mKO2-hCdt1 expression in quiescent Pax7+ satellite cells and led to the authors proposed that myonuclei, which are post-mitotic and mCherry-Cdt1+ were in a G1-like state (de Lima et al., 2014). However, the mKO2-hCdt1 probe used in that study is now known to display variable and sometimes not high enough intensity in several tissues (Abe et al., 2013). In contrast, the mCherry-hCdt1 transgene used in this project is tightly regulated and has been reported to clearly label cells at G0 in other tissues (Oki et al., 2014). Likewise, all myonuclei also expressed high levels of mCherry-hCdt1, confirming that cells in a G0 state were properly labelled.

Satellite cells in *ex vivo* cultures enter the cell cycle within the first 24h, as shown by the expression of Ki67 and the up-regulation of mVenus-hGem. Interestingly, a higher proportion of cycling cells expressing mVenus-hGem than Ki67 was observed (91% versus 32%). This was surprising as Ki67 is generally thought to mark cells at all phases of the cell cycle. However, it should be mentioned that, although the expression of Ki67 at the S phase is generally accepted, its expression during the very initial G1 phase of different cell types has been largely debated (Scholzen et al., 2000). Therefore it is possible that cells in the late G1/early S identified using the Fucci2 system are not labelled with Ki67. This is consistent with the fact that at 24h, 32% of satellite cells incorporated EdU, indicating that they were in S phase. Given that a similar proportion of cells (32%) were labelled with Ki67, it suggests that Ki67 mainly labelled satellite cells in the S phase. This percentage is also very similar to the proportion of cells in S phase detected with the Fucci2 system (24%).

By 48h, satellite cells were actively cycling as shown by Ki67 expression, which is consistent with previous studies (Le Grand et al., 2012). Specifically, most satellite cells were either in S or G2/M phase, as shown by EdU incorporation, PH3 staining and Fucci2 analysis. However, the proportion of cells in S and G2/M phases detected using the Fucci2 system did not entirely match the proportions observed with EdU and PH3 staining. This may be due to the fact that in the Fucci2 system cells in the late S phase do not express mCherry-hCdt1 but do express mVenus-hGem just as cells in the G2 phase do, therefore making it difficult to distinguish them (Sakaue-Sawano et al., 2008). Therefore, it is likely that in *R26p-Fucci2* myofibres the proportion of satellite cells in G2/M was overestimated and that some of these cells were actually still in S phase. EdU co-staining is strongly recommended to overcome this issue but unfortunately, I was not able to optimise this double labelling in the *ex vivo* culture system.

Although some small discrepancies were also found between the Fucci2 system and EdU staining at 72h, the same proliferative trend was observed with both approaches. Importantly, the percentage of cycling cells in satellite cells from *R26p-Fucci2* myofibres

Table 6.1: Distribution of satellite cells in the phases of the cell cycle using different experimental approaches

Time	Proliferation markers			Fucci2			Flow cytometry		
	G0/G1	S	G2/M	G0/G1	S	G2/M	G0/G1	S	G2/M
0h	100%	0%	0%	100%	0%	0%	NA	NA	NA
24h	NA	32%	NA	65%	24%	11%	NA	NA	NA
48h	NA	62%	NA	2%	33%	65%	57%	18%	25%
72h	19%	14%	NA	21%	23%	24%	78%	8%	14%

was similar to the one detected by Ki67 staining (81% and 79%, respectively), which resulted in the same proportion of cells going into G0/G1 phase with both techniques (19% and 21%, respectively). This is also consistent with previous studies (Zammit et al., 2004). Along this line, it is important to discuss the proportion of cells in G0/G1 state obtained by flow cytometry analysis at both 48 and 72h, which is higher than expected. Again, this may be explained by the experimental method used. There, single satellite cells were enzymatically and mechanically isolated from cultured myofibres and it is very likely that myonuclei were present in the final cell solution. Since one single myofibre contains hundreds of myonuclei, this number could have been added up to the final percentage of G0/G1 cells in the analysis. A strategy to solve this problem is the labelling of satellite cells with a fluorescent reporter. Indeed, muscle fibres from Tg:Pax7-EGFP mice were used for some experiments but the GFP fluorescence was lost after ethanol fixation, which is a requirement for PI staining. However, antibody staining can also be performed and this is an approach that is highly recommended for future experiments. Overall, the use of different techniques allowed me to establish a proliferation profile of satellite cells *ex vivo*. This is relevant since a complete analysis of this type in satellite cells *ex vivo* has not been reported and it gives an interesting perspective on the use and scope of cell proliferation markers in our system (Table 6.1).

Most of the knowledge of satellite cell cell cycle dynamics comes from analysis of C₂C₁₂ myoblasts and isolated satellite cells, although some *in vivo* studies on satellite cells have also been reported. Flow cytometry analyses have shown the cell cycle profile of cultured myoblasts and human satellite cells before and after injury or acute exercise (Bellamy et al., 2014, Kollu et al., 2015, Lin et al., 2012, McKay et al., 2010). Furthermore, the dynamics of satellite cell proliferation have been analysed through label retention techniques *in vivo*, including BrdU and [³H]thymidine labelling and doxycycline pulses in TetO-H2B-GFP mice (Chakkalakal et al., 2014, Rocheteau et al., 2012, Schultz, 1996, Shinin et al., 2006). This has contributed to establish the average length of the cell cycle of satellite cells. In my analysis, I observed that satellite cells have a prolonged initial

G1 phase, as 65% of satellite cells were in G1/S and 24-29% in S phase at 24h according to Fucci2 and EdU analysis, which is consistent with previous reports (Rocheteau et al., 2012, Schultz, 1996). I also observed that the number of satellite cells increased by about 3-fold between 24 and 48h, indicating the completion of the first cell division and probably also the second division in a subset of satellite cells. This is also in line with previous studies reporting that satellite cells complete their first cell division between 24 and 48h (Mourikis et al., 2012b, Rocheteau et al., 2012, Schultz, 1996, Siegel et al., 2011) and that subsequent cell divisions occur faster, about every 8 to 10h (Rocheteau et al., 2012, Siegel et al., 2011). This indicates that the cell cycle dynamics of satellite cell *ex vivo* are similar to those found *in vivo*. Additionally, genome-wide analysis of cell cycle regulators has been performed in C₂C₁₂ myoblasts under proliferation and differentiation conditions, demonstrating that the onset of differentiation coincides with down-regulation of cyclins/Cdk complexes and up-regulation of cell cycle exit genes such as p21, p27 and Rb1 (Shen et al., 2003). A similar analysis in satellite cells *ex vivo* would be highly informative and would allow the refinement of the information I present in this chapter.

6.3.2 Shh signalling affects the cell cycle dynamics of satellite cells at two different time points during myogenesis *ex vivo*.

In chapter 5, I showed that activation or inhibition of Shh signalling triggered an increase or a decrease of satellite cell numbers, respectively. Previous studies have reported a role for Shh signalling in the control of myoblast proliferation (Elia et al., 2007, Koleva et al., 2005, Straface et al., 2009) and two studies suggested a beneficial effect of Shh-mediated therapy on satellite cell proliferation *in vivo* (Piccioni et al., 2014a,b). However, the extent to which Shh signalling controls satellite cell proliferation is still poorly understood.

Using the myofibre culture system, I identified two different timing at which Shh signalling is required for satellite cell cycle dynamics. First, within the first 24h of *ex vivo* culture, inhibition of Shh signalling resulted in a decrease in the proportion of proliferating satellite cells as shown by Ki67 and EdU staining. Furthermore, the proportion of cells going into S phase was lower with a concomitant increase in the percentage of satellite cells in G1 phase. These data indicate that Shh signalling is required for the timely initiation of cell cycle in satellite cells, probably by affecting the G1/S transition. The control of the G1/S checkpoint by Shh signalling has been described in other systems, including the zebrafish retina, the chick wing bud and the mouse external genitalia (Seifert et al., 2010, Towers et al., 2008, Wall et al., 2009). The molecular mechanism responsible for this regulation includes the transcriptional control of G1/S regulators, in particular *N-myc*, *CyclinE1*, *CyclinD1*, *Dp1* and *E2f1*. In satellite cells it remains to establish whether Shh

controls directly the transcription of G1/S regulators or acts indirectly via the control of other transcription factors. Further experiments are needed to decipher between these two possibilities.

The second effect of Shh signalling becomes noticeable at 72h: following inhibition of Shh signalling, satellite cells remained in a proliferative state, with most cells in S or G2/M and very few cells in G1 or G0. This indicates that Shh signalling controls cell cycle progression and exit, and thus the number of cells going into terminal differentiation or quiescence. Exit from the cell cycle in senescence, quiescence and differentiation is characterised by a prolonged cell cycle arrest with diploid DNA content and high cyclin dependent kinase inhibitor activity (p27 for quiescence and p21, p19 and p57 for terminal differentiation) (Buttitta and Edgar, 2007). Along this line, Shh signalling directs cell cycle exit through p57 activation in the zebrafish retina (Shkumatava and Neumann, 2005). Even more interesting is the fact that in the *Xenopus laevis* retina, a dual role of Hh signalling in controlling cell cycle dynamics has been described, where Hh signalling stimulates cell proliferation during early development and promotes cell cycle exit at later stages (Locker et al., 2006). Future experiments to analyse the expression of cyclin dependent kinase inhibitors may help identify the molecular targets of Shh signalling in the control of satellite cell cycle. Also, next-generation RNA sequencing (RNA-seq) of FACS-sorted satellite cells depleted of Shh signalling may provide further information of the genes under the control of Shh.

To conclude, during adult myogenesis early transition from G1 to S phase as well as cell cycle progression and exit prior differentiation is under the control of Shh signalling (Fig.6.7). These findings are important as they provide us with a better understanding of the extra-cellular cues that control satellite cell activity and more specifically, satellite cell cell cycle dynamics. This knowledge is also invaluable to design novel protocols for maintaining satellite cells *in vitro* prior to their use for cellular therapies.

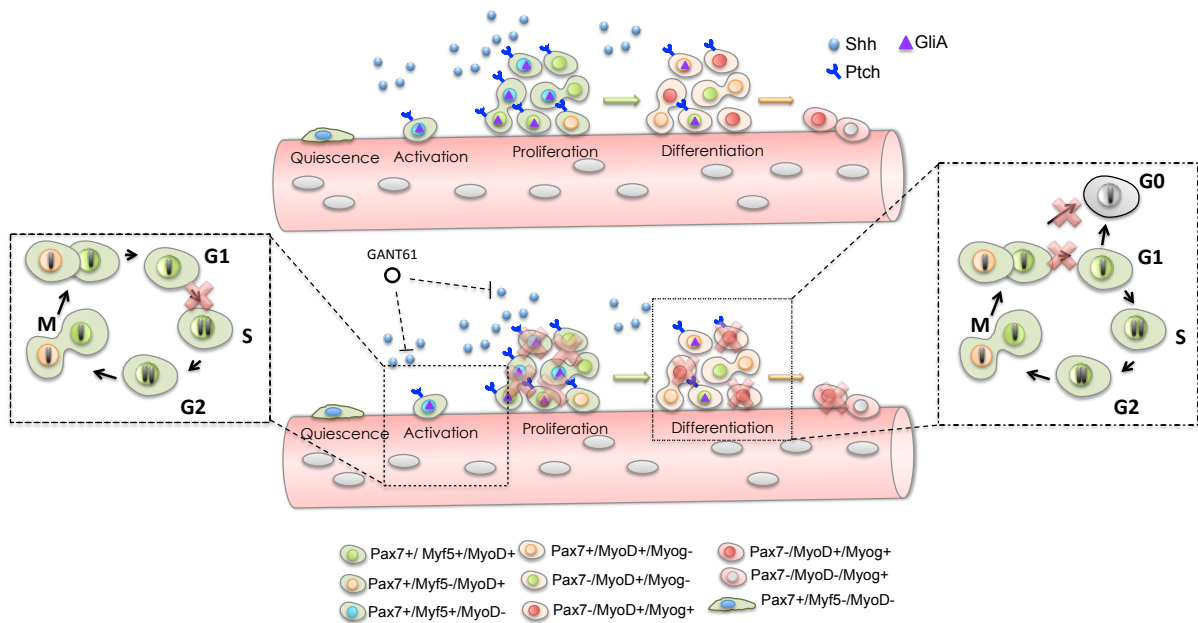


Figure 6.7: Model for satellite cell cell cycle control by Shh signalling. During the activation phase of adult myogenesis (24h), Shh signalling stimulates cell proliferation by affecting the G1-S transition. Conversely, pharmacological inhibition of the Shh pathway in satellite cells during the early differentiation phase (72h) leads to an increase in the proportion of proliferative progenitors, delaying the exit from the cell cycle and reducing the number of satellite cells reaching terminal differentiation.

SKELETAL MUSCLE REGENERATION IS IMPAIRED IN THE ABSENCE OF SHH SIGNALLING

7.1 Introduction

In previous chapters I have shown that activated satellite cells respond to Shh signalling and that this response facilitates the entry and progression of satellite cells through the cell cycle. Blockade of Shh signalling leads to a decrease in the number of satellite cells, delayed cell cycle entry and delayed myogenesis. This evidence suggests that Shh signalling is required for satellite cell activity *ex vivo*. Furthermore, I have shown that following skeletal muscle injury *in vivo*, activated satellite cells respond to Shh signalling. However, the requirement of this pathway in satellite cell function *in vivo* has not been determined yet. One approach to investigate the role of Shh signalling in satellite cell biology *in vivo* is the generation of knockout mice that disrupt Shh signalling transduction. In this study, I used a conditional knockout model, the Pax7^{CreERT2}-Smo^{flox/flox} mice, to specifically delete Smo expression in adult satellite cells.

The Cre-loxP system is the most efficient tool to generate tissue-specific inducible gene deletion. The Cre recombinase catalyzes the reciprocal exchange between two DNA sequences of 34-bp of length, the loxP sites (Hamilton and Abremski, 1984). The inducible system modifies the Cre recombinase by fusion with a mutated oestrogen receptor (ER), which allows temporal control of gene deletion through the binding of the ER antagonist tamoxifen (TM) (Feil, 2007). One of the best known application of this system in skeletal muscles was carried out by Lepper et al. to conditionally delete Pax7 expression in Pax7+ satellite cells (Lepper et al., 2009). Since Pax7 is expressed in muscle progenitor

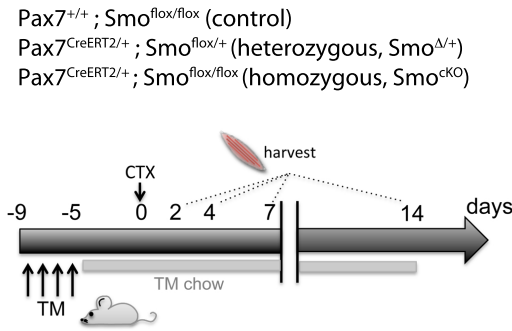


Figure 7.1: Tamoxifen (TM) and cardiotoxin (CTX) regimen and regeneration assay strategy. Mice were injected intraperitoneally for four days with TM. Mice were then fed with TM diet until sacrifice. TA muscles of control, $Smo^{\Delta/+}$ and Smo^{cKO} were injured by a single CTX injection and analysed at various times during regeneration.

cells during embryonic development but only expressed in satellite cells post-natally, the use of an inducible system allowed the deletion of Pax7 specifically in satellite cells from mature muscles (Lepper et al., 2009). Likewise, Shh signalling is indispensable for embryonic development and germline mutations of some of its components, including Smo, are embryonically lethal (Zhang et al., 2001). Therefore, I took advantage of the Cre/Lox inducible system to investigate the requirement of Shh signalling in satellite cell during adult muscle regeneration *in vivo*.

7.1.1 Hypothesis and aim

Given that satellite cells respond to Shh signalling both *ex vivo* and *in vivo* and that pharmacological manipulation of the pathway disrupts satellite cell cell cycle dynamics *ex vivo*, I hypothesised that in the absence of functional Shh signalling, satellite cells ability to repair muscles following injury would be impaired. Therefore, the aim of this chapter is to conditionally delete Smo expression in Pax7+ satellite cells and investigate the requirement of Shh signalling during muscle regeneration *in vivo*.

7.2 Results

7.2.1 Generation of the Pax7^{CreERT2}-Smo^{flox/flox} mutant mice.

To investigate the function of Shh signalling in adult muscles, the Smo receptor was specifically deleted from satellite cells using the Cre/LoxP system. Two original breeding lines of mice ($Smo^{flox/+}$) and ($Pax7^{CreERT2/+}$) were used to generate mutant $Pax7^{CreERT2/+}$ - $Smo^{flox/flox}$ newborns, also referred as Smo^{cKO} , heterozygous $Pax7^{CreERT2/+}$ - $Smo^{flox/-}$, referred as $Smo^{\Delta/+}$, and control $Smo^{flox/flox}$ mice (Fig.7.1).

In this conditional knockout model, the deletion of *Smo* is triggered by administration of tamoxifen (TM). Insufficient dose of TM may cause incomplete recombination (Günther et al., 2013) and too high dose of TM may have cytotoxic effects. Also, prolonged exposure to TM (15 months) can improve body musculature in dystrophic mice, which may have influence on the phenotype caused by Cre recombination (Dorchies et al., 2013). The experimental design of the TM treatment takes into account several factors, including dose, administration and duration, which can lead to variable levels of gene deletion (Günther et al., 2013). Therefore, a long-term treatment (up-to 3 weeks) with relative low doses of TM was adopted for my experiments in order to achieve high percentage of recombination. TM was administered intraperitoneally at 3mg/40g of body weight daily for 4 days before CTX-induced injury. From day 5 mice were fed with TM chow (approximate dose of 40 mg/kg/day) until sacrifice (Fig.7.1). This protocol has been used by others and was found to give over 80% of recombination (von Maltzahn et al., 2013). For the present study, quantification of the Cre recombination rate was done by PhD student Kamalliawati Mohd using Pax7^{CreERT2/+}-*Smo*^{Δ/+} Rosa26-YFP mice. These mice allow to monitor Pax7-expressing satellite cells that have undergone Cre-mediated recombination through the quantification of YFP expression. EDL myofibres from Pax7^{CreERT2/+}-*Smo*^{Δ/+} Rosa26-YFP were analysed by immunofluorescence after 0 and 24h in culture to detect the expression of the satellite cell marker Caveolin-1 and the YFP protein (Fig.7.2, A). This analysis showed that around 83.81% and 90.50% of cultured satellite cells at 0 and 24h underwent recombination after TM injections/diet (Fig.7.2, B). This experimental aspect is crucial when working with inducible knockout systems, as incomplete recombination can mask the deletion phenotype and lead to debatable conclusions.

7.2.2 Effect of satellite cell-specific deletion of *Smo* on muscle architecture following CTX injury.

To test the requirement for Shh signalling pathway during muscle repair, regeneration following CTX-induced injury was analysed in *Smo*^{CKO} mice (Fig.7.1).

First, I examined the morphology of non-injured and CTX-injured TA muscles from control, *Smo*^{CKO} and *Smo*^{Δ/+} mice using hematoxylin and eosin staining (Fig.7.3) and Laminin α -2 immunolabelling to assess the cross sectional area (CSA) of myofibres (Fig.7.4). Healthy non-injured TA muscles from the three different genotypes showed a uniform architecture, myonuclei were located at the periphery of muscle fibres and most of the myofibres were between 1500 and 2000 μ m² of size (Fig.7.3 A-C and Fig.7.4 A-D). At two days post-injury, necrosis and infiltration of mononucleated cells was wide-spread at the site of injury in all mice (Fig.7.3 D-F yellow arrows). This resulted in the damage of the muscle architecture compared to non-injured regions (green arrows) and no evident differ-

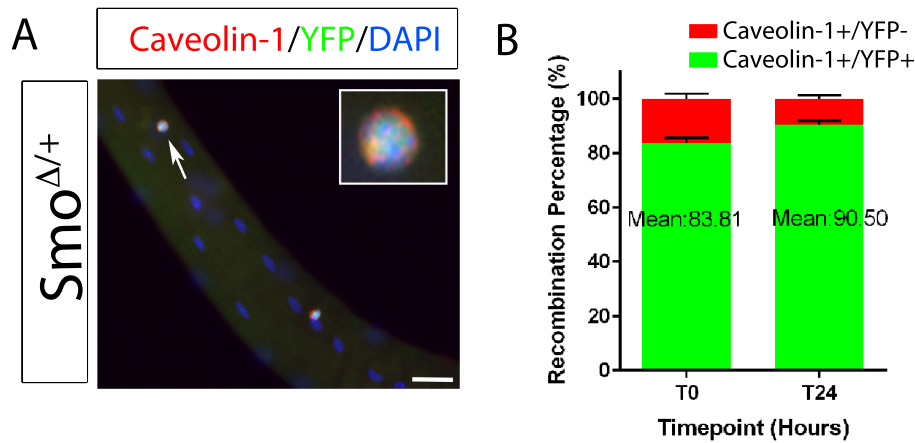


Figure 7.2: Efficiencies of Cre-mediated recombination measured by YFP expression. Pax7^{CreERT2/+}-Smo^{Δ/+} Rosa26-YFP mice were injected intraperitoneally for four days with TM and then fed with TM diet until sacrifice. EDL muscle fibres from these mice were cultured *ex vivo* for 0 and 24h and then immunostained to detect Caveolin-1 and YFP expression. Myonuclei were counterstained with DAPI. (A) Merged image of a 24h-cultured myofibre showing Caveolin-1 and YFP co-expression. Magnified view is also shown (region indicated by an arrow). Scale bar represents 32 μ m. (B) show the quantitative analyses of the percentage of Caveolin-1 and YFP+ cells at 0 and 24h per myofibre. Representative data from two individual mice are shown. Values are mean and SEM.

ence was observed at this point between genotypes. The infiltration of inflammatory cells and satellite cells continued at 4 days post-injury. New fibres with centrally located myonuclei were already visible in both control and Smo^{Δ/+} but hardly detectable in Smo^{cKO} mice (Fig.7.3 G-I). This was consistent with the presence of a higher frequency of small fibres in Smo^{cKO} mice (less than 500 μ m²) than other mice (Fig.7.4 E-H). At 7 days post-injury, newly regenerated myofibres were highly abundant in all mice (Fig.7.3 G-I red arrows). Interestingly, in both Smo^{cKO} and Smo^{Δ/+} accumulation of mononucleated cells was still visible (Fig.7.3 J-L yellow arrows) and persisted until 14 days post-injury (Fig.7.3 M-O). Additionally, the frequency of myofibres with small size was higher in Smo^{cKO} and Smo^{Δ/+} compared to control muscles (Fig.7.4 I-L). Consistent with this observation, myofibres from Smo^{cKO} and Smo^{Δ/+} muscles hardly reached 1500 μ m² in size and most of the fibres were rather small (less than 500 μ m²) whereas control muscles had regenerated myofibres of up to 3000 μ m² in size at 14 days post-injury (Fig.7.4 M-P). Concomitantly, a higher number of regenerating myofibres was observed per section in Smo^{cKO} and Smo^{Δ/+} muscles. Together, this indicates that the partial or total loss of Smo function in satellite cells affects negatively the regeneration process following muscle injury, as shown by the abundance of small-caliber fibres and the accumulation of mononucleated cells at both 7 and 14 days post-injury.

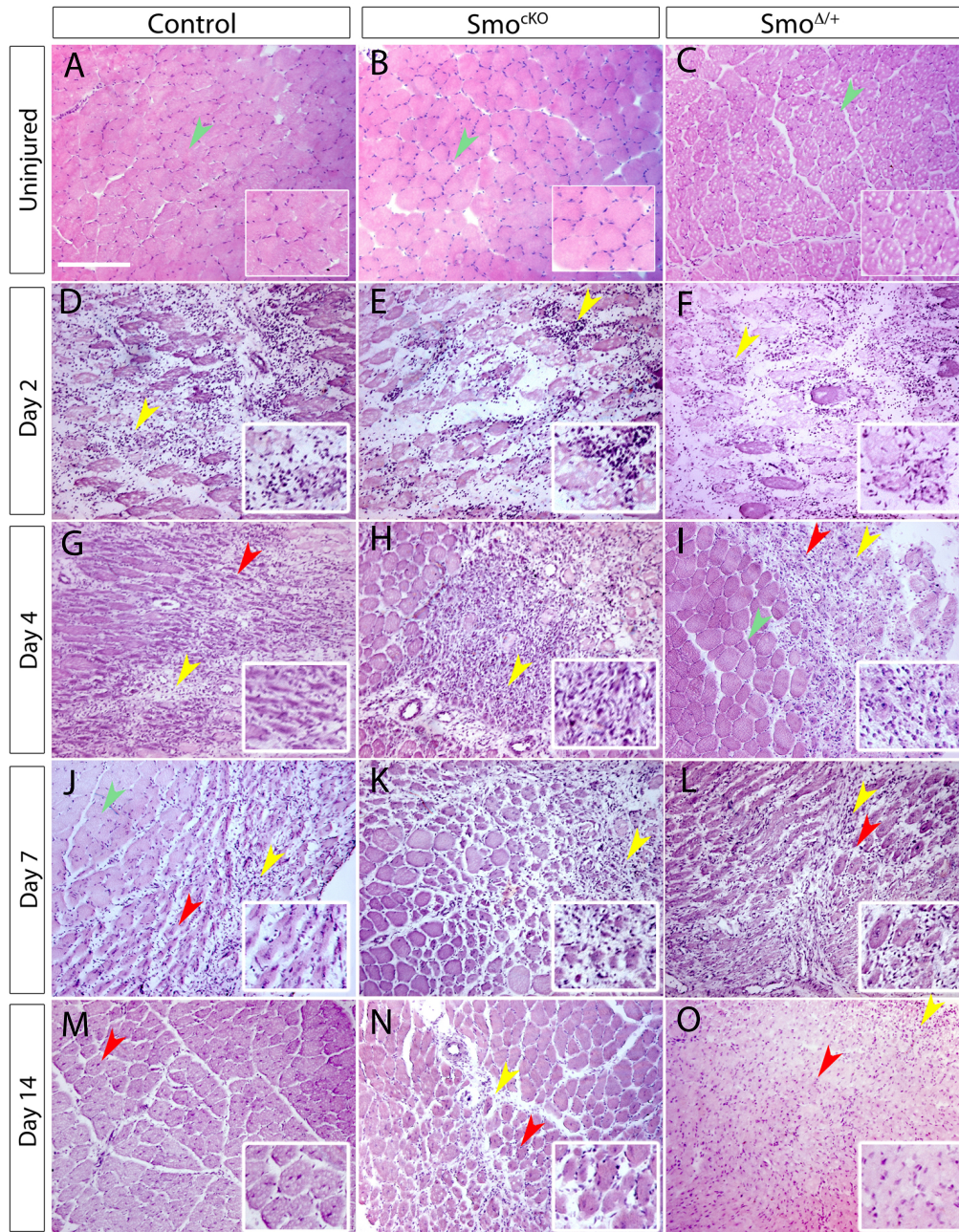


Figure 7.3: Regeneration following CTX-induced muscle injury in Smo^{cKO} mice Uninjured and cardiotoxin-injured (2, 4, 7 and 14 days) TA muscles from control, Smo^{cKO} and Smo^{Δ/+} mice were analysed by H&E staining to assess changes in muscle architecture. Non-injured TA muscle from all mice had fibres with homogeneous size and appearance (A-C). All injured muscles showed similar morphological changes in myofibre shape due to necrosis and cell infiltration of different types of mononuclear cells at 2 (D-F) and 4 days (G-I) post-injury. Newly regenerating myofibres were visible from day 4 in both control and Smo^{Δ/+} but not really detectable in Smo^{cKO} mice. Centrally located nuclei were more evident by day 7 post-injury in control and Smo^{Δ/+} and already visible in Smo^{cKO} mice. (J-L). Muscle architecture was restored by 14 days post-injury in control mice, with the presence of fully regenerated myofibres (M). In contrast, Smo^{Δ/+} and Smo^{cKO} muscles had altered architecture, showing some regenerating regions with small fibres and infiltrating cells (N and O). Non-injured areas, infiltrated cells and fibres with centrally located nuclei are shown with green, yellow and red arrows, respectively. Representative images from three individual mice for each time point are shown. Scale bar represents 200μm.

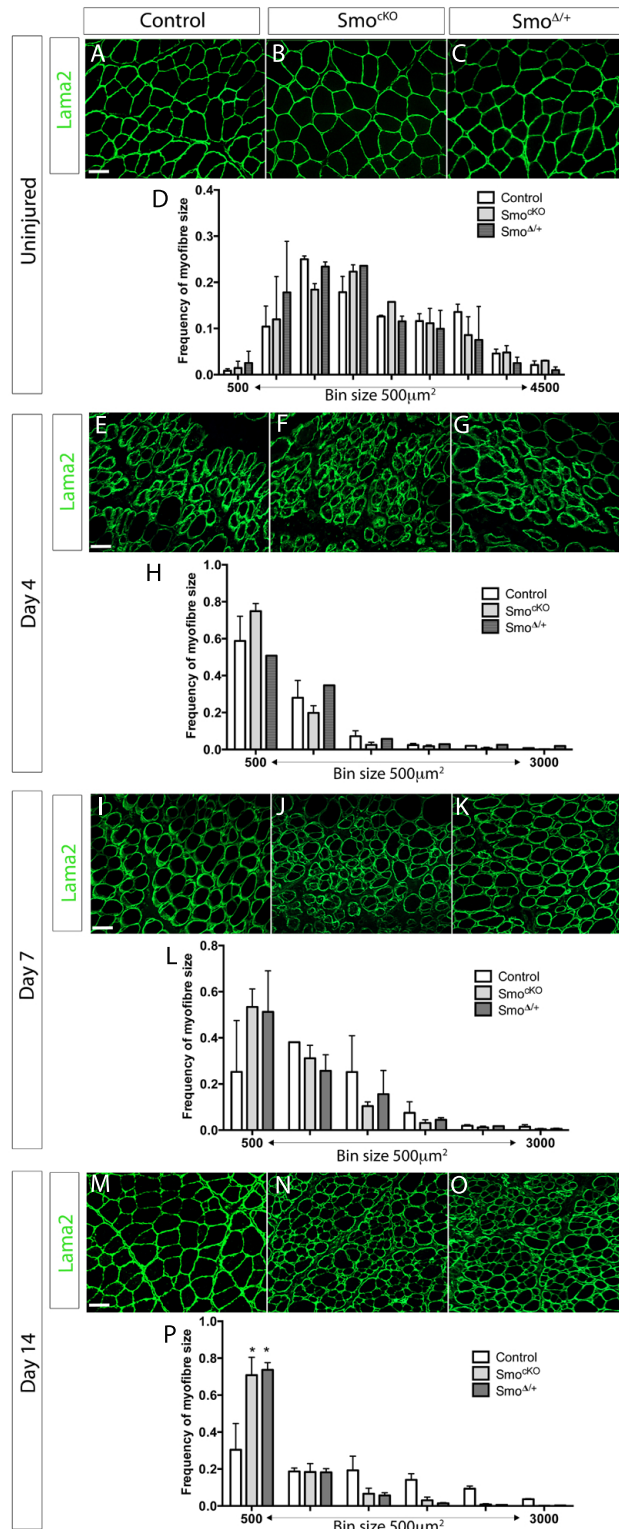


Figure 7.4: Myofibre size declines in regenerating TA muscles of Smo^{cKO} and $Smo^{\Delta/+}$ mice. Uninjured and cardiotoxin-injured (4, 7 and 14 days) TA muscles from control, $Smo^{lox/+}$ and Smo^{cKO} mice were analysed by Laminin alpha-2 (Lama2) immunostaining and the cross sectional area (CSA) of myofibres was analysed. Scale bar represents $50\mu m$. The relative frequency of fibres was plotted against fibre cross-sectional area in μm^2 . A high percentage of small fibres (less than $500\mu m^2$) was observed to be higher at 14 days post-injury in Smo^{cKO} and $Smo^{\Delta/+}$ mice compared to control mice ($p < 0.0001$). Representative data from three individual mice per time point, where three cross-sectional fields (0.154 mm^2) of regenerating muscle per mouse were analysed. Values are mean and error bars show SEM. Statistical analysis was performed using Student's t-test.

7.2.3 Satellite cell-specific deletion of Smo increases fibrosis during muscle regeneration.

Efficient skeletal muscle regeneration is orchestrated by the interplay between satellite cells and non-muscle cells, including inflammatory cells and fibroblasts. Fibroblasts produce extracellular matrix components such as collagen type I, fibronectin, elastin and laminin (Mann et al., 2011). Indeed, transient collagen deposition following CTX-induced injury is a feature of muscle regeneration and it is thought to contribute to muscle stabilisation and to help sequester growth factors that stimulate satellite cell function (Cornelison, 2008, Kääriäinen et al., 2000). However, excessive collagen deposition can lead to fibrosis and interfere with muscle regeneration. Therefore, to assess the extent of fibrosis in regenerating muscles, I performed an immunostaining analysis to detect collagen type I deposition at 7 and 14 days post-injury.

I observed that regenerating control muscles had about 16% of collagen deposition at 7 days post-injury (Fig.7.5 A and G). This percentage was reduced to 9% at 14 days post-injury, indicating that collagen deposition is transient and decreases as regeneration progresses (Fig.7.5 D and G). In contrast, in both Smo^{CKO} and Smo^{Δ/+} muscles, collagen accumulated significantly at 7 days compared to control muscles (deposition of 34.5% and 45.4%, respectively) (Fig.7.5 B, C and G). Furthermore, the amount of collagen deposition remained high at 14 days post-injury in Smo^{CKO} muscles (deposition of 37%), whereas in Smo^{Δ/+} muscles collagen deposition was reduced between 7 and 14 days but was significantly different from the control by 14 days post-injury (deposition of 23%). This suggests that loss of functional Shh signalling in satellite cells had a negative impact on the progression of muscle regeneration, leading to the persistent accumulation of collagen type I.

Next, in order to see if changes in fibre size and accumulation of fibrosis had an impact on the overall size of the muscles, weight ratio of injured and non-injured TA muscles was determined. Against all expectations, the ratio of muscle weight in Smo^{CKO} and Smo^{Δ/+} mice was similar to the control (Fig.7.6), indicating that the knockout of Smo in satellite cells does not cause muscle loss or atrophy. It can be possible, however, that the high accumulation of collagen and the increase in fibre number might compensate for any loss of muscle mass.

7.2.4 The absence of active Shh signalling in satellite cell delays muscle regeneration *in vivo*.

Previous work has established that in the embryonic limb, myogenesis is delayed in the absence of Shh signalling (Anderson et al., 2012). Similarly, *ex vivo* inhibition of the

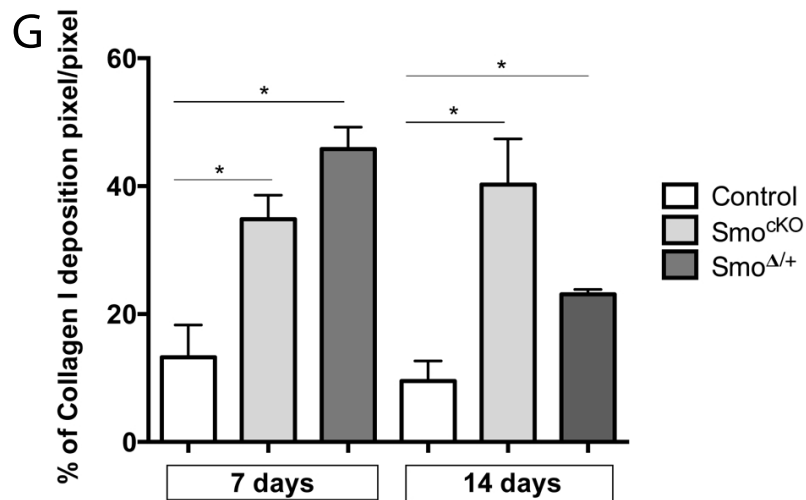
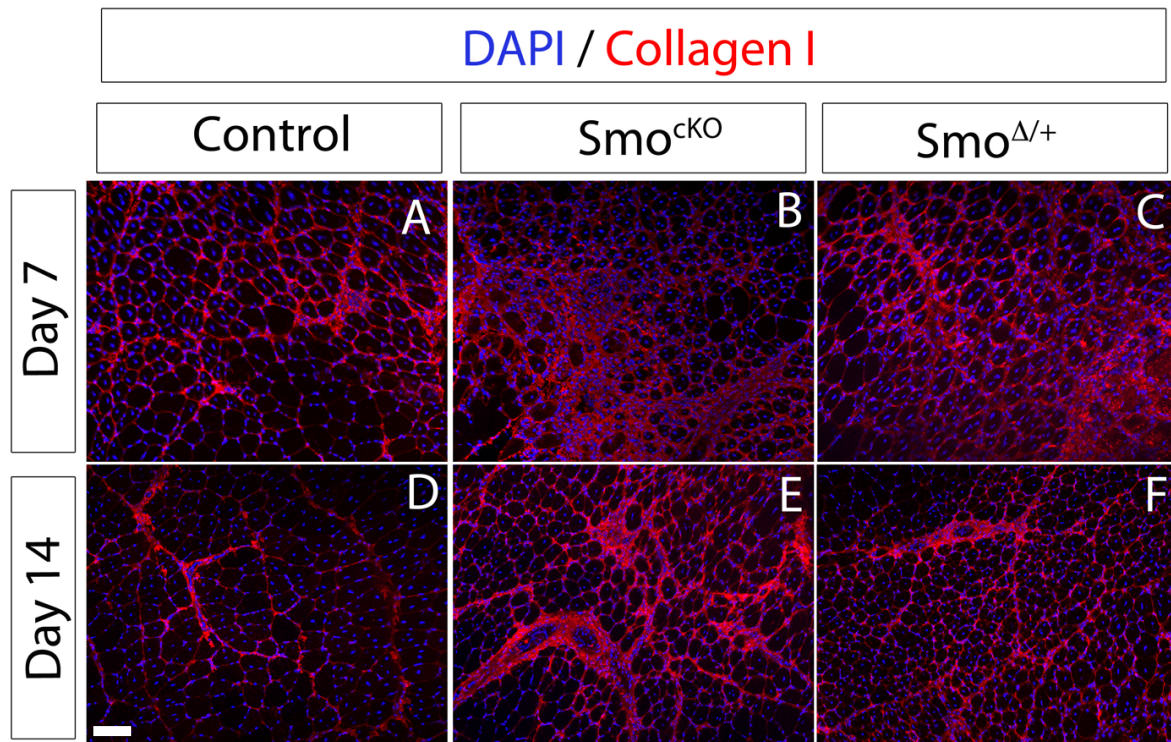


Figure 7.5: Collagen type I deposition increases in Smo^{cKO} and Smo^{Δ/+} regenerating muscles. 7-day (A-C) and 14-day (D-F) CTX-injured TA muscles from control, Smo^{cKO} and Smo^{Δ/+} mice were analysed by collagen type I immunostaining and the percentage of collagen deposition was calculated (G). Myonuclei were counterstained with DAPI. The percentage of fibrosis was calculated by averaging the area of positive collagen staining in multiple sections per TA-injured muscle. There was a significant difference between the amount of collagen in Smo^{cKO} and Smo^{Δ/+} muscles at 7 days compared to control ($p=0.0391$ and $p=0.0335$, respectively). Likewise, the deposition of collagen at 14 days post-injury in Smo^{cKO} and Smo^{Δ/+} muscles was significantly different from the control ($p=0.0464$ and $p=0.0285$, respectively). Representative data from two to three individual mice per time point, where three to four cross-sectional fields (0.154 mm^2) of regenerating muscle per mouse were counted. Values are mean and error bars show SEM. Statistical analysis was performed using Student's t-test.

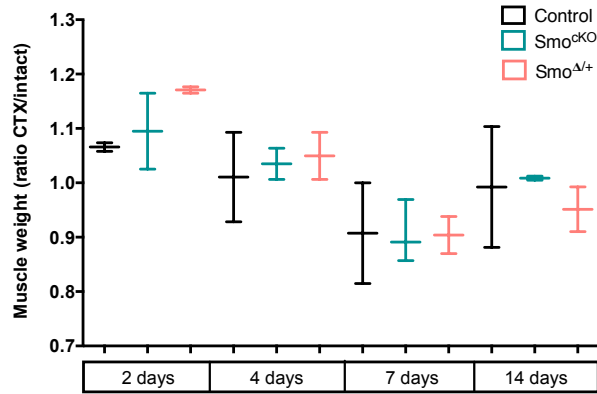


Figure 7.6: Specific deletion of Smo in satellite cells does not affect the weight of regenerating muscles. 2, 4, 7 and 14-day CTX-injured TA muscles from control, Smo^{cKO} and Smo^{Δ/+} mice were weighted and normalised to contralateral uninjured TA muscles (intact). No significant difference was found between genotypes. Boxes represent RQ and whiskers show minimum and maximum values. Representative data based on two to three mice per time point. Statistical analysis was performed using Student's t-test.

Shh signalling pathway in satellite cells leads to a delay in the progression through the myogenic program. Therefore, I decided to test if the lack of functional Shh signalling affected MRF expression in adult satellite cells *in vivo*.

Regenerating TA muscles were harvested at 2, 4, 7 and 14 days after CTX injection and MyoD immunostaining was performed. I observed that total and partial Smo-inactivation in satellite cells resulted in a significant decrease in the number of MyoD+ cells at 2 days post-injury compared to control muscles (37% and 44% reduction for Smo^{cKO} and Smo^{Δ/+}, respectively) (Fig.7.7 A-C and M). Importantly, a 80% decrease in the number of differentiating Myogenin+ cells was also observed in both Smo^{cKO} and Smo^{Δ/+} muscles at 2 days compared to the control (Fig.7.8 A-C and M). At 4 days post-injury, the number of MyoD+ and Myogenin+ cells in Smo^{cKO} and Smo^{Δ/+} muscles was not significantly different from the control, although a trend towards reduced MyoD and Myogenin expression was apparent in Smo^{cKO} muscles (Fig.7.7 D-F and M and Fig.7.8 D-F and M). These data indicate that the absence of Shh signalling affects satellite cell progression through the myogenic program in regenerating adult muscles.

As shown in chapter 3, by 7 days post-injury the number of both MyoD+ and Myogenin+ cells decreases importantly and this coincides with the gradual restoration of the muscle architecture in normal muscles. However, no such decrease was observed in Smo^{cKO} and Smo^{Δ/+} muscles (Fig.7.7 G-I and M and Fig.7.8 G-I and M). By 14 days post-injury, a significant number of MyoD+ and Myogenin+ cells remained present in Smo^{cKO} and Smo^{Δ/+} muscles compared to the control (Fig.7.7 J-L and M and Fig.7.8 J-L and M). More specifically, there was a 2.5 and 5-fold increase in the number of MyoD+ cells and more than a 14-fold increase in the number of Myogenin+ cells was observed for Smo^{cKO} and Smo^{Δ/+} muscles, respectively. This strongly suggests that in the absence of

Shh signalling, satellite cells are delayed in their muscle repair program.

To determine whether Smo^{cKO} and $\text{Smo}^{\Delta/+}$ injured muscles would recover at later time points, I performed immunostaining to analyse MyoD expression in 21-day post-injury muscles. Control muscles had a uniform architecture and most regenerated myofibres with centrally located myonuclei were of similar size. Importantly, similar to the 14-day post-injury muscles, no MyoD expression was detected (Fig.7.9 A and A'). In contrast, the architecture of Smo^{cKO} and $\text{Smo}^{\Delta/+}$ muscles was not homogeneous as small caliber fibres were still present. Moreover, MyoD+ cells were still detected in Smo^{cKO} but not in $\text{Smo}^{\Delta/+}$ muscles (Fig.7.9 B-C'). This indicates that inactivation of Smo in satellite cells causes severe impairment in muscle regeneration in response to injury.

The decrease in the number of MyoD+ and Myogenin+ cells in Smo^{cKO} and $\text{Smo}^{\Delta/+}$ muscles suggests that satellite cells may fail to proliferate in the absence of Shh signalling. Therefore, I examined the expression of the proliferation marker Ki67 in sections from 2, 4, 7 and 14-day CTX-injured muscles. Overall, cell proliferation at 2, 4 and 7 days following acute injury was not significantly different in muscles lacking one or two copies of Smo in satellite cells compared to control muscles (Fig.7.10 A-I and M). In contrast, a 6-fold increase in the number of Ki67+ cells in both Smo^{cKO} and $\text{Smo}^{\Delta/+}$ muscles was observed at 14 days post-injury compared to the control. Most of these Ki67+ cells were in a sublaminar position and hence are likely to be satellite cells (Fig.7.10 J-L and M). This is consistent with the increase of MyoD+ myoblasts at 14 days and strengthens the idea that in the absence of Shh signalling, satellite cells delay their progression into the myogenic program and remain proliferative at late stages of muscle regeneration.

To further investigate the behaviour of Smo-inactivated satellite cells, I analysed how the expansion dynamics of these cells was affected upon loss of Shh signalling. To do so, control and Smo^{cKO} mice were treated with TM and myofibres were isolated after one week on TM diet and cultured for 0, 24, 48 and 72h. Fibres were then immunostained to detect Pax7/Myf5 (0 and 24h), Pax7/MyoD (48h) and Caveolin-1/Myogenin (72h) expression. I observed that the number of Pax7+ cells in freshly isolated myofibres was similar in both control and Smo^{cKO} mice (Fig.7.11 C). Likewise, at 24 and 48h, the number of activated Pax7+/Myf5+ and Pax7+/MyoD+ satellite cells did not change significantly in Smo^{cKO} compared to the control, although there was a tendency towards a reduced number of satellite cell (Fig.7.11 C). In contrast, at 72h in Smo^{cKO} fibres, the number of Caveolin-1+/Myogenin- and Caveolin+/Myogenin+ satellite cell was reduced by 45% and 55%, respectively, whereas the differentiated Caveolin-1-/Myogenin+ population completely disappeared (Fig.7.11 A-C). These results are consistent with my previous experiments using GANT61 and cyclopamine to block Shh signalling. Together, these data confirm that in the absence of Shh signalling, satellite cells delay their progression through the myogenic program with a concomitant reduction in satellite cell numbers.

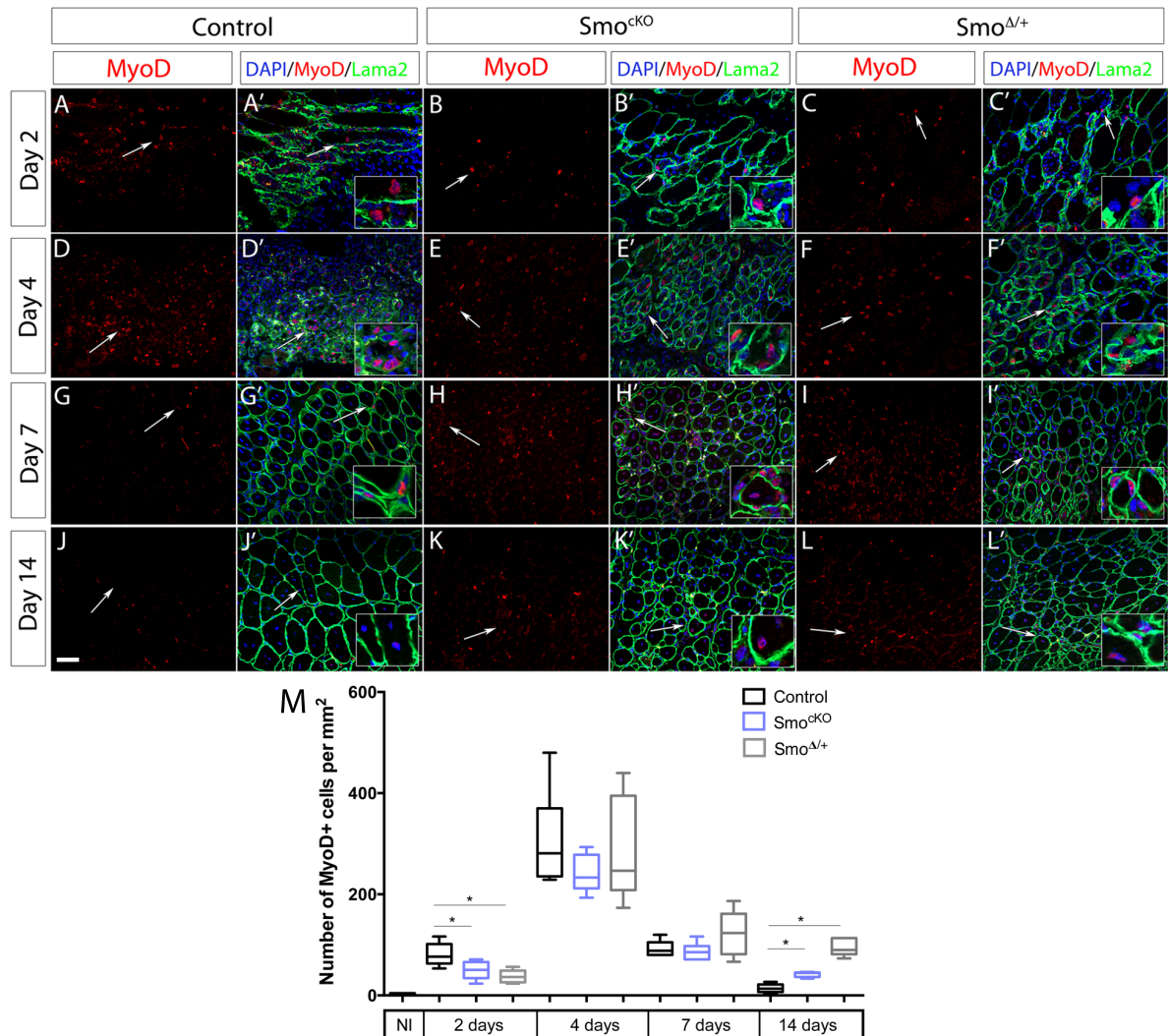


Figure 7.7: Loss of Smo affects the number of MyoD+ satellite cells in regenerating muscles. CTX-injured (2, 4, 7 and 14 days) TA muscles from control, Smo^{cKO} and Smo^{Δ/+} mice were analysed by immunofluorescence to detect MyoD (red). Cell nuclei were counterstained using DAPI (blue) and muscles fibres were outlined with Laminin alpha 2 (green). Merge images from three channels are shown for each genotype at 2, 4, 7 and 14 day-injured muscles in A' to L'. Magnified views for merged images are shown (regions indicated by an arrow). Scale bar represents 50μm. There was a significant difference in the number of MyoD+ cells at 2 days in Smo^{cKO} and Smo^{Δ/+} muscles compared to the control (p=0.0057 and p=0.0229, respectively). Moreover, a significant increase in MyoD+ cells was observed at 14 days in Smo^{cKO} and Smo^{Δ/+} muscles compared to control (p=0.0340 and p=0.0444, respectively). Representative data from three individual mice per time point, where four to six cross-sectional fields (0.154 mm²) of regenerating muscle per mouse were counted. Boxes represent RQ and whiskers show minimum and maximum values. Statistical analysis was performed using Student's t-test.

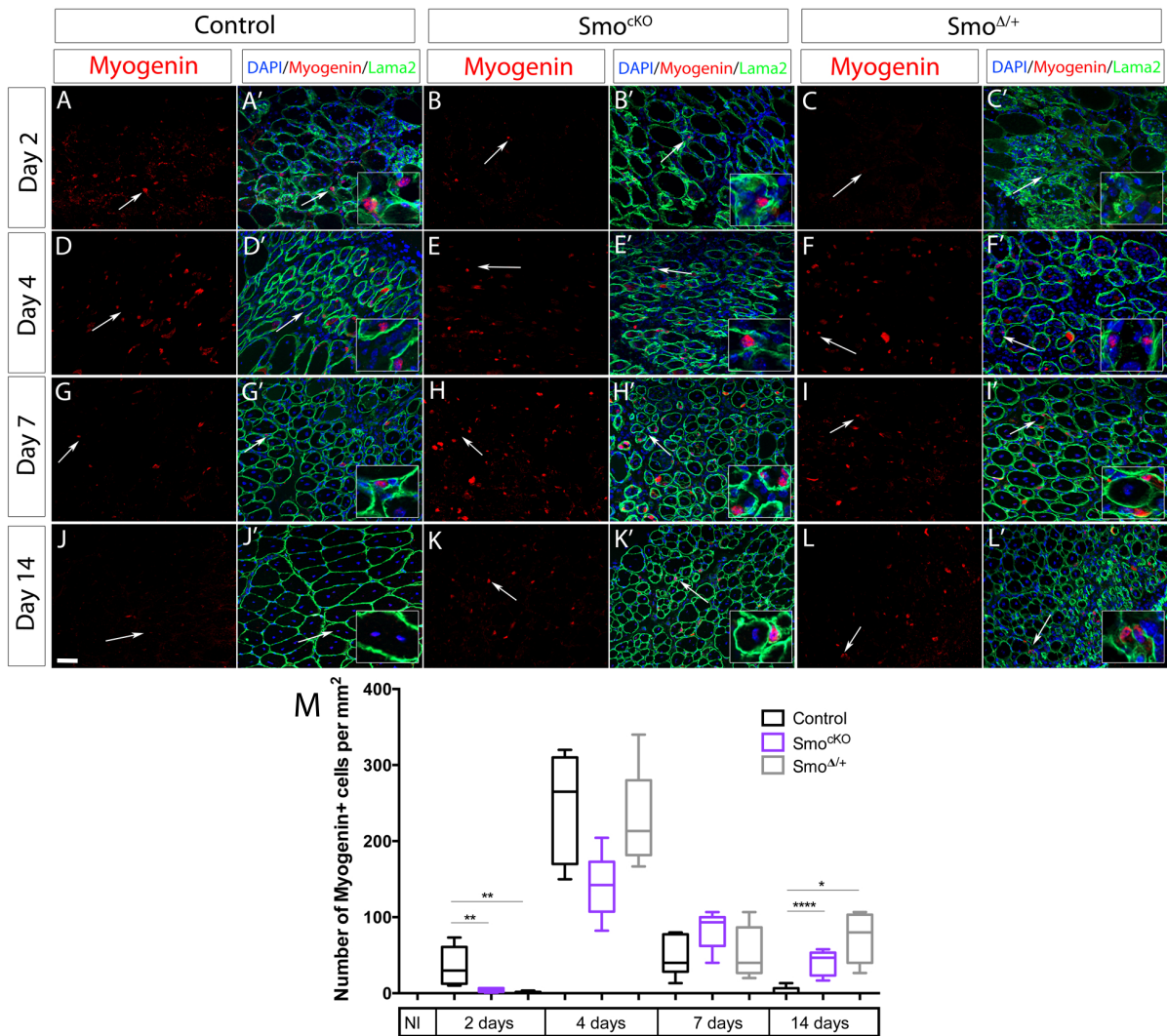


Figure 7.8: Decrease of satellite cell differentiation in the absence of Shh signalling. CTX-injured (2, 4, 7 and 14 days) TA muscles from control, Smo^{cKO} and $\text{Smo}^{\Delta/+}$ mice were analysed by immunofluorescence to detect Myogenin (red). Cell nuclei were counterstained using DAPI (blue) and muscles fibres were outlined with Laminin alpha 2 (green). Merge images from three channels are shown for each genotype at 2, 4, 7 and 14 day-injured muscles in A' to L'. Magnified views for merged images are shown (regions indicated by an arrow). Scale bar represents $50\mu\text{m}$. There was a significant difference in the number of Myogenin+ cells at 2 days in Smo^{cKO} and $\text{Smo}^{\Delta/+}$ muscles compared to control ($p=0.0081$ and $p=0.0019$, respectively). Similarly, there was a significant increase in the number of Myogenin+ cells at 14 days in Smo^{cKO} and $\text{Smo}^{\Delta/+}$ muscles compared to control ($p < 0.0001$ and $p=0.0150$, respectively). Representative data from three individual mice per time point, where four to six cross-sectional fields (0.154 mm^2) of regenerating muscle per mouse were counted. Boxes represent RQ and whiskers show minimum and maximum values. Statistical analysis was performed using Student's t-test.

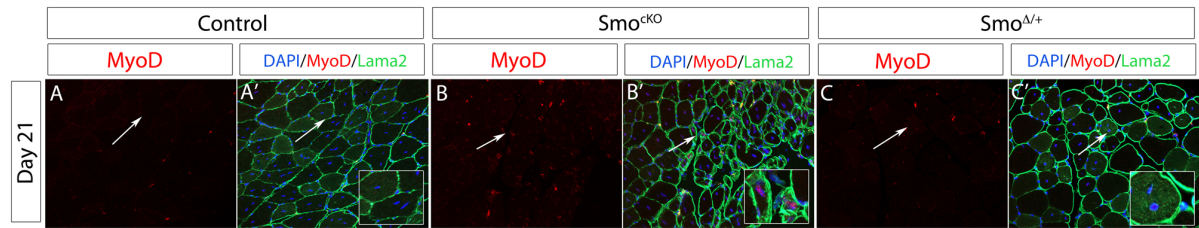


Figure 7.9: Regeneration at 21 days post-injury in Smo^{cKO} and Smo^{Δ/+} CTX-injured muscles. CTX-injured TA muscles from control (A-A'), Smo^{cKO} (B-B') and Smo^{Δ/+} (C-C') mice were analysed by immunofluorescence to detect MyoD (red). Cell nuclei were counterstained using DAPI (blue) and muscles fibres were outlined with Laminin alpha 2 (green). Merge images from three channels are shown for each genotype. Magnified views for merged images are shown (regions indicated by an arrow). Regenerating muscles at 21 days post-injury exhibit a homogeneous architecture made up of fibres with centrally located myonuclei and no MyoD expression. On the other hand, Smo^{cKO} and Smo^{Δ/+} muscles had smaller fibres and MyoD-expressing cells were still detectable in Smo^{cKO} mice. Representative images from one individual mouse per phenotype.

7.3 Discussion

7.3.1 The absence of Shh signalling impairs muscle regeneration *in vivo*.

In this chapter, I used Pax7^{CreERT2/+}-Smo^{flox/flox} mice to induce deletion of Smo in satellite cells and investigate muscle regeneration for up to 21 days following CTX injury. I observed that deletion of Smo in satellite cells leads to impaired muscle regeneration: 1) Satellite-cell specific deletion of one or two Smo alleles leads to reduced fibre size in 7 and 14-day regenerating muscles; 2) The reduced fibre caliber is accompanied by an increased deposition of collagen type I; 3) An overall delay in the progression through the myogenic program was observed in Smo^{cKO} and Smo^{Δ/+} muscles.

Although previous studies reported that disrupting Shh signalling impairs muscle regeneration (Renault et al., 2013a,b, Straface et al., 2009), this is the first report of a direct requirement for Shh signalling in satellite cells. Indeed, previous studies reported that transfection of injured and dystrophic adult muscles with a plasmid encoding human Shh improved muscle regeneration in mice (Piccioni et al., 2014a,b). However, the direct effect of Shh on satellite cells was not assessed and the authors presumed that Shh signalling was positively affecting both angiogenesis and myogenesis. Loss-of-function approaches have consisted so far in analysing muscle repair following the systemic administration of cyclopamine. This resulted in impaired muscle regeneration with low numbers of activated satellite cells (Straface et al., 2009). In another report using a conditional knockout model to delete Gli3 in post-mitotic skeletal muscles (using a human α -skeletal actin promoter) (HSACre^{ERT2}; Gli3^{flox/flox}), the authors observed delayed ischemia-induced myogenesis (Renault et al., 2013b). However, the significance of these observations is unclear as Gli3

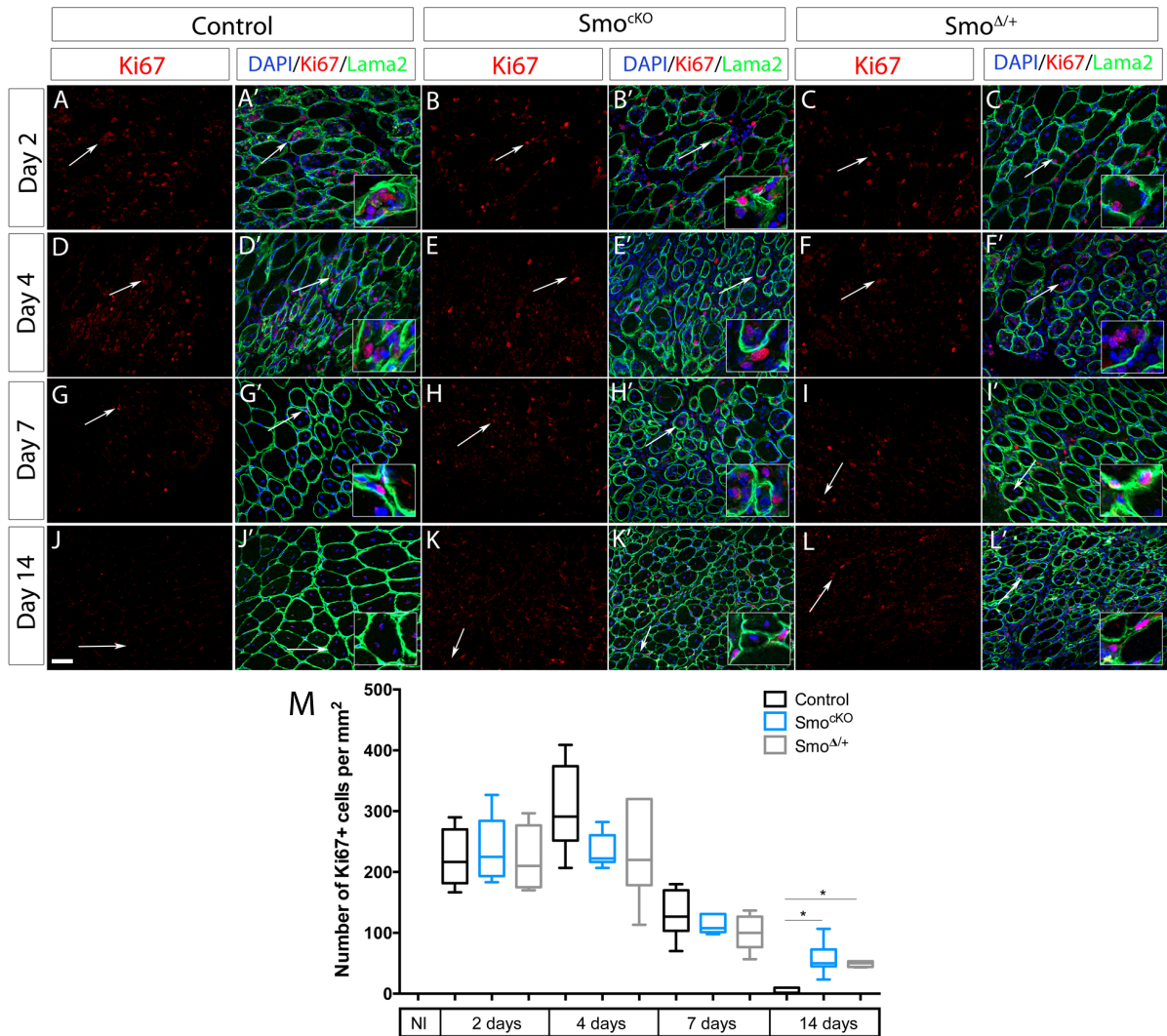


Figure 7.10: Satellite cells remain proliferative at late stages of regeneration in the absence of Shh signalling. CTX-injured (2, 4, 7 and 14 days post-injury) TA muscles from control, Smo^{cKO} and $Smo^{\Delta/+}$ mice were analysed by immunofluorescence to detect the proliferation marker Ki67 (red). Cell nuclei were counterstained using DAPI (blue) and muscles fibres were outlined with Laminin alpha 2 (green). Merge images from three channels are shown for each genotype at 2, 4, 7 and 14 day-injured muscles in A' to L'. Magnified views for merged images are shown (regions indicated by an arrow). Scale bar represents 50 μ m. There was a significant difference in the number of Ki67+ cells at 14 days in Smo^{cKO} and $Smo^{\Delta/+}$ muscles compared to control muscles ($p=0.0166$ and $p=0.0190$, respectively). Representative data from three individual mice per time point, where four to six cross-sectional fields (0.154 mm²) of regenerating muscle per mouse were counted. Boxes represent RQ and whiskers show minimum and maximum values. Statistical analysis was performed using Student's t-test.

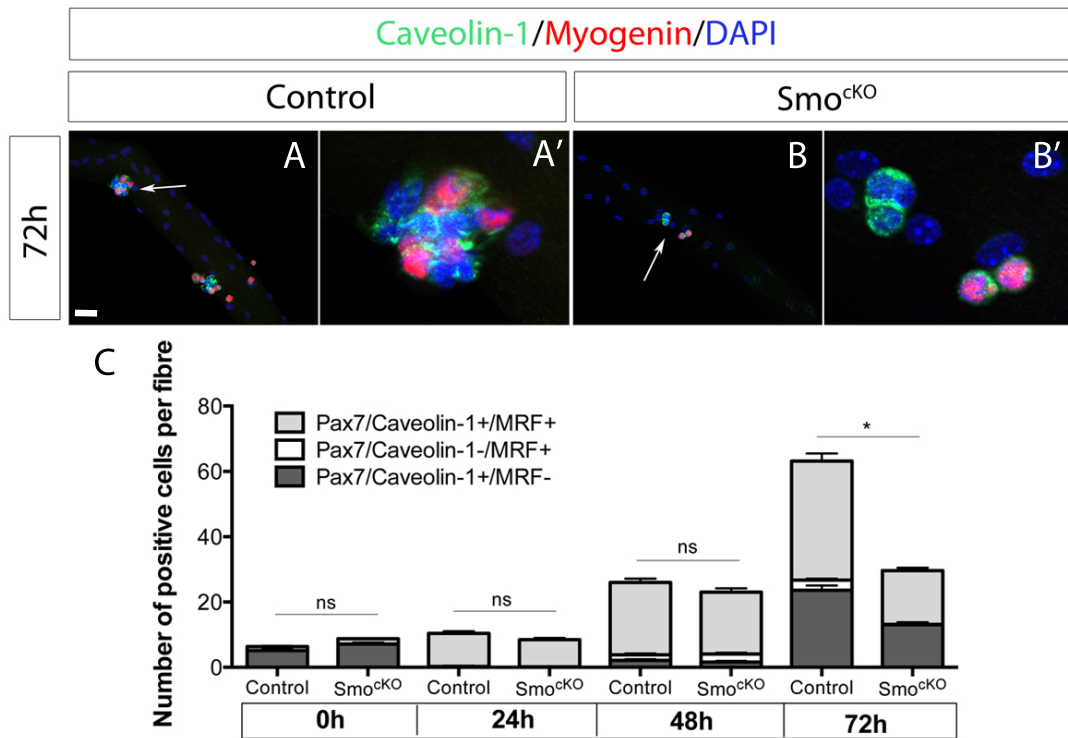


Figure 7.11: Smo deletion impairs the expansion of activated satellite cells. EDL muscle fibres from control and Smo^{ckO} mice were cultured for 0, 24, 48 and 72h. 0 and 24h-cultured myofibres were immunostained to detect Pax7 and Myf5; 48h-cultured myofibres for Pax7 and MyoD and 72h-cultured fibres for Caveolin-1 and Myogenin. Merged images for 72h-cultures are shown in A and B. Magnified views for every image are shown in A' and B'. Scale bar represents 20 μ m. Quantification of immunofluorescence analysis is shown in C. Smo deletion caused a decrease in the number of both Caveolin-1+/Myogenin- (p=0.0214), Caveolin-1-/Myogenin+ (p=0.05) and Caveolin-1+/Myogenin+ (p=0.0125) cells at 72h. Representative data from two individual mice are shown, with 14 to 31 individual fibres per mouse for each time point. Values are mean and SEM. Statistical analysis was performed using Student's t-test.

was in this case removed from myofibres but not satellite cells, and I have shown using the Tg(GBS-GFP) mice that only satellite cells respond to Shh signalling in myofibre preparations. Finally, a study using Smo heterozygous mice demonstrated that the loss of a single copy of Smo altered muscle repair (Renault et al., 2013a). However, in this study Smo deletion occurred before birth, which, given the role of Shh in embryonic myogenesis (Anderson et al., 2009, 2012, Borycki et al., 1999b, Kruger et al., 2001), opens the possibility that the phenotype observed in adult muscles originates during embryonic development. Therefore, although these studies reported a general impairment of skeletal muscle regeneration linked to the disruption of Shh signalling, including increased fibrosis, decreased MRF expression and reduction of angiogenesis (Renault et al., 2013a,b, Straface et al., 2009), a direct requirement for Shh signalling in satellite cells was not demonstrated. Here, the study of Pax7^{CreERT2}-Smo^{flox/flox} conditional knockout mice allowed me to overcome the requirement of Shh signalling during embryonic myogenesis and to demonstrate a specific role of Shh signalling in satellite cell-mediated adult myogenesis.

7.3.2 Shh signalling is required for satellite cell progression through the myogenic program.

Following injury, Smo^{ckO} and Smo^{Δ/+} muscles presented showed aberrant progression through the myogenic program, as fewer MyoD+ and Myogenin+ cells were observed at 2 days post-injury compared to control muscles. Moreover, sustained expression of MyoD+ and Myogenin+ cells was observed in Smo^{ckO} and Smo^{Δ/+} muscles at 14 days post-injury, indicating a delay in myogenesis. The MyoD+ and Myogenin+ satellite cells observed in Smo^{ckO} and Smo^{Δ/+} muscles at 14 days post-injury are likely to be cycling, as shown by the corresponding numbers of Ki67+ cells at that time point. However, double immunofluorescence analysis with a satellite cell marker is needed to confirm this possibility. Although I cannot rule out that cell proliferation in Smo^{ckO} and Smo^{Δ/+} satellite cells is normal, as no satellite cell marker was used along with Ki67, my analysis of Smo^{ckO} cultured myofibres uncovered a 50% decrease in the number of differentiating cells at 72h in the absence of Smo, suggesting a defect in satellite cells expansion. These findings are consistent with the loss-of-function experiments reported in chapter 5 and with the role of Shh signalling in the control of satellite cell proliferation described in chapter 6. Shh signalling has been shown previously to control the proliferation of other adult stem cells, including neural progenitor cells, bulge stem cells, hematopoietic stem cells and lung progenitor cells (Hsu et al., 2014, Krause et al., 2010, Petrova et al., 2013, Trowbridge et al., 2006). Although little is known about the mechanisms mediating Shh-induced proliferation in these adult stem cells, it has been shown that Shh signalling up-regulates the expression of the G1 regulator *cyclin D1* during the proliferation of

hematopoietic stem cells (Trowbridge et al., 2006). Whether this mechanism is conserved in other stem cell types has not been demonstrated yet. However, my *ex vivo* analysis of satellite cell cell cycle dynamics suggests a delay in G1/S transition in the absence of Shh signalling, which is consistent with fewer MyoD+ cells observed at 2 days post-injury in Smo^{CKO} mice compared to control mice. Further analysis of the expression of cell cycle regulators would be needed to confirm this.

7.3.3 Dose-dependent effect of Shh signalling in satellite cell function

I observed that mice heterozygous for Smo (Smo^{Δ/+}) behaved similarly to their homozygous counterpart (Smo^{CKO}), suggesting that the removal of a single allele of Smo is sufficient to impair skeletal muscle regeneration. This also suggests that Shh signalling has a dose-dependent effect on satellite cell activity and cell cycle progression. Such dose-dependent effect has been described in other systems and thus, may be a conserved feature of Shh signalling. For instance, Shh signalling is essential for neurogenesis in the subventricular zone of the adult brain, and the generation of olfactory bulb cells is sensitive to the level of Shh signalling, specifically to activity levels of the Gli3 repressor (Petrova et al., 2013). The dose-dependent effect of Shh signalling during embryonic development is also well known. In this case, a gradient of Shh is established along the dorso-ventral axis of the neural tube so that cells close to the ventral region are exposed to higher concentrations of the Shh ligand, which translates into the induction of different transcription factors in a dose-dependent manner (Chamberlain et al., 2008, Ribes and Briscoe, 2009). How does this dose-dependent effect impact the transduction of Shh signals? It has been shown that increasing levels of Shh ligand induce high levels of Smo phosphorylation, which in turn promotes the accumulation of Smo in the primary cilia and the degree of pathway activation downstream of Smo (Chen et al., 2011, Jia et al., 2004, Su et al., 2011). This corresponds to different levels of intracellular signalling driven by changes in the balance between Gli repressor and Gli activator forms. Thus, high levels of Shh induce high levels of Smo phosphorylation and blockade of Gli processing into repressor forms to favour the production of Gli activators (increased ratio of Gli full-length/repressor) (Hui and Angers, 2011). In contrast, low levels of Shh results in low Smo phosphorylation and in little production of both Gli activator and repressor forms. Finally, no Shh leads to inactivation of Smo and the processing of Gli proteins into repressor forms (decreased ratio of Gli full-length/repressor) (Hooper, 2003). How are reduced levels of Smo sensed at the level of gene transcription? if Smo levels decrease, as in the case of Smo^{Δ/+} mice, the ratio of Gli activator/repressor may be reduced, resulting in the repression of Shh target genes. It may also be possible that Shh target genes containing high affinity Gli

binding sites may be activated but those with low affinity may not (Ashe and Briscoe, 2006). Alternatively, the transcription of Shh target genes with multiple Gli binding sites may not be induced when Smo levels are reduced (Vokes et al., 2007). All these mechanisms may result in aberrant or unbalanced transcriptional activity in Smo Δ / $+$ mice and hence the phenotypic similarity to Smo cKO mice.

7.3.4 The role of Shh signalling in adult muscles differs from its role in embryonic myogenesis.

Shh signalling is a well-conserved molecular pathway with multiple roles in patterning and morphogenesis during early vertebrate development (Briscoe and Thérond, 2013, Ingham and McMahon, 2001). The Shh protein is secreted by the notochord and the zone of polarising activity of the limb bud and patterns the ventral neural tube, the somite, hind gut and the limb (Ribes and Briscoe, 2009, Riddle et al., 1993). Thus, mutations of the *Shh* gene in the mouse embryo is lethal and leads to several defects in the development of the anterior central nervous system (cyclopia, forebrain reduction and separation of the dorsal midline), limb (truncation of limb, lack of digits), somite derivatives (absence of ribs, sternum, defects on muscle patterning) (Chiang et al., 1996). *Smo* $^{-/-}$ mutant mouse embryos have growth retardation and stronger developmental defects compared to *Shh* $^{-/-}$ mutants. Also, *Smo* $^{-/-}$ mice die earlier than *Shh* $^{-/-}$ and *Ihh* $^{-/-}$ mice as a result of blocking the transduction of both ligands (Zhang et al., 2001).

In embryonic myogenesis, Shh signalling controls muscle progenitor cell specification (through direct control of *Myf5* transcription) (Anderson et al., 2012, Borycki et al., 1999b, Hu et al., 2012), muscle patterning (through its control of Laminin α 1 production, a component of the myotomal basement membrane) (Anderson et al., 2009), muscle precursor cell migration (distal limb muscles) (Hu et al., 2012) and proliferation (Towers et al., 2008). In the adult, Shh signalling controls satellite cell proliferation, affecting the progression through the myogenic program. Although analysis of cultured myofibres from Smo cKO mice showed a decrease in the number of Pax7+/Myf5+ satellite cells at 24h, it is unlikely that Shh signalling controls *Myf5* transcription in satellite cells, as around 90% of quiescent satellite cells already express *Myf5* (Kuang et al., 2007). It is also possible that Shh signalling may control satellite cell patterning, as previous work from the lab has shown that inhibition of Shh signalling in satellite cells cultured *ex vivo* causes a reduction in the number of Laminin α 1+ satellite cells (Rayagiri, 2014). However, the extent of this effect needs to be explored further. Likewise, the role of Shh signalling in satellite cell migration needs to be investigated, as part of satellite cell activation involves their migration to the site of injury (Siegel et al., 2009). Finally, my study strongly supports a role of Shh signalling in the control of satellite cell proliferation. This effect was not

unexpected, since Shh signalling controls the proliferation of muscle progenitor cells in embryonic limb muscles (Chinnaiya et al., 2014, Towers et al., 2008). Importantly, I used EDL satellite cells in my experiments, which are derived from limb muscles during embryogenesis. Indeed, it has been shown that satellite cells from different muscles behave differently, suggesting the existence of satellite cell heterogeneity depending on the muscle of origin in which they reside. For instance, satellite cells from head muscles have distinct characteristics than satellite cells from the trunk, including different embryonic origin and mechanisms of gene expression (Harel et al., 2009, Ono et al., 2010, Sambasivan et al., 2009). Therefore, it would be interesting to see if the control of Shh signalling on the proliferation of satellite cells is also conserved in other muscles, such as trunk and head muscles.

FINAL DISCUSSION

8.1 Thesis summary

In this thesis, I investigated the role of Shh signalling in satellite cell-mediated myogenesis. I hypothesised that Shh signalling controls satellite cell function in mammalian adult muscles in a manner reminiscent to its effect in muscle progenitor cells in the embryo. Through a combination of *ex vivo* and *in vivo* approaches, I showed that, unlike quiescent satellite cells, activated satellite cells respond to Shh signalling, as following injury Shh response occurs in activated satellite cells and persists during the satellite cell expansion phase before declining when satellite cells enter differentiation. I also demonstrated that Shh signalling contributes *ex vivo* and *in vivo* to muscle regeneration and to satellite cell proliferation. Further analysis of the effect of Shh on the cell cycle showed that Shh signalling promotes the entry of satellite cells into the cell cycle and their progression through S phase. Together, these observations led me to propose a model for the role of Shh signalling in the control of satellite cell-mediated myogenesis whereby satellite cell progression through the cell cycle and through myogenesis requires Shh signalling (Fig.8.1).

8.2 Shh signalling activity is recapitulated during adult myogenesis

Adult muscle regeneration recapitulates, to a certain extent, the events occurring during embryonic myogenesis to generate differentiated myofibres in response to exercise, injury or congenital diseases such as muscular dystrophies. This involves the redeployment of signalling pathways implicated in embryonic myogenesis for adult myogenesis. Indeed, a role for FGF, BMP, Notch and Wnt signalling has been reported previously (Chakkalakal

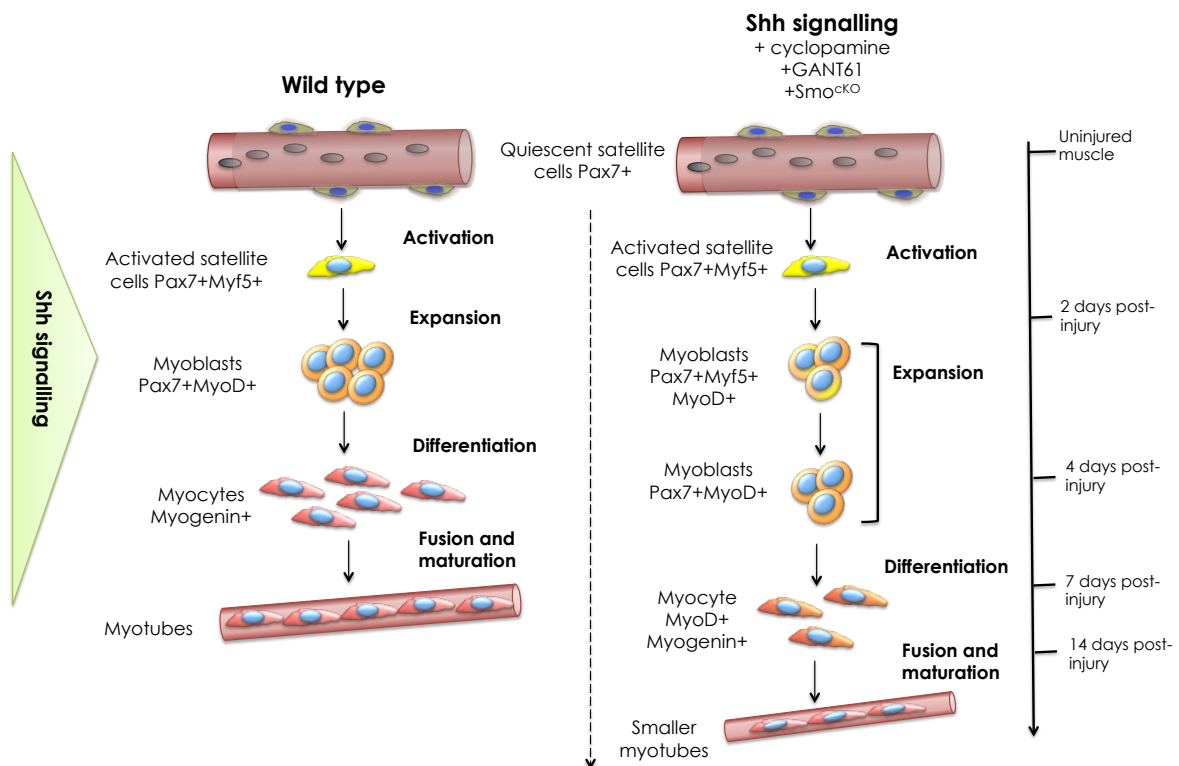


Figure 8.1: Shh signalling during adult muscle regeneration. Quiescent satellite cells do not respond to Shh signalling. By contrast, activated satellite cells become responsive to Shh signalling and this response is required for their progression through the cell cycle and myogenesis. In the absence of Shh signalling (via pharmacological inhibition or in Smo^{CKO} mice), satellite cells progression through the cell cycle and myogenesis is impaired, resulting in delayed regeneration following muscle injury.

et al., 2012, Le Grand et al., 2009, Mourikis et al., 2012b, Ono et al., 2011, Yablonka-Reuveni et al., 1999b). In contrast, Shh signalling has not been investigated in satellite cell biology. My findings add now Shh signalling to the list of signalling pathways with dual activity in embryonic and adult myogenesis.

I have demonstrated that quiescent satellite cells do not respond to Shh signals, which is consistent with previous reports showing absence of Shh activity in healthy skeletal muscles (Pola et al., 2003, Straface et al., 2009). The absence of Shh activity in resting skeletal muscles may be linked to the low turnover rate of this tissue. Indeed, in adult tissues with a high turnover such as the skin, Shh signalling appears to be present and active: in resting hair follicles (telogen), *Gli2* and *Gli3* are broadly expressed, and *Gli1* and *Ptch1* expression is readily detected in resting epithelial cells of the dermal bulge, which allows for a quick response to Shh signalling during regeneration (Brownell et al., 2011). Likewise, in the resting adult intestinal tract, Hh-responsive cells (*Ptch1+* and *Gli1+*) are numerous at the crypts and in the submucosa, indicating an ongoing Shh response during homeostasis (Kolterud et al., 2009). Therefore, Shh signalling response may have adapted to fulfil the requirements of adult stem cells with different cell cycle dynamics, and may explain why Shh signalling is inactive in quiescent satellite cells.

Shh signalling activity appears to be regulated spatio-temporally in adult skeletal muscles, since Shh response in satellite cells is detected as cells become activated following injury or *ex vivo* culture. The onset of Shh response may be controlled in different ways, which are not necessarily mutually exclusive. First, Shh response may be modulated by the availability of Shh ligands, which can be sequestered by ECM components (Blaess et al., 2004, Pons et al., 2001). It is possible that the disruption of the ECM that accompanies muscle injuries facilitates release of Shh, while the gradual restoration of the muscle architecture that follows satellite cell differentiation and muscle repair triggers a decline of Shh response through the capture of Shh ligands into the restored ECM. Second, it is possible that Shh ligand is synthesised during muscle injury, as suggested by the increase and decrease in the levels of *Shh* mRNA in whole muscles in response to injury (Straface et al., 2009). Although the precise source of the Shh ligand in skeletal muscles remains unknown, I have shown that neither myofibres nor satellite cells are able to synthesise *Shh* mRNA. Biochemical evidence suggests that the Shh protein is able to diffuse at long ranges in the form of soluble multimeres (Zeng et al., 2001), opening the possibility that Shh may originate from distant sources such as blood capillaries, lymphatic vessels or nerves (Brownell et al., 2011, Dierks et al., 2007, Yao et al., 2014). Finally, it has been shown that follicular dendritic cells in peripheral lymphoid tissue secrete Shh (Sacedón et al., 2005), opening the possibility that immune cells may deliver Shh proteins following muscle injury (Sacedón et al., 2005).

My findings demonstrate that Shh response in satellite cells is required for their entry

into the cell cycle and that this response persists during the expansion phase (48h *ex vivo* and 2 days post-injury *in vivo*). Importantly, Shh response is gradually lost over time, especially in self-renewing satellite cells and terminally differentiated cells. This down-regulation of Shh signalling response may be related to the availability of the ligand, to the specific down-regulation of components of the Shh response pathway or to the negative regulators of the pathway such as Gli3 and Hip, as well as to the negative feedback exerted by increased Ptch1 expression. Dampening of Shh signalling activity in satellite cells may be important for signal relay and to prime satellite cells to respond to other signalling molecules. For instance, mesenchymal cells in the developing limb bud are primed by Shh signalling to create a gradient of BMP activity that determines digit identity (Dahn and Fallon, 2000, Drossopoulou et al., 2000). In skeletal muscles, BMP signalling has been proposed to control the balance between proliferation and differentiation of satellite cells (Ono et al., 2011). Therefore, it may be possible that Shh signalling acts synergistically with BMP signalling to control satellite cell function. However, further experiments would be needed to identify the signalling pathways acting up and downstream of Shh signalling in satellite cells.

8.3 Control of cell cycle progression by Shh signalling

The results presented in this thesis identified two different phases at which Shh signalling regulates satellite cell cell cycle dynamics. First, I have shown that Shh signalling controls the initial progression of satellite cells into the cell cycle, specifically through the G1/S transition. Second, Shh signalling controls satellite cell exit from the cell cycle, affecting the overall number of cells going into terminal differentiation or quiescence. The mechanisms by which Shh signalling induces a mitogenic response in other tissues are diverse, and can involve the direct control of cell cycle regulators or the modulation of signalling pathways known to control cell proliferation. For instance, Shh signalling promotes progression through G1/S by regulating *N-myc*, *CyclinE1*, *CyclinD1*, *Dp1* and *E2f1* in the zebrafish retina, chick wing bud, mouse epidermis, mouse cerebellar granular neural precursors (CGNPs) and mouse external genitalia (Kenney et al., 2004, Mill et al., 2003, Oliver et al., 2003, Seifert et al., 2010, Towers et al., 2008, Wall et al., 2009). Other mechanisms of cell cycle regulation by Shh signalling include blockade of p21-mediated growth arrest (Fan and Khavari, 1999) and the sequestration of Cyclin B1 by Ptch1, which acts as a tumour suppressor of basal cell carcinoma (BBC) to repress the G2/M transition (Barnes et al., 2001). Finally, Hh signalling can promote cell cycle exit through the control of the cyclin kinase inhibitors p57 and p27 in the vertebrate retina (Masai et al., 2005, Shkumatava and Neumann, 2005). These different cell cycle regulators are attractive candidate targets of Shh signalling in our system and additional experiments

to identify such targets are under way.

On the other hand, Shh signalling may stimulate cell proliferation through the activation of mitogenic molecules such as receptor tyrosine kinase (RTK)-mediated signalling pathways. For instance, Shh signalling acts synergistically with PI3K/Akt and mTOR signalling to induce proliferation of CGNPs in the cerebellum (Kenney et al., 2004, Mainwaring and Kenney, 2011). Shh signalling also stimulates the activity of the p38 MAPK signalling to control astrocyte proliferation (Atkinson et al., 2009). This is interesting as Shh signalling can promote myoblast proliferation through PI3K/Akt and ERK1/2 signalling (Elia et al., 2007, Madhala-Levy et al., 2012). Also, Shh signalling can stimulate proliferation of mouse embryonic stem (ES) cells by activating the Ca^{2+} /PKC pathway, which in turn transactivates the epidermal growth factor receptor (EGFR) pathway (Heo et al., 2007). In skeletal muscles, growth factors such as FGF and IGF-1 activate the PI3K/Akt and ERK1/2 signalling and cyclin D/Cdk2, 4 and 6 complexes to stimulate proliferation while restricting differentiation (Guo et al., 1999, Yablonka-Reuveni et al., 1999b). This promotes the regulation of other cyclins to allow cell cycle progression. Eventually, down-regulation of ERK1/2 signalling activity leads to the inhibition of cell proliferation (Knight and Kothary, 2011). Therefore, modulation of RTK-mediated signalling pathways by Shh signalling is a highly plausible strategy to regulate cell cycle progression in satellite cells.

Not only Shh signalling blockade in satellite cells delays their progression through the cell cycle, but it also affects how satellite cells progress through the myogenic program. These observations raise the possibility that Shh signalling may affect myogenic differentiation by controlling the orientation of cell division in satellite cells. Consistent with this idea, inhibition of Shh signalling in postnatal CGNPs causes an increase in the proportion of symmetric cell divisions, indicating that Shh signalling normally stimulates CGNP asymmetric division (Haldipur et al., 2015). Conversely, constitutive activation of Shh signalling in neural stem cell of the subependymal zone results in an increase in the number of symmetric cell divisions (Ferent et al., 2014). This suggests that Shh signalling can regulate both symmetric and asymmetric cell divisions. Therefore, it remains possible that Shh controls the fate of satellite cells (differentiation) via its control of cell division orientation.

Finally, a whole body of evidence from cancer models has demonstrated that activating mutations of Shh signalling components lead to cancer formation. For instance, Gorlin syndrome is a rare autosomal-dominant inherited disease characterised by an increased incidence of tumours like BBCs, medulloblastomas and embryonic rhabdomyosarcomas (eRMS), a tumour of skeletal muscles (Scotting et al., 2005). Heterozygous loss-of-function mutation in *PTCH* accounts for the occurrence of this syndrome, as well as *SUFU* mutations and over-expression of *GLI1* (Hahn et al., 1996, Johnson et al., 1996, Tostar et al.,

2006). Although some evidence suggests that eRMS are not generated by Shh signalling overactivation in satellite cells, eRMS tumours up-regulate both myogenic and Shh signalling genes (Rajurkar et al., 2013). Moreover, it has recently been demonstrated that Shh signalling is required for self-renewal and tumorigenicity of eRMS (Satheesha et al., 2015), which is in line with the role of Shh signalling in the control of satellite cell proliferation. Therefore, understanding the function of Shh signalling in satellite cell cell cycle dynamics is also relevant to therapeutically target eRMS.

8.4 A requirement of Shh signalling in adult skeletal muscles

To investigate the role of Shh signalling in adult skeletal muscles *in vivo*, I used tamoxifen-induced conditional knockout mice to delete Smo expression specifically in Pax7+ satellite cells (Smo^{CKO}). Following cardiotoxin-mediated muscle injury, Shh signalling inactivation in satellite cells resulted in impaired muscle regeneration, with reduced fibre size, increased collagen deposition and delay in the progression through the myogenic program. Although previous studies have reported that disrupting Shh signalling impairs muscle regeneration (Renault et al., 2013a,b, Straface et al., 2009), this is the first evidence of a direct requirement for Shh signalling in satellite cell-mediated muscle regeneration.

Smo gene inactivation in satellite cells led to an aberrant progression through the myogenic program and an overall reduction in the number of satellite cells, which results in reduced myogenic fusion and insufficient myonuclei contribution to new myofibres. Smo^{CKO} injured muscles do not recover even after 21 days-post injury, indicating a drastic failure in the repair process. Interestingly, I observed that MyoD+ satellite cells are still present in regenerating muscles of Smo^{CKO} mice. How is it possible that even in the presence of activated satellite cells muscle repair does not occur? Failure to successfully repair muscle damage leads to the alteration of the architecture and an increased proliferation of fibroblasts, which can impair the myogenic process (Mann et al., 2011). It may be possible that once fibrosis occurs, regeneration cannot take place. Indeed, following muscle injury, fibroblasts proliferate in close association with satellite cell so that both populations peak at 5 days post-injury and gradually decrease from day 7 post-injury (Murphy et al., 2011). Therefore, satellite cells face a race against time, where the precise timing of their activity may overcome the deleterious effects of fibroblasts. Consistent with this, conditional ablation of Pax7+ satellite cells in BaCl₂-injured muscles causes a complete loss of muscle regeneration, which is accompanied by a dramatic increase in fibrosis (Murphy et al., 2011). My results indicate that impaired satellite cell-mediated myogenesis in Smo^{CKO} mice favours fibroblast activity, which leads to over-deposition of

collagen between regenerating fibres.

8.5 Shh signalling and implications in muscular diseases and therapies

Loss of muscle mass and fibrosis are common features of muscular disorders including age-related sarcopenia and muscular dystrophies. This is also accompanied by a progressive reduction of satellite cell numbers, which affects the regenerative potential of skeletal muscles (Boldrin et al., 2009, Chakkalakal et al., 2012, Liu et al., 2013). Shh signalling response has been shown to be reduced in aged and dystrophic mice, and thus may contribute to the loss of regenerative capacity of older skeletal muscles (Piccioni et al., 2014a,b). Cell and gene therapy are two of the most promising tools for the treatment of muscle disorders. In the case of gene therapy, injection of a plasmid encoding human Shh into normal, dystrophic and aged mouse muscles has been shown to improve muscle regeneration following injury, including reduction of fibrosis and increase in the number of regenerating myofibres (Palladino et al., 2011, Piccioni et al., 2014a,b). These effects are quite robust and are likely to involve both a systemic mechanism on angiogenesis and a direct stimulation of myogenesis.

The treatment of degenerated muscles may involve also cellular therapies and previous attempts have made use of non-myogenic as well as myogenic cells. Non-myogenic cells such as bone marrow-derived cells (hematopoietic and mesenchymal stem cells) (Dezawa et al., 2005, Torrente et al., 2004), mesoangioblasts (Sampaolesi et al., 2006, 2003), embryonic stem (ES) cells (Albini et al., 2013, Darabi et al., 2008, Salani et al., 2012, Shelton et al., 2014) and induced pluripotent stem (iPS) cells (Li et al., 2015, Tedesco et al., 2012) have been harnessed towards the myogenic lineage for therapeutical purposes. For instance, iPS cells from limb-girdle muscular dystrophy type 2D (LGMD2D) patients have been generated, differentiated into mesoangioblast-like cells and genetically corrected to express α -sarcoglycan protein. Injection of these cells into LGMD2D mice has restored α -sarcoglycan expression and functionally improved the dystrophic phenotype (Tedesco et al., 2012). Similar approaches have been used to treat Duchenne muscular dystrophy (DMD) (Darabi et al., 2012, Filareto et al., 2013, Kazuki et al., 2010). Strategies to treat muscle disorders using muscle cells include the transplantation of intact myofibres and satellite cells expanded *in vitro* (Hall et al., 2010, Marg et al., 2014). Unfortunately, several challenges arise with the use of both non-myogenic and myogenic cells for transplantation. First, large quantities of cells with high purity are needed and in the case of satellite cells, it has been shown that their expansion *in vitro* decreases their regenerative capacity, compromising their clinical application (Montarras et al., 2005). Second, the

maintenance of stemness (self-renewal potential) is required, so that transplanted cells can contribute to several cycles of regeneration (Sacco et al., 2008). Third, most of the protocols to generate muscle cells involve the ectopic expression of myogenic regulatory factors of genetic correction, which requires immortalization or extensive cell expansion (Ousterout et al., 2013). Finally, the delivery of transplanted cells has mainly been achieved by direct injection into recipient muscles and this represents a major barrier for the treatment of muscle disorders. How can all these challenges be overcome? The ideal system would use a source of cells that allow easy purification, amplification and the derivation to myogenic cells without introduction of genes. Specifically, new strategies to maintain myogenic cells *in vitro* using specific signalling molecules to recreate their natural microenvironment along with systemic delivery methods are highly desirable (Cosgrove et al., 2009). Indeed, the manipulation of intrinsic and extrinsic signalling factors in satellite cells are currently being undertaken, which has improved their expansion *in vitro* (Charville et al., 2015, Fu et al., 2015). The data presented in this thesis support a role of Shh signalling in the control of satellite cell myogenesis and cell cycle progression, which might contribute to improve the *in vitro* expansion of satellite cells for clinical applications.

8.6 Future directions

The data presented in this thesis report a role for Shh signalling in the control of satellite cell cell cycle progression and its requirement during skeletal muscle regeneration. Further work is required and is underway to determine the molecular mechanism by which Shh controls cell cycle progression in satellite cells. Smo-deficient mouse satellite cells Pax7^{CreERT2/+}; Smo^{flox/flox}; Rosa26-YFP are being isolated by FACS at 4 days following muscle injury in order to carry out a genome-wide RNA-seq analysis to identify target genes under the control of Shh signalling. Another question that we need to address is whether Shh signalling affects satellite self-renewal. This may be achieved by monitoring symmetric and asymmetric cell divisions in Smo^{CKO} or GANT61-treated wild type myofibres, and combine this to repeated injuries in Smo^{CKO} mice. Finally, it would be interesting to examine the effects of constitutive activation of Shh signalling in satellite cells *in vivo* to complement the gain-of-function experiments described in chapter 4. This could be achieved by either using a conditional activated allele of Smo (SmoA2) or a conditional loss of function allele of Ptch1 (Ptch1^{flox/flox}) and Pax7^{CreERT2} mice (Hallahan et al., 2004). One prediction would be that constitutive activation of Shh signalling results in an increase in the number of activated satellite cells. Finally, the identity of non-muscle cells responding to Shh signalling during muscle regeneration *in vivo* should be determined in order to see the requirement of Shh signalling in non-myogenic cells using the Cre-Lox technology. Finally, it would be interesting to include Shh in protocols

to drive mesenchymal stem cells into the myogenic lineage and explore its effects on their expansion *in vitro*.

8.7 Final remarks

The role of Shh signalling in adult skeletal muscles was until recently poorly understood, with contradicting evidence supporting cell proliferation and differentiation of satellite cells. However, the exogenous administration of a plasmid encoding Shh into injured and dystrophic muscles was known to enhance muscle repair (Piccioni et al., 2014a,b). The present study demonstrates that Shh signalling is required for adult skeletal muscle regeneration and provides novel insights into the role of Shh signalling in the control of satellite cell progression through the cell cycle and through myogenesis. Understanding how Shh signalling affects satellite behaviour is important for skeletal muscle biology and add to our knowledge of Shh function in other adult stem cell systems, including neural, hair follicle, crypt and lung stem cells (Petrova and Joyner, 2014). Finally, the requirement of Shh signalling in satellite cells provides a novel framework for designing approaches to drive expansion of satellite cells or generate myogenic progenitor cells from stem cells useful for therapeutical purpose.

BIBLIOGRAPHY

- Abe, T., Sakaue-Sawano, A., Kiyonari, H., Shioi, G., Inoue, K.-i., Horiuchi, T., Nakao, K., Miyawaki, A., Aizawa, S., and Fujimori, T. (2013). Visualization of cell cycle in mouse embryos with Fucci2 reporter directed by Rosa26 promoter. *Development*, 140(1):237–246.
- Agyeman, A., Jha, B. K., Mazumdar, T., and Houghton, J. A. (2014). Mode and specificity of binding of the small molecule GANT61 to GLI determines inhibition of GLI-DNA binding. *Oncotarget*, 5(12):4492.
- Ahn, S. and Joyner, A. L. (2005). In vivo analysis of quiescent adult neural stem cells responding to sonic hedgehog. *Nature*, 437(7060):894–897.
- Albini, S., Coutinho, P., Malecova, B., Giordani, L., Savchenko, A., Forcales, S. V., and Puri, P. L. (2013). Epigenetic reprogramming of human embryonic stem cells into skeletal muscle cells and generation of contractile myospheres. *Cell Reports*, 3(3):661–670.
- Albini, S., Toto, P. C., Dall’Agnese, A., Malecova, B., Cenciarelli, C., Felsani, A., Caruso, M., Bultman, S. J., and Puri, P. L. (2015). Brahma is required for cell cycle arrest and late muscle gene expression during skeletal myogenesis. *EMBO Reports*, page e201540159.
- Alcedo, J., Ayzenzon, M., Von Ohlen, T., Noll, M., and Hooper, J. E. (1996). The Drosophila smoothed gene encodes a seven-pass membrane protein, a putative receptor for the Hedgehog signal. *Cell*, 86(2):221–232.
- Alderton, J. M. and Steinhardt, R. A. (2000). Calcium influx through calcium leak channels is responsible for the elevated levels of calcium-dependent proteolysis in dystrophic myotubes. *Journal of Biological Chemistry*, 275(13):9452–9460.
- Alexandre, C., Jacinto, A., and Ingham, P. W. (1996). Transcriptional activation of hedgehog target genes in Drosophila is mediated directly by the cubitus interruptus protein, a member of the GLI family of zinc finger DNA-binding proteins. *Genes&Development*, 10(16):2003–2013.
- Allbrook, D. (1962). An electron microscopic study of regenerating skeletal muscle. *Journal of Anatomy*, 96(Pt 2):137.
- Allen, B. L., Song, J. Y., Izzi, L., Althaus, I. W., Kang, J.-S., Charron, F., Krauss, R. S., and McMahon, A. P. (2011). Overlapping roles and collective requirement for the coreceptors GAS1, CDO, and BOC in SHH pathway function. *Developmental Cell*, 20(6):775–787.

- Allen, R. E., Sheehan, S. M., Taylor, R. G., Kendall, T. L., and Rice, G. M. (1995). Hepatocyte growth factor activates quiescent skeletal muscle satellite cells in vitro. *Journal of Cellular Physiology*, 165(2):307–312.
- Anderson, C., Thorsteinsdóttir, S., and Borycki, A.-G. (2009). Sonic hedgehog-dependent synthesis of laminin $\alpha 1$ controls basement membrane assembly in the myotome. *Development*, 136(20):3495–3504.
- Anderson, C., Williams, V. C., Moyon, B., Daubas, P., Tajbakhsh, S., Buckingham, M. E., Shiroishi, T., Hughes, S. M., and Borycki, A.-G. (2012). Sonic hedgehog acts cell-autonomously on muscle precursor cells to generate limb muscle diversity. *Genes&Development*, 26(18):2103–2117.
- Anderson, C., Winder, S. J., and Borycki, A.-G. (2007). Dystroglycan protein distribution coincides with basement membranes and muscle differentiation during mouse embryogenesis. *Developmental Dynamics*, 236(9):2627–2635.
- Anderson, J. E. (2000). A role for nitric oxide in muscle repair: nitric oxide-mediated activation of muscle satellite cells. *Molecular Biology of the Cell*, 11(5):1859–1874.
- Armand, O., Boutineau, A., Mauger, A., Pautou, M., and Kieny, M. (1982). Origin of satellite cells in avian skeletal muscles. *Archives d'Anatomie Microscopique et de Morphologie Experimentale*, 72(2):163–181.
- Arnold, L., Henry, A., Poron, F., Baba-Amer, Y., Van Rooijen, N., Plonquet, A., Gherardi, R. K., and Chazaud, B. (2007). Inflammatory monocytes recruited after skeletal muscle injury switch into anti-inflammatory macrophages to support myogenesis. *The Journal of Experimental Medicine*, 204(5):1057–1069.
- Asakura, A., Seale, P., Girgis-Gabardo, A., and Rudnicki, M. A. (2002). Myogenic specification of side population cells in skeletal muscle. *The Journal of Cell Biology*, 159(1):123–134.
- Ashe, H. L. and Briscoe, J. (2006). The interpretation of morphogen gradients. *Development*, 133(3):385–394.
- Atkinson, P. J., Dellovade, T., Albers, D., Von Schack, D., Saraf, K., Needle, E., Reinhart, P. H., and Hirst, W. D. (2009). Sonic Hedgehog signaling in astrocytes is dependent on p38 mitogen-activated protein kinase and G-protein receptor kinase 2. *Journal of Neurochemistry*, 108(6):1539–1549.
- Auffray, C., Fogg, D., Garfa, M., Elain, G., Join-Lambert, O., Kayal, S., Sarnacki, S., Cumano, A., Lauvau, G., and Geissmann, F. (2007). Monitoring of blood vessels and tissues by a population of monocytes with patrolling behavior. *Science*, 317(5838):666–670.
- Aza-Blanc, P. and Kornberg, T. B. (1999). Ci: a complex transducer of the hedgehog signal. *Trends in Genetics*, 15(11):458–462.
- Aza-Blanc, P., Lin, H.-Y., Altaba, A. R., and Kornberg, T. B. (2000). Expression of the vertebrate Gli proteins in Drosophila reveals a distribution of activator and repressor activities. *Development*, 127(19):4293–4301.
- Aza-Blanc, P., Ramírez-Weber, F.-A., Laget, M.-P., Schwartz, C., and Kornberg, T. B. (1997). Proteolysis that is inhibited by Hedgehog targets Cubitus interruptus protein to the nucleus and converts it to a repressor. *Cell*, 89(7):1043–1053.

- Bai, C. B., Auerbach, W., Lee, J. S., Stephen, D., and Joyner, A. L. (2002). Gli2, but not Gli1, is required for initial Shh signaling and ectopic activation of the Shh pathway. *Development*, 129(20):4753–4761.
- Bajanca, F., Luz, M., Raymond, K., Martins, G. G., Sonnenberg, A., Tajbakhsh, S., Buckingham, M., and Thorsteinsdóttir, S. (2006). Integrin $\alpha6\beta1$ -laminin interactions regulate early myotome formation in the mouse embryo. *Development*, 133(9):1635–1644.
- Bajard, L., Relaix, F., Lagha, M., Rocancourt, D., Daubas, P., and Buckingham, M. E. (2006). A novel genetic hierarchy functions during hypaxial myogenesis: Pax3 directly activates Myf5 in muscle progenitor cells in the limb. *Genes&Development*, 20(17):2450–2464.
- Balaskas, N., Ribeiro, A., Panovska, J., Dessaud, E., Sasai, N., Page, K. M., Briscoe, J., and Ribes, V. (2012). Gene regulatory logic for reading the Sonic Hedgehog signaling gradient in the vertebrate neural tube. *Cell*, 148(1):273–284.
- Barnes, E. A., Kong, M., Ollendorff, V., and Donoghue, D. J. (2001). Patched1 interacts with cyclin B1 to regulate cell cycle progression. *The EMBO Journal*, 20(9):2214–2223.
- Bartel, D. P. (2004). MicroRNAs: genomics, biogenesis, mechanism, and function. *Cell*, 116(2):281–297.
- Baxendale, S., Davison, C., Muxworthy, C., Wolff, C., Ingham, P. W., and Roy, S. (2004). The B-cell maturation factor Blimp-1 specifies vertebrate slow-twitch muscle fiber identity in response to Hedgehog signaling. *Nature Genetics*, 36(1):88–93.
- Beauchamp, J. R., Heslop, L., David, S., Tajbakhsh, S., Kelly, R. G., Wernig, A., Buckingham, M. E., Partridge, T. A., and Zammit, P. S. (2000). Expression of CD34 and Myf5 defines the majority of quiescent adult skeletal muscle satellite cells. *The Journal of Cell Biology*, 151(6):1221–1234.
- Bekoff, A. and Betz, W. (1977). Properties of isolated adult rat muscle fibres maintained in tissue culture. *The Journal of Physiology*, 271(2):537–547.
- Bellaiche, Y., The, I., Perrimon, N., et al. (1998). Tout-velu is a Drosophila homologue of the putative tumour suppressor EXT-1 and is needed for Hh diffusion. *Nature*, 394(6688):85–88.
- Bellamy, L. M., Joannisse, S., Grubb, A., Mitchell, C. J., McKay, B. R., Phillips, S. M., Baker, S., and Parise, G. (2014). The acute satellite cell response and skeletal muscle hypertrophy following resistance training. *PLoS One*, page e109739.
- Bendris, N., Lemmers, B., Blanchard, J.-M., and Arsic, N. (2011). Cyclin A2 mutagenesis analysis: a new insight into CDK activation and cellular localization requirements. *PLoS One*, 6(7):e22879.
- Bentzinger, C. F., Wang, Y. X., Dumont, N. A., and Rudnicki, M. A. (2013a). Cellular dynamics in the muscle satellite cell niche. *EMBO Reports*, 14(12):1062–1072.
- Bentzinger, C. F., Wang, Y. X., von Maltzahn, J., Soleimani, V. D., Yin, H., and Rudnicki, M. A. (2013b). Fibronectin regulates Wnt7a signaling and satellite cell expansion. *Cell Stem Cell*, 12(1):75–87.
- Berkes, C. A. and Tapscott, S. J. (2005). MyoD and the transcriptional control of myogenesis. In *Seminars in Cell&Developmental Biology*, volume 16, pages 585–595. Elsevier.

- Berry, L. D. and Gould, K. L. (1996). Regulation of Cdc2 activity by phosphorylation at T14/Y15. In *Progress in Cell Cycle Research*, pages 99–105. Springer.
- Bianco, P., Riminucci, M., Gronthos, S., and Robey, P. G. (2001). Bone marrow stromal stem cells: nature, biology, and potential applications. *Stem Cells*, 19(3):180–192.
- Bischoff, R. (1975). Regeneration of single skeletal muscle fibers in vitro. *The Anatomical Record*, 182(2):215–235.
- Bischoff, R. (1986). Proliferation of muscle satellite cells on intact myofibers in culture. *Developmental Biology*, 115(1):129–139.
- Bitgood, M. J. and McMahon, A. P. (1995). Hedgehog and Bmp Genes Are Coexpressed at Many Diverse Sites of Cell–Cell Interaction in the Mouse Embryo. *Developmental Biology*, 172(1):126–138.
- Bitgood, M. J., Shen, L., and McMahon, A. P. (1996). Sertoli cell signaling by Desert Hedgehog regulates the male germline. *Current Biology*, 6(3):298–304.
- Bjornson, C. R., Cheung, T. H., Liu, L., Tripathi, P. V., Steeper, K. M., and Rando, T. A. (2012). Notch signaling is necessary to maintain quiescence in adult muscle stem cells. *Stem Cells*, 30(2):232–242.
- Blaess, S., Graus-Porta, D., Belvindrah, R., Radakovits, R., Pons, S., Littlewood-Evans, A., Senften, M., Guo, H., Li, Y., Miner, J. H., et al. (2004). β 1-integrins are critical for cerebellar granule cell precursor proliferation. *The Journal of Neuroscience*, 24(13):3402–3412.
- Blau, H. M., Pavlath, G. K., Hardeman, E. C., Chiu, C.-P., Silberstein, L., Webster, S. G., Miller, S. C., and Webster, C. (1985). Plasticity of the differentiated state. *Science*, 230(4727):758–766.
- Boldrin, L., Neal, A., Zammit, P. S., Muntoni, F., and Morgan, J. E. (2012). Donor satellite cell engraftment is significantly augmented when the host niche is preserved and endogenous satellite cells are incapacitated. *Stem Cells*, 30(9):1971–1984.
- Boldrin, L., Zammit, P. S., Muntoni, F., and Morgan, J. E. (2009). Mature adult dystrophic mouse muscle environment does not impede efficient engrafted satellite cell regeneration and self-renewal. *Stem Cells*, 27(10):2478–2487.
- Borycki, A., Brown, A., and Emerson, C. (2000). Shh and Wnt signaling pathways converge to control Gli gene activation in avian somites. *Development*, 127(10):2075–2087.
- Borycki, A., Li, J., Jin, F., Emerson, C., and Epstein, J. (1999a). Pax3 functions in cell survival and in pax7 regulation. *Development*, 126(8):1665–1674.
- Borycki, A.-G., Brunk, B., Tajbakhsh, S., Buckingham, M., Chiang, C., and Emerson, C. (1999b). Sonic hedgehog controls epaxial muscle determination through Myf5 activation. *Development*, 126(18):4053–4063.
- Borycki, A.-G., Mendham, L., and Emerson, C. (1998). Control of somite patterning by Sonic hedgehog and its downstream signal response genes. *Development*, 125(4):777–790.

- Bowers, M., Eng, L., Lao, Z., Turnbull, R. K., Bao, X., Riedel, E., Mackem, S., and Joyner, A. L. (2012). Limb anterior–posterior polarity integrates activator and repressor functions of GLI2 as well as GLI3. *Developmental Biology*, 370(1):110–124.
- Brack, A. S., Conboy, I. M., Conboy, M. J., Shen, J., and Rando, T. A. (2008). A temporal switch from notch to Wnt signaling in muscle stem cells is necessary for normal adult myogenesis. *Cell Stem Cell*, 2(1):50–59.
- Bren-Mattison, Y. and Olwin, B. B. (2002). Sonic hedgehog inhibits the terminal differentiation of limb myoblasts committed to the slow muscle lineage. *Developmental Biology*, 242(2):130–148.
- Briscoe, J. and Théron, P. P. (2013). The mechanisms of Hedgehog signalling and its roles in development and disease. *Nature Reviews Molecular Cell Biology*, 14(7):416–429.
- Brownell, I., Guevara, E., Bai, C. B., Loomis, C. A., and Joyner, A. L. (2011). Nerve-derived Sonic hedgehog defines a niche for hair follicle stem cells capable of becoming epidermal stem cells. *Cell Stem Cell*, 8(5):552–565.
- Bryson-Richardson, R. J. and Currie, P. D. (2008). The genetics of vertebrate myogenesis. *Nature Reviews Genetics*, 9(8):632–646.
- Buckingham, M. (2001). Skeletal muscle formation in vertebrates. *Current Opinion in Genetics&Development*, 11(4):440–448.
- Bumcrot, D. A., Takada, R., and McMahon, A. P. (1995). Proteolytic processing yields two secreted forms of Sonic hedgehog. *Molecular and Cellular Biology*, 15(4):2294–2303.
- Burke, R., Nellen, D., Bellotto, M., Hafen, E., Senti, K.-A., Dickson, B. J., and Basler, K. (1999). Dispatched, a novel sterol-sensing domain protein dedicated to the release of cholesterol-modified hedgehog from signaling cells. *Cell*, 99(7):803–815.
- Burkhart, D. L. and Sage, J. (2008). Cellular mechanisms of tumour suppression by the retinoblastoma gene. *Nature Reviews Cancer*, 8(9):671–682.
- Buttitta, L. A. and Edgar, B. A. (2007). Mechanisms controlling cell cycle exit upon terminal differentiation. *Current Opinion in Cell Biology*, 19(6):697–704.
- Cairns, J. (2006). Mutation selection and the natural history of cancer. *Science of Aging Knowledge Environment*, 2006(10):cp1.
- Capdevila, J., Pariente, F., Sampedro, J., Alonso, J. L., and Guerrero, I. (1994). Subcellular localization of the segment polarity protein patched suggests an interaction with the wingless reception complex in *Drosophila* embryos. *Development*, 120(4):987–998.
- Carlson, B. M. (1973). The regeneration of skeletal muscle—a review. *American Journal of Anatomy*, 137(2):119–149.
- Carnwath, J. W. and Shotton, D. M. (1987). Muscular dystrophy in the mdx mouse: histopathology of the soleus and extensor digitorum longus muscles. *Journal of the Neurological Sciences*, 80(1):39–54.

- Carpenter, D., Stone, D. M., Brush, J., Ryan, A., Armanini, M., Frantz, G., Rosenthal, A., and De Sauvage, F. J. (1998). Characterization of two patched receptors for the vertebrate hedgehog protein family. *Proceedings of the National Academy of Sciences*, 95(23):13630–13634.
- Cayuso, J., Ulloa, F., Cox, B., Briscoe, J., and Martí, E. (2006). The Sonic hedgehog pathway independently controls the patterning, proliferation and survival of neuroepithelial cells by regulating Gli activity. *Development*, 133(3):517–528.
- Chakkalakal, J. V., Christensen, J., Xiang, W., Tierney, M. T., Boscolo, F. S., Sacco, A., and Brack, A. S. (2014). Early forming label-retaining muscle stem cells require p27kip1 for maintenance of the primitive state. *Development*, 141(8):1649–1659.
- Chakkalakal, J. V., Jones, K. M., Basson, M. A., and Brack, A. S. (2012). The aged niche disrupts muscle stem cell quiescence. *Nature*, 490(7420):355–360.
- Chakravarthy, M. V., Abraha, T. W., Schwartz, R. J., Fiorotto, M. L., and Booth, F. W. (2000). Insulin-like Growth Factor-I Extends in Vitro Replicative Life Span of Skeletal Muscle Satellite Cells by Enhancing G1/S Cell Cycle Progression via the Activation of Phosphatidylinositol 3-Kinase/Akt Signaling Pathway. *Journal of Biological Chemistry*, 275(46):35942–35952.
- Chamberlain, C. E., Jeong, J., Guo, C., Allen, B. L., and McMahon, A. P. (2008). Notochord-derived shh concentrates in close association with the apically positioned basal body in neural target cells and forms a dynamic gradient during neural patterning. *Development*, 135(6):1097–1106.
- Charge, S. B. and Rudnicki, M. A. (2004). Cellular and molecular regulation of muscle regeneration. *Physiological Reviews*, 84(1):209–238.
- Charville, G. W., Cheung, T. H., Yoo, B., Santos, P. J., Lee, G. K., Shrager, J. B., and Rando, T. A. (2015). Ex vivo expansion and in vivo self-renewal of human muscle stem cells. *Stem Cell Reports*.
- Chen, J.-F., Tao, Y., Li, J., Deng, Z., Yan, Z., Xiao, X., and Wang, D.-Z. (2010a). microRNA-1 and microRNA-206 regulate skeletal muscle satellite cell proliferation and differentiation by repressing Pax7. *The Journal of Cell Biology*, 190(5):867–879.
- Chen, J. K., Taipale, J., Cooper, M. K., and Beachy, P. A. (2002a). Inhibition of Hedgehog signaling by direct binding of cyclopamine to Smoothened. *Genes&Development*, 16(21):2743–2748.
- Chen, J. K., Taipale, J., Young, K. E., Maiti, T., and Beachy, P. A. (2002b). Small molecule modulation of Smoothened activity. *Proceedings of the National Academy of Sciences*, 99(22):14071–14076.
- Chen, M.-H., Wilson, C. W., Li, Y.-J., Law, K. K. L., Lu, C.-S., Gacayan, R., Zhang, X., Hui, C.-c., and Chuang, P.-T. (2009). Cilium-independent regulation of Gli protein function by Sufu in Hedgehog signaling is evolutionarily conserved. *Genes&Development*, 23(16):1910–1928.
- Chen, X. and Li, Y. (2009). Role of matrix metalloproteinases in skeletal muscle: migration, differentiation, regeneration and fibrosis. *Cell Adhesion&Migration*, 3(4):337–341.
- Chen, Y., Cardinaux, J.-R., Goodman, R. H., and Smolik, S. M. (1999). Mutants of cubitus interruptus that are independent of PKA regulation are independent of hedgehog signaling. *Development*, 126(16):3607–3616.

- Chen, Y., Li, S., Tong, C., Zhao, Y., Wang, B., Liu, Y., Jia, J., and Jiang, J. (2010b). G protein-coupled receptor kinase 2 promotes high-level Hedgehog signaling by regulating the active state of Smo through kinase-dependent and kinase-independent mechanisms in *Drosophila*. *Genes&Development*, 24(18):2054–2067.
- Chen, Y., Sasai, N., Ma, G., Yue, T., Jia, J., Briscoe, J., and Jiang, J. (2011). Sonic Hedgehog dependent phosphorylation by CK1 α and GRK2 is required for ciliary accumulation and activation of smoothened. *PLoS Biology*.
- Chen, Y. and Struhl, G. (1996). Dual roles for patched in sequestering and transducing Hedgehog. *Cell*, 87(3):553–563.
- Cheng, L., Alvares, L. E., Ahmed, M. U., El-Hanfy, A. S., and Dietrich, S. (2004). The epaxial–hypaxial subdivision of the avian somite. *Developmental Biology*, 274(2):348–369.
- Cheung, T. H., Quach, N. L., Charville, G. W., Liu, L., Park, L., Edalati, A., Yoo, B., Hoang, P., and Rando, T. A. (2012). Maintenance of muscle stem-cell quiescence by microRNA-489. *Nature*, 482(7386):524–528.
- Cheung, T. H. and Rando, T. A. (2013). Molecular regulation of stem cell quiescence. *Nature Reviews Molecular Cell Biology*, 14(6):329–340.
- Chiang, C., Litingtung, Y., Harris, M. P., Simandl, B. K., Li, Y., Beachy, P. A., and Fallon, J. F. (2001). Manifestation of the limb prepattern: limb development in the absence of sonic hedgehog function. *Developmental Biology*, 236(2):421–435.
- Chiang, C., Litingtung, Y., Lee, E., Young, K. E., Corden, J. L., Westphal, H., and Beachy, P. A. (1996). Cyclopia and defective axial patterning in mice lacking Sonic hedgehog gene function. *Nature*.
- Chinnaiya, K., Tickle, C., and Towers, M. (2014). Sonic hedgehog-expressing cells in the developing limb measure time by an intrinsic cell cycle clock. *Nature Communications*, 5(4320).
- Chong, Y. C., Mann, R. K., Zhao, C., Kato, M., and Beachy, P. A. (2015). Bifurcating action of Smoothened in Hedgehog signaling is mediated by Dlg5. *Genes&Development*, 29(3):262–276.
- Christ, B. and Brand-Saberi, B. (2002). Limb muscle development. *International Journal of Developmental Biology*, 46(7):905–914.
- Christov, C., Chrétien, F., Abou-Khalil, R., Bassez, G., Vallet, G., Authier, F.-J., Bassaglia, Y., Shinin, V., Tajbakhsh, S., Chazaud, B., et al. (2007). Muscle satellite cells and endothelial cells: close neighbors and privileged partners. *Molecular Biology of the Cell*, 18(4):1397–1409.
- Ciciliot, S., Rossi, A. C., Dyar, K. A., Blaauw, B., and Schiaffino, S. (2013). Muscle type and fiber type specificity in muscle wasting. *The International Journal of Biochemistry&Cell Biology*, 45(10):2191–2199.
- Clarke, M., Khakee, R., and McNeil, P. L. (1993). Loss of cytoplasmic basic fibroblast growth factor from physiologically wounded myofibers of normal and dystrophic muscle. *Journal of Cell Science*, 106(1):121–133.

- Coller, H. A. (2007). What's taking so long? S-phase entry from quiescence versus proliferation. *Nature Reviews Molecular Cell Biology*, 8(8):667–670.
- Collins, C. A., Olsen, I., Zammit, P. S., Heslop, L., Petrie, A., Partridge, T. A., and Morgan, J. E. (2005). Stem cell function, self-renewal, and behavioral heterogeneity of cells from the adult muscle satellite cell niche. *Cell*, 122(2):289–301.
- Collins, C. A. and Zammit, P. S. (2009). Isolation and grafting of single muscle fibres. In *Stem Cells in Regenerative Medicine*, pages 319–330. Springer.
- Collins, C. A., Zammit, P. S., Ruiz, A. P., Morgan, J. E., and Partridge, T. A. (2007). A population of myogenic stem cells that survives skeletal muscle aging. *Stem cells*, 25(4):885–894.
- Conboy, I. M. and Rando, T. A. (2002). The regulation of Notch signaling controls satellite cell activation and cell fate determination in postnatal myogenesis. *Developmental Cell*, 3(3):397–409.
- Cooper, R., Tajbakhsh, S., Mouly, V., Cossu, G., Buckingham, M., and Butler-Browne, G. (1999). In vivo satellite cell activation via Myf5 and MyoD in regenerating mouse skeletal muscle. *Journal of Cell Science*, 112(17):2895–2901.
- Cornelison, D. (2008). Context matters: in vivo and in vitro influences on muscle satellite cell activity. *Journal of Cellular Biochemistry*, 105(3):663–669.
- Cornelison, D., Filla, M. S., Stanley, H. M., Rapraeger, A. C., and Olwin, B. B. (2001). Syndecan-3 and syndecan-4 specifically mark skeletal muscle satellite cells and are implicated in satellite cell maintenance and muscle regeneration. *Developmental Biology*, 239(1):79–94.
- Corrales, J. D., Blaess, S., Mahoney, E. M., and Joyner, A. L. (2006). The level of Sonic hedgehog signaling regulates the complexity of cerebellar foliation. *Development*, 133(9):1811–1821.
- Cosgrove, B. D., Sacco, A., Gilbert, P. M., and Blau, H. M. (2009). A home away from home: challenges and opportunities in engineering in vitro muscle satellite cell niches. *Differentiation*, 78(2):185–194.
- Cossu, G. and Bianco, P. (2003). Mesoangioblasts—vascular progenitors for extravascular mesodermal tissues. *Current Opinion in Genetics&Development*, 13(5):537–542.
- Cossu, G., Kelly, R., Tajbakhsh, S., Di Donna, S., Vivarelli, E., and Buckingham, M. (1996). Activation of different myogenic pathways: myf-5 is induced by the neural tube and MyoD by the dorsal ectoderm in mouse paraxial mesoderm. *Development*, 122(2):429–437.
- Crist, C. G., Montarras, D., and Buckingham, M. (2012). Muscle satellite cells are primed for myogenesis but maintain quiescence with sequestration of Myf5 mRNA targeted by microRNA-31 in mRNP granules. *Cell Stem Cell*, 11(1):118–126.
- Cruz-Migoni, S. B. and Borycki, A.-G. (2014). Hedgehog Signalling. *eLS*, <http://onlinelibrary.wiley.com/doi/10.1002/9780470015902.a0000806.pub2/abstract>.
- Currie, P. D. and Ingham, P. W. (1996). Induction of a specific muscle cell type by a hedgehog-like protein in zebrafish. *Nature*, 382(6590):452–455.

- Dahn, R. D. and Fallon, J. F. (2000). Interdigital regulation of digit identity and homeotic transformation by modulated BMP signaling. *Science*, 289(5478):438–441.
- Darabi, R., Arpke, R. W., Irion, S., Dimos, J. T., Grskovic, M., Kyba, M., and Perlingeiro, R. C. (2012). Human ES- and iPS-derived myogenic progenitors restore Dystrophin and improve contractility upon transplantation in dystrophic mice. *Cell Stem Cell*, 10(5):610–619.
- Darabi, R., Gehlbach, K., Bachoo, R. M., Kamath, S., Osawa, M., Kamm, K. E., Kyba, M., and Perlingeiro, R. C. (2008). Functional skeletal muscle regeneration from differentiating embryonic stem cells. *Nature Medicine*, 14(2):134–143.
- Davies, K. E. and Nowak, K. J. (2006). Molecular mechanisms of muscular dystrophies: old and new players. *Nature Reviews Molecular Cell Biology*, 7(10):762–773.
- De Angelis, L., Berghella, L., Coletta, M., Lattanzi, L., Zanchi, M., Gabriella, M., Ponzetto, C., and Cossu, G. (1999). Skeletal myogenic progenitors originating from embryonic dorsal aorta coexpress endothelial and myogenic markers and contribute to postnatal muscle growth and regeneration. *The Journal of Cell Biology*, 147(4):869–878.
- de Lima, J. E., Bonnin, M.-A., Bourgeois, A., Parisi, A., Le Grand, F., and Duprez, D. (2014). Specific pattern of cell cycle during limb fetal myogenesis. *Developmental Biology*, 392(2):308–323.
- Dellavalle, A., Sampaolesi, M., Tonlorenzi, R., Tagliafico, E., Sacchetti, B., Perani, L., Innocenzi, A., Galvez, B. G., Messina, G., Morosetti, R., et al. (2007). Pericytes of human skeletal muscle are myogenic precursors distinct from satellite cells. *Nature Cell Biology*, 9(3):255–267.
- Delloye-Bourgeois, C., Gibert, B., Rama, N., Delcros, J.-G., Gadot, N., Scoazec, J.-Y., Krauss, R., Bernet, A., and Mehlen, P. (2013). Sonic Hedgehog promotes tumor cell survival by inhibiting CDON pro-apoptotic activity. *PLoS Biology*, 11(8):e1001623.
- Delloye-Bourgeois, C., Rama, N., Brito, J., Le Douarin, N., and Mehlen, P. (2014). Sonic Hedgehog promotes the survival of neural crest cells by limiting apoptosis induced by the dependence receptor CDON during branchial arch development. *Biochemical and Biophysical Research Communications*, 452(3):655–660.
- Dezawa, M., Ishikawa, H., Itokazu, Y., Yoshihara, T., Hoshino, M., Takeda, S.-i., Ide, C., and Nabeshima, Y.-i. (2005). Bone marrow stromal cells generate muscle cells and repair muscle degeneration. *Science*, 309(5732):314–317.
- Dierks, C., Grbic, J., Zirlik, K., Beigi, R., Englund, N. P., Guo, G.-R., Veelken, H., Engelhardt, M., Mertelsmann, R., Kelleher, J. F., et al. (2007). Essential role of stromally induced hedgehog signaling in B-cell malignancies. *Nature Medicine*, 13(8):944–951.
- Doherty, M. J., Ashton, B. A., Walsh, S., Beresford, J. N., Grant, M. E., and Canfield, A. E. (1998). Vascular pericytes express osteogenic potential in vitro and in vivo. *Journal of Bone and Mineral Research*, 13(5):828–838.
- Domen, J., Wagers, A., and Weissman, I. L. (2006). 2. bone marrow (hematopoietic) stem cells. *Regenerative Medicine*, page 13.

- Dorchies, O. M., Reutenauer-Patte, J., Dahmane, E., Ismail, H. M., Petermann, O., Patthey-Vuadens, O., Comyn, S. A., Gayi, E., Piacenza, T., Handa, R. J., et al. (2013). The anticancer drug tamoxifen counteracts the pathology in a mouse model of duchenne muscular dystrophy. *The American Journal of Pathology*, 182(2):485–504.
- Drossopoulou, G., Lewis, K., Sanz-Ezquerro, J., Nikbakht, N., McMahon, A., Hofmann, C., and Tickle, C. (2000). A model for anteroposterior patterning of the vertebrate limb based on sequential long-and short-range Shh signalling and Bmp signalling. *Development*, 127(7):1337–1348.
- Dumont, N. A., Bentzinger, C. F., Sincennes, M.-C., and Rudnicki, M. A. (2015a). Satellite cells and skeletal muscle regeneration. *Comprehensive Physiology*, 5(3):1027–59.
- Dumont, N. A., Wang, Y. X., and Rudnicki, M. A. (2015b). Intrinsic and extrinsic mechanisms regulating satellite cell function. *Development*, 142(9):1572–1581.
- Duprez, D., Fournier-Thibault, C., and Le Douarin, N. (1998). Sonic Hedgehog induces proliferation of committed skeletal muscle cells in the chick limb. *Development*, 125(3):495–505.
- Eisenberg, B. R. (1983). Quantitative ultrastructure of mammalian skeletal muscle. *Comprehensive Physiology*, 10:73–112.
- El-Zaatari, M., Daignault, S., Tessier, A., Kelsey, G., Travnikar, L. A., Cantu, E. F., Lee, J., Plonka, C. M., Simeone, D. M., Anderson, M. A., et al. (2012). Plasma Shh levels reduced in pancreatic cancer patients. *Pancreas*, 41(7):1019.
- Elia, D., Madhala, D., Ardon, E., Reshef, R., and Halevy, O. (2007). Sonic hedgehog promotes proliferation and differentiation of adult muscle cells: Involvement of MAPK/ERK and PI3K/Akt pathways. *Biochimica et Biophysica Acta (BBA)-Molecular Cell Research*, 1773(9):1438–1446.
- Ericson, J., Morton, S., Kawakami, A., Roelink, H., and Jessell, T. M. (1996). Two critical periods of Sonic Hedgehog signaling required for the specification of motor neuron identity. *Cell*, 87(4):661–673.
- Eugster, C., Panáková, D., Mahmoud, A., and Eaton, S. (2007). Lipoprotein-heparan sulfate interactions in the Hh pathway. *Developmental Cell*, 13(1):57–71.
- Fabian, S. L., Penchev, R. R., St-Jacques, B., Rao, A. N., Sipilä, P., West, K. A., McMahon, A. P., and Humphreys, B. D. (2012). Hedgehog-Gli pathway activation during kidney fibrosis. *The American Journal of Pathology*, 180(4):1441–1453.
- Fan, C.-W., Chen, B., Franco, I., Lu, J., Shi, H., Wei, S., Wang, C., Wu, X., Tang, W., Roth, M. G., et al. (2014). The Hedgehog Pathway Effector Smoothed Exhibits Signaling Competency in the Absence of Ciliary Accumulation. *Chemistry&Biology*, 21(12):1680–1689.
- Fan, H. and Khavari, P. A. (1999). Sonic hedgehog opposes epithelial cell cycle arrest. *The Journal of Cell Biology*, 147(1):71–76.
- Feil, R. (2007). Conditional somatic mutagenesis in the mouse using site-specific recombinases. In *Conditional Mutagenesis: An Approach to Disease Models*, pages 3–28. Springer.
- Feldman, J. L. and Stockdale, F. E. (1992). Temporal appearance of satellite cells during myogenesis. *Developmental Biology*, 153(2):217–226.

- Feng, X.-H. and Derynck, R. (2005). Specificity and versatility in TGF- β signaling through Smads. *Annu. Rev. Cell Dev. Biol.*, 21:659–693.
- Ferent, J., Cochard, L., Faure, H., Taddei, M., Hahn, H., Ruat, M., and Traiffort, E. (2014). Genetic activation of Hedgehog signaling unbalances the rate of neural stem cell renewal by increasing symmetric divisions. *Stem Cell Reports*, 3(2):312–323.
- Ferrari, G., Angelis, D., Coletta, M., Paolucci, E., Stornaiuolo, A., Cossu, G., Mavilio, F., et al. (1998). Muscle regeneration by bone marrow-derived myogenic progenitors. *Science*, 279(5356):1528–1530.
- Filareto, A., Parker, S., Darabi, R., Borges, L., Iacovino, M., Schaaf, T., Mayerhofer, T., Chamberlain, J. S., Ervasti, J. M., McIvor, R. S., et al. (2013). An ex vivo gene therapy approach to treat muscular dystrophy using inducible pluripotent stem cells. *Nature Communications*, 4:1549.
- Fingas, C. D., Mertens, J. C., Razumilava, N., Sydor, S., Bronk, S. F., Christensen, J. D., Rizvi, S. H., Canbay, A., Treckmann, J. W., Paul, A., et al. (2013). Polo-like kinase 2 is a mediator of hedgehog survival signaling in cholangiocarcinoma. *Hepatology*, 58(4):1362–1374.
- Fombonne, J., Bissey, P.-A., Guix, C., Sadoul, R., Thibert, C., and Mehlen, P. (2012). Patched dependence receptor triggers apoptosis through ubiquitination of caspase-9. *Proceedings of the National Academy of Sciences*, 109(26):10510–10515.
- Forbes, A., Nakano, Y., Taylor, A., and Ingham, P. (1992). Genetic analysis of hedgehog signalling in the Drosophila embryo. *Development*, pages 115–124.
- Friedrichs, M., Wirsdörfer, F., Flohé, S. B., Schneider, S., Wuelling, M., and Vortkamp, A. (2011). Bmp signaling balances proliferation and differentiation of muscle satellite cell descendants. *BMC Cell Biology*, 12(1):26.
- Fu, W., Asp, P., Canter, B., and Dynlacht, B. D. (2014). Primary cilia control hedgehog signaling during muscle differentiation and are deregulated in rhabdomyosarcoma. *Proceedings of the National Academy of Sciences*, 111(25):9151–9156.
- Fu, X., Xiao, J., Wei, Y., Li, S., Liu, Y., Yin, J., Sun, K., Sun, H., Wang, H., Zhang, Z., et al. (2015). Combination of inflammation-related cytokines promotes long-term muscle stem cell expansion. *Cell Research*, 25:655–673.
- Fukada, S.-i., Uezumi, A., Ikemoto, M., Masuda, S., Segawa, M., Tanimura, N., Yamamoto, H., Miyagoe-Suzuki, Y., and Takeda, S. (2007). Molecular signature of quiescent satellite cells in adult skeletal muscle. *Stem Cells*, 25(10):2448–2459.
- Fukada, S.-i., Yamaguchi, M., Kokubo, H., Ogawa, R., Uezumi, A., Yoneda, T., Matev, M. M., Motohashi, N., Ito, T., Zolkiewska, A., et al. (2011). Hes1 and Hes3 are essential to generate undifferentiated quiescent satellite cells and to maintain satellite cell numbers. *Development*, 138(21):4609–4619.
- Gang, E. J., Darabi, R., Bosnakovski, D., Xu, Z., Kamm, K. E., Kyba, M., and Perlingeiro, R. C. (2009). Engraftment of mesenchymal stem cells into dystrophin-deficient mice is not accompanied by functional recovery. *Experimental Cell Research*, 315(15):2624–2636.

- Ge, X., McFarlane, C., Vajjala, A., Lokireddy, S., Ng, Z. H., Tan, C. K., Tan, N. S., Wahli, W., Sharma, M., and Kambadur, R. (2011). Smad3 signaling is required for satellite cell function and myogenic differentiation of myoblasts. *Cell Research*, 21(11):1591–1604.
- Ghorpade, D. S., Holla, S., Kaveri, S. V., Bayry, J., Patil, S. A., and Balaji, K. N. (2013). Sonic hedgehog-dependent induction of microRNA 31 and microRNA 150 regulates Mycobacterium bovis BCG-driven toll-like receptor 2 signaling. *Molecular and Cellular Biology*, 33(3):543–556.
- Gilbert, P. M., Havenstrite, K. L., Magnusson, K. E., Sacco, A., Leonardi, N. A., Kraft, P., Nguyen, N. K., Thrun, S., Lutolf, M. P., and Blau, H. M. (2010). Substrate elasticity regulates skeletal muscle stem cell self-renewal in culture. *Science*, 329(5995):1078–1081.
- Girard, F., Strausfeld, U., Fernandez, A., and Lamb, N. J. (1991). Cyclin A is required for the onset of DNA replication in mammalian fibroblasts. *Cell*, 67(6):1169–1179.
- Gnocchi, V. F., White, R. B., Ono, Y., Ellis, J. A., and Zammit, P. S. (2009). Further characterisation of the molecular signature of quiescent and activated mouse muscle satellite cells. *PLoS One*, 4(4):e5205.
- Gonzatti-Haces, M., Seth, A., Park, M., Copeland, T., Oroszlan, S., and Woude, G. V. (1988). Characterization of the TPR-MET oncogene p65 and the MET protooncogene p140 protein-tyrosine kinases. *Proceedings of the National Academy of Sciences*, 85(1):21–25.
- Goodell, M. A., Brose, K., Paradis, G., Conner, A. S., and Mulligan, R. C. (1996). Isolation and functional properties of murine hematopoietic stem cells that are replicating in vivo. *The Journal of Experimental Medicine*, 183(4):1797–1806.
- Goodrich, L. V., Milenković, L., Higgins, K. M., and Scott, M. P. (1997). Altered neural cell fates and medulloblastoma in mouse patched mutants. *Science*, 277(5329):1109–1113.
- Goulding, M., Lumsden, A., and Paquette, A. J. (1994). Regulation of Pax-3 expression in the dermomyotome and its role in muscle development. *Development*, 120(4):957–971.
- Gros, J., Manceau, M., Thomé, V., and Marcelle, C. (2005). A common somitic origin for embryonic muscle progenitors and satellite cells. *Nature*, 435(7044):954–958.
- Gros, J., Scaal, M., and Marcelle, C. (2004). A two-step mechanism for myotome formation in chick. *Developmental Cell*, 6(6):875–882.
- Grounds, M. D., Garrett, K. L., Lai, M. C., Wright, W. E., and Beilharz, M. W. (1992). Identification of skeletal muscle precursor cells in vivo by use of MyoD1 and myogenin probes. *Cell and Tissue Research*, 267(1):99–104.
- Gruss, P. and Walther, C. (1992). Pax in development. *Cell*, 69(5):719–722.
- Günther, S., Kim, J., Kostin, S., Lepper, C., Fan, C.-M., and Braun, T. (2013). Myf5-positive satellite cells contribute to Pax7-dependent long-term maintenance of adult muscle stem cells. *Cell Stem Cell*, 13(5):590–601.

- Guo, S., Rena, G., Cichy, S., He, X., Cohen, P., and Unterman, T. (1999). Phosphorylation of serine 256 by protein kinase B disrupts transactivation by FKHR and mediates effects of insulin on insulin-like growth factor-binding protein-1 promoter activity through a conserved insulin response sequence. *Journal of Biological Chemistry*, 274(24):17184–17192.
- Gussoni, E., Soneoka, Y., Strickland, C. D., Buzney, E. A., Khan, M. K., Flint, A. F., Kunkel, L. M., and Mulligan, R. C. (1999). Dystrophin expression in the mdx mouse restored by stem cell transplantation. *Nature*, 401(6751):390–394.
- Gustafsson, M. K., Pan, H., Pinney, D. F., Liu, Y., Lewandowski, A., Epstein, D. J., and Emerson, C. P. (2002). Myf5 is a direct target of long-range Shh signaling and Gli regulation for muscle specification. *Genes&Development*, 16(1):114–126.
- Hahn, H., Wicking, C., Zaphiropoulos, P. G., Gailani, M. R., Shanley, S., Chidambaram, A., Vorechovsky, I., Holmberg, E., Uden, A. B., Gillies, S., et al. (1996). Mutations of the human homolog of Drosophila patched in the nevoid basal cell carcinoma syndrome. *Cell*, 85(6):841–851.
- Haldipur, P., Sivaprakasam, I., Babu, V., Govindan, S., and Mani, S. (2015). Asymmetric cell division of granule neuron progenitors in the external granule layer of the mouse cerebellum. *Biology Open*, pages bio-009886.
- Halevy, O., Piestun, Y., Allouh, M. Z., Rosser, B. W., Rinkevich, Y., Reshef, R., Rozenboim, I., Wleklinski-Lee, M., and Yablonka-Reuveni, Z. (2004). Pattern of pax7 expression during myogenesis in the posthatch chicken establishes a model for satellite cell differentiation and renewal. *Developmental Dynamics*, 231(3):489–502.
- Hall, J. K., Banks, G. B., Chamberlain, J. S., and Olwin, B. B. (2010). Prevention of muscle aging by myofiber-associated satellite cell transplantation. *Science Translational Medicine*, 2(57):57ra83–57ra83.
- Hallahan, A. R., Pritchard, J. I., Hansen, S., Benson, M., Stoeck, J., Hatton, B. A., Russell, T. L., Ellenbogen, R. G., Bernstein, I. D., Beachy, P. A., et al. (2004). The SmoA1 mouse model reveals that notch signaling is critical for the growth and survival of sonic hedgehog-induced medulloblastomas. *Cancer Research*, 64(21):7794–7800.
- Hamilton, D. L. and Abremski, K. (1984). Site-specific recombination by the bacteriophage P1 lox-Cre system: Cre-mediated synapsis of two lox sites. *Journal of Molecular Biology*, 178(2):481–486.
- Han, J., Pedersen, J. S., Kwon, S. C., Belair, C. D., Kim, Y.-K., Yeom, K.-H., Yang, W.-Y., Haussler, D., Belloch, R., and Kim, V. N. (2009). Posttranscriptional crossregulation between Drosha and DGCR8. *Cell*, 136(1):75–84.
- Hans, F. and Dimitrov, S. (2001). Histone H3 phosphorylation and cell division. *Oncogene*, 20(24):3021–3027.
- Hanson, J. and Huxley, H. E. (1953). Structural basis of the cross-striations in muscle. *Nature*, 172:530–532.
- Harel, I., Nathan, E., Tirosch-Finkel, L., Zigdon, H., Guimarães-Camboa, N., Evans, S. M., and Tzahor, E. (2009). Distinct origins and genetic programs of head muscle satellite cells. *Developmental Cell*, 16(6):822–832.

- Hartman, T. R., Zinshteyn, D., Schofield, H. K., Nicolas, E., Okada, A., and O'Reilly, A. M. (2010). *Drosophila* Boi limits Hedgehog levels to suppress follicle stem cell proliferation. *The Journal of Cell Biology*, 191(5):943–952.
- Hasty, P., Bradley, A., Morris, J. H., Edmondson, D. G., Venuti, J. M., Olson, E. N., and Klein, W. H. (1993). Muscle deficiency and neonatal death in mice with a targeted mutation in the myogenin gene. *Nature*, 364(6437):501–6.
- Heo, J. S., Lee, M. Y., and Han, H. J. (2007). Sonic hedgehog stimulates mouse embryonic stem cell proliferation by cooperation of Ca²⁺/protein kinase C and epidermal growth factor receptor as well as Gli1 activation. *Stem Cells*, 25(12):3069–3080.
- Heredia, J. E., Mukundan, L., Chen, F. M., Mueller, A. A., Deo, R. C., Locksley, R. M., Rando, T. A., and Chawla, A. (2013). Type 2 innate signals stimulate fibro/adipogenic progenitors to facilitate muscle regeneration. *Cell*, 153(2):376–388.
- Hollway, G. E. and Currie, P. D. (2003). Myotome meanderings. *EMBO Reports*, 4(9):855–860.
- Holtz, A. M., Peterson, K. A., Nishi, Y., Morin, S., Song, J. Y., Charron, F., McMahon, A. P., and Allen, B. L. (2013). Essential role for ligand-dependent feedback antagonism of vertebrate hedgehog signaling by PTCH1, PTCH2 and HHIP1 during neural patterning. *Development*, 140(16):3423–3434.
- Hooper, J. E. (2003). Smoothed translates hedgehog levels into distinct responses. *Development*, 130(17):3951–3963.
- Hosoyama, T., Nishijo, K., Prajapati, S. I., Li, G., and Keller, C. (2011). Rb1 gene inactivation expands satellite cell and postnatal myoblast pools. *Journal of Biological Chemistry*, 286(22):19556–19564.
- Hsu, Y.-C., Li, L., and Fuchs, E. (2014). Transit-amplifying cells orchestrate stem cell activity and tissue regeneration. *Cell*, 157(4):935–949.
- Hu, J. K.-H., McGlenn, E., Harfe, B. D., Kardon, G., and Tabin, C. J. (2012). Autonomous and nonautonomous roles of Hedgehog signaling in regulating limb muscle formation. *Genes&Development*, 26(18):2088–2102.
- Hu, M. C., Mo, R., Bhella, S., Wilson, C. W., Chuang, P.-T., Hui, C.-c., and Rosenblum, N. D. (2006). GLI3-dependent transcriptional repression of Gli1, Gli2 and kidney patterning genes disrupts renal morphogenesis. *Development*, 133(3):569–578.
- Huang, P., Xiong, F., Megason, S. G., and Schier, A. F. (2012). Attenuation of Notch and Hedgehog signaling is required for fate specification in the spinal cord. *PLoS Genetics*, 8(6):e1002762–e1002762.
- Huangfu, D. and Anderson, K. V. (2005). Cilia and Hedgehog responsiveness in the mouse. *Proceedings of the National Academy of Sciences*, 102(32):11325–11330.
- Huangfu, D., Liu, A., Rakeman, A. S., Murcia, N. S., Niswander, L., and Anderson, K. V. (2003). Hedgehog signalling in the mouse requires intraflagellar transport proteins. *Nature*, 426(6962):83–87.
- Hui, C.-c. and Angers, S. (2011). Gli proteins in development and disease. *Annual Review of Cell and Developmental Biology*, 27:513–537.

- Hui, C.-c. and Joyner, A. L. (1993). A mouse model of Greig cephalo-polysyndactyly syndrome: the extra-toesJ mutation contains an intragenic deletion of the Gli3 gene. *Nature Genetics*, 3(3):241–246.
- Huxley, H. (1957). The double array of filaments in cross-striated muscle. *The Journal of Biophysical and Biochemical Cytology*, 3(5):631–648.
- i Altaba, A. R. (1998). Combinatorial Gli gene function in floor plate and neuronal inductions by Sonic hedgehog. *Development*, 125(12):2203–2212.
- Ingham, P., Taylor, A., and Nakano, Y. (1991). Role of the *Drosophila* patched gene in positional signalling. *Nature*, 353(6340):184–187.
- Ingham, P. W. and McMahon, A. P. (2001). Hedgehog signaling in animal development: paradigms and principles. *Genes&Development*, 15(23):3059–3087.
- Irintchev, A., Zeschnigk, M., Starzinski-Powitz, A., and Wernig, A. (1994). Expression pattern of M-cadherin in normal, denervated, and regenerating mouse muscles. *Developmental Dynamics*, 199(4):326–337.
- Jeong, J. and McMahon, A. P. (2005). Growth and pattern of the mammalian neural tube are governed by partially overlapping feedback activities of the hedgehog antagonists patched 1 and Hhip1. *Development*, 132(1):143–154.
- Jia, J., Amanai, K., Wang, G., Tang, J., Wang, B., and Jiang, J. (2002). Shaggy/GSK3 antagonizes Hedgehog signalling by regulating Cubitus interruptus. *Nature*, 416(6880):548–552.
- Jia, J., Tong, C., and Jiang, J. (2003). Smoothed transduces Hedgehog signal by physically interacting with Costal2/Fused complex through its C-terminal tail. *Genes&Development*, 17(21):2709–2720.
- Jia, J., Tong, C., Wang, B., Luo, L., and Jiang, J. (2004). Hedgehog signalling activity of smoothed requires phosphorylation by protein kinase a and casein kinase i. *Nature*, 432(7020):1045–1050.
- Jiang, J. and Struhl, G. (1998). Regulation of the Hedgehog and Wingless signalling pathways by the F-box/WD40-repeat protein Slimb. *Nature*, 391(6666):493–496.
- Joe, A. W., Yi, L., Natarajan, A., Le Grand, F., So, L., Wang, J., Rudnicki, M. A., and Rossi, F. M. (2010). Muscle injury activates resident fibro/adipogenic progenitors that facilitate myogenesis. *Nature Cell Biology*, 12(2):153–163.
- Johnson, R. L., Rothman, A. L., Xie, J., Goodrich, L. V., Bare, J. W., Bonifas, J. M., Quinn, A. G., Myers, R. M., Cox, D. R., Epstein, E. H., et al. (1996). Human homolog of patched, a candidate gene for the basal cell nevus syndrome. *Science*, 272(5268):1668–1671.
- Johnson, R. L. and Tabin, C. J. (1997). Molecular models for vertebrate limb development. *Cell*, 90(6):979–990.
- Jones, N. C., Fedorov, Y. V., Rosenthal, R. S., and Olwin, B. B. (2001). ERK1/2 is required for myoblast proliferation but is dispensable for muscle gene expression and cell fusion. *Journal of Cellular Physiology*, 186(1):104–115.

- Jones, N. C., Tyner, K. J., Nibarger, L., Stanley, H. M., Cornelison, D. D., Fedorov, Y. V., and Olwin, B. B. (2005). The p38 functions as a molecular switch to activate the quiescent satellite cell. *The Journal of Cell Biology*, 169(1):105–116.
- Jostes, B., Walther, C., and Gruss, P. (1990). The murine paired box gene, Pax7, is expressed specifically during the development of the nervous and muscular system. *Mechanisms of Development*, 33(1):27–37.
- Kääriäinen, M., Järvinen, T., Järvinen, M., Rantanen, J., and Kalimo, H. (2000). Relation between myofibers and connective tissue during muscle injury repair. *Scandinavian Journal of Medicine & Science in Sports*, 10(6):332–337.
- Kablar, B., Krastel, K., Ying, C., Asakura, A., Tapscott, S. J., and Rudnicki, M. A. (1997). MyoD and Myf-5 differentially regulate the development of limb versus trunk skeletal muscle. *Development*, 124(23):4729–4738.
- Kahane, N., Ribes, V., Kicheva, A., Briscoe, J., and Kalcheim, C. (2013). The transition from differentiation to growth during dermomyotome-derived myogenesis depends on temporally restricted hedgehog signaling. *Development*, 140(8):1740–1750.
- Kalluri, R. and Zeisberg, M. (2006). Fibroblasts in cancer. *Nature Reviews Cancer*, 6(5):392–401.
- Kassar-Duchossoy, L., Gayraud-Morel, B., Gomès, D., Rocancourt, D., Buckingham, M., Shinin, V., and Tajbakhsh, S. (2004). Mrf4 determines skeletal muscle identity in Myf5: MyoD double-mutant mice. *Nature*, 431(7007):466–471.
- Kassar-Duchossoy, L., Giaccone, E., Gayraud-Morel, B., Jory, A., Gomès, D., and Tajbakhsh, S. (2005). Pax3/Pax7 mark a novel population of primitive myogenic cells during development. *Genes & Development*, 19(12):1426–1431.
- Katagiri, T., Akiyama, S., Namiki, M., Komaki, M., Yamaguchi, A., Rosen, V., Wozney, J. M., Fujisawa-Sehara, A., and Suda, T. (1997). Bone morphogenetic protein-2 inhibits terminal differentiation of myogenic cells by suppressing the transcriptional activity of MyoD and myogenin. *Experimental Cell Research*, 230(2):342–351.
- Kawabe, Y.-i., Wang, Y. X., McKinnell, I. W., Bedford, M. T., and Rudnicki, M. A. (2012). Carm1 regulates Pax7 transcriptional activity through MLL1/2 recruitment during asymmetric satellite stem cell divisions. *Cell Stem Cell*, 11(3):333–345.
- Kazuki, Y., Hiratsuka, M., Takiguchi, M., Osaki, M., Kajitani, N., Hoshiya, H., Hiramatsu, K., Yoshino, T., Kazuki, K., Ishihara, C., et al. (2010). Complete genetic correction of ips cells from Duchenne muscular dystrophy. *Molecular Therapy*, 18(2):386–393.
- Kenney, A. M., Widlund, H. R., and Rowitch, D. H. (2004). Hedgehog and PI-3 kinase signaling converge on Nmyc1 to promote cell cycle progression in cerebellar neuronal precursors. *Development*, 131(1):217–228.
- Khaliullina, H., Panáková, D., Eugster, C., Riedel, F., Carvalho, M., and Eaton, S. (2009). Patched regulates Smoothed trafficking using lipoprotein-derived lipids. *Development*, 136(24):4111–4121.

- Kitzmann, M., Carnac, G., Vandromme, M., Primig, M., Lamb, N. J., and Fernandez, A. (1998). The muscle regulatory factors MyoD and myf-5 undergo distinct cell cycle-specific expression in muscle cells. *The Journal of Cell Biology*, 142(6):1447–1459.
- Knight, J. and Kothary, R. (2011). The myogenic kinome: protein kinases critical to mammalian skeletal myogenesis. *Skeletal Muscle*, 1:29.
- Knoblich, J. A. (2008). Mechanisms of asymmetric stem cell division. *Cell*, 132(4):583–597.
- Koleva, M., Kappler, R., Vogler, M., Herwig, A., Fulda, S., and Hahn, H. (2005). Pleiotropic effects of sonic hedgehog on muscle satellite cells. *Cellular and Molecular Life Sciences CMLS*, 62(16):1863–1870.
- Kollu, S., Abou-Khalil, R., Shen, C., and Brack, A. S. (2015). The spindle assembly checkpoint safeguards genomic integrity of skeletal muscle satellite cells. *Stem Cell Reports*, 4(6):1061–1074.
- Kolterud, Å., Grosse, A. S., Zacharias, W. J., Walton, K. D., Kretovich, K. E., Madison, B. B., Waghray, M., Ferris, J. E., Hu, C., Merchant, J. L., et al. (2009). Paracrine Hedgehog signaling in stomach and intestine: new roles for hedgehog in gastrointestinal patterning. *Gastroenterology*, 137(2):618–628.
- Kong, J. H., Yang, L., Dessaud, E., Chuang, K., Moore, D. M., Rohatgi, R., Briscoe, J., and Novitch, B. G. (2015). Notch Activity Modulates the Responsiveness of Neural Progenitors to Sonic Hedgehog Signaling. *Developmental Cell*, 33(4):373–387.
- Konigsberg, U. R., Lipton, B. H., and Konigsberg, I. R. (1975). The regenerative response of single mature muscle fibers isolated in vitro. *Developmental Biology*, 45(2):260–275.
- Kopan, R. (2012). Notch signaling. *Cold Spring Harbor Perspectives in Biology*, 4(10):a011213.
- Korthuis, R. J. (2011). Skeletal muscle circulation. In *Colloquium Series on Integrated Systems Physiology: From Molecule to Function*, volume 3, pages 1–144. Morgan & Claypool Life Sciences.
- Krause, A., Xu, Y., Joh, J., Hubner, R., Gess, A., Ilic, T., and Worgall, S. (2010). Overexpression of sonic Hedgehog in the lung mimics the effect of lung injury and compensatory lung growth on pulmonary Sca-1 and CD34 positive cells. *Molecular Therapy*, 18(2):404–412.
- Krause, D., Ito, T., Fackler, M., Smith, O., Collector, M., Sharkis, S., and May, W. S. (1994). Characterization of murine CD34, a marker for hematopoietic progenitor and stem cells. *Blood*, 84(3):691–701.
- Krauss, S., Concordet, J.-P., and Ingham, P. (1993). A functionally conserved homolog of the Drosophila segment polarity gene hh is expressed in tissues with polarizing activity in zebrafish embryos. *Cell*, 75(7):1431–1444.
- Kruger, M., Mennerich, D., Fees, S., Schafer, R., Mundlos, S., and Braun, T. (2001). Sonic hedgehog is a survival factor for hypaxial muscles during mouse development. *Development*, 128(5):743–752.
- Kuang, S., Chargé, S. B., Seale, P., Huh, M., and Rudnicki, M. A. (2006). Distinct roles for Pax7 and Pax3 in adult regenerative myogenesis. *The Journal of Cell Biology*, 172(1):103–113.
- Kuang, S., Kuroda, K., Le Grand, F., and Rudnicki, M. A. (2007). Asymmetric self-renewal and commitment of satellite stem cells in muscle. *Cell*, 129(5):999–1010.

- Kusano, K. F., Pola, R., Murayama, T., Curry, C., Kawamoto, A., Iwakura, A., Shintani, S., Ii, M., Asai, J., Tkebuchava, T., et al. (2005). Sonic hedgehog myocardial gene therapy: tissue repair through transient reconstitution of embryonic signaling. *Nature Medicine*, 11(11):1197–1204.
- Lane, S. W., Williams, D. A., and Watt, F. M. (2014). Modulating the stem cell niche for tissue regeneration. *Nature Biotechnology*, 32(8):795–803.
- Lauth, M., Bergström, Å., Shimokawa, T., and Toftgård, R. (2007). Inhibition of GLI-mediated transcription and tumor cell growth by small-molecule antagonists. *Proceedings of the National Academy of Sciences*, 104(20):8455–8460.
- Le Grand, F., Grifone, R., Mourikis, P., Houbron, C., Gigaud, C., Pujol, J., Maillet, M., Pagès, G., Rudnicki, M., Tajbakhsh, S., et al. (2012). Six1 regulates stem cell repair potential and self-renewal during skeletal muscle regeneration. *The Journal of Cell Biology*, 198(5):815–832.
- Le Grand, F., Jones, A. E., Seale, V., Scimè, A., and Rudnicki, M. A. (2009). Wnt7a activates the planar cell polarity pathway to drive the symmetric expansion of satellite stem cells. *Cell Stem Cell*, 4(6):535–547.
- Lee, J., Platt, K. A., Censullo, P., and Altaba, A. R. (1997). Gli1 is a target of Sonic hedgehog that induces ventral neural tube development. *Development*, 124(13):2537–2552.
- Lee, J. J., Ekker, S. C., von Kessler, D. P., Porter, J. A., Sun, B. I., and Beachy, P. A. (1994). Autoproteolysis in hedgehog protein biogenesis. *Science*, 266(5190):1528–1537.
- Lepper, C., Conway, S. J., and Fan, C.-M. (2009). Adult satellite cells and embryonic muscle progenitors have distinct genetic requirements. *Nature*, 460(7255):627–631.
- Lepper, C., Partridge, T. A., and Fan, C.-M. (2011). An absolute requirement for Pax7-positive satellite cells in acute injury-induced skeletal muscle regeneration. *Development*, 138(17):3639–3646.
- Li, H. L., Fujimoto, N., Sasakawa, N., Shirai, S., Ohkame, T., Sakuma, T., Tanaka, M., Amano, N., Watanabe, A., Sakurai, H., et al. (2015). Precise correction of the dystrophin gene in duchenne muscular dystrophy patient induced pluripotent stem cells by TALEN and CRISPR-Cas9. *Stem Cell Reports*, 4(1):143–154.
- Li, X., Blagden, C. S., Bildsoe, H., Bonnin, M. A., Duprez, D., and Hughes, S. M. (2004). Hedgehog can drive terminal differentiation of amniote slow skeletal muscle. *BMC Developmental Biology*, 4(1):9.
- Lieber, R. L. (2002). *Skeletal muscle structure, function, and plasticity*. Lippincott Williams&Wilkins.
- Lin, X., Yang, X., Li, Q., Ma, Y., Cui, S., He, D., Lin, X., Schwartz, R. J., and Chang, J. (2012). Protein tyrosine phosphatase-like A regulates myoblast proliferation and differentiation through MyoG and the cell cycling signaling pathway. *Molecular and Cellular Biology*, 32(2):297–308.
- Lindner, D., Zietsch, C., Becher, P. M., Schulze, K., Schultheiss, H.-P., Tschöpe, C., and Westermann, D. (2012). Differential expression of matrix metalloproteases in human fibroblasts with different origins. *Biochemistry Research International*, 2012.
- Litingtung, Y. and Chiang, C. (2000). Specification of ventral neuron types is mediated by an antagonistic interaction between Shh and Gli3. *Nature Neuroscience*, 3(10):979–985.

- Liu, L., Cheung, T. H., Charville, G. W., Hurgo, B. M. C., Leavitt, T., Shih, J., Brunet, A., and Rando, T. A. (2013). Chromatin modifications as determinants of muscle stem cell quiescence and chronological aging. *Cell Reports*, 4(1):189–204.
- Liu, N., Nelson, B. R., Bezprozvannaya, S., Shelton, J. M., Richardson, J. A., Bassel-Duby, R., and Olson, E. N. (2014). Requirement of MEF2A, C, and D for skeletal muscle regeneration. *Proceedings of the National Academy of Sciences*, 111(11):4109–4114.
- Locker, M., Agathocleous, M., Amato, M. A., Parain, K., Harris, W. A., and Perron, M. (2006). Hedgehog signaling and the retina: insights into the mechanisms controlling the proliferative properties of neural precursors. *Genes&Development*, 20(21):3036–3048.
- Londhe, P. and Davie, J. K. (2011). Gamma interferon modulates myogenesis through the major histocompatibility complex class II transactivator, CIITA. *Molecular and Cellular Biology*, 31(14):2854–2866.
- Long, F., Zhang, X. M., Karp, S., Yang, Y., and McMahon, A. P. (2001). Genetic manipulation of hedgehog signaling in the endochondral skeleton reveals a direct role in the regulation of chondrocyte proliferation. *Development*, 128(24):5099–5108.
- Luz, M., Marques, M., and Santo Neto, H. (2002). Impaired regeneration of dystrophin-deficient muscle fibers is caused by exhaustion of myogenic cells. *Brazilian Journal of Medical and Biological Research*, 35(6):691–695.
- Machida, S., Spangenburg, E. E., and Booth, F. W. (2003). Forkhead transcription factor FoxO1 transduces insulin-like growth factor’s signal to p27Kip1 in primary skeletal muscle satellite cells. *Journal of Cellular Physiology*, 196(3):523–531.
- Madhala-Levy, D., Williams, V., Hughes, S., Reshef, R., and Halevy, O. (2012). Cooperation between Shh and IGF-I in promoting myogenic proliferation and differentiation via the MAPK/ERK and PI3K/Akt pathways requires smo activity. *Journal of Cellular Physiology*, 227(4):1455–1464.
- Madine, M. A., Swietlik, M., Pelizon, C., Romanowski, P., Mills, A. D., and Laskey, R. A. (2000). The roles of the MCM, ORC, and Cdc6 proteins in determining the replication competence of chromatin in quiescent cells. *Journal of Structural Biology*, 129(2):198–210.
- Madsen, P. and Celis, J. E. (1985). S-phase patterns of cyclin (PCNA) antigen staining resemble topographical patterns of DNA synthesis: a role for cyclin in DNA replication? *FEBS Letters*, 193(1):5–11.
- Mainwaring, L. A. and Kenney, A. M. (2011). Divergent functions for eIF4E and S6 kinase by sonic hedgehog mitogenic signaling in the developing cerebellum. *Oncogene*, 30(15):1784–1797.
- Mann, C. J., Perdiguero, E., Kharraz, Y., Aguilar, S., Pessina, P., Serrano, A. L., and Muñoz-Cánoves, P. (2011). Aberrant repair and fibrosis development in skeletal muscle. *Skeletal Muscle*, 1(1):21–21.
- Mansouri, A., Hallonet, M., and Gruss, P. (1996). Pax genes and their roles in cell differentiation and development. *Current Opinion in Cell Biology*, 8(6):851–857.
- Marg, A., Escobar, H., Gloy, S., Kufeld, M., Zacher, J., Spuler, A., Birchmeier, C., Izsvák, Z., and Spuler, S. (2014). Human satellite cells have regenerative capacity and are genetically manipulable. *The Journal of Clinical Investigation*, 124(10):4257.

- Maroto, M., Reshef, R., Münsterberg, A. E., Koester, S., Goulding, M., and Lassar, A. B. (1997). Ectopic Pax-3 activates MyoD and Myf-5 expression in embryonic mesoderm and neural tissue. *Cell*, 89(1):139–148.
- Martinelli, D. C. and Fan, C.-M. (2007). Gas1 extends the range of Hedgehog action by facilitating its signaling. *Genes&Development*, 21(10):1231–1243.
- Masai, I., Yamaguchi, M., Tonou-Fujimori, N., Komori, A., and Okamoto, H. (2005). The hedgehog-PKA pathway regulates two distinct steps of the differentiation of retinal ganglion cells: the cell-cycle exit of retinoblasts and their neuronal maturation. *Development*, 132(7):1539–1553.
- Mauro, A. (1961). Satellite cell of skeletal muscle fibers. *The Journal of Biophysical and Biochemical Cytology*, 9(2):493–495.
- McCarthy, J. J., Mula, J., Miyazaki, M., Erfani, R., Garrison, K., Farooqui, A. B., Srikuea, R., Lawson, B. A., Grimes, B., Keller, C., et al. (2011). Effective fiber hypertrophy in satellite cell-depleted skeletal muscle. *Development*, 138(17):3657–3666.
- McCroskery, S., Thomas, M., Maxwell, L., Sharma, M., and Kambadur, R. (2003). Myostatin negatively regulates satellite cell activation and self-renewal. *The Journal of Cell Biology*, 162(6):1135–1147.
- McDermott, A., Gustafsson, M., Elsam, T., Hui, C.-C., Emerson, C. P., and Borycki, A.-G. (2005). Gli2 and Gli3 have redundant and context-dependent function in skeletal muscle formation. *Development*, 132(2):345–357.
- McKay, B. R., Toth, K. G., Tarnopolsky, M. A., and Parise, G. (2010). Satellite cell number and cell cycle kinetics in response to acute myotrauma in humans: immunohistochemistry versus flow cytometry. *The Journal of Physiology*, 588(17):3307–3320.
- McKinnell, I. W., Ishibashi, J., Le Grand, F., Punch, V. G., Addicks, G. C., Greenblatt, J. F., Dilworth, F. J., and Rudnicki, M. A. (2008). Pax7 activates myogenic genes by recruitment of a histone methyltransferase complex. *Nature Cell Biology*, 10(1):77–84.
- McKinney-Freeman, S. L., Jackson, K. A., Camargo, F. D., Ferrari, G., Mavilio, F., and Goodell, M. A. (2002). Muscle-derived hematopoietic stem cells are hematopoietic in origin. *Proceedings of the National Academy of Sciences*, 99(3):1341–1346.
- McLennan, I. S. (1993). Resident macrophages (ED2-and ED3-positive) do not phagocytose degenerating rat skeletal muscle fibres. *Cell and Tissue Research*, 272(1):193–196.
- McPherron, A. C., Lawler, A. M., and Lee, S.-J. (1997). Regulation of skeletal muscle mass in mice by a new TGF- β superfamily member. *Nature*, 387(6628):83–90.
- Merly, F., Lescaudron, L., Rouaud, T., Crossin, F., and Gardahaut, M. F. (1999). Macrophages enhance muscle satellite cell proliferation and delay their differentiation. *Muscle&Nerve*, 22(6):724–732.
- Mill, P., Mo, R., Fu, H., Grachtchouk, M., Kim, P. C., Dlugosz, A. A., and Hui, C.-c. (2003). Sonic hedgehog-dependent activation of Gli2 is essential for embryonic hair follicle development. *Genes&Development*, 17(2):282–294.

- Mille, F., Thibert, C., Fombonne, J., Rama, N., Guix, C., Hayashi, H., Corset, V., Reed, J. C., and Mehlen, P. (2009). The Patched dependence receptor triggers apoptosis through a DRAL-caspase-9 complex. *Nature Cell Biology*, 11(6):739–746.
- Mo, R., Freer, A. M., Zinyk, D. L., Crackower, M. A., Michaud, J., Heng, H., Chik, K. W., Shi, X.-M., Tsui, L.-C., Cheng, S. H., et al. (1997). Specific and redundant functions of Gli2 and Gli3 zinc finger genes in skeletal patterning and development. *Development*, 124(1):113–123.
- Mokalled, M. H., Johnson, A. N., Creemers, E. E., and Olson, E. N. (2012). MASTR directs MyoD-dependent satellite cell differentiation during skeletal muscle regeneration. *Genes&Development*, 26(2):190–202.
- Molkentin, J. D. and Olson, E. N. (1996). Defining the regulatory networks for muscle development. *Current Opinion in Genetics&Development*, 6(4):445–453.
- Montarras, D., L'honoré, A., and Buckingham, M. (2013). Lying low but ready for action: the quiescent muscle satellite cell. *FEBS Journal*, 280(17):4036–4050.
- Montarras, D., Morgan, J., Collins, C., Relaix, F., Zaffran, S., Cumano, A., Partridge, T., and Buckingham, M. (2005). Direct isolation of satellite cells for skeletal muscle regeneration. *Science*, 309(5743):2064–2067.
- Morgan, D. O. (2007). *The cell cycle: principles of control*. New Science Press.
- Morita, H., Yoshimura, A., Inui, K., Ideura, T., Watanabe, H., Wang, L., Soinenen, R., and Tryggvason, K. (2005). Heparan sulfate of perlecan is involved in glomerular filtration. *Journal of the American Society of Nephrology*, 16(6):1703–1710.
- Moss, F. and Leblond, C. (1971). Satellite cells as the source of nuclei in muscles of growing rats. *The Anatomical Record*, 170(4):421–435.
- Motoyama, J., Liu, J., Mo, R., Ding, Q., Post, M., and Hui, C.-c. (1998). Essential function of Gli2 and Gli3 in the formation of lung, trachea and oesophagus. *Nature Genetics*, 20(1):54–57.
- Mourikis, P., Gopalakrishnan, S., Sambasivan, R., and Tajbakhsh, S. (2012a). Cell-autonomous Notch activity maintains the temporal specification potential of skeletal muscle stem cells. *Development*, 139(24):4536–4548.
- Mourikis, P., Sambasivan, R., Castel, D., Rocheteau, P., Bizzarro, V., and Tajbakhsh, S. (2012b). A critical requirement for notch signaling in maintenance of the quiescent skeletal muscle stem cell state. *Stem Cells*, 30(2):243–252.
- Mozzetta, C., Consalvi, S., Saccone, V., Tierney, M., Diamantini, A., Mitchell, K. J., Marazzi, G., Borsellino, G., Battistini, L., Sassoon, D., et al. (2013). Fibroadipogenic progenitors mediate the ability of HDAC inhibitors to promote regeneration in dystrophic muscles of young, but not old Mdx mice. *EMBO Molecular Medicine*, 5(4):626–639.
- Muir, A., Kanji, A., and Allbrook, D. (1965). The structure of the satellite cells in skeletal muscle. *Journal of Anatomy*, 99(Pt 3):435.

- Münsterberg, A., Kitajewski, J., Bumcrot, D. A., McMahon, A. P., and Lassar, A. B. (1995). Combinatorial signaling by Sonic hedgehog and Wnt family members induces myogenic bHLH gene expression in the somite. *Genes&Development*, 9(23):2911–2922.
- Murdoch, J. N. and Copp, A. J. (2010). The relationship between Sonic Hedgehog signaling, cilia, and neural tube defects. *Birth Defects Research Part A: Clinical and Molecular Teratology*, 88(8):633–652.
- Murphy, M. M., Keefe, A. C., Lawson, J. A., Flygare, S. D., Yandell, M., and Kardon, G. (2014). Transiently active Wnt/ β -catenin signaling is not required but must be silenced for stem cell function during muscle regeneration. *Stem Cell Reports*, 3(3):475–488.
- Murphy, M. M., Lawson, J. A., Mathew, S. J., Hutcheson, D. A., and Kardon, G. (2011). Satellite cells, connective tissue fibroblasts and their interactions are crucial for muscle regeneration. *Development*, 138(17):3625–3637.
- Nakano, Y., Guerrero, I., Hidalgo, A., Taylor, A., Whittle, J., and Ingham, P. (1989). A protein with several possible membrane-spanning domains encoded by the Drosophila segment polarity gene patched. *Nature*, 341(6242):508–513.
- Nieuwenhuis, E., Motoyama, J., Barnfield, P. C., Yoshikawa, Y., Zhang, X., Mo, R., Crackower, M. A., and Hui, C.-c. (2006). Mice with a targeted mutation of patched2 are viable but develop alopecia and epidermal hyperplasia. *Molecular and Cellular Biology*, 26(17):6609–6622.
- Nolan-Stevaux, O., Lau, J., Truitt, M. L., Chu, G. C., Hebrok, M., Fernández-Zapico, M. E., and Hanahan, D. (2009). GLI1 is regulated through Smoothed-independent mechanisms in neoplastic pancreatic ducts and mediates PDAC cell survival and transformation. *Genes&Development*, 23(1):24–36.
- Nurse, P. (1994). Ordering S phase and M phase in the cell cycle. *Cell*, 79(4):547–550.
- Nüsslein-Volhard, C. and Wieschaus, E. (1980). Mutations affecting segment number and polarity in Drosophila. *Nature*, 287(5785):795–801.
- Ochoa, O., Sun, D., Reyes-Reyna, S. M., Waite, L. L., Michalek, J. E., McManus, L. M., and Shireman, P. K. (2007). Delayed angiogenesis and VEGF production in CCR2^{-/-} mice during impaired skeletal muscle regeneration. *American Journal of Physiology-Regulatory, Integrative and Comparative Physiology*, 293(2):R651–R661.
- Oki, T., Nishimura, K., Kitaura, J., Togami, K., Maehara, A., Izawa, K., Sakaue-Sawano, A., Niida, A., Miyano, S., Aburatani, H., et al. (2014). A novel cell-cycle-indicator, mVenus-p27K⁻, identifies quiescent cells and visualizes G0-G1 transition. *Scientific Reports*, 4(4012).
- Olguin, H. C. and Olwin, B. B. (2004). Pax-7 up-regulation inhibits myogenesis and cell cycle progression in satellite cells: a potential mechanism for self-renewal. *Developmental Biology*, 275(2):375–388.
- Oliver, T. G., Grasfeder, L. L., Carroll, A. L., Kaiser, C., Gillingham, C. L., Lin, S. M., Wickramasinghe, R., Scott, M. P., and Wechsler-Reya, R. J. (2003). Transcriptional profiling of the Sonic hedgehog response: a critical role for N-myc in proliferation of neuronal precursors. *Proceedings of the National Academy of Sciences*, 100(12):7331–7336.

- Ono, Y., Boldrin, L., Knopp, P., Morgan, J. E., and Zammit, P. S. (2010). Muscle satellite cells are a functionally heterogeneous population in both somite-derived and branchiomic muscles. *Developmental Biology*, 337(1):29–41.
- Ono, Y., Calhabeu, F., Morgan, J. E., Katagiri, T., Amthor, H., and Zammit, P. S. (2011). BMP signalling permits population expansion by preventing premature myogenic differentiation in muscle satellite cells. *Cell Death&Differentiation*, 18(2):222–234.
- Ono, Y., Masuda, S., Nam, H.-s., Benezra, R., Miyagoe-Suzuki, Y., and Takeda, S. (2012). Slow-dividing satellite cells retain long-term self-renewal ability in adult muscle. *Journal of Cell Science*, 125(5):1309–1317.
- Otto, A., Collins-Hooper, H., Patel, A., Dash, P. R., and Patel, K. (2011). Adult skeletal muscle stem cell migration is mediated by a blebbing/amoeboid mechanism. *Rejuvenation Research*, 14(3):249–260.
- Ousterout, D. G., Perez-Pinera, P., Thakore, P. I., Kabadi, A. M., Brown, M. T., Qin, X., Fedrigo, O., Mouly, V., Tremblay, J. P., and Gersbach, C. A. (2013). Reading frame correction by targeted genome editing restores dystrophin expression in cells from Duchenne muscular dystrophy patients. *Molecular Therapy*, 21(9):1718–1726.
- Pajcini, K. V., Corbel, S. Y., Sage, J., Pomerantz, J. H., and Blau, H. M. (2010). Transient inactivation of Rb and ARF yields regenerative cells from postmitotic mammalian muscle. *Cell Stem Cell*, 7(2):198–213.
- Palladino, M., Gatto, I., Neri, V., Straino, S., Silver, M., Tritarelli, A., Piccioni, A., Smith, R. C., Gaetani, E., Losordo, D. W., et al. (2011). Pleiotropic beneficial effects of sonic hedgehog gene therapy in an experimental model of peripheral limb ischemia. *Molecular Therapy*, 19(4):658–666.
- Pallafacchina, G., Francois, S., Regnault, B., Czarny, B., Dive, V., Cumano, A., Montarras, D., and Buckingham, M. (2010). An adult tissue-specific stem cell in its niche: a gene profiling analysis of in vivo quiescent and activated muscle satellite cells. *Stem Cell Research*, 4(2):77–91.
- Pannérec, A., Marazzi, G., and Sassoon, D. (2012). Stem cells in the hood: the skeletal muscle niche. *Trends in Molecular Medicine*, 18(10):599–606.
- Pappenheimer, A. (1939). The pathology of nutritional muscular dystrophy in young rats. *The American Journal of Pathology*, 15(2):179.
- Pardee, A. B. (1974). A restriction point for control of normal animal cell proliferation. *Proceedings of the National Academy of Sciences*, 71(4):1286–1290.
- Parisi, A., Lacour, F., Giordani, L., Colnot, S., Maire, P., and Le Grand, F. (2015). APC is required for muscle stem cell proliferation and skeletal muscle tissue repair. *The Journal of Cell Biology*, pages jcb-201501053.
- Park, H., Bai, C., Platt, K., Matise, M., Beeghly, A., Hui, C., Nakashima, M., and Joyner, A. (2000). Mouse Gli1 mutants are viable but have defects in SHH signaling in combination with a Gli2 mutation. *Development*, 127(8):1593–1605.
- Pastoret, C. and Seville, A. (1995). Age-related differences in regeneration of dystrophic (mdx) and normal muscle in the mouse. *Muscle & nerve*, 18(10):1147–1154.

- Pasut, A., Jones, A. E., and Rudnicki, M. A. (2013). Isolation and culture of individual myofibers and their satellite cells from adult skeletal muscle. *Journal of Visualized Experiments: JoVE*, (73).
- Pepinsky, R. B., Zeng, C., Wen, D., Rayhorn, P., Baker, D. P., Williams, K. P., Bixler, S. A., Ambrose, C. M., Garber, E. A., Miatkowski, K., et al. (1998). Identification of a palmitic acid-modified form of human Sonic hedgehog. *Journal of Biological Chemistry*, 273(22):14037–14045.
- Petrova, R., Garcia, A. D. R., and Joyner, A. L. (2013). Titration of GLI3 repressor activity by Sonic hedgehog signaling is critical for maintaining multiple adult neural stem cell and astrocyte functions. *The Journal of Neuroscience*, 33(44):17490–17505.
- Petrova, R. and Joyner, A. L. (2014). Roles for Hedgehog signaling in adult organ homeostasis and repair. *Development*, 141(18):3445–3457.
- Piccioni, A., Gaetani, E., Neri, V., Gatto, I., Palladino, M., Silver, M., Smith, R. C., Giarretta, I., Pola, E., Hlatky, L., et al. (2014a). Sonic hedgehog therapy in a mouse model of age-associated impairment of skeletal muscle regeneration. *The Journals of Gerontology Series A: Biological Sciences and Medical Sciences*, 69(3):245–252.
- Piccioni, A., Gaetani, E., Palladino, M., Gatto, I., Smith, R., Neri, V., Marcantoni, M., Giarretta, I., Silver, M., Straino, S., et al. (2014b). Sonic hedgehog gene therapy increases the ability of the dystrophic skeletal muscle to regenerate after injury. *Gene Therapy*, 21(4):413–421.
- Poggeff, I. A. and Murray, M. R. (1946). Form and behavior of adult mammalian skeletal muscle in vitro. *The Anatomical Record*, 95(3):321–335.
- Pola, R., Ling, L. E., Aprahamian, T. R., Barban, E., Bosch-Marce, M., Curry, C., Corbley, M., Kearney, M., Isner, J. M., and Losordo, D. W. (2003). Postnatal recapitulation of embryonic Hedgehog pathway in response to skeletal muscle ischemia. *Circulation*, 108(4):479–485.
- Pons, S., Trejo, J. L., Martínez-Morales, J. R., and Martí, E. (2001). Vitronectin regulates Sonic hedgehog activity during cerebellum development through CREB phosphorylation. *Development*, 128(9):1481–1492.
- Porter, J. A., Young, K. E., and Beachy, P. A. (1996). Cholesterol modification of Hedgehog signaling proteins in animal development. *Science*, 274(5285):255–259.
- Pownall, M. E., Gustafsson, M. K., and Emerson Jr, C. P. (2002). Myogenic regulatory factors and the specification of muscle progenitors in vertebrate embryos. *Annual Review of Cell and Developmental Biology*, 18(1):747–783.
- Purslow, P. P. and Trotter, J. A. (1994). The morphology and mechanical properties of endomysium in series-fibred muscles: variations with muscle length. *Journal of Muscle Research & Cell Motility*, 15(3):299–308.
- Rajurkar, M., Huang, H., Cotton, J., Brooks, J., Sicklick, J., McMahon, A., and Mao, J. (2013). Distinct cellular origin and genetic requirement of Hedgehog-Gli in postnatal rhabdomyosarcoma genesis. *Oncogene*, 33(46):5370–5378.
- Rando, T. A. and Blau, H. M. (1994). Primary mouse myoblast purification, characterization, and transplantation for cell-mediated gene therapy. *The Journal of Cell Biology*, 125(6):1275–1287.

- Rawls, A., Valdez, M. R., Zhang, W., Richardson, J., Klein, W. H., and Olson, E. N. (1998). Overlapping functions of the myogenic bHLH genes MRF4 and MyoD revealed in double mutant mice. *Development*, 125(13):2349–2358.
- Rayagiri, S. (2014). *Analysis of the Remodelling of the Satellite Cell Basal Lamina During Skeletal Muscle Regeneration*. PhD thesis, University of Sheffield.
- Reisz-Porszasz, S., Bhasin, S., Artaza, J. N., Shen, R., Sinha-Hikim, I., Hogue, A., Fielder, T. J., and Gonzalez-Cadavid, N. F. (2003). Lower skeletal muscle mass in male transgenic mice with muscle-specific overexpression of myostatin. *American Journal of Physiology-Endocrinology and Metabolism*, 285(4):E876–E888.
- Relaix, F., Montarras, D., Zaffran, S., Gayraud-Morel, B., Rocancourt, D., Tajbakhsh, S., Mansouri, A., Cumano, A., and Buckingham, M. (2006). Pax3 and Pax7 have distinct and overlapping functions in adult muscle progenitor cells. *The Journal of Cell Biology*, 172(1):91–102.
- Relaix, F., Rocancourt, D., Mansouri, A., and Buckingham, M. (2005). A Pax3/Pax7-dependent population of skeletal muscle progenitor cells. *Nature*, 435(7044):948–953.
- Relaix, F. and Zammit, P. S. (2012). Satellite cells are essential for skeletal muscle regeneration: the cell on the edge returns centre stage. *Development*, 139(16):2845–2856.
- Renault, M.-A., Robbesyn, F., Chapouly, C., Yao, Q., Vandierdonck, S., Reynaud, A., Belloc, I., Traiffort, E., Ruat, M., Desgranges, C., et al. (2013a). Hedgehog-dependent regulation of angiogenesis and myogenesis is impaired in aged mice. *Arteriosclerosis, Thrombosis, and Vascular Biology*, 33(12):2858–2866.
- Renault, M.-A., Vandierdonck-Leymond, S., Chapouly, C., Yu, Y., Qin, G., Metras, A., Couffinhal, T., Losordo, D. W., Yao, Q., Reynaud, A., et al. (2013b). Gli3-regulation of myogenesis is necessary for ischemia-induced angiogenesis. *Circulation Research*, 113(10):1148–1158.
- Reznik, M. (1969). Thymidine-3H uptake by satellite cells of regenerating skeletal muscle. *The Journal of Cell Biology*, 40(2):568.
- Ribes, V. and Briscoe, J. (2009). Establishing and interpreting graded Sonic Hedgehog signaling during vertebrate neural tube patterning: the role of negative feedback. *Cold Spring Harbor Perspectives in Biology*, 1(2):a002014.
- Richter, E. A., Garetto, L. P., Goodman, M. N., and Ruderman, N. B. (1982). Muscle glucose metabolism following exercise in the rat: increased sensitivity to insulin. *Journal of Clinical Investigation*, 69(4):785.
- Riddle, R. D., Johnson, R. L., Laufer, E., and Tabin, C. (1993). Sonic hedgehog mediates the polarizing activity of the ZPA. *Cell*, 75(7):1401–1416.
- Robbins, D. J., Nybakken, K. E., Kobayashi, R., Sisson, J. C., Bishop, J. M., and Thérond, P. P. (1997). Hedgehog elicits signal transduction by means of a large complex containing the kinesin-related protein costal2. *Cell*, 90(2):225–234.

- Rocheteau, P., Gayraud-Morel, B., Siegl-Cachedenier, I., Blasco, M. A., and Tajbakhsh, S. (2012). A subpopulation of adult skeletal muscle stem cells retains all template DNA strands after cell division. *Cell*, 148(1):112–125.
- Rodgers, J. T., King, K. Y., Brett, J. O., Cromie, M. J., Charville, G. W., Maguire, K. K., Brunson, C., Mastey, N., Liu, L., Tsai, C.-R., et al. (2014). mTORC1 controls the adaptive transition of quiescent stem cells from G0 to GAlert. *Nature*, 510(7505):393–396.
- Rohatgi, R., Milenkovic, L., Corcoran, R. B., and Scott, M. P. (2009). Hedgehog signal transduction by Smoothed: pharmacologic evidence for a 2-step activation process. *Proceedings of the National Academy of Sciences*, 106(9):3196–3201.
- Rosenblatt, J. D. (1992). A time course study of the isometric contractile properties of rat extensor digitorum longus muscle injected with bupivacaine. *Comparative Biochemistry and Physiology Part A: Physiology*, 101(2):361–367.
- Rosenblatt, J. D., Lunt, A. I., Parry, D. J., and Partridge, T. A. (1995). Culturing satellite cells from living single muscle fiber explants. *In Vitro Cellular&Developmental Biology-Animal*, 31(10):773–779.
- Rowbotham, N. J., Hager-Theodorides, A. L., Cebecauer, M., Shah, D. K., Drakopoulou, E., Dyson, J., Outram, S. V., and Crompton, T. (2007). Activation of the Hedgehog signaling pathway in T-lineage cells inhibits TCR repertoire selection in the thymus and peripheral T-cell activation. *Blood*, 109(9):3757–3766.
- Roy, S., Wolff, C., and Ingham, P. W. (2001). The u-boot mutation identifies a Hedgehog-regulated myogenic switch for fiber-type diversification in the zebrafish embryo. *Genes&Development*, 15(12):1563–1576.
- Rudnicki, M. A., Braun, T., Hinuma, S., and Jaenisch, R. (1992). Inactivation of MyoD in mice leads to up-regulation of the myogenic HLH gene Myf-5 and results in apparently normal muscle development. *Cell*, 71(3):383–390.
- Sacco, A., Doyonnas, R., Kraft, P., Vitorovic, S., and Blau, H. M. (2008). Self-renewal and expansion of single transplanted muscle stem cells. *Nature*, 456(7221):502–506.
- Saccone, V., Consalvi, S., Giordani, L., Mozzetta, C., Barozzi, I., Sandoná, M., Ryan, T., Rojas-Muñoz, A., Madaro, L., Fasanaro, P., et al. (2014). HDAC-regulated myomiRs control BAF60 variant exchange and direct the functional phenotype of fibro-adipogenic progenitors in dystrophic muscles. *Genes&Development*, 28(8):841–857.
- Sacedón, R., Díez, B., Nuñez, V., Hernández-López, C., Gutierrez-Frías, C., Cejalvo, T., Outram, S. V., Crompton, T., Zapata, A. G., Vicente, A., et al. (2005). Sonic hedgehog is produced by follicular dendritic cells and protects germinal center B cells from apoptosis. *The Journal of Immunology*, 174(3):1456–1461.
- Sachidanandan, C., Sambasivan, R., and Dhawan, J. (2002). Tristetraprolin and LPS-inducible CXC chemokine are rapidly induced in presumptive satellite cells in response to skeletal muscle injury. *Journal of Cell Science*, 115(13):2701–2712.

- Saclier, M., Yacoub-Youssef, H., Mackey, A. L., Arnold, L., Ardjoune, H., Magnan, M., Sailhan, F., Chelly, J., Pavlath, G. K., Mounier, R., et al. (2013). Differentially activated macrophages orchestrate myogenic precursor cell fate during human skeletal muscle regeneration. *Stem Cells*, 31(2):384–396.
- Sakaue-Sawano, A., Kurokawa, H., Morimura, T., Hanyu, A., Hama, H., Osawa, H., Kashiwagi, S., Fukami, K., Miyata, T., Miyoshi, H., et al. (2008). Visualizing spatiotemporal dynamics of multicellular cell-cycle progression. *Cell*, 132(3):487–498.
- Salani, S., Donadoni, C., Rizzo, F., Bresolin, N., Comi, G. P., and Corti, S. (2012). Generation of skeletal muscle cells from embryonic and induced pluripotent stem cells as an in vitro model and for therapy of muscular dystrophies. *Journal of Cellular and Molecular Medicine*, 16(7):1353–1364.
- Salic, A. and Mitchison, T. J. (2008). A chemical method for fast and sensitive detection of DNA synthesis in vivo. *Proceedings of the National Academy of Sciences*, 105(7):2415–2420.
- Sambasivan, R., Gayraud-Morel, B., Dumas, G., Cimper, C., Paisant, S., Kelly, R. G., and Tajbakhsh, S. (2009). Distinct regulatory cascades govern extraocular and pharyngeal arch muscle progenitor cell fates. *Developmental Cell*, 16(6):810–821.
- Sambasivan, R., Yao, R., Kissenpfennig, A., Van Wittenberghe, L., Paldi, A., Gayraud-Morel, B., Genuou, H., Malissen, B., Tajbakhsh, S., and Galy, A. (2011). Pax7-expressing satellite cells are indispensable for adult skeletal muscle regeneration. *Development*, 138(17):3647–3656.
- Sampaolesi, M., Blot, S., D’antona, G., Granger, N., Tonlorenzi, R., Innocenzi, A., Mognol, P., Thibaud, J.-L., Galvez, B. G., Barthélémy, I., et al. (2006). Mesoangioblast stem cells ameliorate muscle function in dystrophic dogs. *Nature*, 444(7119):574–579.
- Sampaolesi, M., Torrente, Y., Innocenzi, A., Tonlorenzi, R., D’Antona, G., Pellegrino, M. A., Barresi, R., Bresolin, N., De Angelis, M. G. C., Campbell, K. P., et al. (2003). Cell therapy of α -sarcoglycan null dystrophic mice through intra-arterial delivery of mesoangioblasts. *Science*, 301(5632):487–492.
- Sartore, S., Mascarello, F., Rowlerson, A., Gorza, L., Ausoni, S., Vianello, M., and Schiaffino, S. (1987). Fibre types in extraocular muscles: a new myosin isoform in the fast fibres. *Journal of Muscle Research&Cell Motility*, 8(2):161–172.
- Sasaki, H., Nishizaki, Y., Hui, C.-c., Nakafuku, M., and Kondoh, H. (1999). Regulation of Gli2 and Gli3 activities by an amino-terminal repression domain: implication of Gli2 and Gli3 as primary mediators of Shh signaling. *Development*, 126(17):3915–3924.
- Satheesha, S., Manzella, G., Bovay, A., Casanova, E., Bode, P., Belle, R., Feuchtgruber, S., Jaaks, P., Dogan, N., Koscielniak, E., et al. (2015). Targeting Hedgehog signaling reduces self-renewal in embryonal rhabdomyosarcoma. *Oncogene*.
- Schaaf, G. (2012). Ex-vivo expansion of muscle-regenerative cells for the treatment of muscle disorders. *Journal of Stem Cell Research&Therapy*, 2:1–15.
- Scharner, J. and Zammit, P. S. (2011). The muscle satellite cell at 50: the formative years. *Skeletal Muscle*, 1(1):28–28.
- Schiaffino, S. and Reggiani, C. (1994). Myosin isoforms in mammalian skeletal muscle. *Journal of Applied Physiology*, 77(2):493–501.

- Schiaffino, S. and Reggiani, C. (2011). Fiber types in mammalian skeletal muscles. *Physiological Reviews*, 91(4):1447–1531.
- Schienda, J., Engleka, K. A., Jun, S., Hansen, M. S., Epstein, J. A., Tabin, C. J., Kunkel, L. M., and Kardon, G. (2006). Somitic origin of limb muscle satellite and side population cells. *Proceedings of the National Academy of Sciences*, 103(4):945–950.
- Schmalbruch, H. and Hellhammer, U. (1976). The number of satellite cells in normal human muscle. *The Anatomical Record*, 185(3):279–287.
- Scholzen, T., Gerdes, J., et al. (2000). The Ki-67 protein: from the known and the unknown. *Journal of Cellular Physiology*, 182(3):311–322.
- Schultz, E. (1996). Satellite cell proliferative compartments in growing skeletal muscles. *Developmental Biology*, 175(1):84–94.
- Schultz, E. and McCormick, K. M. (1994). Skeletal muscle satellite cells. In *Reviews of Physiology, Biochemistry and Pharmacology, Volume 123*, pages 213–257. Springer.
- Scotting, P. J., Walker, D. A., and Perilongo, G. (2005). Childhood solid tumours: a developmental disorder. *Nature Reviews Cancer*, 5(6):481–488.
- Seale, P., Ishibashi, J., Scime, A., and Rudnicki, M. A. (2004). Pax7 is necessary and sufficient for the myogenic specification of CD45⁺: Sca1⁺ stem cells from injured muscle. *PLoS Biology*, 2(5):664–672.
- Seale, P., Sabourin, L. A., Girgis-Gabardo, A., Mansouri, A., Gruss, P., and Rudnicki, M. A. (2000). Pax7 is required for the specification of myogenic satellite cells. *Cell*, 102(6):777–786.
- Sebastian, S., Sreenivas, P., Sambasivan, R., Cheedipudi, S., Kandalla, P., Pavlath, G. K., and Dhawan, J. (2009). MLL5, a trithorax homolog, indirectly regulates H3K4 methylation, represses cyclin A2 expression, and promotes myogenic differentiation. *Proceedings of the National Academy of Sciences*, 106(12):4719–4724.
- Seidel, K., Ahn, C. P., Lyons, D., Nee, A., Ting, K., Brownell, I., Cao, T., Carano, R. A., Curran, T., Schober, M., et al. (2010). Hedgehog signaling regulates the generation of ameloblast progenitors in the continuously growing mouse incisor. *Development*, 137(22):3753–3761.
- Seifert, A. W., Zheng, Z., Ormerod, B. K., and Cohn, M. J. (2010). Sonic hedgehog controls growth of external genitalia by regulating cell cycle kinetics. *Nature Communications*, 1:23.
- Semesarian, C., Wu, M., Yu, Y., Marciniak, T., Yeoh, T., Allen, T., Harvey, P., and Graham, R. (1999). Skeletal muscle hypertrophy is mediated by a Ca²⁺-dependent calcineurin signaling pathway. *Nature*, 400:576–581.
- Serrano, A. L., Baeza-Raja, B., Perdiguero, E., Jardí, M., and Muñoz-Cánoves, P. (2008). Interleukin-6 is an essential regulator of satellite cell-mediated skeletal muscle hypertrophy. *Cell Metabolism*, 7(1):33–44.
- Shea, K. L., Xiang, W., LaPorta, V. S., Licht, J. D., Keller, C., Basson, M. A., and Brack, A. S. (2010). Sprouty1 regulates reversible quiescence of a self-renewing adult muscle stem cell pool during regeneration. *Cell Stem Cell*, 6(2):117–129.

- Shefer, G., Van de Mark, D. P., Richardson, J. B., and Yablonka-Reuveni, Z. (2006). Satellite-cell pool size does matter: defining the myogenic potency of aging skeletal muscle. *Developmental Biology*, 294(1):50–66.
- Shefer, G. and Yablonka-Reuveni, Z. (2005). Isolation and culture of skeletal muscle myofibers as a means to analyze satellite cells. In *Basic Cell Culture Protocols*, pages 281–304. Springer.
- Shelton, M., Metz, J., Liu, J., Carpenedo, R. L., Demers, S.-P., Stanford, W. L., and Skerjanc, I. S. (2014). Derivation and expansion of pax7-positive muscle progenitors from human and mouse embryonic stem cells. *Stem Cell Reports*, 3(3):516–529.
- Shen, X., Collier, J. M., Hlaing, M., Zhang, L., Delshad, E. H., Bristow, J., and Bernstein, H. S. (2003). Genome-wide examination of myoblast cell cycle withdrawal during differentiation. *Developmental Dynamics*, 226(1):128–138.
- Shenghui, H., Nakada, D., and Morrison, S. J. (2009). Mechanisms of stem cell self-renewal. *Annual Review of Cell and Developmental*, 25:377–406.
- Shinin, V., Gayraud-Morel, B., Gomès, D., and Tajbakhsh, S. (2006). Asymmetric division and cosegregation of template DNA strands in adult muscle satellite cells. *Nature Cell Biology*, 8(7):677–682.
- Shkumatava, A. and Neumann, C. J. (2005). Shh directs cell-cycle exit by activating p57Kip2 in the zebrafish retina. *EMBO Reports*, 6(6):563–569.
- Siegel, A. L., Atchison, K., Fisher, K. E., Davis, G. E., and Cornelison, D. (2009). 3d timelapse analysis of muscle satellite cell motility. *Stem Cells*, 27(10):2527–2538.
- Siegel, A. L., Kuhlmann, P. K., and Cornelison, D. (2011). Muscle satellite cell proliferation and association: new insights from myofiber time-lapse imaging. *Skeletal Muscle*, 1(1):7.
- Snow, M. H. (1977). The effects of aging on satellite cells in skeletal muscles of mice and rats. *Cell and Tissue Research*, 185(3):399–408.
- Snow, M. H. (1978). An autoradiographic study of satellite cell differentiation into regenerating myotubes following transplantation of muscles in young rats. *Cell and Tissue Research*, 186(3):535–540.
- Sorichter, S., Mair, J., Koller, A., Pelsers, M., Puschendorf, B., and Glatz, J. (1998a). Early assessment of exercise induced skeletal muscle injury using plasma fatty acid binding protein. *British Journal of Sports Medicine*, 32(2):121–124.
- Sorichter, S., Puschendorf, B., and Mair, J. (1998b). Skeletal muscle injury induced by eccentric muscle action: muscle proteins as markers of muscle fiber injury. *Exercise Immunology Review*, 5:5–21.
- St-Jacques, B., Hammerschmidt, M., and McMahon, A. P. (1999). Indian hedgehog signaling regulates proliferation and differentiation of chondrocytes and is essential for bone formation. *Genes&Development*, 13(16):2072–2086.
- St Pierre, B. and Tidball, J. G. (1994). Differential response of macrophage subpopulations to soleus muscle reloading after rat hindlimb suspension. *Journal of Applied Physiology*, 77(1):290–297.

- Stasiulewicz, M., Gray, S., Mastromina, I., Silva, J. C., Bjorklund, M., Seymour, P. A., Booth, D., Thompson, C., Green, R., Hall, E. A., et al. (2015). A conserved role for Notch in priming the cellular response to Shh through ciliary localisation of the key Shh transducer, Smoothened. *Development*, pages dev-125237.
- Stecca, B., Mas, C., Clement, V., Zbinden, M., Correa, R., Piguet, V., Beermann, F., and Altaba, A. R. (2007). Melanomas require HEDGEHOG-GLI signaling regulated by interactions between GLI1 and the RAS-MEK/AKT pathways. *Proceedings of the National Academy of Sciences*, 104(14):5895–5900.
- Straface, G., Aprahamian, T., Flex, A., Gaetani, E., Biscetti, F., Smith, R. C., Pecorini, G., Pola, E., Angelini, F., Stigliano, E., et al. (2009). Sonic hedgehog regulates angiogenesis and myogenesis during post-natal skeletal muscle regeneration. *Journal of Cellular and Molecular Medicine*, 13(8b):2424–2435.
- Strutt, H., Thomas, C., Nakano, Y., Stark, D., Neave, B., Taylor, A., and Ingham, P. (2001). Mutations in the sterol-sensing domain of Patched suggest a role for vesicular trafficking in Smoothened regulation. *Current Biology*, 11(8):608–613.
- Strutz, F., Okada, H., Lo, C. W., Danoff, T., Carone, R. L., Tomaszewski, J. E., and Neilson, E. G. (1995). Identification and characterization of a fibroblast marker: FSP1. *The Journal of Cell Biology*, 130(2):393–405.
- Su, Y., Ospina, J. K., Zhang, J., Michelson, A. P., Schoen, A. M., and Zhu, A. J. (2011). Sequential phosphorylation of Smoothened transduces graded Hedgehog signaling. *Science Signaling*, 4(180):ra43.
- Szent-Györgyi, A. G. (2004). The early history of the biochemistry of muscle contraction. *The Journal of General Physiology*, 123(6):631–641.
- Tabata, T., Eaton, S., and Kornberg, T. (1992). The Drosophila hedgehog gene is expressed specifically in posterior compartment cells and is a target of engrailed regulation. *Genes&Development*, 6:2635–2635.
- Taipale, J., Chen, J. K., Cooper, M. K., Wang, B., Mann, R. K., Milenkovic, L., Scott, M. P., and Beachy, P. A. (2000). Effects of oncogenic mutations in Smoothened and Patched can be reversed by cyclopamine. *Nature*, 406(6799):1005–1009.
- Taipale, J., Cooper, M., Maiti, T., and Beachy, P. (2002). Patched acts catalytically to suppress the activity of Smoothened. *Nature*, 418(6900):892–896.
- Tajbakhsh, S. and Buckingham, M. (2000). The birth of muscle progenitor cells in the mouse: spatiotemporal considerations. *Current Topics in Developmental Biology*, 48:225–260.
- Tajbakhsh, S., Rocancourt, D., Cossu, G., and Buckingham, M. (1997). Redefining the genetic hierarchies controlling skeletal myogenesis: Pax-3 and Myf-5 act upstream of MyoD. *Cell*, 89(1):127–138.
- Tatsumi, R., Hattori, A., Ikeuchi, Y., Anderson, J. E., and Allen, R. E. (2002). Release of hepatocyte growth factor from mechanically stretched skeletal muscle satellite cells and role of pH and nitric oxide. *Molecular Biology of the Cell*, 13(8):2909–2918.
- Tedesco, F. S., Gerli, M. F., Perani, L., Benedetti, S., Ungaro, F., Cassano, M., Antonini, S., Tagliafico, E., Artusi, V., Longa, E., et al. (2012). Transplantation of genetically corrected human iPSC-derived progenitors in mice with limb-girdle muscular dystrophy. *Science Translational Medicine*, 4(140):140ra89–140ra89.

- Thibert, C., Teillet, M.-A., Lapointe, F., Mazelin, L., Le Douarin, N. M., and Mehlen, P. (2003). Inhibition of neuroepithelial Patched-induced apoptosis by Sonic hedgehog. *Science*, 301(5634):843–846.
- Tidball, J. G. (1995). Inflammatory cell response to acute muscle injury. *Medicine and Science in Sports and Exercise*, 27(7):1022–1032.
- Torrente, Y., Belicchi, M., Sampaolesi, M., Pisati, F., Meregalli, M., D’Antona, G., Tonlorenzi, R., Porretti, L., Gavina, M., Mamchaoui, K., et al. (2004). Human circulating AC133+ stem cells restore dystrophin expression and ameliorate function in dystrophic skeletal muscle. *Journal of Clinical Investigation*, 114(2):182.
- Tosney, K. W., Dehnbostel, D. B., and Erickson, C. A. (1994). Neural crest cells prefer the myotome’s basal lamina over the sclerotome as a substratum. *Developmental Biology*, 163(2):389–406.
- Tostar, U., Malm, C. J., Meis-Kindblom, J. M., Kindblom, L.-G., Toftgård, R., and Undén, A. B. (2006). Deregulation of the Hedgehog signalling pathway: a possible role for the PTCH and SUFU genes in human rhabdomyoma and rhabdomyosarcoma development. *The Journal of Pathology*, 208(1):17–25.
- Towers, M., Mahood, R., Yin, Y., and Tickle, C. (2008). Integration of growth and specification in chick wing digit-patterning. *Nature*, 452(7189):882–886.
- Toyoshima, H. and Hunter, T. (1994). p27, a novel inhibitor of G1 cyclin-Cdk protein kinase activity, is related to p21. *Cell*, 78(1):67–74.
- Trowbridge, J. J., Scott, M. P., and Bhatia, M. (2006). Hedgehog modulates cell cycle regulators in stem cells to control hematopoietic regeneration. *Proceedings of the National Academy of Sciences*, 103(38):14134–14139.
- Troy, A., Cadwallader, A. B., Fedorov, Y., Tyner, K., Tanaka, K. K., and Olwin, B. B. (2012). Coordination of satellite cell activation and self-renewal by Par-complex-dependent asymmetric activation of p38 α/β MAPK. *Cell Stem Cell*, 11(4):541–553.
- Tseng, T.-T., Gratwick, K. S., Kollman, J., Park, D., Nies, D. H., Goffeau, A., and Saier Jr, M. H. (1999). The RND permease superfamily: an ancient, ubiquitous and diverse family that includes human disease and development proteins. *Journal of Molecular Microbiology and Biotechnology*, 1(1):107–125.
- Tumbar, T., Guasch, G., Greco, V., Blanpain, C., Lowry, W. E., Rendl, M., and Fuchs, E. (2004). Defining the epithelial stem cell niche in skin. *Science*, 303(5656):359–363.
- Uezumi, A., Fukada, S.-i., Yamamoto, N., Takeda, S., and Tsuchida, K. (2010). Mesenchymal progenitors distinct from satellite cells contribute to ectopic fat cell formation in skeletal muscle. *Nature Cell Biology*, 12(2):143–152.
- Urciuolo, A., Quarta, M., Morbidoni, V., Gattazzo, F., Molon, S., Grumati, P., Montemurro, F., Tedesco, F. S., Blaauw, B., Cossu, G., et al. (2013). Collagen VI regulates satellite cell self-renewal and muscle regeneration. *Nature Communications*, 4.
- Varjosalo, M., Björklund, M., Cheng, F., Syvänen, H., Kivioja, T., Kilpinen, S., Sun, Z., Kallioniemi, O., Stunnenberg, H. G., He, W.-W., et al. (2008). Application of active and kinase-deficient kinome collection for identification of kinases regulating Hedgehog signaling. *Cell*, 133(3):537–548.

- Venuti, J. M., Morris, J. H., Vivian, J. L., Olson, E. N., and Klein, W. H. (1995). Myogenin is required for late but not early aspects of myogenesis during mouse development. *The Journal of Cell Biology*, 128(4):563–576.
- Vokes, S. A., Ji, H., McCuine, S., Tenzen, T., Giles, S., Zhong, S., Longabaugh, W. J., Davidson, E. H., Wong, W. H., and McMahon, A. P. (2007). Genomic characterization of Gli-activator targets in Sonic hedgehog-mediated neural patterning. *Development*, 134(10):1977–1989.
- von Maltzahn, J., Jones, A. E., Parks, R. J., and Rudnicki, M. A. (2013). Pax7 is critical for the normal function of satellite cells in adult skeletal muscle. *Proceedings of the National Academy of Sciences*, 110(41):16474–16479.
- Walker, B. E. (1962). A radioautographic study of muscle regeneration in dystrophic mice. *The American Journal of Pathology*, 41(1):41.
- Wall, D. S., Mears, A. J., McNeill, B., Mazerolle, C., Thurig, S., Wang, Y., Kageyama, R., and Wallace, V. A. (2009). Progenitor cell proliferation in the retina is dependent on Notch-independent Sonic hedgehog/Hes1 activity. *The Journal of Cell Biology*, 184(1):101–112.
- Walsh, K. and Perlman, H. (1997). Cell cycle exit upon myogenic differentiation. *Current Opinion in Genetics&Development*, 7(5):597–602.
- Wang, X., Ono, Y., Tan, S. C., Chai, R. J., Parkin, C., and Ingham, P. W. (2011). Prdm1a and miR-499 act sequentially to restrict Sox6 activity to the fast-twitch muscle lineage in the zebrafish embryo. *Development*, 138(20):4399–4404.
- Wang, Y. and Thorlacius, H. (2005). Mast cell-derived tumour necrosis factor- α mediates macrophage inflammatory protein-2-induced recruitment of neutrophils in mice. *British Journal of Pharmacology*, 145(8):1062–1068.
- Wang, Y., Zhou, Z., Walsh, C. T., and McMahon, A. P. (2009). Selective translocation of intracellular Smoothened to the primary cilium in response to Hedgehog pathway modulation. *Proceedings of the National Academy of Sciences*, 106(8):2623–2628.
- Wang, Y. X. and Rudnicki, M. A. (2012). Satellite cells, the engines of muscle repair. *Nature Reviews Molecular Cell Biology*, 13(2):127–133.
- Wechsler-Reya, R. J. and Scott, M. P. (1999). Control of neuronal precursor proliferation in the cerebellum by Sonic Hedgehog. *Neuron*, 22(1):103–114.
- Wen, Y., Bi, P., Liu, W., Asakura, A., Keller, C., and Kuang, S. (2012). Constitutive Notch activation upregulates Pax7 and promotes the self-renewal of skeletal muscle satellite cells. *Molecular and Cellular Biology*, 32(12):2300–2311.
- Whalen, R. G., Harris, J. B., Butler-Browne, G. S., and Sesodia, S. (1990). Expression of myosin isoforms during notexin-induced regeneration of rat soleus muscles. *Developmental Biology*, 141(1):24–40.
- Williams, B. A. and Ordahl, C. P. (1994). Pax-3 expression in segmental mesoderm marks early stages in myogenic cell specification. *Development*, 120(4):785–796.

- Wolff, C., Roy, S., and Ingham, P. W. (2003). Multiple muscle cell identities induced by distinct levels and timing of Hedgehog activity in the zebrafish embryo. *Current Biology*, 13(14):1169–1181.
- Yablonka-Reuveni, Z. and Rivera, A. J. (1994). Temporal expression of regulatory and structural muscle proteins during myogenesis of satellite cells on isolated adult rat fibers. *Developmental Biology*, 164(2):588–603.
- Yablonka-Reuveni, Z., Rudnicki, M. A., Rivera, A. J., Primig, M., Anderson, J. E., and Natanson, P. (1999a). The transition from proliferation to differentiation is delayed in satellite cells from mice lacking MyoD. *Developmental Biology*, 210(2):440–455.
- Yablonka-Reuveni, Z., Seger, R., and Rivera, A. J. (1999b). Fibroblast growth factor promotes recruitment of skeletal muscle satellite cells in young and old rats. *Journal of Histochemistry&Cytochemistry*, 47(1):23–42.
- Yaffe, D. and Saxel, O. (1977). Serial passaging and differentiation of myogenic cells isolated from dystrophic mouse muscle. *Nature*, 270(5639):725–727.
- Yamada, M., Tatsumi, R., Kikuri, T., Okamoto, S., Nonoshita, S., Mizunoya, W., Ikeuchi, Y., Shimokawa, H., Sunagawa, K., and Allen, R. E. (2006). Matrix metalloproteinases are involved in mechanical stretch-induced activation of skeletal muscle satellite cells. *Muscle&Nerve*, 34(3):313–319.
- Yamane, H., Ihara, S., Kuroda, M., and Nishikawa, A. (2011). Adult-type myogenesis of the frog *Xenopus laevis* specifically suppressed by notochord cells but promoted by spinal cord cells in vitro. *In Vitro Cellular&Developmental Biology-Animal*, 47(7):470–483.
- Yan, Z., Choi, S., Liu, X., Zhang, M., Schageman, J. J., Lee, S. Y., Hart, R., Lin, L., Thurmond, F. A., and Williams, R. S. (2003). Highly coordinated gene regulation in mouse skeletal muscle regeneration. *Journal of Biological Chemistry*, 278(10):8826–8836.
- Yang, N., Li, L., Eguether, T., Sundberg, J. P., Pazour, G. J., and Chen, J. (2015). Intraflagellar transport 27 is essential for Hedgehog signaling but dispensable for ciliogenesis during hair follicle morphogenesis. *Development*, pages dev-115261.
- Yang, Y., Drossopoulou, G., Chuang, P., Duprez, D., Marti, E., Bumcrot, D., Vargesson, N., Clarke, J., Niswander, L., McMahon, A., et al. (1997). Relationship between dose, distance and time in Sonic Hedgehog-mediated regulation of anteroposterior polarity in the chick limb. *Development*, 124(21):4393–4404.
- Yao, Q., Renault, M.-A., Chapouly, C., Vandierdonck, S., Belloc, I., Jaspard-Vinassa, B., Daniel-Lamazière, J.-M., Laffargue, M., Merched, A., Desgranges, C., et al. (2014). Sonic Hedgehog mediates a novel pathway of PDGF-BB-dependent vessel maturation. *Blood*, 123(15):2429–2437.
- Yennek, S., Burute, M., Théry, M., and Tajbakhsh, S. (2014). Cell adhesion geometry regulates non-random DNA segregation and asymmetric cell fates in mouse skeletal muscle stem cells. *Cell Reports*, 7(4):961–970.
- Yin, H., Price, F., and Rudnicki, M. A. (2013). Satellite cells and the muscle stem cell niche. *Physiological Reviews*, 93(1):23–67.

- Zammit, P. S., Golding, J. P., Nagata, Y., Hudon, V., Partridge, T. A., and Beauchamp, J. R. (2004). Muscle satellite cells adopt divergent fates a mechanism for self-renewal? *The Journal of Cell Biology*, 166(3):347–357.
- Zammit, P. S., Heslop, L., Hudon, V., Rosenblatt, J. D., Tajbakhsh, S., Buckingham, M. E., Beauchamp, J. R., and Partridge, T. A. (2002). Kinetics of myoblast proliferation show that resident satellite cells are competent to fully regenerate skeletal muscle fibers. *Experimental Cell Research*, 281(1):39–49.
- Zammit, P. S., Relaix, F., Nagata, Y., Ruiz, A. P., Collins, C. A., Partridge, T. A., and Beauchamp, J. R. (2006). Pax7 and myogenic progression in skeletal muscle satellite cells. *Journal of Cell Science*, 119(9):1824–1832.
- Zeng, X., Goetz, J. A., Suber, L. M., Scott, W. J., Schreiner, C. M., and Robbins, D. J. (2001). A freely diffusible form of Sonic Hedgehog mediates long-range signalling. *Nature*, 411(6838):716–720.
- Zhang, T., Günther, S., Looso, M., Künne, C., Krüger, M., Kim, J., Zhou, Y., and Braun, T. (2015). Prmt5 is a regulator of muscle stem cell expansion in adult mice. *Nature Communications*, 6(7140).
- Zhang, X. M., Ramalho-Santos, M., and McMahon, A. P. (2001). Smoothed mutants reveal redundant roles for Shh and Ihh signaling including regulation of L/R asymmetry by the mouse node. *Cell*, 105(6):781–792.
- Zhao, H., Feng, J., Seidel, K., Shi, S., Klein, O., Sharpe, P., and Chai, Y. (2014). Secretion of Shh by a neurovascular bundle niche supports mesenchymal stem cell homeostasis in the adult mouse incisor. *Cell Stem Cell*, 14(2):160–173.
- Zhao, M., Qiao, M., Harris, S. E., Chen, D., Oyajobi, B. O., and Mundy, G. R. (2006). The zinc finger transcription factor Gli2 mediates bone morphogenetic protein 2 expression in osteoblasts in response to Hedgehog signaling. *Molecular and Cellular Biology*, 26(16):6197–6208.
- Zhou, Z. and Bornemann, A. (2001). MRF4 protein expression in regenerating rat muscle. *Journal of Muscle Research&Cell Motility*, 22(4):311–316.